AD-A036 406 GTE SYLVANIA INC NEEDHAM HEIGHTS MASS COMMUNICATIONS--ETC F/G 17/2
ELF COMMUNICATIONS SEAFARER PROGRAM. SITE SURVEY, MICHIGAN REGI--ETC(U)
APR 76 N00093-75-C-0309

UNCLASSIFIED NL

1 OF 3
AD A036406

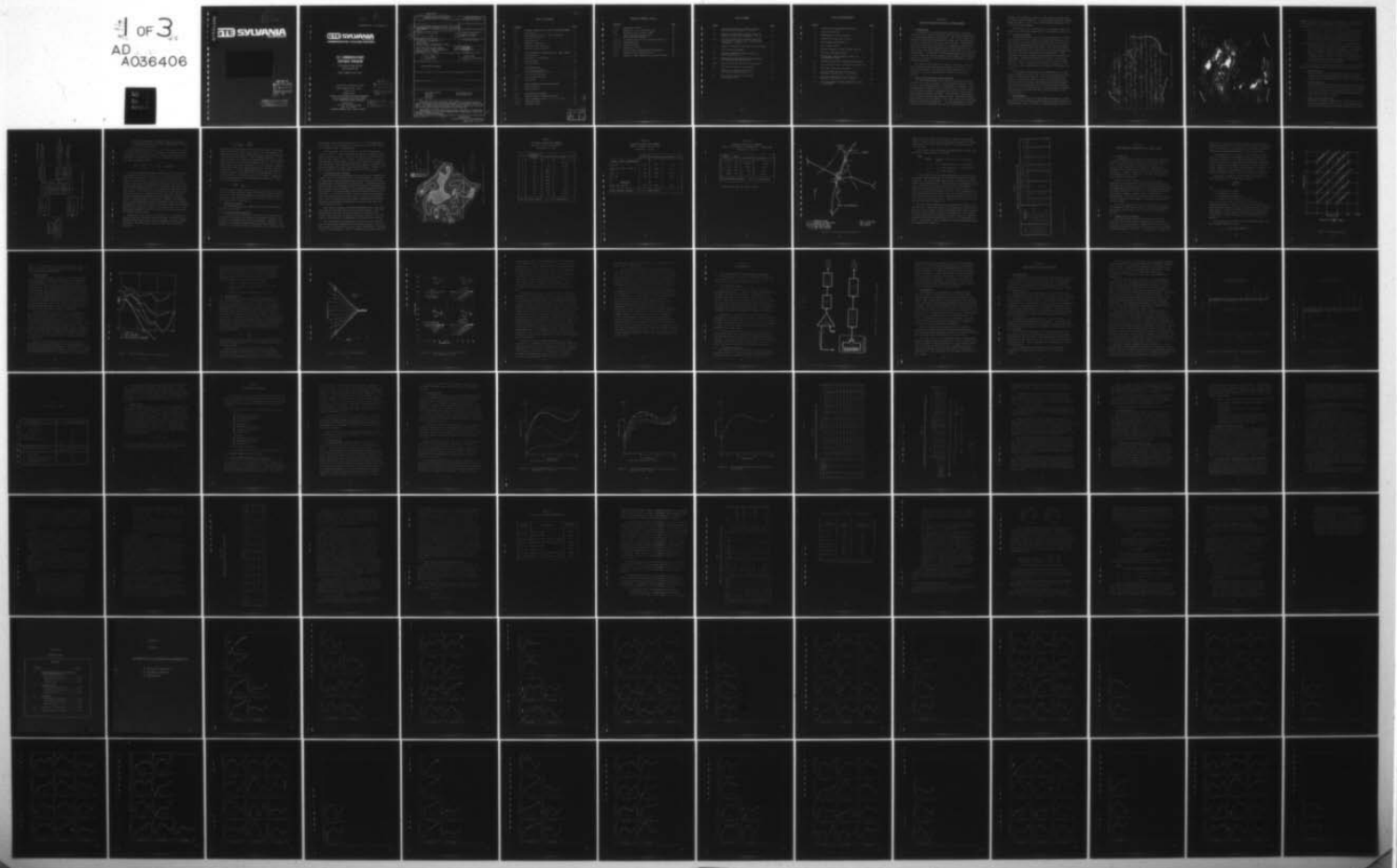

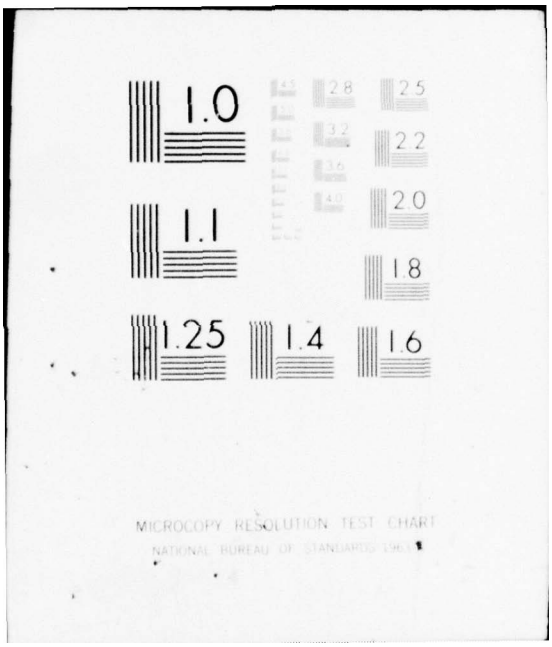
1.0
1.1
1.25
1.4
1.6
2.8
2.5
3.2
2.2
3.6
2.0
4.0
1.8
MICROCOPY RESOLUTION TEST CHART
NATIONAL BUREAU OF STANDARDS 1963-A

AD A036406

(1) NW

GTE SYLVANIA
INCORPORATED

DDC
MAR 4 1977
A

DISTRIBUTION STATEMENT A
Approved for public release;
Distribution Unlimited

CONTROL NO: 0309-B006-001

GTE SYLVANIA
INCORPORATED
COMMUNICATION SYSTEMS DIVISION

ELF COMMUNICATIONS SEAFARER PROGRAM

SITE SURVEY FINAL REPORT MICHIGAN REGION

EARTH CONDUCTIVITY DATA

DDC
RECEIVED
MAR 4 1977
A

Contract No. N00039-75-C-0309
CDRL SEQUENCE NO. B006
April 1976
Prepared for:
NAVAL ELECTRONIC SYSTEMS COMMAND
Special Communications Project Office
ELF COMMUNICATIONS DIVISION

DISTRIBUTION STATEMENT A
Approved for public release;
Distribution Unlimited

Prepared by:
GTE Sylvania Incorporated
189 " B " Street
Needham Heights, Massachusetts 02194

UNCLASSIFIED

SECURITY CLASSIFICATION OF THIS PAGE (When Data Entered)

REPORT DOCUMENTATION PAGE	READ INSTRUCTIONS BEFORE COMPLETING FORM
1. REPORT NUMBER	2. GOVT ACCESSION NO. 3. RECIPIENT'S CATALOG NUMBER
4. TITLE (and Subtitle) (6) ELF Communications Seafarer Program. Site Survey, **Final Report**, Michigan Region. Earth Conductivity Data.	5. TYPE OF REPORT & PERIOD COVERED 6. PERFORMING ORG. REPORT NUMBER
7. AUTHOR(s) (9) Final rept.	8. CONTRACT OR GRANT NUMBER(s) (15) N00039-75-C-0309 ✓
9. PERFORMING ORGANIZATION NAME AND ADDRESS GTE Sylvania Incorporated ✓ 189 B Street Needham Heights, Massachusetts 02194	10. PROGRAM ELEMENT, PROJECT, TASK AREA & WORK UNIT NUMBERS
11. CONTROLLING OFFICE NAME AND ADDRESS (10) Naval Electronic Systems Command Special Communications Project Office Washington, D. C. 20360	12. REPORT DATE April 1976 ✓ 13. NUMBER OF PAGES 192
14. MONITORING AGENCY NAME & ADDRESS (if different from Controlling Office) (12) 214p.	15. SECURITY CLASS. (of this report) Unclassified 15a. DECLASSIFICATION/DOWNGRADING SCHEDULE

16. DISTRIBUTION STATEMENT (of this Report)

Distribution Unlimited

17. DISTRIBUTION STATEMENT (of the abstract entered in Block 20, if different from Report)

18. SUPPLEMENTARY NOTES

19. KEY WORDS (Continue on reverse side if necessary and identify by block number)

ELF Communications
Seafarer
Site Survey
Michigan
Environmental Data
Earth Conductivity

20. ABSTRACT (Continue on reverse side if necessary and identify by block number)

An earth conductivity survey has been completed in the Upper Peninsula region of Michigan with confirming measurements at the Wisconsin Test Facility (WTF). The results define the geological distributions within the survey area and identify average conductivity values for each rock type.

Measurements at the WTF were used to provide a data base for comparative evaluation between the scalar audio magnetotelluric method used in the survey and other available techniques.

HB

DD FORM 1 JAN 73 1473 EDITION OF 1 NOV 65 IS OBSOLETE

UNCLASSIFIED

SECURITY CLASSIFICATION OF THIS PAGE (When Data Entered)

406 355

TABLE OF CONTENTS

SECTION		PAGE
1.0	SEAFARER CONDUCTIVITY SURVEY PROGRAM SUMMARY	1
1.1	Introduction	1
1.2	Audio Magnetotelluric (AMT) Technique . . .	1
1.3	Conduct of Survey	2
1.4	Data Analysis	2
1.5	Summary of Resulty	8
1.5.1	Michigan Upper Peninsula	8
1.5.2	Wisconsin Test Facility	9
2.0	AUDIO-FREQUENCY MAGNETOTELLURIC (AMT) THEORY	17
2.1	Introduction	17
2.2	Principle of the Method	17
2.3	Source Fields	20
2.4	Interpretation	22
3.0	INSTRUMENTATION	27
3.1	E- & H-Field Sensors and Interference Analyzer	27
3.1.1	E- & H-Field Sensors	27
3.1.2	Interference Analyzer	27
3.2	Calibration	29
4.0	ERROR ANALYSIS AND SYSTEM SCALING	30
4.1	Error Analysis	30
4.2	System Sizing	35
5.0	DISCUSSION OF RESULTS	36
5.1	Michigan Upper Peninsula Results	36
5.1.1	Depth Sounding Cirves - Log ρ vs. Log f . .	36
5.1.2	Pseudosections	37
5.1.3	Residual Plots	38

BY
DISTRIBUTION/AVAILABILITY CODES
DIST. AVAIL. and/or SPECIAL

TABLE OF CONTENTS (Cont.)

SECTION		PAGE
5.1.4	Anisotropy TE/TM	45
5.1.5	Summary of 35 Hz and 95 Hz Data	45
5.2	Wisconsin Test Facility (WTF)	46
5.2.1	Short Electrode AMT Results Along E/W Antenna ROW	46
5.2.1.1	Log Resistivity vs Log Frequency Results . .	47
5.2.1.2	Pseudosections	49
5.2.1.3	Residual Plots	51
5.2.1.4	Anisotropy TE/TM	51
5.2.2	Half and Full Antenna AMT Measurements . . .	52
5.2.3	Layered Earth Interpretation	57
5.2.4	Summary of WTF Conductivity Survey Results .	60

LIST OF TABLES

TABLE		PAGE
I	Michigan Conductivity Summary Based on E/W Profiles (Frequency - 95 Hz).	11
II	Michigan Conductivity Summary Based on Bedrock Geology Map (Frequency - 95 Hz) . . .	12
III	Michigan Conductivity Summary Based on University of Toronto Log ρ Contour Map (Frequency - 95 Hz)	13
IV	Summary of Results from Various WTF Studies .	16
V	Error Analysis Summary	34
VI	Averaged Apparent Resistivities for Each Traverse Line	42
VII	Weighted Average Apparent Resistivities For Michigan Upper Peninsula	43
VIII	Mean Resistivity WTF (E/W Antenna Line) . . .	50
IX	AMT E-Field Sensor Configuration	53
X	Summary of Conductivity Results for the WTF Antenna Array	55
XI	Statistical Analysis of the WTF Measurement Data	56

LIST OF ILLUSTRATIONS

FIGURE		PAGE
1	Conductivity Measurement Locations	3
2	Study Area Geology	4
3	Methodology of Data Analysis	6
4	Conductivity Contours - 95 Hz	10
5	WTF Antenna Configuration	14
6	Skin Depth Curves	19
7	Typical Magnetic Field Strength Spectra . . .	21
8	Two-Layer Sounding Curves	23
9	Three-Layer Curves Showing Effect of Intermediate Layers	24
10	Schematic Diagram of Detection Equipment . .	28
11	Salt Lake Test Data: Average Square Root of ρ	32
12	Salt Lake Test Data: Average ρ	33
13	Line Averaged Resistivity Plots for Michigan - Lines A, B, C, D, and E	39
14	Line Averaged Resistivity Plots for Michigan - Lines F, G, H, I, and J	40
15	"Area Weighted" Average Resistivity Plot for Michigan	41

SECTION 1

SEAFARER CONDUCTIVITY SURVEY PROGRAM SUMMARY

1.1 INTRODUCTION

A conductivity survey has been completed in the Upper Peninsula (UP) region of Michigan with confirming measurements at the Wisconsin Test Facility (WTF). The results define the geological distributions within the survey area and identify average conductivity values for each rock type. Measurements at the WTF provided a data base for comparative evaluation between the scalar Audio Magnetotelluric (AMT) method used in this survey and other methods such as Tensor AMT, H/I, E/H, and Schlumberger. In addition, the WTF measurement program establishes a basis for scaling system current moment (IL) requirements from an area of known propagation performance to other Michigan locations.

The survey instrumentation, support personnel, and computer analysis were provided by University of Toronto. Geologic interpretations in this report were made by Dr. D. Strangway, Chairman, Department of Geology, University of Toronto.

1.2 AUDIO MAGNETOTELLURIC (AMT) TECHNIQUE

The AMT method measures the ratio of horizontal electric field at the earth's surface to the orthogonal magnetic field to yield earth resistivities as a function of frequency. The instrumentation consists of a horizontal dipole E-field sensor, a coil H-field sensor, a prewhitening filter box and a variable frequency analyzer receiver. The receiver integrates the E- and H-field signals and forms the ratio, from which subsurface conductivity is inferred. The signal source is terrestrial spherics (lightning discharges). At each measurement location, two 200-foot wire antennas are laid out perpendicular to one

another, the termination being a stake inserted no more than 12 inches below the surface. Then orthogonal pairs of measurements are made at each of ten predetermined frequencies over a range of three decades.

The output of the receiver plus a calibration factor is equal to ten times the logarithm of the apparent resistivity.

1.3 CONDUCT OF SURVEY

In the Michigan UP region, the low conductivity geological formations tend to run in a north-south direction. For this reason, the area was sectionalized into a grid configuration where measurements were made along lines of latitude spaced approximately six miles apart. Site locations were then evaluated based on a review of the existing conductivity data base, geology, ownership, and accessibility. Sites located in National Forests and near population centers were eliminated. Selection criteria were based on access and ownership data, with State-owned property given highest priority. Figure 1 shows the measurement locations of the 106 sites in the survey region, and Figure 2 illustrates the geology.

In Wisconsin, AMT conductivity measurements were taken along the WTF E/W antenna line at 20 sites identified by the existing antenna pole numbers. The area weighted-average method to define bulk resistivities was not suitable here, so the resistivities were interpolated between measurement stations and then averaged at 115 equally spaced locations along the 13.1 mile antenna line. Long-wire AMT measurements were also made utilizing the WTF overhead antenna as the E-field sensor.

1.4 DATA ANALYSIS

The data are taken via scalar AMT measurements at sites selected for their geological characteristics and proximity to predetermined lines of latitude. Each measurement site is as-

Figure 1. Conductivity Measurement Locations

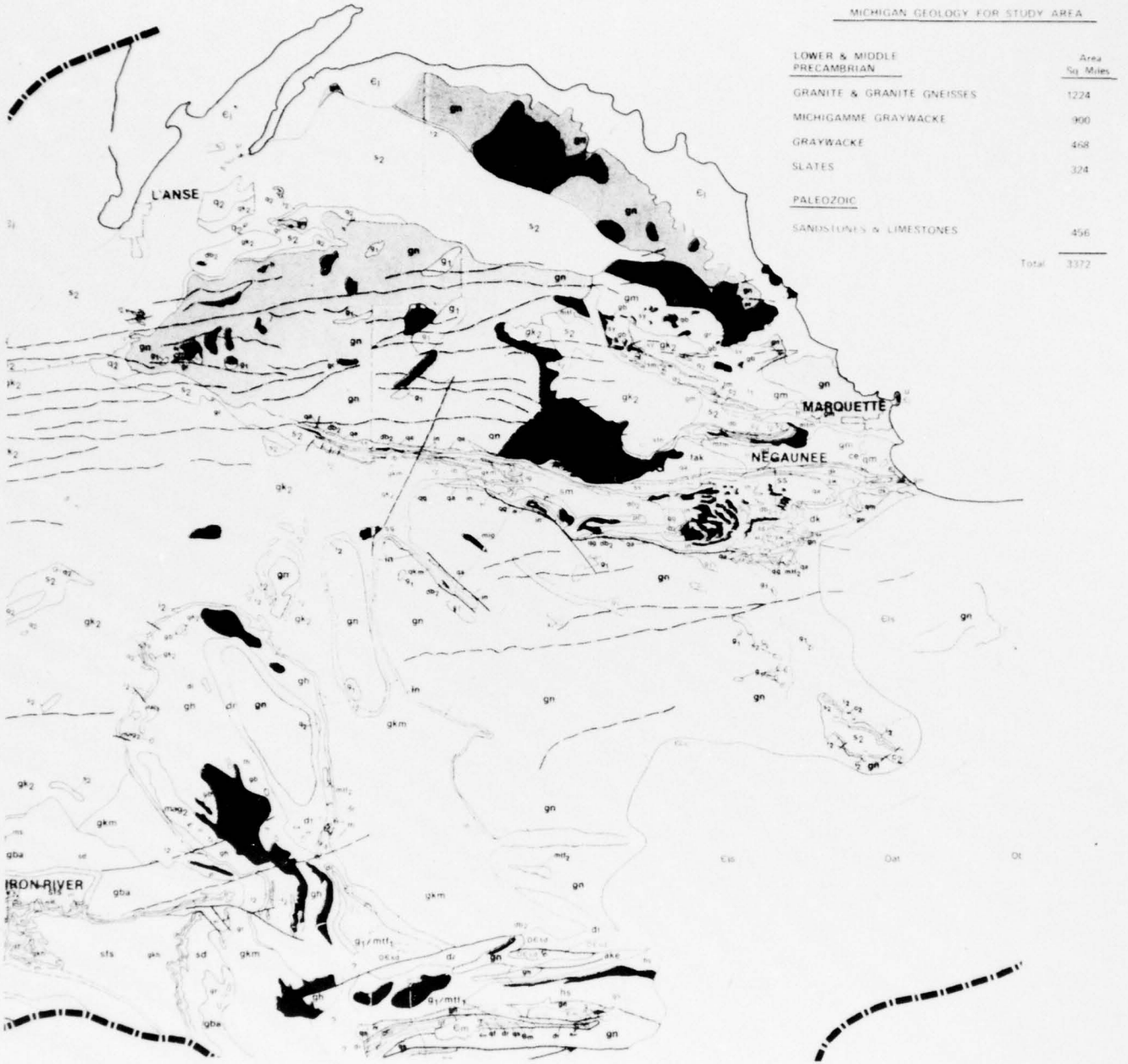

Figure 2. Study Area Geology

signed to a given line traverse to accommodate a lateral profiling analysis. The methodology of analysis is illustrated by Figure 3, with the major steps described below:

- Depth sounding curves are developed from smoothed data which show the actual field observations plotted station-by-station on a log ρ versus log f plot. This method shows the sense of resistivity with depth from which layered earth structures can be interpreted.
- Pseudosections are developed from a measurement traverse of the area and show the resistivity variations as a function of frequency and distance. The development of pseudosections is an important step in the analysis in that it allows locally wide variations to be subordinated to achieve a resistivity profile and countour maps that can be reasonably integrated for ELF antenna performance predictions.

From this basic analysis, the survey area can be characterized by the following data interpretations and illustrations:

a. Lines Analysis
Lateral profiles are developed which show resistivity gradients along the measurement traverse (residuals), layered earth interpretations and anisotropy indications.

b. Geology Analysis
The geologic distributions within the survey area can be used as a basis to represent the total area if the geology is well charted and the resistivities of the various rock types are known. This requires many measurements to be taken in each rock type.

c. Conductivity Countour Map
Contours of constant conductivity for the survey area are generated from the data along a given measurement traverse and interpolation between measurement locations

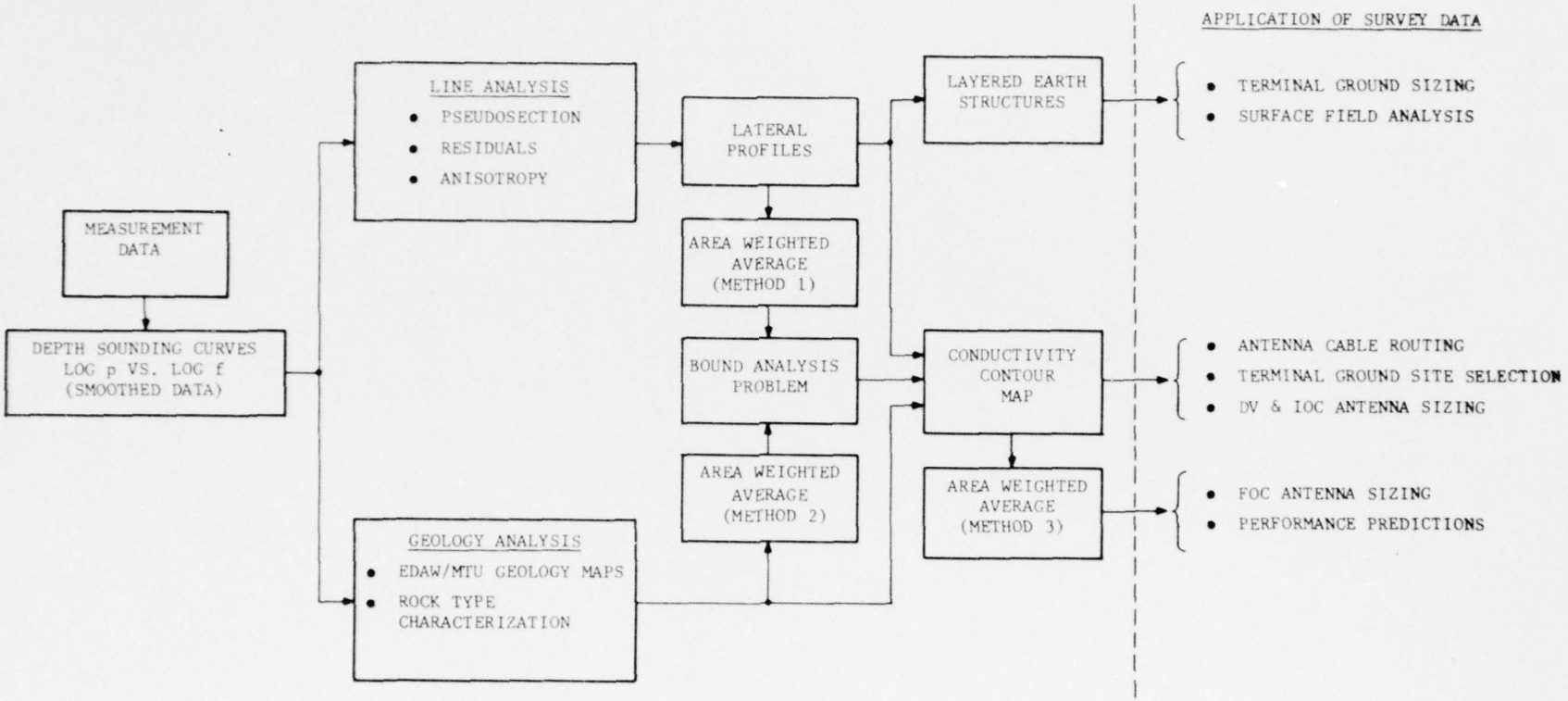

Figure 3. Methodology of Data Analysis

along each traverse and between lines of latitude. In areas where data are sparse, geology maps are used as an aid in contouring.

The average resistivities for the survey area can be computed for each of these three approaches. Letting A_i be the individual line traverse lengths or subordinated areas associated with each method, and ρ_i be the respective resistivity, the area weighted average is

$$\rho \text{ area} = \left[\frac{1}{\sum_{1}^{n} A_i} \sum_{1}^{n} \sqrt{\rho_i} \; A_i \right]^2 \quad \text{ohm-meters.}$$

The area weighted averages associated with line analysis and geology are useful in bounding the analysis problem in that one technique gives a one-dimensional profile along ten lines of latitude with no definition between lines (6 miles apart), while the geology method characterizes the survey area by rock type based on the heuristic assumption that each rock type and its associated areas can be correctly identified (geologic noise). The accuracy of each method in characterising the survey area is an unknown quantity since the analysis is really a two-dimensional problem and the degree of geologic "noise" is always subject to question. However, the combination of these approaches, heavily weighted by the line analysis pseudosections, can give the best available answer from measurement data in achieving the main survey objective, i.e., a two-dimensional conductivity contour map and its associated weighted average conductivities.

Knowledge of the effective resistivity ρ_e is necessary to determine the ELF excitation factor in order to predict propagation effects from a given site and thereby size the transmitter array. The excitation factor is given by the following equation:

$$E = \frac{1}{\sqrt{h^2 \sigma (c/v)}} = \frac{\sqrt{\rho_e}}{\sqrt{h^2 c/v}}$$

Estimation of the values of the excitation factor and atmospheric attenuation rate (i.e., E and α) for the purposes of SEAFARER sizing has been conducted largely with data from one controlled source, the WTF. The estimates presently in use are the result of an analysis conducted by NUSC using a model which shows that E and the attenuation rate, α, are coupled, which implies that some knowledge of ρ_e is required. Because the GTE Sylvania (1976) AMT measurement at the WTF yielded a conductivity of 0.26 millimhos/meter under the East-West antenna as opposed to the NUSC (1973) H/I measurement of 0.32 millimho/meter, a correction factor is required. Consequently, for the purpose of sizing systems, the effective conductivity is taken to be

$$\sigma_e = \frac{3.2}{2.6} \quad \frac{1}{\rho_{area}}$$

This approach decreases the excitation factor used for sizing by 0.9 dB from that which would be obtained by direct application of the 1976 AMT measurements and should therefore be conservative. This scaling factor has not been applied to the data presented in this report.

1.5 SUMMARY OF RESULTS

The following sections summarize the survey results for Michigan and the WTF.

1.5.1 Michigan Upper Peninsula

The rocks of the central UP region have low conductivity, reflecting the presence of massive pre-Cambrian gneisses. To the east, the conductivity increases somewhat, indicating the presence of conductive Cambrian and Ordovician sediments. This limestone and sandstone cover is relatively thin, since the con-

ductivities still remain fairly low at 2 - 5 x 10^{-4} mhos/meter. At a depth of a few kilometers the conductivity increases sharply to values around .01 mhos/meters.

These patterns are illustrated by the 95 Hz contour map shown in Figure 4. The contour map is based on averaged, smoothed data for 106 stations. Larger scale maps are to be found inside the back cover of this volume. On the 95 Hz map, a set of observations taken by NUSC at 75 are also shown and included in the contouring. These observations are in general agreement with ours and completely support the above conclusions. Tables I, II, and III summarize the measurement results of this program.

1.5.2 Wisconsin Test Facility

AMT conductivity measurements were taken along the WTF E/W antenna line at 20 locations (200' E-field sensors). Profiles of resistivity versus frequency were plotted, and the data were smoothed using a third-order polynomial fit. Pseudosections were generated with the smoothed data and contoured by interpolation due to uneven station spacing. Data between measurement stations were derived from linear interpolation of the square-root of resistivity. A resistivity profile versus distance was generated with data points every 600 feet along a 13.1 mile E/W antenna line. The 115 data points were equally weighted and averaged to determine the effective conductivity as seen by each half and full E/W antenna line.

Half and full antenna line AMT measurements were also made utilizing the overhead WTF lines as E-field sensors. Over 250 measurements were taken during the period of Octover 1975 - January 1976 utilizing morning and afternoon spherics. The WTF antenna configuration is schematically illustrated by Figure 5.

The E/W antenna long and short line test results indicate that the geological layered-earth structure consists of three to four layers; low resistivity at the lower frequencies is typically about 1000 ohm-meters. This is overlain by a high resistivity

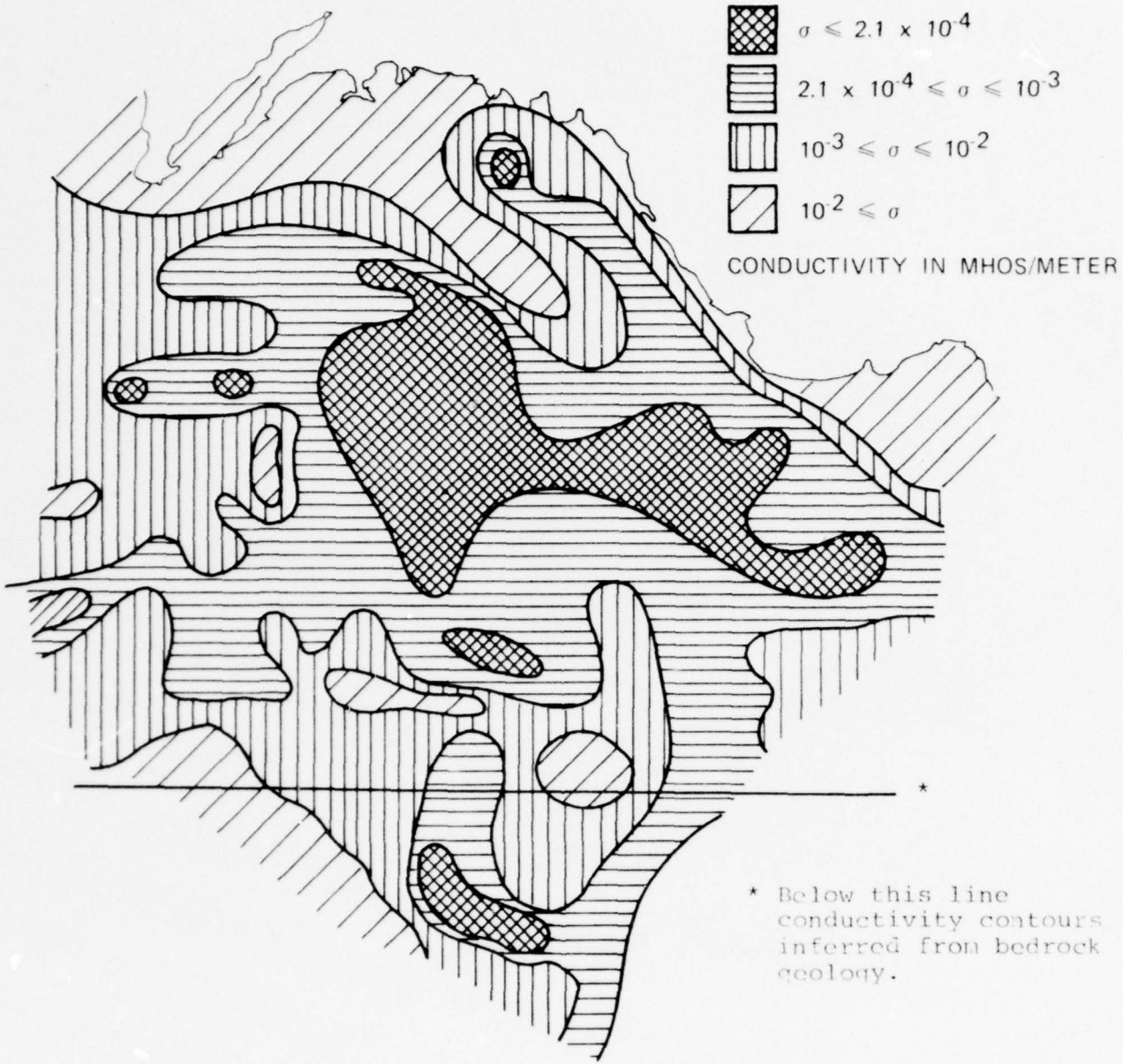

Figure 4. Conductivity Contours - 95 Hz.

TABLE I

MICHIGAN CONDUCTIVITY SUMMARY
BASED ON E/W LATITUDE PROFILES
(Frequency - 95 Hz)

LINE	EXTENT OF INTERPOLATION (MILES)	$\bar{\rho}$ OHM-METERS	$\bar{\sigma}$ MHOS/METERS x 10^{-4}
A	44	31	323.00
B	56	355	28.00
C	68	2884	3.47
D	46	2691	3.72
E	95	3802	2.63
F	94	2884	3.47
G	98	2630	3.80
H	94	1660	6.02
I	86	955	10.50
J	71	646	15.50
AREA WEIGHTED AVERAGE - 5.67 x 10^{-4} MHOS/METER			

TABLE II

MICHIGAN CONDUCTIVITY SUMMARY
BASED ON BEDROCK GEOLOGY MAP
(Frequency - 95 Hz)

	AREA SQ MILES	$\bar{\rho}$ OHM-METERS	$\bar{\sigma}$ MHOS/METER x 10^{-4}
LOWER & MIDDLE PRECAMBRIAN			
GN, GR	1244	5747	1.74
GKM, GKA, GB, GH, GKH, H, DR	900	1020	9.8
GK2, G2	468	893	11.2
S2, SM	324	238	42.0
PALEOZOIC			
OAT, ELS, EM, EJ	456	1538	6.5
AREA WEIGHTED AVERAGE - 4.48×10^{-4} MHOS/METER			

TABLE III

MICHIGAN CONDUCTIVITY SUMMARY
BASED ON UNIVERSITY OF TORONTO LOG ρ CONTOUR MAP
(Frequency - 95 Hz)

CONTOUR RANGE $\sigma \times 10^{-4}$	AREA SQ MILES	$\bar{\rho}$ OHM-METERS	$\bar{\sigma}$ MHOS/METERS $\times 10^{-4}$
$\sigma \leq 2.1$	599	10,129	0.987
2.1 - 10	1479	2,197	4.55
10 - 100	920	435	23.0
$\sigma \geq 100$	431	70	143.0
AREA WEIGHTED AVERAGE* - 5.06×10^{-4} MHOS/METER			

*Conductivity used for system sizing.

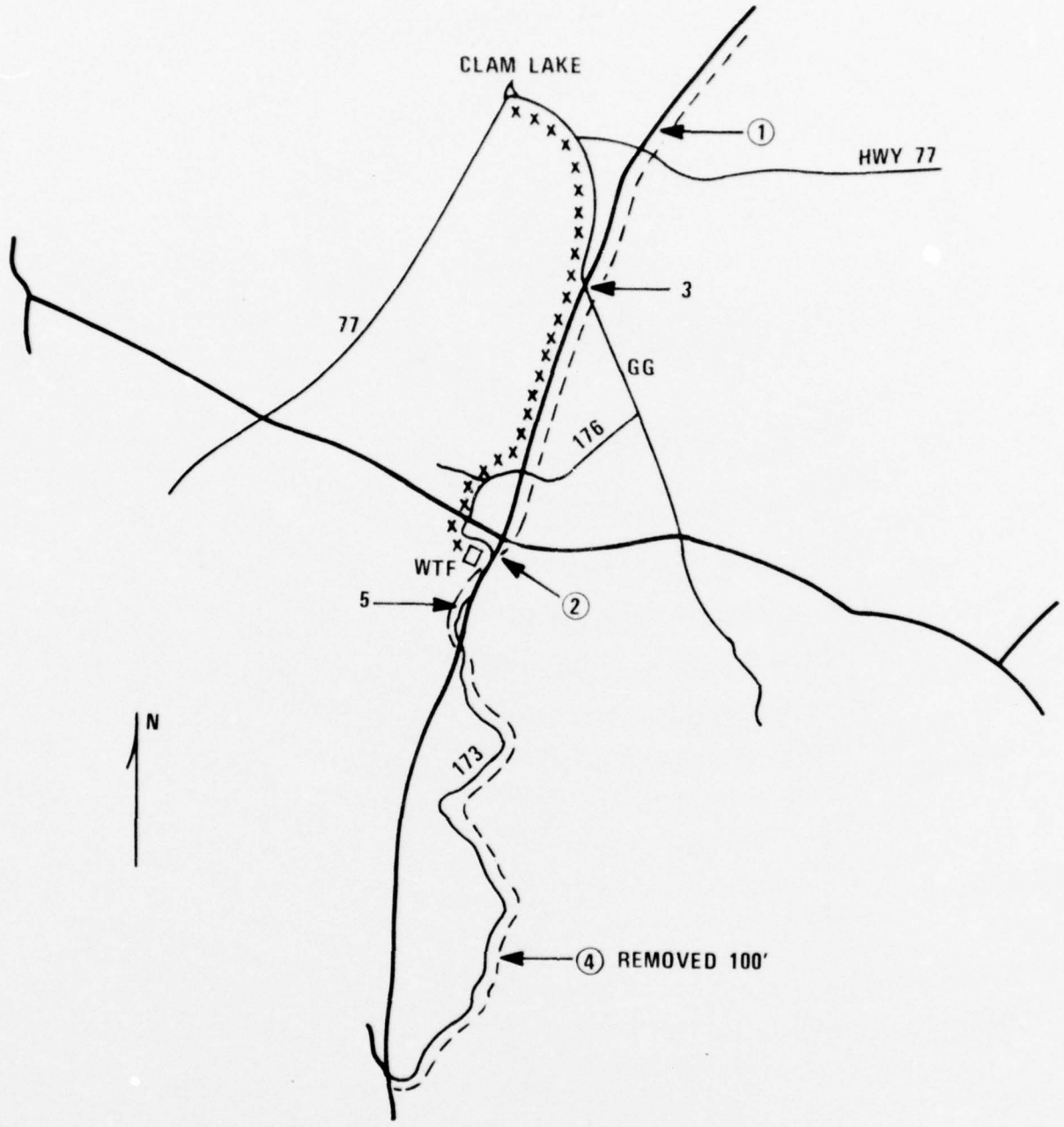

Figure 5. WTF Antenna Configuration

layer with peak values in the range of 7,000 to 10,000 ohm-meters. Nearer the surface, the resistivity appears to become lower with a hint that locally there is a high resistivity surface layer.

This leads to the following one-dimensional layered earth structure interpretation for the WTF:

Layer		
1	Surface	Strongly anisotropic - a few meters thick
2	_____	$\rho_2 \approx 1700$ ohm-meter; $h_2 \approx 600$ meters
3	_____	$\rho_3 \approx 6600$ ohm-meter; $h_3 \approx 4600$ meters
4	_____	$\rho_4 \ll 1000$ ohm-meter

Recent (1976) long line AMT measurements along the N/S antenna add a second dimension to the above layered earth interpretation. The results show that areas to the north and west exhibit low conductivities. The GTE Sylvania Schlumberger (1972) data, combined with the E/W residual plots and measurements, suggest a general E/W geologic fracturing in the bedrock. A simplistic model would consist of a shear line intersecting the north leg 1500 meters from the center and extending to the west leg 5600 meters from the center. Everything north of the shear line would be highly conductive. Anisotropy near the center of the array could be as high as 2.

The WTF survey emphasis was on measurements along the E/W antenna line. Data were taken at 20 locations to laterally profile the area, and full antenna measurements were made to determine the overall antenna effective conductivity. The results of these measurements and analysis indicate that the effective conductivity along the E/W antenna is 2.6×10^{-4} mhos/meter at 80 Hz. The results of this survey and various other WTF studies are summarized in Table IV.

TABLE IV

SUMMARY OF RESULTS FROM VARIOUS WTF STUDIES

STUDY	MEASUREMENT TECHNIQUE	ANTENNA DATA - MHOS/METER x 10^{-4}							
		σ_E	σ_W	σ_{EW} PREDICTED	σ_{EW} MEASURED	σ_S	σ_N	σ_{NS} PREDICTED	σ_{NS} MEASURED
RCA 1968	2 km H/I	1.71	1.76	1.70	-	1.77	1.70	1.70	-
GTE 1972	16 km Schlumberger	3.98	-	3.10	-	-	-	3.30	-
NUSC 1972	22 km H/I	-	-	-	3.20	-	-	-	2.2
NUSC 1973	H/I Half Ant.	2.50	3.00	2.80	-	1.40	3.50	2.20	-
GTE 1975	61 m AMT.	2.07	2.84	2.40	-	-	-	-	-
GTE 1976	AMT. Half Ant.	2.36	2.87	2.60	-	1.32	6.53*	2.52	-
	AMT. Full Ant.	-	-	-	2.59	-	-	-	4.20*

*Possible parasitic contamination.

SECTION 2

AUDIO-FREQUENCY MAGNETOTELLURIC (AMT) THEORY

2.1 INTRODUCTION

The magnetotelluric method for determining subsurface electrical conductivity structure was first recognized in 1950. Since then, most magnetotelluric studies have utilized low frequencies to investigate deep-seated features such as sedimentary basins or the earth's crust and mantle. However, Cagniard (1953) explicitly outlined the extension of this technique to shallow exploration by using higher frequencies.

During the early summer of 1963, initial field observations were made by Kennecott Copper Corporation to determine the feasibility of determining ground resistivity by magnetotelluric measurements in the audio-frequency range. The field program was carried out in conjunction with DECO Electronics, Boulder, Colorado, now a subsidiary of Westinghouse. Sufficient encouragement was realized then to justify Kennecott's development of equipment specifically for the purpose.

For mineral exploration where resistivity data alone are diagnostic, AMT has been found to have both advantages and disadvantages compared with conventional electrical methods.

2.2 PRINCIPLE OF THE METHOD

The magnetotelluric method has been described by Cagniard (1953), Wait (1962), Vozoff (1972), and others. Basically, the electromagnetic impedance - the ratio of the horizontal electric field (E) in the ground to the orthogonal horizontal magnetic field (H) - is measured at a number of

frequencies to yield earth resistivities as a function of frequency, resulting in a form of depth sounding. Operationally the technique is quite simple in that depth sounding is conducted by making measurements at only one location.

The magnetotelluric field can be described in terms of either a propagating electromagnetic wave interacting with the earth's surface, or an inductive phenomenon in which telluric currents are induced by the fluctuating geomagnetic field. Whereas the incident horizontal magnetic field is roughly doubled at the surface and uniform in the absence of lateral contrasts in resistivity, the electric field is directly dependent upon the earth's conductivity structure.

The depth of sounding can be related to frequency by using the concept of the skin depth given as

$$\delta = \sqrt{\frac{1}{\pi \mu \sigma f}} \ ,$$

where

δ is skin depth in meters

f is frequency in hertz

σ is conductivity in mhos/m

μ is magnetic permeability in henries/m

Plots of skin depths as a function of resistivity and frequency are shown in Figure 6. This figure shows that the audio-frequency range of (10 Hz to 10 kHz) covers the desired depth range. As such, the AMT method can be considered as a supplement to other methods for determining near-surface resistivities such as conventional DC or AC resistivity surveys.

The apparent resistivity can be determined simply from the measured impedance (E/H) by

$$\rho_a = \frac{1.26 \times 10^5 \times (E/H)^2}{f} \ ,$$

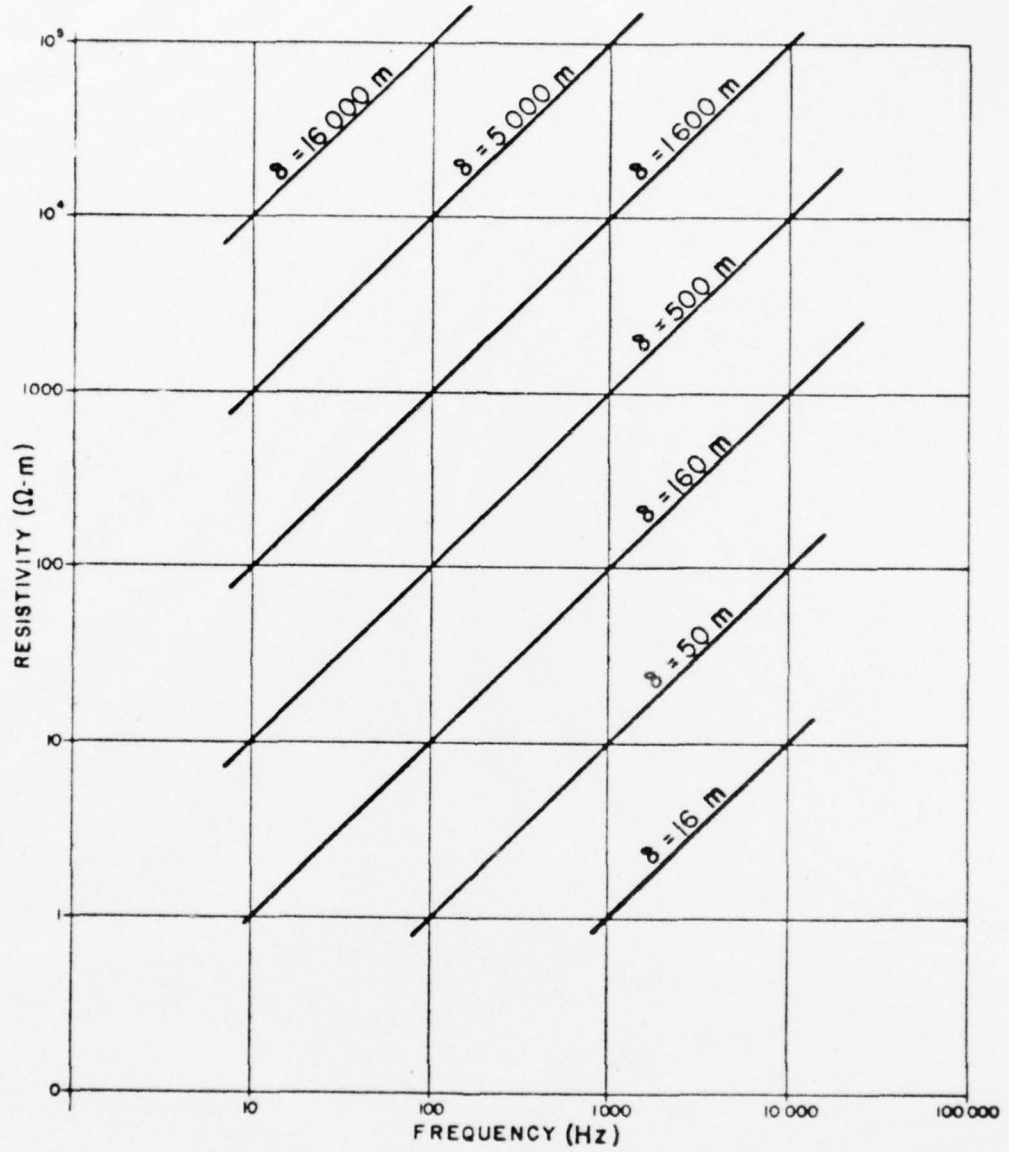

Figure 6. Skin Depth Curves

where E is in volts/m, and H in ampere-turns/m. Data can then be plotted on log-log paper to form the standard magnetotelluric sounding curve.

2.3 SOURCE FIELDS

The problem of source fields in the audio-frequency range has been considered by many workers in studies of radio propagation. Interest in natural noise fields is therefore considerable, and several extensive studies have been reported. The audio-frequency magnetotelluric technique commonly used in geophysical exploration also makes use of natural audio-frequency signals at 150 Hz and 500 Hz. It is well known and understood that the main source of natural noise is thunderstorms, which are extensively concentrated in the tropics and tend to peak in their activity in the early afternoon, local time. The generated energy propagates around the world, trapped in the waveguide formed between the earth's surface and the ionosphere.

Full treatment of the nature of this propagation has been given by various authors and only a few pertinent details will be given here. The source itself contains a wide spectrum of frequencies; but due to the characteristics of the waveguide, many of these tend to be attenuated. Thus a pulse at the source spreads out geometrically, as well as having certain preferred frequencies or rejected frequencies. Among the better known of these are the Schumann resonances at 8, 14, 20 and 25 Hz in which fairly strong energy peaks are observed. The waveguide also has a strong absorption at about 2 kHz.

Figure 7 shows horizontal magnetic field strength curves for morning and afternoon on a typical summer day in the western United States and Canada. Note that in all cases the amplitude decreases with increasing frequency up to about 2 kHz, but that this effect is much greater in the morning,

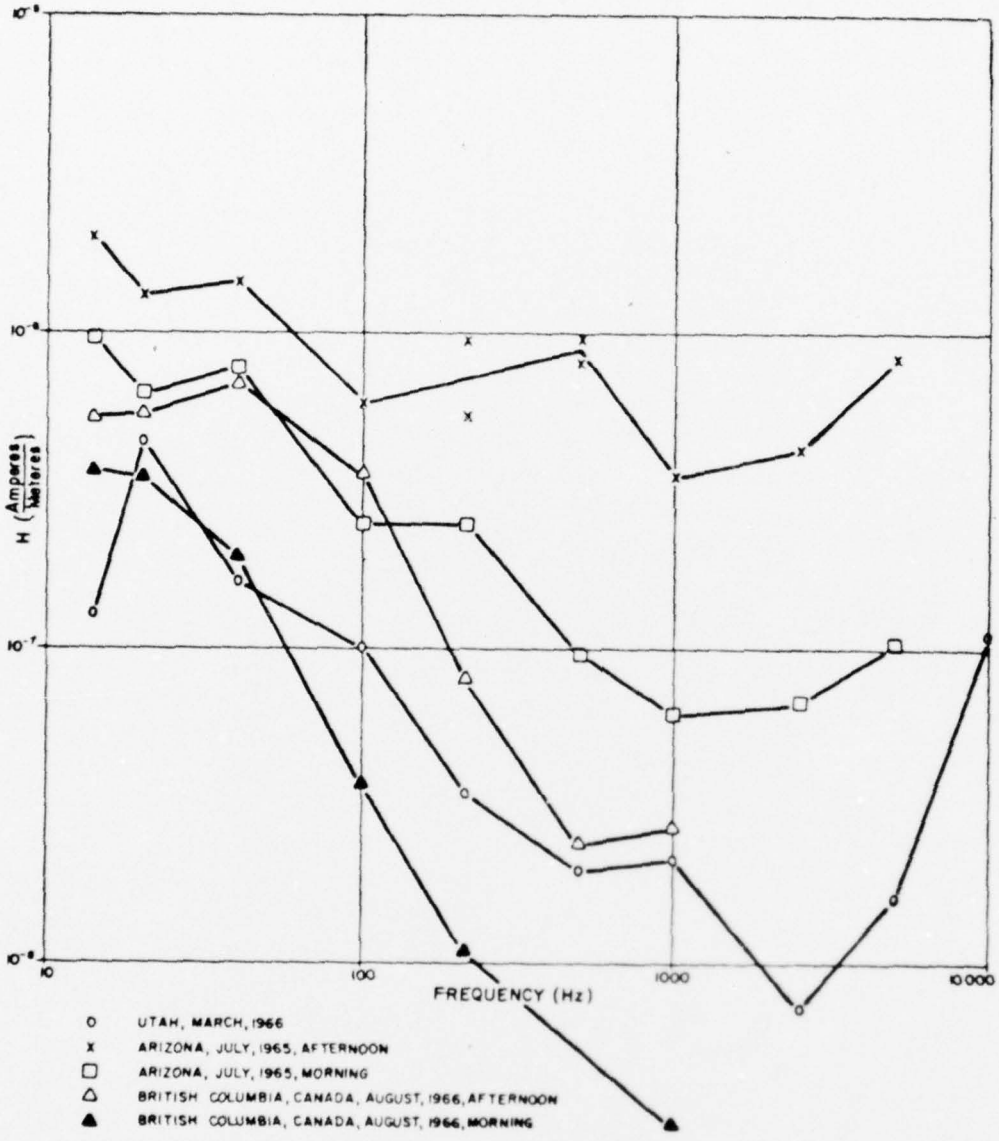

Figure 7. Typical Magnetic Field Strength Spectra

due to the fact that the sources are much farther away and the waveguide attenuation at 2-3 kHz is relatively much greater. In the afternoon, local thunderstorm activity is present and the decrease at 2 kHz is much less important. Otherwise, the absolute field strength level is dependent on the proximity to sources so that in general:

a. Levels are higher in lower latitudes;

b. Levels are higher in the afternoon than in the morning; and

c. Levels are higher in summer than in winter.

2.4 INTERPRETATION

The simplest method of interpreting magnetotelluric data is the comparison of the sounding curves obtained in the field with theoretical curves. Several workers have published theoretical apparent resistivity versus frequency curves for two- and three-layer cases, and the calculation for multi-layer cases is quite simple. Typical curves for a two-layer configuration are given in Figure 8. Because of the law of electromagnetic similitude, these layered-media curves can be used for any combination of layer thickness and resistivity. Specifically, if we consider any configuration, and multiply all lengths by K_L and all resistivities by K_ρ, the original curve is correct if all frequencies are multiplied by the factor

$$K_F = \frac{K_\rho}{K_L^2}$$

This operation essentially keeps constant the electromagnetic response parameter kd (or $k^2d^2 = i\mu\omega\sigma d^2$, where d is a representative length).

Theoretical curves to show the effect of a layer sandwiched between an upper layer and a lower half-space are given in Figure 9. Essentially, it is not possible to detect a conducting middle layer which is 1/100 the thickness

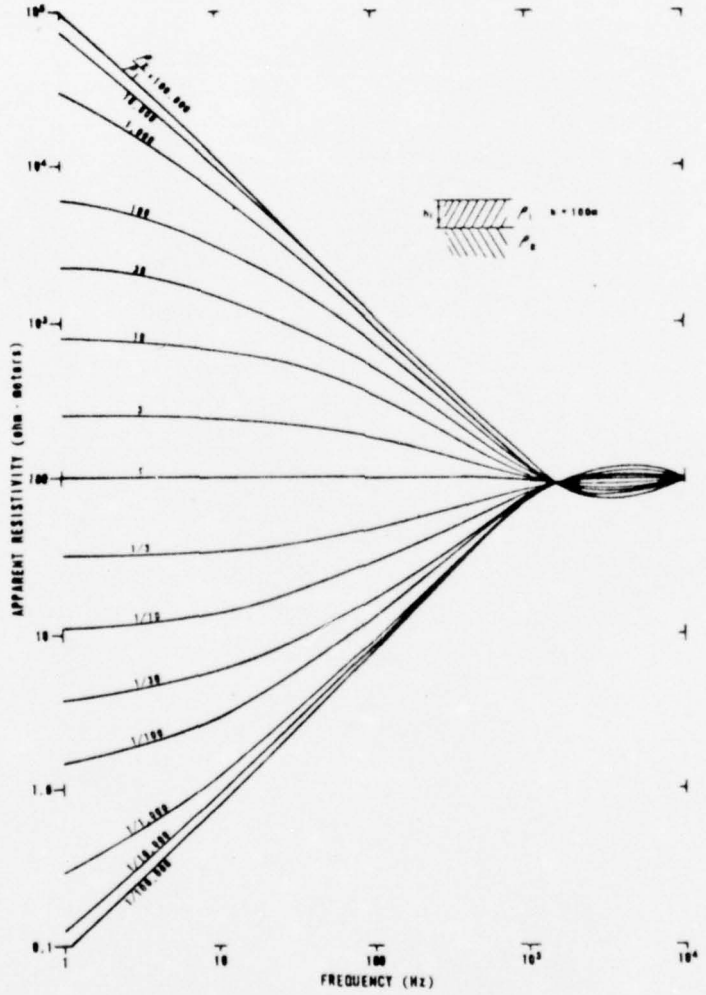

Figure 8. Two-Layer Sounding Curves

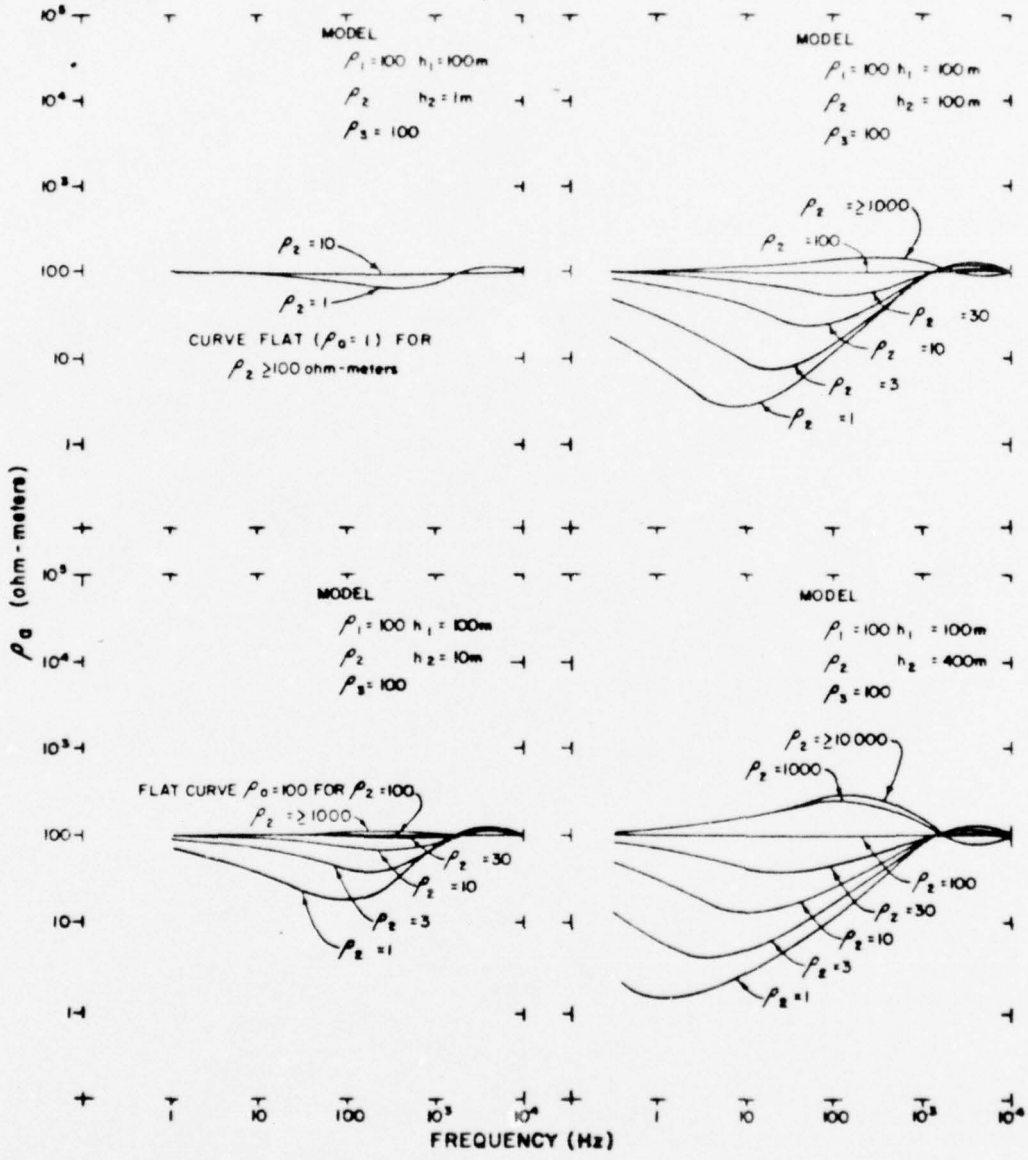

Figure 9. Three-Layer Curves Showing Effect of Intermediate Layers

of the upper layer. On the other hand, if the thickness of the middle layer is as little as 1/30 that of the upper layer and it is a very good conductor, clear indications should be present. Layers of high resistivity, however, are hard to detect; and it is not until the thickness of the middle layer is two or three times that of the upper layer that it becomes detectable as a separate layer. Limitations in measurements thus lead to the fact that true and accurate depth sounding is very difficult. This particular method is, however, as are other inductive techniques, well-suited to searching for low-resistivity zones.

Fundamentally, electrical current tends to flow into a medium of high conductivity; therefore, current induced by the geomagnetic field may flow in a direction controlled by the local geology rather than in a perpendicular direction, as expected when no lateral resistivity contrast is present. Moreover, lateral resistivity variations result in a vertical magnetic field component, as used in AFMAG. Therefore, field complications arise because the measured impedance at the surface of the earth is no longer independent of either (1) the orientation of the orthogonal fields measured, or (2) the polarization of the incoming source field. As a result, the measured apparent resistivity in the vicinity of lateral resistivity contrasts can have very poor repeatability in time, especially over periods of hours when source-field thunderstorms may have changed position. Similarly, two measurements using field recording orientations rotated 90 degrees can show drastic differences in the observed apparent resistivity curves.

Because the magnetotelluric impedance is a tensor quantity for a two-dimensional earth resistivity structure, simultaneous phase-sensitive measurement of both orthogonal components of the electric and magnetic fields is required for a complete description. Broad-band, four-channel recording and subsequent Fourier analysis is commonly utilized in low-frequency magnetotelluric studies, as

discussed by Cantwell (1960), Bostick and Smith (1962), and Swift (1967), among others.

The light, field-portable equipment used during this survey was designed to measure only scalar resistivities; thus, strictly valid data are obtained only when the measuring orientation is aligned with the resistivity structure. By making closely spaced readings, however, the position of lateral contacts can be exceedingly well defined and those regions where anisotropies exist can be clearly delineated.

With the AMT apparatus aligned with the resistivity structure, it is possible to directly measure the impedance for "E-parallel" or "E-perpendicular" polarizations, terms which refer to the electric-source, field-oriented parallel to or across the structure, respectively. Apparent resistivities obtained from these impedances can then be compared with theoretical two-dimensional curves corresponding to the appropriate source polarization. Theoretical, apparent resistivities for arbitrary two-dimensional resistivity structures are now available by use of a computer modeling technique developed by T. R. Madden of M.I.T. This procedure recognizes the analogy between Maxwell's equations for a two-dimensional geometry and the transmission line, and constructs an electrical network in which the circuit elements depend upon the resistivity structure and the frequency; and the voltage and current relate to the electric and magnetic field values. The technique is discussed by Madden and Swift (1969), and is elaborated upon by Swift (1971).

SECTION 3

INSTRUMENTATION

3.1 E- & H-FIELD SENSORS AND INTERFERENCE ANALYZER

The instrumentation used in this survey consists of two sensors (electric and magnetic field), a prewhitening filter box and a variable frequency analyzer.

3.1.1 E- & H-Field Sensors

The electric field sensor is simply a long cable grounded at both ends. In general, either 500 or 200 feet of dipole was used for the sensor. Although shorter lengths could have been utilized, it was felt that the antenna should be as long as possible in order to average out very local effects. In Michigan and Wisconsin, all data were taken using 200-foot dipoles due to the problem of laying out longer wires in heavy brush. A schematic diagram of the detection equipment is shown as Figure 10.

The magnetic field sensor is a ferrite-cored coil developed at the University of Toronto. It has a frequency response that is linear from 10 Hz to 10 kHz, and contains a series of separate segments, each with its own preamplifier to reduce the total capacitance and thereby provide a wide bandwidth in a single coil.

Preconditioning provides rejection of 60 Hz and prewhitens the signal before presentation to the analyzer. This preconditioning also consists of band limiting the signals, since large signals from VLF stations and broadcast stations can saturate the AMT system while it tries to detect very small signals at a frequency of interest.

3.1.2 Interference Analyzer

The analyzer used was assembled by Kennecott Copper Corporation and is on long-term loan to the University of Toronto. The unit contains a central oscillator and a

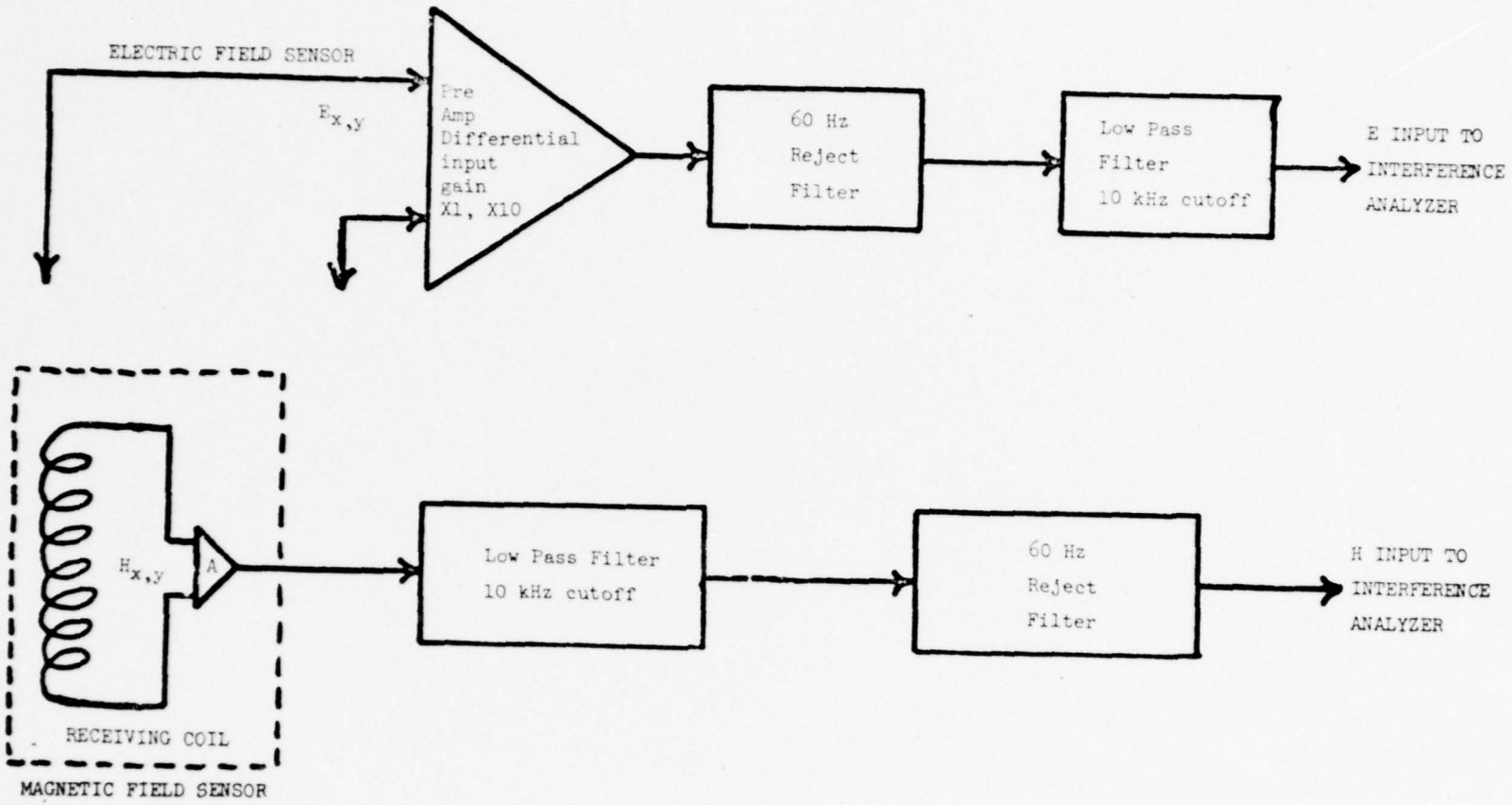

Figure 10. Schematic Diagram of Detection Equipment

heterodyning system to measure the ratio of two signals fed to it. The filtering characteristics of this system are very sharp and provide narrow-band detection at the center frequency. In addition, the skirts are very sharp, since the system is required to detect very small signals in the presence of large, nearby ones. Skirt rejections of 10^5 or more are inherent. The results are presented in the form of a logarithmic ratio which, together with the gain settings and a calibration factor, can be used to derive directly the value of log resistivity.

3.2 CALIBRATION

The AMT system is calibrated in a number of ways. The coil itself is calibrated by laying a large single loop antenna on the ground with the coil vertical in the middle. The single loop is then energized at each frequency to be used with a known magnetic moment, and the coil output measured. The rest of the system is then simply calibrated by measuring gain of the separate stages. As the system measures the ratio of E/H and the channels are essentially the same, there is no temperature effect to a first approximation. The coil is not common to both E- and H-field systems and hence its temperature sensitivity is important. However, as the coil is not particularly sensitive to temperature, results are nearly temperature independent.

Other calibration procedures used have involved energizing the coil and the E-field input simultaneously, and then calibrating directly in terms of the ratio measured. This procedure gives essentially the same results.

The final check on calibration has been to make runs in areas of known resistivity structure. For this purpose, one area in Southern Ontario and one on the Salt Flats in Utah have been used, the latter having a uniformly very low resistivity medium and, hence, providing an excellent calibration site. Data from this site are shown in Section 5 of this volume.

SECTION 4

ERROR ANALYSIS AND SYSTEM SCALING

4.1 ERROR ANALYSIS

An estimation of errors associated with measuring resistivity can be analyzed by identifying the major sources of dispersion in the result. One is the normal dispersion to instrumental errors that can be measured in the laboratory, and another is dispersion in the resistivity measurement itself, i.e., measurement repeatability.

The instrument can be separated into the receiving coil, the preamplifiers, and the interference analyzer. The contribution of each to the total error can be measured and converted to an equivalent resistivity error. The receiving coil must be calibrated with a known magnetic field at each of the measurement frequencies. The accuracy of the calibration results in the errors in the resistivity of 2 to 3 percent. The variation in the true sensitivity of the coil deduced from calibrations that were repeated several months later gives resistivity errors of 10 to 15 percent.

The gain of the preamplifiers was measured before and after the Michigan and Wisconsin field trips. The maximum gain errors were $\pm$.1 dB resulting in resistivity errors of $\pm$4 percent. The sensitivity of the gain to temperature variations has not been measured.

The Interference Analyzer also has measurement errors in the value of the ratio of voltages measured and in the center frequency "F_o" of its filter. The repeatability of the ratio is within $\pm$.3 dB, which is equivalent to a resistivity error of $\pm$7 percent of F_o. Center frequency F_o is repeatable to within $\pm$ 2 Hz ($\pm$1% f_o).

The instrumental and calibration errors give total uncertainty of approximately $\pm$29 percent in resistivity readings.

The second source of dispersion can be estimated by making repeat soundings at one station where the resistivity structure is well known. Repeatability measurements were made on the Bonneville Salt Flats in Utah where the resistivity is known to be in the range .25 to .32 ohm-meters essentially independent of frequency for these particular measurement frequencies.

The data from the repeat readings at each measurement frequency for all orientations of the electric field sensor were averaged and a standard deviation calculated. In one case, the square roots of the resistivities were averaged, which is equivalent to averaging the electric fields; in the other case, the resistivities were averaged directly. The results of these calculations are shown in Figures 11 and 12. The 1 kHz and 2 kHz data have associated with them substantially larger standard deviations than are observed at the other frequencies. The average values appear to come reasonably close to other published data, excepting the frequencies just mentioned that have anomalously high values.

These data provide a test of the repeatability of the measurements at one particular station during a six-hour measurement period. The different values of resistivity that are measured are not the result of instrumental errors (that are less than $\pm$10% in this case), although they incorporate some of these error sources, but are related more to the fact that during each measurement period the instrument is, in fact, seeing different signals from different sources where orthogonal components of the electric and magnetic fields are not necessarily related by Cagniards' formula for the apparent resistivity. That is, they may be what is referred to as uncorrelated transients from local sources and, hence, give "apparent resistivities" that are different from the true apparent resistivity.

The error analysis summary is shown in Table V. If the distribution of instrumentation errors are all biased in one direction, then the worst-case resistivity error would be 29 percent. On the other hand, if the error bias is randomly distributed, instrumentation errors would normally be less than 10 percent.

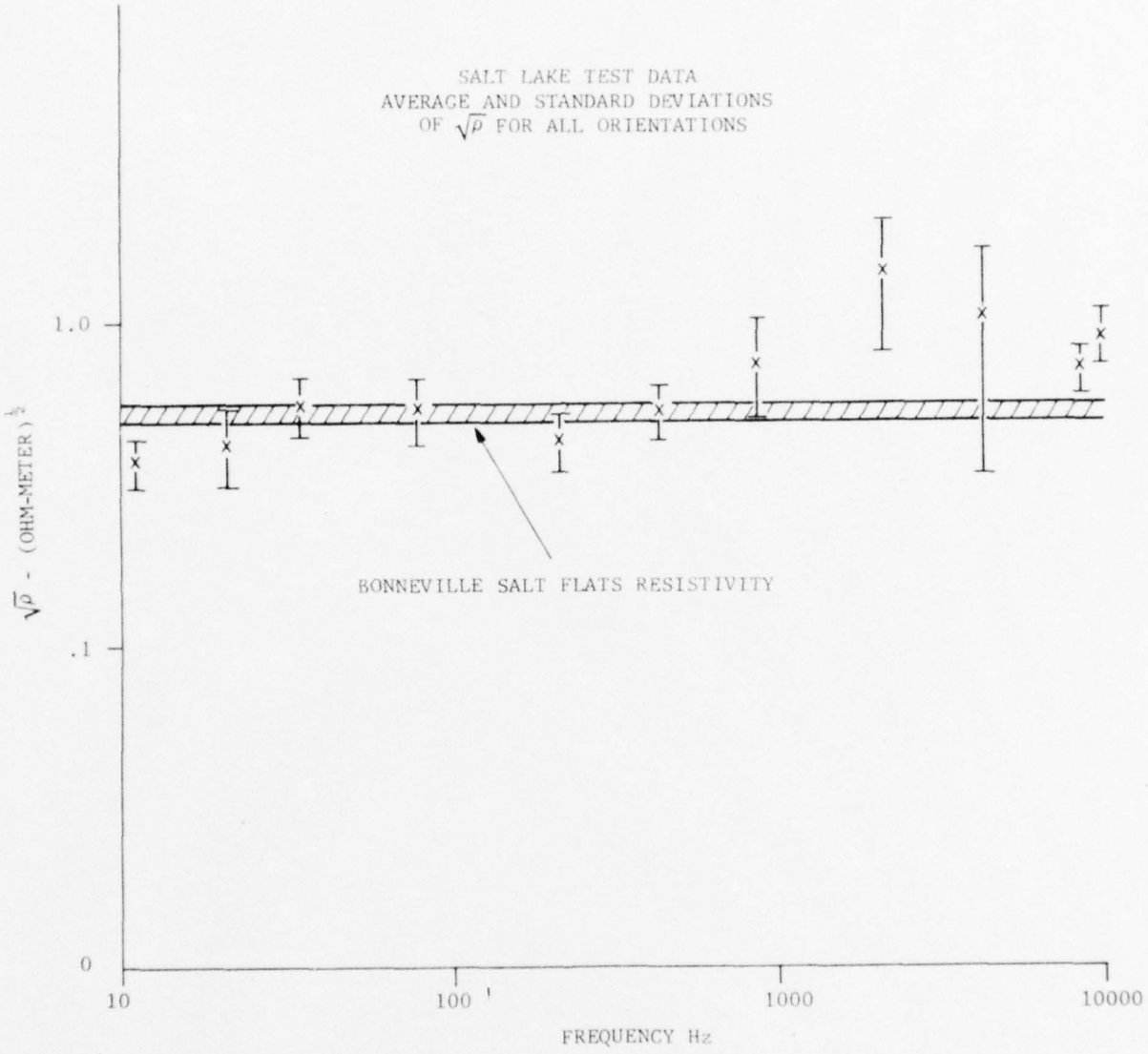

Figure 11. Salt Lake Test Data: Average Square Root of ρ

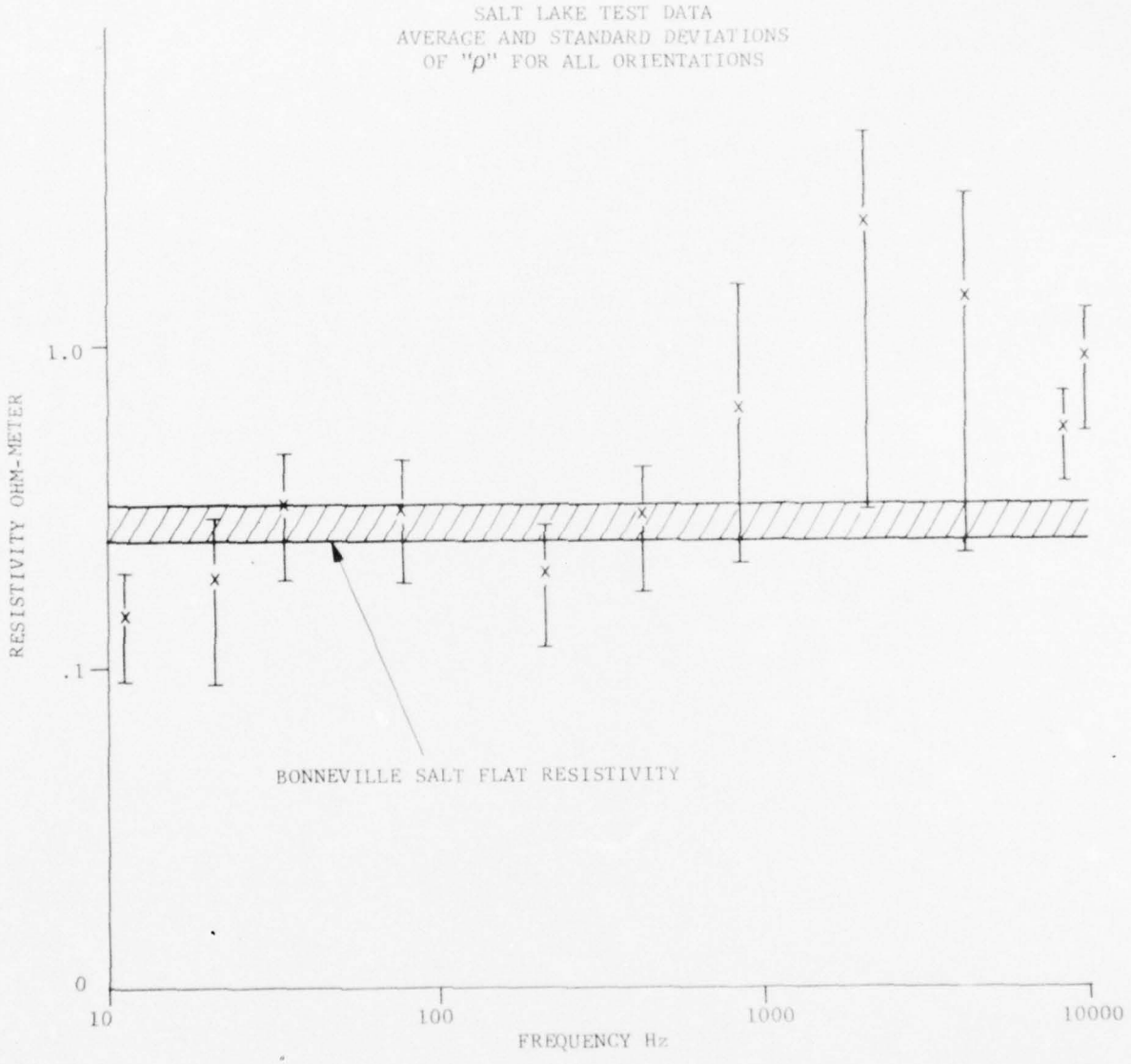

Figure 12. Salt Lake Test Data: Average ρ

TABLE V

ERROR ANALYSIS SUMMARY

INSTRUMENTATION	PERCENT ERROR IN ρ
COIL CALIBRATION:	
Repeatability	$\pm$ 3.0
True Sensitivity	$\pm$15.0
PREAMPLIFIER GAIN	$\pm$ 4.0
INTERFERENCE ANALYZER	$\pm$ 7.0
TOTAL	$\pm$29.0
MEASUREMENT REPEATABILITY	Percent Standard Deviation in ρ at 79 Hz
1 MEASUREMENT	$\pm$42.0
20 AVERAGED MEASUREMENT (WTF)	$\pm$ 9.39
106 AVERAGED MEASUREMENTS (MICHIGAN)	$\pm$ 4.08

The technique itself produces errors that are larger than the instrumentation errors for a few data samples. In the Michigan site survey, the resistivity data from 106 measurement stations were averaged, which reduces the percent standard deviation in resistivity from 42 percent to 4.08 percent. In the WTF survey, the percent standard deviation in resistivity is 9.34.

4.2 SYSTEM SIZING

As indicated in section 1.4, system sizing parameters for SEAFARER have been developed largely from data obtained from a single controlled source, the WTF. Sizing of systems to meet communication objectives for other sites is basically a process of scaling WTF performance as a function of location and electrical properties of the candidate site. Because the NUSC analysis giving present estimates of ELF propagation parameters used for SEAFARER sizing recognizes coupling between excitation factor E and attenuation rate α and shows that α is a slowly varying function of E, it has been deemed appropriate to employ the expression

$$\sigma_e = \frac{3.2}{2.6} \frac{1}{\rho_{area}}$$

developed in section 1.4. This scaling restores the self-consistency of the propagation parameters determined by NUSC, and yields somewhat conservative excitation factors.

SECTION 5

DISCUSSION OF RESULTS

The following sections discuss the AMT measurement results in Michigan and the WTF with detailed graphs and computer analysis contained in Appendixes A and B, respectively. In general, the discussions and graphs are subdivided as follows:

1. Log Resistivity vs. Log Frequency with Polynomial Fits
   - North-South Orientation
   - East-West Orientation
   - Averaged Data
2. Pseudosections
   - North-South Orientation
   - East-West Orientation
   - Averaged Data
3. Residuals
   - North-South Orientation
   - East-West Orientation
   - Averaged Data
4. Anisotropy (TE/TM Ratio)
5. Measurement Locations, Latitude and Longitude

5.1 MICHIGAN UPPER PENINSULA RESULTS

5.1.1 Depth Sounding Curves - Log ρ vs. Log f

The first set of data shown in Appendix A.1 is the actual field observations plotted station by station on a log resistivity - log frequency plot. This system shows the sense of resistivity with depth in a general way in that decreasing frequency means increasing depth. There are 106

stations of date. Results were obtained using 200-foot electrode arrays (end to end) oriented both N/S and E/W. The squares on each plot are the actual observations. In general, a number of important features can be seen immediately. The resistivity drops with frequency for most stations. At a significant number of stations, there is also a low at approximately 2 - 4 kHz. This low may or may not represent true ground resistivity since the signal strengths become very weak at these frequencies especially in winter. There is also a general smoothing of the curves when both E/W and N/S observations are combined into one.

The curves shown on these plots represent a smoothing of the observations using a third order polynomial. Such a polynomial roughly smooths data to the level of resolution that can be expected for magnetotelluric observations. Subsequent plots, therefore, use the data derived by smoothing as their basis.

Stations marked with a K represent repeat observations or poor data and are simply included here for the record and not used for analysis.

5.1.2 Pseudosections

The pseudosections shown in Appendix section A.2 portray the resistivity distribution in a two-dimensional array. Lower frequency represents greater depths. The data are contoured using interpolation between stations at two-minute intervals. This interpolation is based on the square root of the resistivity and, therefore, simulates the actual observations based on the electrical field. As one moves from line to line, some consistent pattern can be seen. First, line A is highly conductive compared to the other lines. As we will see, this is due to the fact that most of Line A is on Precambrian sediments or on slates which are relatively conductive. Further south the resistivities are generally higher in the main Precambrian gneiss and granite areas.

A number of sharp lateral contrasts exists, but the decrease with depth shows up consistently on all pseudo-sections.

5.1.3 Residual Plots

The residual plots are a form of data presentation designed to emphasize the differences along lines. The profiles are based on interpolated data and are shown in Appendix A.3. On the basis of these interpolations, it is possible to derive a mean resistivity for each line at each frequency. This value is based on the length of the line on which observations were made and was determined by averaging $\sqrt{\rho}$ at each two-minute interval. These values are tabulated as a function of frequency for each line traverse in Table VI. Table VII summarizes the area weighted averages for all lines as a function of frequency.

In the depth sounding and residual plots, the pattern of lower resistivities at low frequencies and the sense of increasing resistivity in the middle lines are seen. One can also quite clearly see the presence of an additional low resistivity layer at the higher frequencies in the range of 1 to 4 kHz.

These values have in turn been used to derive an overall weighted curve for the region. This curve is weighted in terms of the length of the lines and hence represents an overall weighted average for the region surveyed, the weighting being in terms of the area sampled. The line average and area weighted resistivity plots are shown in Figures 13, 14, and 15.

A preliminary attempt has been made to interpret this as a two-layer structure. A rough approximation is for a top layer two kilometers thick with a resistivity of about 2000 ohm-meters. This overlies a very good conductor which has a resistivity less than 50 ohm-meters. While there are

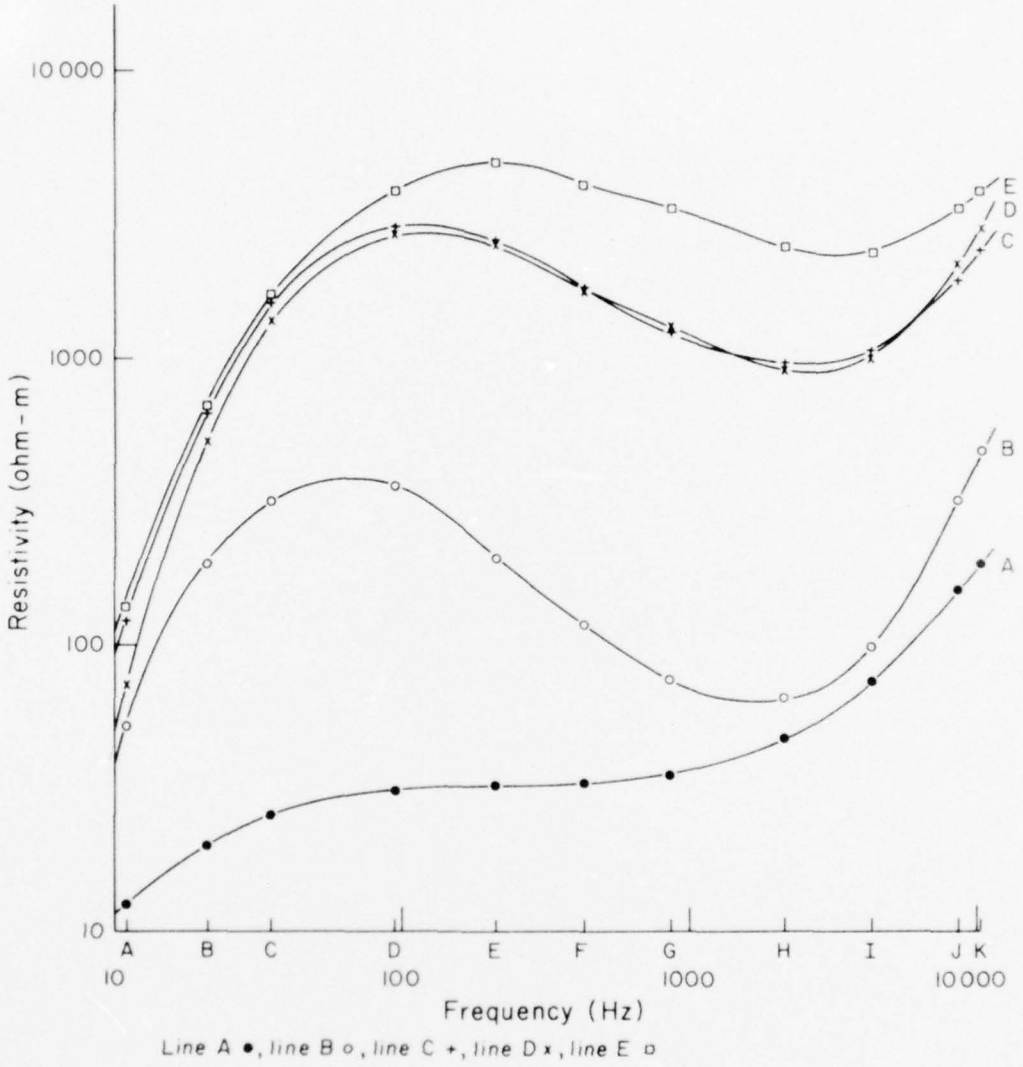

Figure 13. Line Averaged Resistivity Plots for Michigan - Lines A, B, C, D, and E

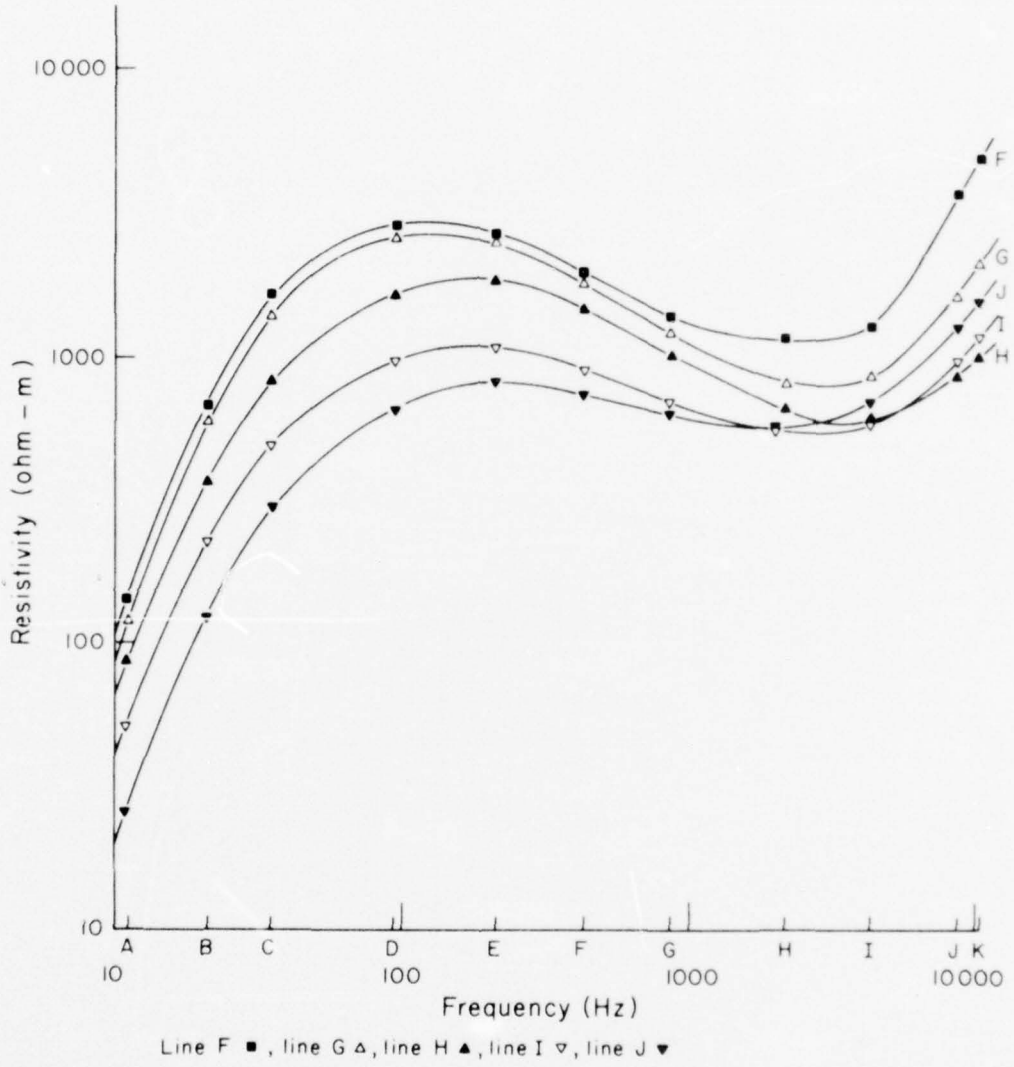

Figure 14. Line Averaged Resistivity Plots for Michigan - Lines F, G, H, I, and J

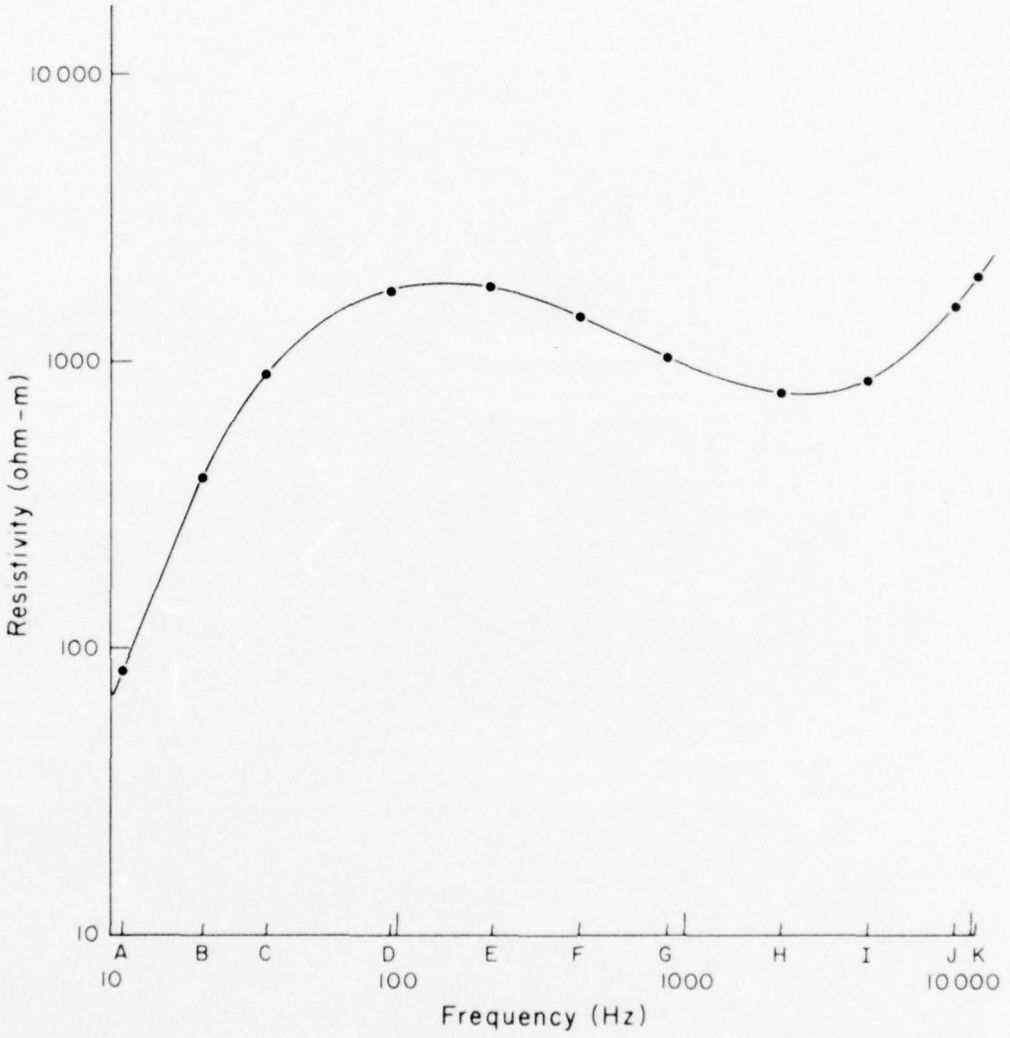

Figure 15. "Area Weighted" Average Resistivity Plot for Michigan

TABLE VI

AVERAGED APPARENT RESISTIVITIES FOR EACH TRAVERSE LINE

LINE	LENGTH OF INTERPOLATION (MILES)	FREQUENCIES - Hz										
		11	21	35	95	213	430	864	2160	4310	8650	10,100
A	44	12.3	20.0	25.7	30.9	32.4	33.1	35.5	46.8	74.1	154.9	190.5
B	56	52.5	190.5	316.2	354.8	199.5	117.5	75.9	64.6	97.7	316.2	467.7
C	68	120.2	645.7	1548.8	2884.0	2570.4	1778.3	1230.3	955.0	1047.1	1862.1	2344.2
D	46	72.4	512.9	1349.0	2691.5	2511.9	1737.8	1288.2	933.3	1000.0	2089.3	2818.4
E	95	134.9	676.1	1659.6	3801.9	4786.3	4073.8	3235.9	2454.7	2344.2	3311.3	3801.9
F	94	141.3	676.1	1548.8	2884.0	2691.5	1949.8	1380.4	1148.2	1548.8	3630.8	4897.8
G	98	120.2	616.6	1412.5	2630.3	2511.9	1819.7	1202.3	812.8	851.1	1621.8	2089.3
H	94	87.1	371.5	831.8	1659.6	1862.1	1479.1	1023.3	660.7	602.6	851.1	1000.0
I	86	51.3	223.9	489.8	955.0	1071.5	891.3	691.8	549.5	588.8	955.0	1148.2
J	71	21.5	123.0	295.1	645.7	812.8	741.3	631.0	575.4	676.1	1258.9	1548.8

TABLE VII

WEIGHTED AVERAGE APPARENT RESISTIVITIES FOR MICHIGAN UPPER PENINSULA

	FREQUENCIES - Hz										
	11	21	35	95	213	430	864	2160	4310	8650	10,100
Apparent Resistivity (OHM-Meters)	82.9	396.5	909.0	1761.8	1817.3	443.4	1030.5	786.3	855.3	1547.7	1951.2

NOTE: Formulae used for calculating weighted apparent resistivity average:

(a) For total length of traverse lines $L = \sum_{i = \text{line A}}^{\text{line J}} \ell_i = 655'$

where ℓ is the length of each line in minutes

(b) $$\rho_{AV} = \left[\frac{1}{L} \sum_{i = \text{line A}}^{\text{line J}} \ell_i \ \rho_i^{\frac{1}{2}} \right]^2$$

significant variations from place to place, this overall weighting probably represents typical, shallow Precambrian crust.

The residual profiles show the deviation from the line-by-line means at each frequency. On the basis of these plots, one can trace the deviations from the average quite well. For example, the resistivity at depth on the west end of Line A is below the average.

On line B the resistivity at the east end is high, precisely where the stations are located on granite gneiss. The sparse sampling on the west end is on slates or sediments and shows low resistivities.

Again, on Line C the granite gneiss is resistive, the slates conductive. Stations S33 and S34 are also relatively conductive, showing that the graywackes are conductive. Station N12 is highly resistive and on granite. This same pattern can be seen on Line D; in fact, over the whole area we see that the highs on the residual plots essentially correspond to the granites and the granite gneisses of the region.

Line E shows essentially the same pattern although station S48 does not follow the pattern. At the east end of the line, stations S3, S1, S4, S4B and S2 are all on the Paleozoic cover. The residual plots show the effect of this quite clearly, the more conductive sediments thickening to the east so that at station S2 the data are hardly affected by the underlying Precambrian.

The pattern for Line F continues to show the same information with high resistivities for the major areas of granite gneiss. The Paleozoic sedimentary cover at the east end is quite thin as seen both by a window of Precambrian and by the lack of low resistivities, suggesting that the sediments here are quite thin.

Line G continues to have the same pattern of highs over the granite gneisses and lows over the graywackes. The Paleozoic sediments are likely quite thin as they scarcely influence the observed resistivity values out to station S9.

On line H, the high resistivity regions shown again very closely reflect the granite gneiss areas. The sedimentary cover at the east appears to be substantial at stations S54 and S-55 but not closer to the Precambrian contact.

The same situation is repeated on both Line I and Line J.

5.1.4 Anisotropy TE/TM

The final sets of plots shown in Appendix section A.4 are the ratios of the N/S to E/W components (differences in log domain) which can be used to study lateral variations. Where the values differ substantially from each other, these plots emphasize the differences. In general, the region is not highly anisotropic, nor does it seem to have an overall regional effect. A number of the sharp changes do seem to correspond roughly to sharp lateral changes in resistivity. This is not always the case; but where it is, it is undoubtedly due to the coupling of the source energy to the lateral contact giving a large apparent anistropy.

5.1.5 Summary of 35 Hz and 95 Hz Data

In order to present a simple summary of the regional variations in resistivity, the average value of resistivity at 35 Hz and 95 Hz has been plotted on two separate countour maps (see Maps 1 and 2, respectively). These data represent the smoothed average values for the 106 stations and are shown as log ρ values which have been contoured on an interval of 0.33 log ρ. Figure 4 in section 1 illustrates four ranges in conductivity over the survey region at 95 Hz. On the 95 Hz map, a set of observations taken by NUSC at 75 Hz,

are also shown and included in the contouring. These observations are in general agreement with ours and completely support the foregoing conclusions. In general, nearby stations give similar results, thus corroborating our data by totally independent observations.

The overall regional pattern can be summarized as follows:

a. The granites and granite gneisses are high in resistivity.

b. The graywackes and slates are fairly low in resistivity.

c. The sedimentary cover in the south-east part of the area is relatively low in resistivity, but it appears to be very thin and, hence, influences the observations at only a few places.

5.2 WISCONSIN TEST FACILITY (WTF)

During the period of October 1975 - January 1976, AMT conductivity measurements were taken along the WTF E/W and N/S antenna lines. Short line measurements (200' E-field sensors) were taken at 20 locations along the E/W antenna right-of-way (ROW). Half and full antenna measurements (7/14 mile, E-field sensors) were also taken, utilizing the existing WTF overhead antenna lines. The following subsections discuss the results of these measurements with particular emphasis on the E/W line data, since this will be used as a basis for scaling system current moment (IL) requirements from an area (WTF) of known propagation performance to other locations.

5.2.1 Short Electrode AMT Results Along E/W Antenna ROW

AMT conductivity measurements were taken along the WTF E/W antenna line at 20 locations (200' E-field sensors). Profiles of resistivity versus frequency were plotted, and the data were smoothed using a third-order polynomial fit. Pseudosections were generated with the smoothed data and contoured by interpolation due to uneven station spacing.

Data between measurement stations were derived from linear interpolation of the square-root of resistivity. A resistivity profile versus distance was generated with data points every 600 feet along a 13.1 mile E/W antenna line. The 115 data points were equally weighted and averaged to determine the effective conductivity as seen by each half and full E/W antenna line.

The following paragraphs discuss the measured results from the depth sounding data and the respective pseudosections, residual plots, and anisotropy data.

5.2.1.1 Log Resistivity vs Log Frequency Results

Appendix B.1 contains the Log ρ vs Log f plots for each sounding made at the WTF. These consist of observations made at 20 stations along the east-west transmitter line. The station numbers correspond to pole numbers (which are located at roughly 100 meter intervals). The first letter on these plots refer to a half of the transmitter line: east (E) or west (W). The next letter(s) refers to the electric field: N/S (N), E/W (W); or to the average (AVG). The data points shown refer to the actual field calculation of the apparent resistivity. Many soundings at a specific frequency were repeated. In these cases, the value which gave the smoothest curve in the resistivity-frequency plot was chosen. The raw data can be verified by referring to the original field data on file both at the University of Toronto and GTE Sylvania.

It is worth noting that, in general, the values of resistivity tend to be low at 2160 Hz and at the adjacent frequencies of 864 and 4310. These low values may be related to very weak source fields encountered at the time of observation, and are believed to be a result of problems in measuring these very low signals.

The smooth curve through each set of data represents a least squares third-order polynomial fit. The choice of a

third-order polynomial is logical, albeit somewhat arbitrary, because it permits the detection of four layers of resistivity, which is about the limit of detectability for the three decades of frequency used. The E/W and N/S data are somewhat "noisier" than the averaged data. (The average was determined by taking the square root of the resistivity and summing and squaring.) This calculation leads to the smoothed curves shown in the appendix.

At this time, criteria for rejecting individual observations have not been developed, and the effect that individual points have on determining the polynomials remain to be studied in the future. In general, however, it is noted that the smoothed polynomial fits the observed data points quite well, especially at the frequencies of interest to this project. (In preparing the appended plots one extreme data point at 79 Hz at station EW 112 was eliminated.)

The data suggests that the structure consists of three to four layers. Low resistivity at the lowest frequencies is typically about 1000 ohm-meters. This is overlain by a high resistivity layer with peak values in the range of 7000 to 10,000 ohm-meters. Nearer the surface, the resistivity appears to become lower, hinting that locally there is a high resistivity surface layer. It is pertinent to make a few further observations:

a. The data were collected along the WTF east-west line, and there is some concern that this might have had some effect on the observed results. In general the N/S electric field observations are higher than the E/W observations, although there are exceptions. This difference may be related either to a preferred geologic grain or to the cable. One station (57W) was measured 100 feet off the line, and the same pattern was observed,

which suggests that the effect is geological. A general E/W geologic fracturing or jointing, with some water filling the sheers, would account for these observations.

b. At the highest frequencies, an unusual anisotropy was detected. It seems possible that this was a result of coupling in some way to the overhead antenna cable. It is, of course, also possible that the local overburden has filled small bedrock valleys that have a preferred orientation.

5.2.1.2 Pseudosections

Pseudosections are an attempt to present the variation in resistivity both as a function of frequency and as a function of position along a line. Since the soundings were not made at equal intervals, an interpolation procedure was developed. For the WTF, 200 meters (the distance between 56W and 58W) was chosen as the interpolation spacing. Polynomial fits at each sounding point were used as the basis, then interpolated between stations using $(\text{resistivity})^{1/2}$. This calculation method was chosen because it most closely represents an attempt to consider how the electric field would be averaged. These data are then contoured to give a graphic view of the way in which the resistivity varies laterally with frequency. Appendix B.2 shows the pseudosections for the E/W antenna line.

Examining the N/S data along the E/W antenna line, one sees immediately that at 79 Hz the resistivity is generally in the range of 2,000 to 20,000 ohm-meters. The average values are tabulated in Table VIII. This average is based on taking the square root of each resistivity value in the interpolated data set and including only one data point beyond the ends of the observation interval. In effect, this means that resistivity value is properly weighted to consider the variations from station to station.

TABLE VIII

MEAN RESISTIVITY - WTF (E/W ANTENNA LINE)

POLARIZATION	FREQUENCIES - Hz										
	11	21	35	79	213	430	864	2,160	4,310	8,650	10,110
N/S	1,480	4,790	7,760	8,910	5,500	3,240	1,950	1,320	1,510	3,470	4,790
E/W	676	1,860	3,090	4,170	3,090	2,000	1,200	617	447	437	467
AVG. ρ	1,020	3,240	5,370	6,610	4,170	2,510	1,510	977	977	1,660	2,090

As noted earlier, the resistivity drops to low values at low frequencies with a low resistivity sequence at around 2 kHz. We believe this to be the result of weak fields that make the observations difficult. The pattern for the E/W observations is similar, except that the values tend to be lower due to the anisotropy already mentioned.

5.2.1.3 Residual Plots

The residual plots shown in Appendix B.3 are designed to emphasize the deviation from the mean in the apparent resistivity. The mean values of resistivity determined along a line have been used as baseline values and are tabulated in Table VIII. The data are interpolated on 200 meter intervals (note ticks at actual observation points), and are plotted so that the vertical scale is as shown in units of 10 log ρ ($\rho \sim$ ohm-m). An examination of the profiles permits one to quickly see the regions of high and low resistivity and how these vary with frequency. In a general way, the north-south and east-west components show quite similar patterns - for example, low resistivities at low frequencies near station 113W and general lows near stations 12W and 26W. Different positions for the anomalies at the two polarizations are, however, quite clear and distinct in several cases. This pattern is expected across lateral contrasts in resistivities and confirms the existence of such contrasts. A good example of this is at station 30E where the east-west component is high and the north-south component is low.

Taking the square root average of these data results in the last figure of this set in which the deviations from the mean are much subdued (note reduced scale), so that the sharp effects at lateral contacts have been smoothed. These graphic displays are a useful way of displaying the deviations from the simple patterns otherwise observed.

5.2.1.4 Anisotropy TE/TM

Separate plots designed to emphasize the anisotropy between the two observing directions have been determined at

each frequency as a function of distance along the traverse line and are shown in Appendix B.4. The data have been interpolated to a 200 meter spacing and the ratio of the two components shown directly. Again, the vertical scale is logarithmic so that a simple perspective is obtained. As already noted, it is quite striking that the north-south resistivity is consistently higher than the east-west resistivity. This implies a strong anisotropy to the whole region, an effect which can be attributed largely to the presence of east-west oriented fracturing, perhaps controlled by a few major shear zones in that general direction. It is possible, of course, that some of this anisotropy is due to the presence of the transmitter cable, which seems to be unlikely, except at the two highest frequencies where the discrepancy is considerable. Only at station 26W is there a general local reversal of the anisotropy pattern of high values in a north-south direction and low values in an east-west direction. Again, this discrepancy appears to be a result of sharp lateral changes as already seen in the residual plots (see Appendix B.3).

5.2.2 Half and Full Antenna AMT Measurements

During the period of October 1975 - January 1976, AMT measurements were taken at the WTF utilizing the E/W and N/S antenna lines as E-field sensors. Over 250 measurements were taken during this period utilizing morning and afternoon spherics. The E-field sensor configuration is tabulated in Table IX, and the WTF overhead antenna array is schematically illustrated by Figure 5.

The measurement data were weighted equally for frequencies 70, 85, and 95 Hz. Data averaging was accomplished in the usual manner as follows:

$$\bar{\rho} = \left[\frac{1}{n} \sum_{1}^{n} \sqrt{\rho_i} \right]^2$$

n = number of data points.

TABLE IX

AMT E-FIELD SENSOR CONFIGURATION

E-FIELD SENSOR	CONFIGURATION	MEASUREMENT LOCATION
East Leg	P112E to WTF	P112E
West Leg	P112W to WTF	P112W
E/W Antenna	P112E to West Terminal Ground	P112E
W/E Antenna	P112W to East Terminal Ground	P112W
North Leg	P100N to WTF	P100N
South Leg	P74S to WTF	P74S
N/S Antenna	P100N to South Terminal Ground	P100N
S/N Antenna	P74S to North Terminal Ground	P74S

Data were not smoothed, since a large percentage of the measurements were taken over a limeted frequency range between 35 and 213 Hz. The measurement results are summarized in Table X with the mean and standard deviations listed in Table XI.

The existing N/S overhead antenna has in its near proximity several cables which could be considered parasitic elements. Figure 14 illustrates the situation where a faulted buried line is within 25 meters of the overhead antenna over a 7-mile length of the north line. In addition, a recent rerouting of telephone cable from Hwy GG to the north leg ROW places a parasitic element within 10 meters of the overhead line over a length of 2-1/2 miles. Such proximity of these cables is bound to influence the E/H wave impedance measurement as well as any WTF propagation or pattern steering experiments. Recent NUSC pattern steering measurements bear out the fact that the WTF antenna has changed since 1973. (Private Communication, P. Bannister, NUSC) Phasing of the various antenna elements are different by 20° to 30° from previously measured azimuthal patterns.

The south overhead antenna does not seem to be affected by the faulted buried cable near the overhead line. This is probably due to the fact that the buried cable is only in the ROW over 5 percent of its length and has an average spacing of 0.2δ.

The measurement results for the conductivity under the south antenna leg is consistent with previous studies, while σ_N and $\sigma_{N/S}$ values are questionable, suggesting parasitic contamination. Measurement errors associated with contamination could be caused by one of the following factors:

a. It has been shown from modeling and measurement verification that a grounded long wire parasitic line (Z_p = 100 ohms) located within 0.01δ (40 meters)

TABLE X

SUMMARY OF CONDUCTIVITY RESULTS FOR THE WTF ANTENNA ARRAY

ANTENNA SEGMENT	NUMBER OF OBSERVATIONS	E-FIELD SENSOR	$\bar{\rho}$ OHM-METERS	$\bar{\sigma}$ MHOS/METER x 10^{-4}	REMARKS
West Leg	49	West Leg	3485	2.87	Measured.
West Leg	11	200' along West Leg	3515	2.84	Predicted from interpolated results of 11 observations.
East Leg	37	East Leg	4240	2.36	Measured.
East Leg	9	200' along East Leg	4821	2.07	Predicted from interpolated results of 9 observations.
Full E/W Ant.	63	E/W Antenna Line	3860	2.59	Measured.
Full E/W Ant.	86	Half Antenna Line	3850	2.6	Predicted from half leg measurements.
Full E/W Ant.	20	200' along E/W Ant.	4167	2.4	Predicted from interpolated results of 20 observations.
North Leg	18	North Leg	1532	6.53*	Measured.
South Leg	36	South Leg	7589	1.32	Measured.
Full N/S Ant.	60	N/S Antenna Line	2381	4.2*	Measured.
Full N/S Ant.	54	Half Antenna Line	3965	2.52	Half leg measurements.

* Possible parasitic contamination.

TABLE XI

STATISTICAL ANALYSIS OF THE WTF MEASUREMENT DATA

ANTENNA CONFIGURATION	$\bar{x}$ MEAN OHM-METERS	$\bar{\sigma}$ STANDARD DEVIATION OHM-METERS
North Leg	1556	575
South Leg	7802	2625
East Leg	4392	1945
West Leg	3721	1893
N/S Predicted	4679	2687
N/S Measured	2497	1086
E/W Predicted	4056	2714
E/W Measured	4065	1305

NOTE: Predicted standard deviations assume normally distributed independent half leg distributions.

of the E/H field sensors, can produce a wave impedance measurement error in σ of 2.5:1. (Effects of a Grounded Parasitic Line on Earth Conductivity Measurements, DECO Report 30, p. 14, dated July 1966.)

b. E-field contamination can be expected from a nearby telephone cable parasitic element when the common mode impedance is less than 200 ohms.

c. For the antenna configuration shown in Figure 14, it would seem that the major contamination is in the E-field. A long wire grounded parasitic near the AMT long wire E-field sensor would have the effect of moving a ground plane closer to the sensing antenna (shielding), thereby reducing the fields measured by the receiver. The H-field sensor, on the other hand, is not as sensitive to single-ended long wire parasitics, since it sees only a small volume of the area over which the parasitic H-field exists. For the case of a single long wire parasitic line, grounded remotely from the H-field sensor locations, the H-field contamination would probably be less than 10 percent.

The GTE Schlumberger (1972) expansions for the E/W and N/S antenna lines show a relatively consistent anisotropic $\bar{\rho}$ profile in both directions suggesting, once again, an erroneous, measured 5:1 anisotropy contrast between the N/S legs.

5.2.3 Layered Earth Interpretation

The results of this survey are in general agreement with previous GTE Schlumberger (1972) studies at this site which modelled the following layered earth structure:

E/W LINE		N/S LINE	
670 Ω-m	40 m	670 Ω-m	40 m
17000	240 m	26700	240 m
350	340 m	270	340 m
6800		9035	
(4170)TM		(8910)TE	

The E/W antenna depth sounding curves and lateral profiling can be interpreted as describing a layered earth structure consisting of a low resistivity layer at the surface followed by a high resistivity middle layer and another low resistivity layer at depth. The upper layer of the AMT data probably corresponds to the upper three layers of the Schlumberger data where the high resistivity layer is not detectable. The recent AMT results at 79 Hz (the maximum) should reflect the properties of the lower layer determined in the Schlumberger work.

	N/S	E/W
AMT* (maximum value)	8,910	4,170
Lower Layers Schlumberger	9,035	6,810

*Two polarizations along E/W antenna line.

The agreement of the values and of the sense of the anisotropy is surprisingly good. This data and the full antenna measurements suggest a shear pattern with an east-west strike in the bedrock.

The depth sounding results shown in Figure 15 represent the average resistivities over the full E/W antenna at the sampled intervals for two polarizations.

These data suggest quite clearly the presence of a four-layer earth. Because the top layer is only a few tens of meters thick and quite strongly anisotropic (if these data are

taken at face value), a simple three-layer interpretation (a high resistivity layer sandwiched between two low resistivity layers) can be postulated. Koziar (Ph.D. thesis, in preparation) shows that this situation can be inverted, using the peak resistivity value and the frequency at this peak. The following conclusions can be drawn:

a. The upper layer can be characterized by the value of h_2/ρ_2 or the ratio of its thickness to its resistivity

$$\frac{h_2}{\rho_2} = \frac{.252}{(\rho \text{ max} \quad f \text{ max})^{1/2}} \qquad \begin{array}{l}\rho \text{ - k } \Omega\text{-m} \\ f \text{ - kHz}\end{array}$$

b. The resistivity of the middle layer cannot be determined precisely but must be $>\rho$ max.

c. The thickness of the middle layer is given by

$$h_3 = 503 \left(\frac{\rho \text{ max}}{f \text{ max}}\right)^{1/2}$$

d. The resistivity of the bottom layer (ρ_4) $\ll \rho_3$ and less than the lowest observed value.

This leads to the following one-dimensional interpretation for the layered-earth structure at the WTF:

Layer		
1	Surface	Strongly anisotropic - a few tens of meters thick
2	_____	$\rho_2 \approx$ 1700 ohm-meter; $h_2 \approx$ 600 meters
3	_____	$\rho_3 >$ 6600 Ω-m; $h_3 \approx$ 4.6 km
4	_____	$\rho_4 \ll$ 1000 Ω-m

The full antenna AMT measurements along the N/S antenna add a second dimension to the above layered earth interpretation. The results show that areas to the north and west exhibit low conductivities. The GTE Sylvania Schlumberger (1972) data, combined with the E/W residual plots and half-leg measure-

ments, suggest a general E/W geologic fracturing in the bedrock. A simplistic model would consist of a shear line intersecting a north leg 1500 meters from the center and extending to the west leg 5600 meters from the center. Everything north of the shear line would be highly conductive. Anisotropy near the center of the array could be as high as 2.

5.2.4 Summary of WTF Conductivity Survey Results

The results from the October AMT lateral profiling and the January half and full antenna measurements show once again the WTF area to be geoelectrically complex and highly anisotropic.

The survey emphasis was on conductivity measurements along the WTF E/W antenna line. The program included lateral profiling from 20 measuring stations, half and full antenna line measurements. The analysis showed the effective conductivity for the E/W antenna line at 80 Hz to be 2.6×10^{-4} mhos/meter. The results of this survey and various other WTF studies are summarized in Table XI.

Some observations can be made from the results of this survey and past WTF studies. These are as follows:

- The GTE Sylvania and NUSC half-antenna and predicted full antenna conductivities are in good agreement, within ± 8 percent. Statistical analysis has shown that the GTE Sylvania measured E/W antenna conductivity data has the lowest standard deviation of all other independent half or full antenna measurements.
- Effective conductivities predicted from interpolative and numerical averaging of many short electrode AMT measurements consistently produce values lower than long line measurements. One possible explanation is that 200' AMT electric dipoles do very little volume averaging, and consequently the measurements along the E/W antenna might not impact the

high conductive regions to the north and west. Eleven kilometer electrodes would certainly see this geologic fracturing much sooner.

- GTE Sylvania-measured σ_S is in good agreement with previous studies, while σ_N and $\sigma_{N/S}$ values seem to be in error, suggesting parasitic contamination. The GTE Sylvania Schlumberger (1972) expansions for the E/W and N/S antenna lines show a relatively consistent anisotropic $\bar{\rho}$ profile in both directions suggesting, once again, an erroneous, measured 5:1 anisotropy contrast between the N/S legs.

APPENDIX A

MICHIGAN DATA

CONTENTS

SECTION		PAGE
A.1	Log Resistivity vs. Log Frequency with Polynomial Fits	
	North-South Orientation	A-3
	East-West Orientation	A-19
	Averaged Data	A-35
A.2	Psendosections	
	North-South Orientation	A-52
	East-West Orientation	A-57
	Averaged Data	A-62
A.3	Residuals	
	North-South Orientation	A-68
	East-West Orientation	A-78
	Averaged Data	A-88
A.4	Anisotropy (TE/TM Radio)	A-98
A.5	Michigan Station Location	A-110

SECTION A.1

MICHIGAN

LOG RESISTIVITY VS. LOG FREQUENCY WITH POLYNOMIAL FITS

- NORTH-SOUTH ORIENTATION
- EAST-WEST ORIENTATION
- AVERAGED DATA

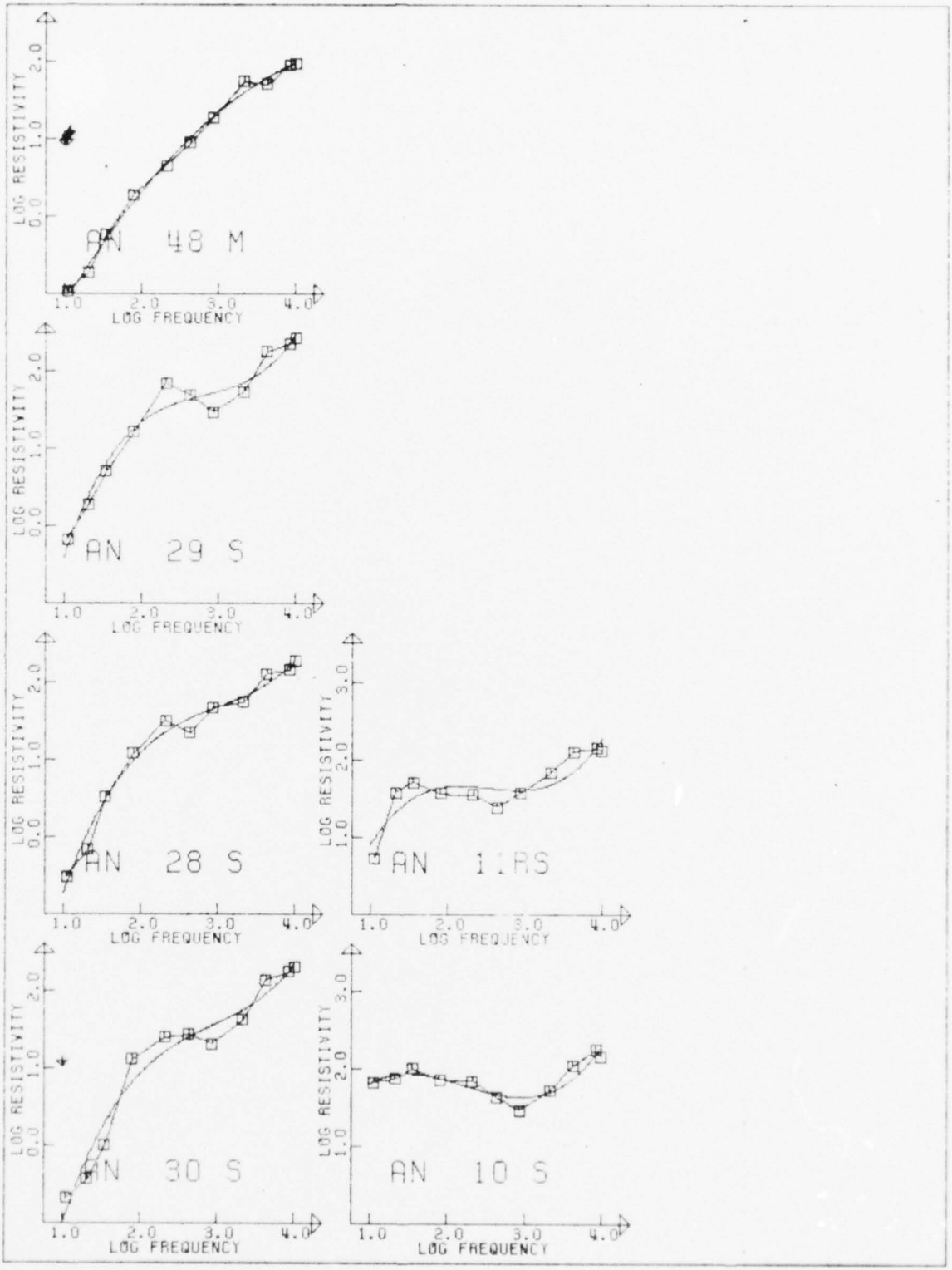
LOG RESISTIVITY
LOG FREQUENCY
AN 48 M
AN 29 S
AN 28 S
AN 11RS
AN 30 S
AN 10 S

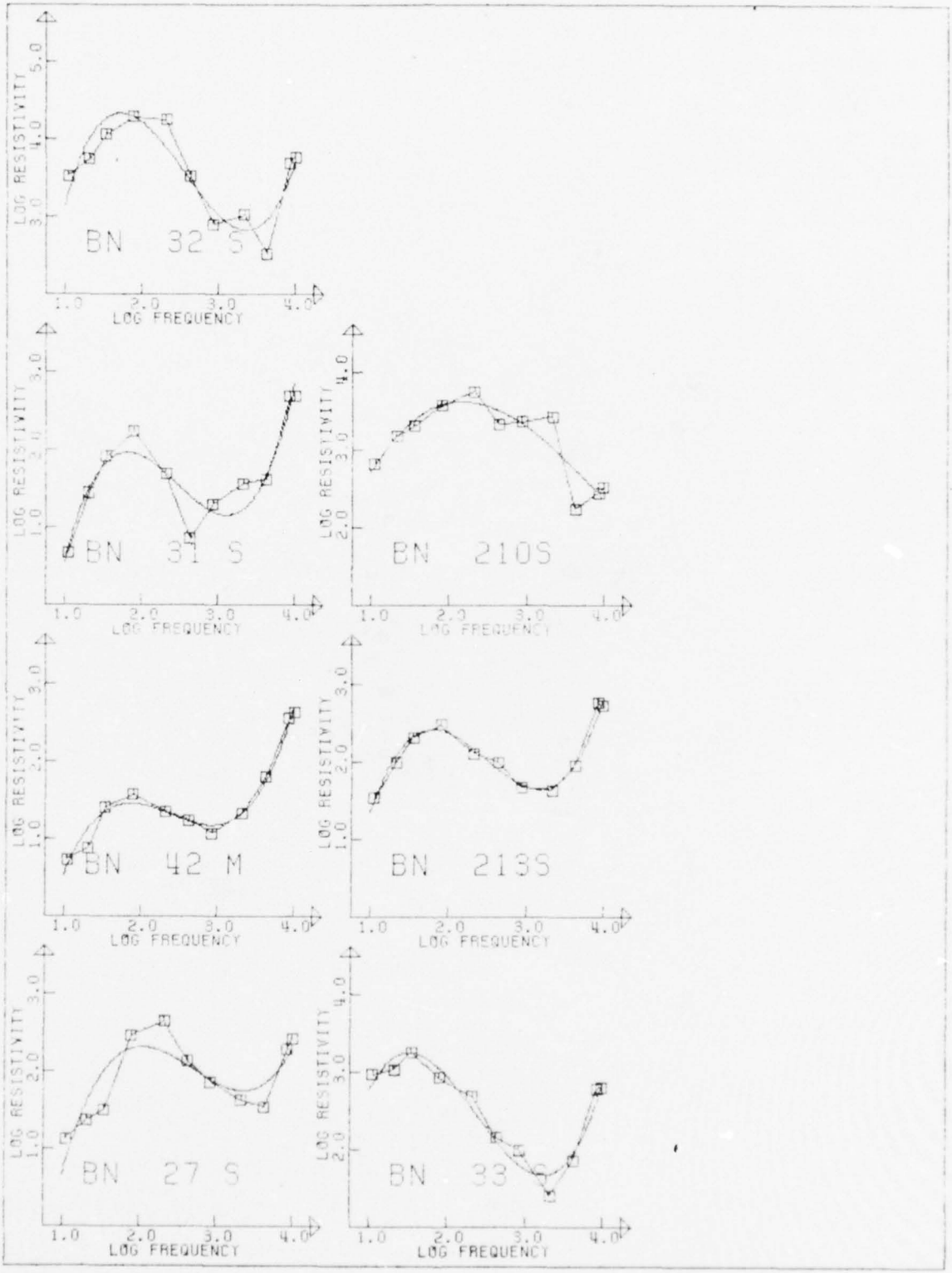
LOG RESISTIVITY
LOG FREQUENCY
BN 32 S
BN 31 S
BN 210S
BN 42 M
BN 213S
BN 27 S
BN 33 S
1.0
2.0
3.0
4.0
5.0

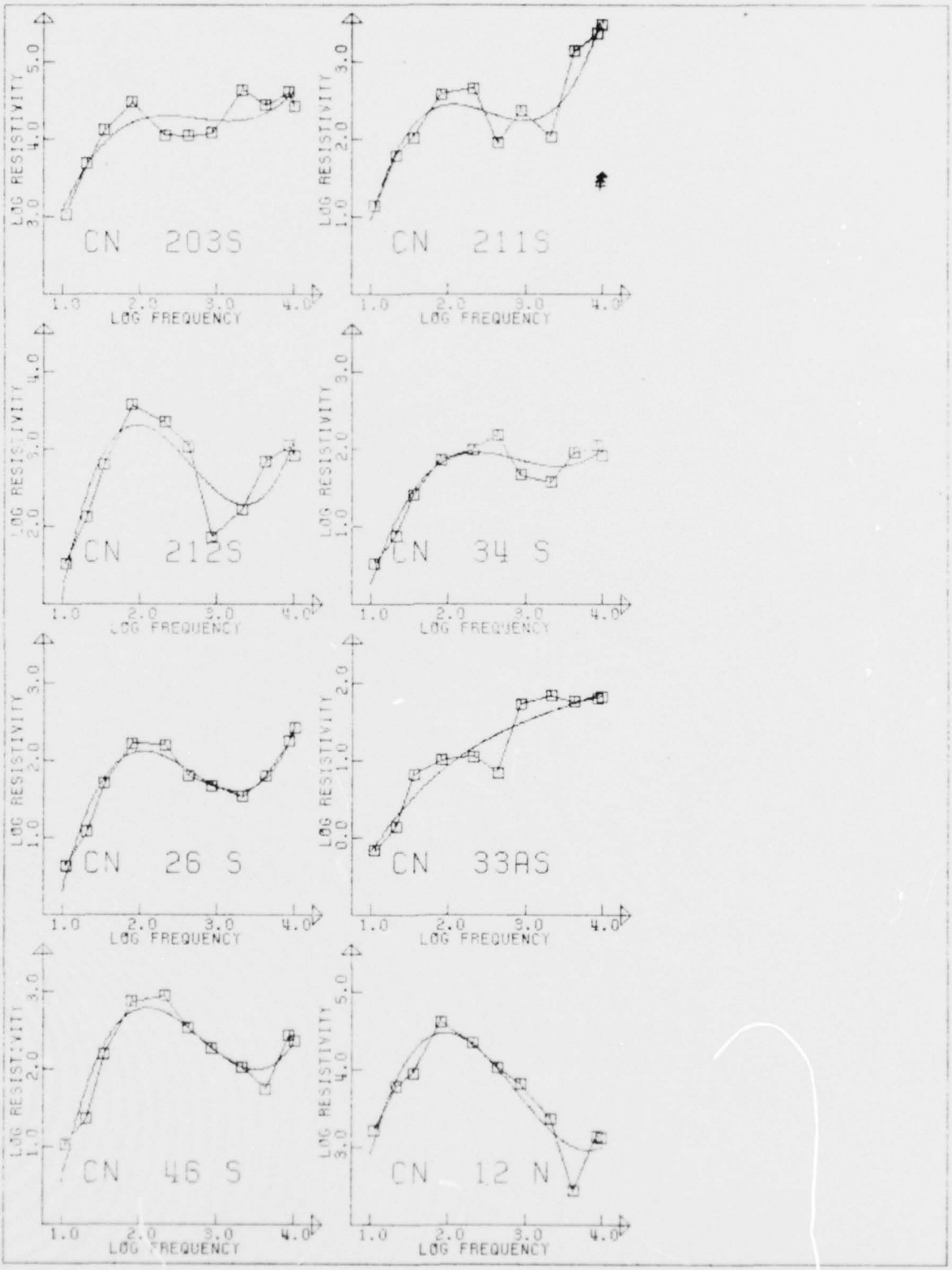
CN 203S
CN 211S
CN 212S
CN 34 S
CN 26 S
CN 33AS
CN 46 S
CN 12 N
LOG RESISTIVITY
LOG FREQUENCY
1.0
2.0
3.0
4.0

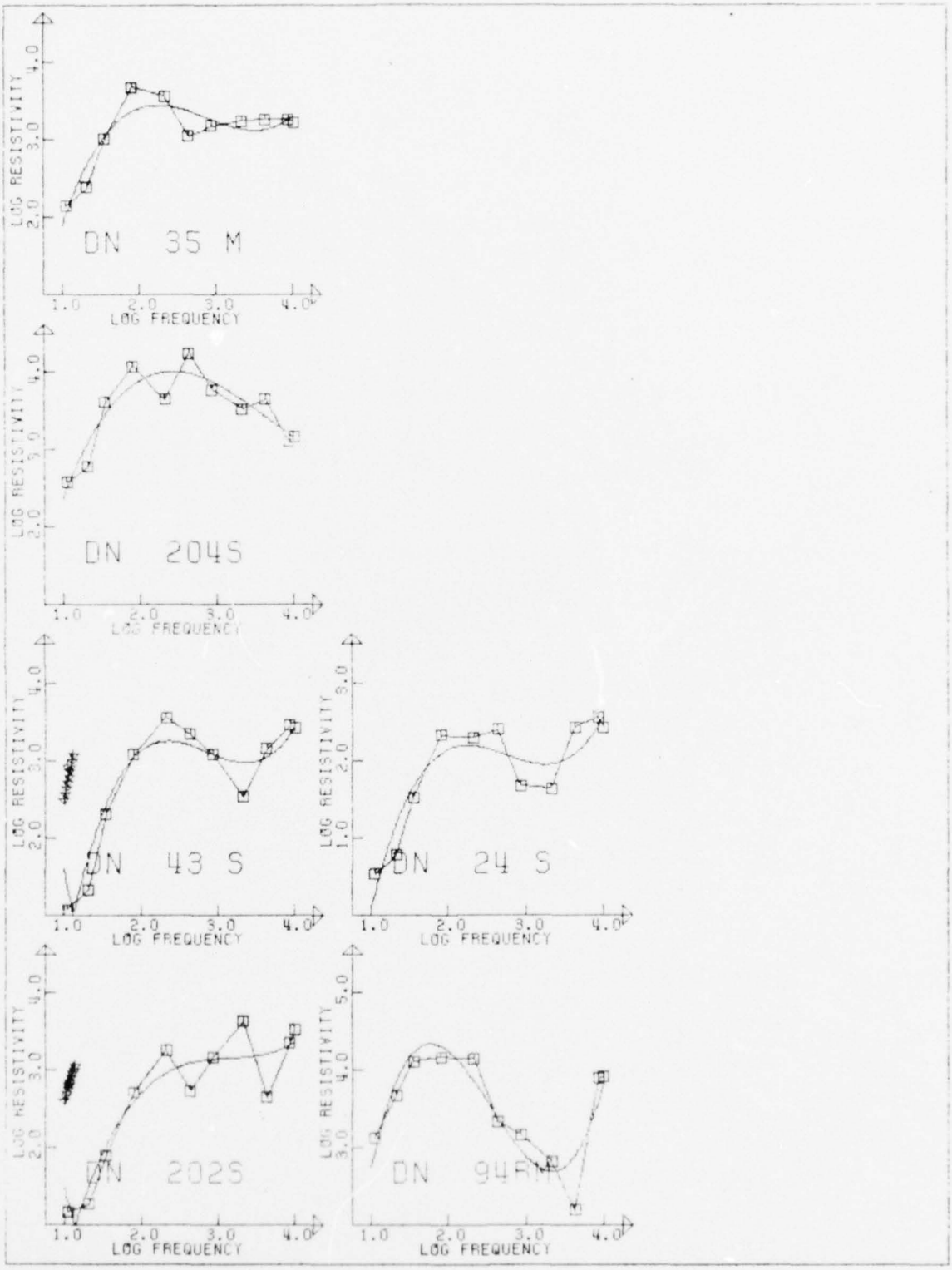
LOG RESISTIVITY
LOG FREQUENCY
DN 35 M
DN 204S
DN 43 S
DN 24 S
DN 202S
DN 94RM

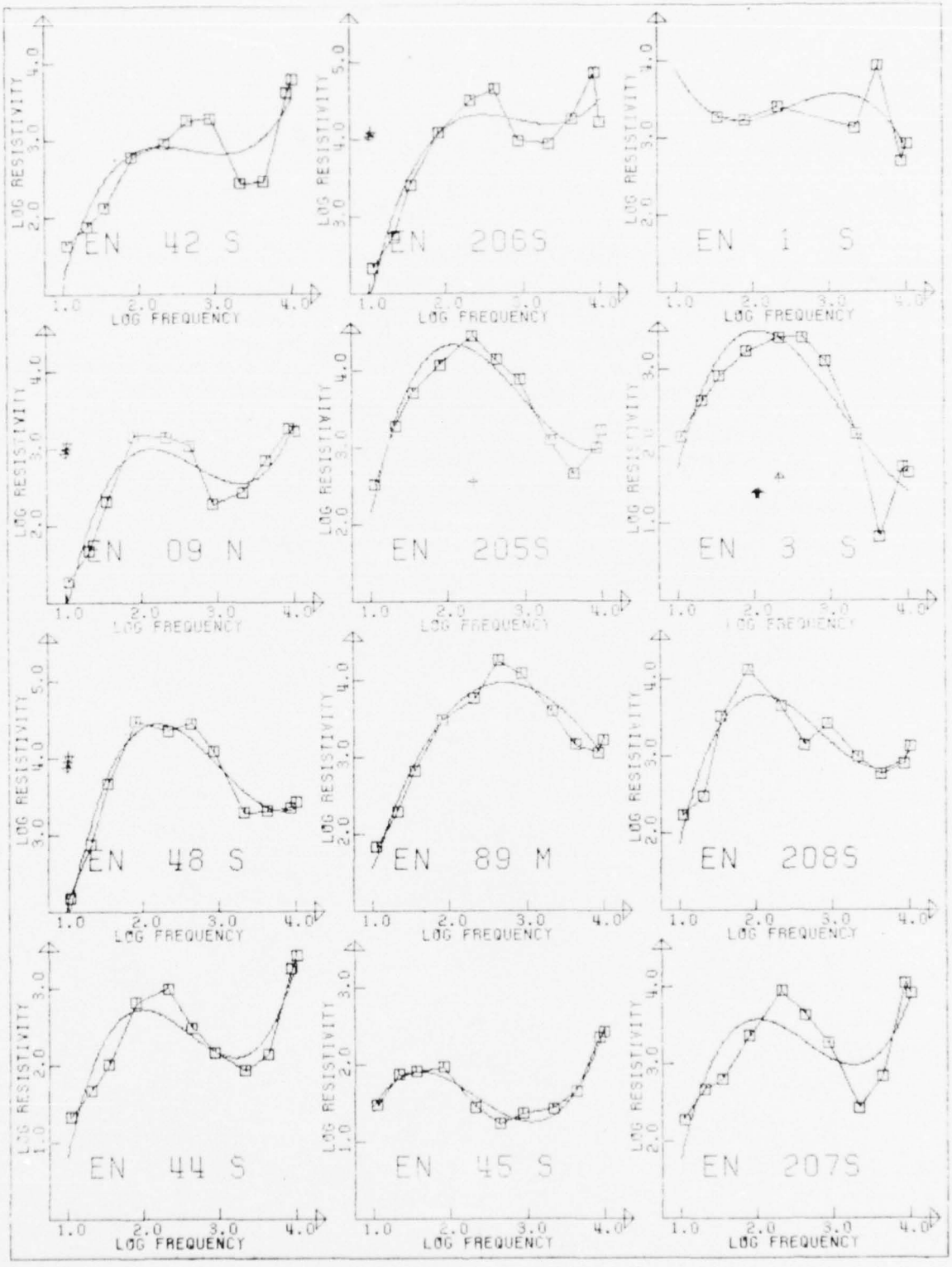
LOG RESISTIVITY
LOG FREQUENCY
EN 42 S
EN 206S
EN 1 S
EN 09 N
EN 205S
EN 3 S
EN 48 S
EN 89 M
EN 208S
EN 44 S
EN 45 S
EN 207S

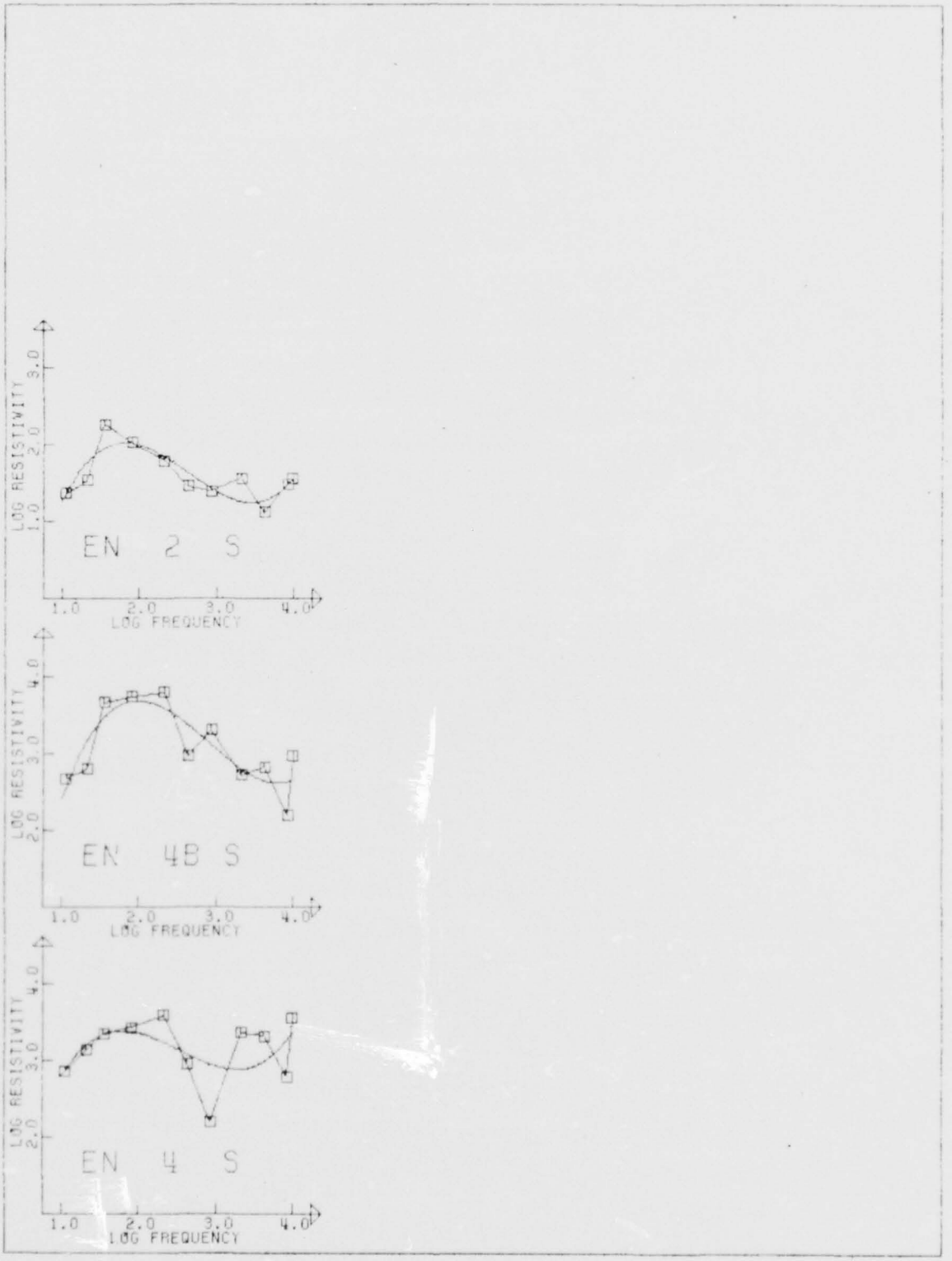
LOG RESISTIVITY
3.0
2.0
1.0
EN 2 S
1.0
2.0
3.0
4.0
LOG FREQUENCY
LOG RESISTIVITY
4.0
3.0
2.0
EN 4B S
1.0
2.0
3.0
4.0
LOG FREQUENCY
LOG RESISTIVITY
4.0
3.0
2.0
EN 4 S
1.0
2.0
3.0
4.0
LOG FREQUENCY

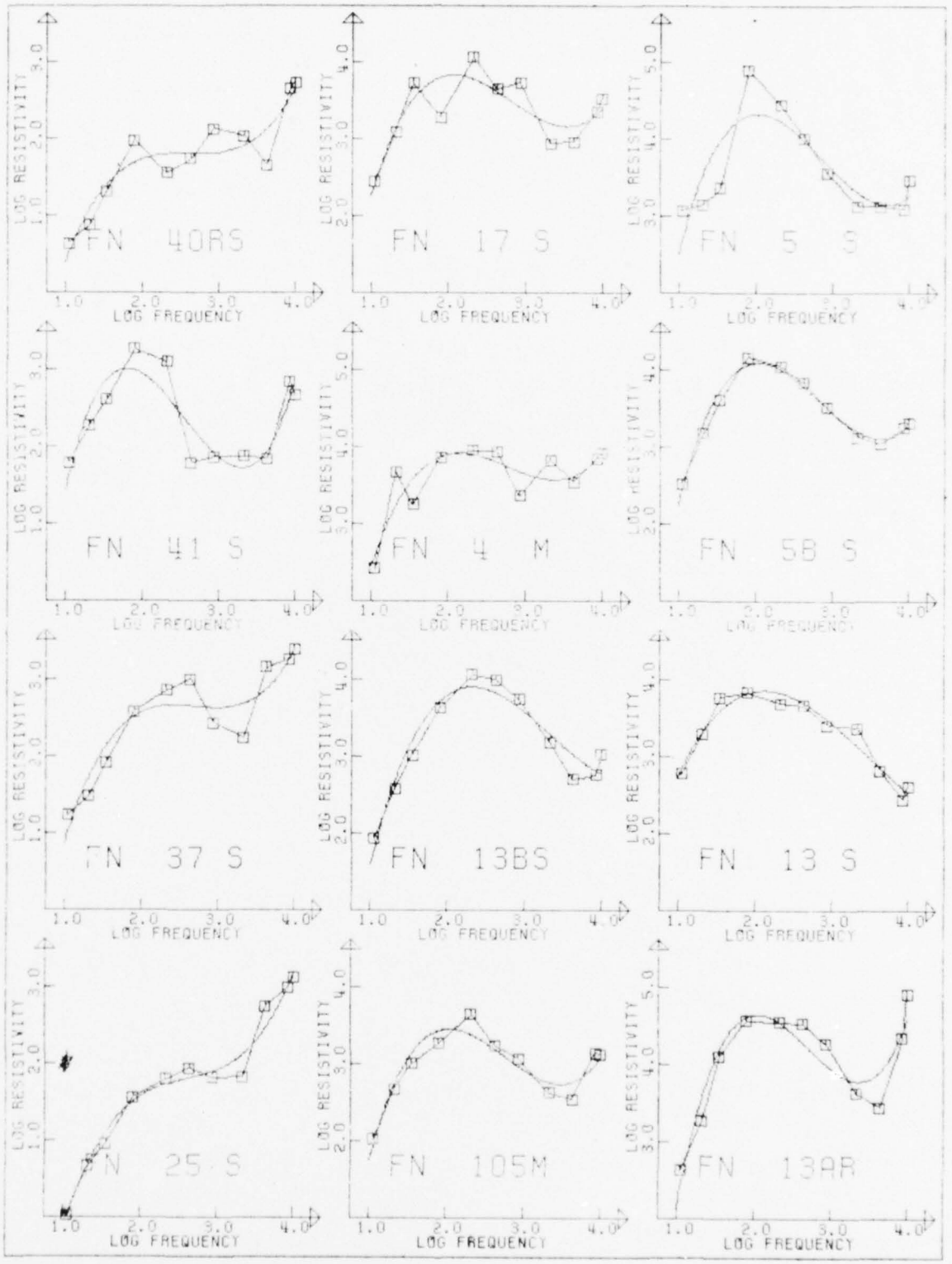
FN 40RS
FN 17 S
FN 5 S
FN 41 S
FN 4 M
FN 58 S
FN 37 S
FN 13BS
FN 13 S
N 25 S
FN 105M
FN 13AR
LOG RESISTIVITY
LOG FREQUENCY

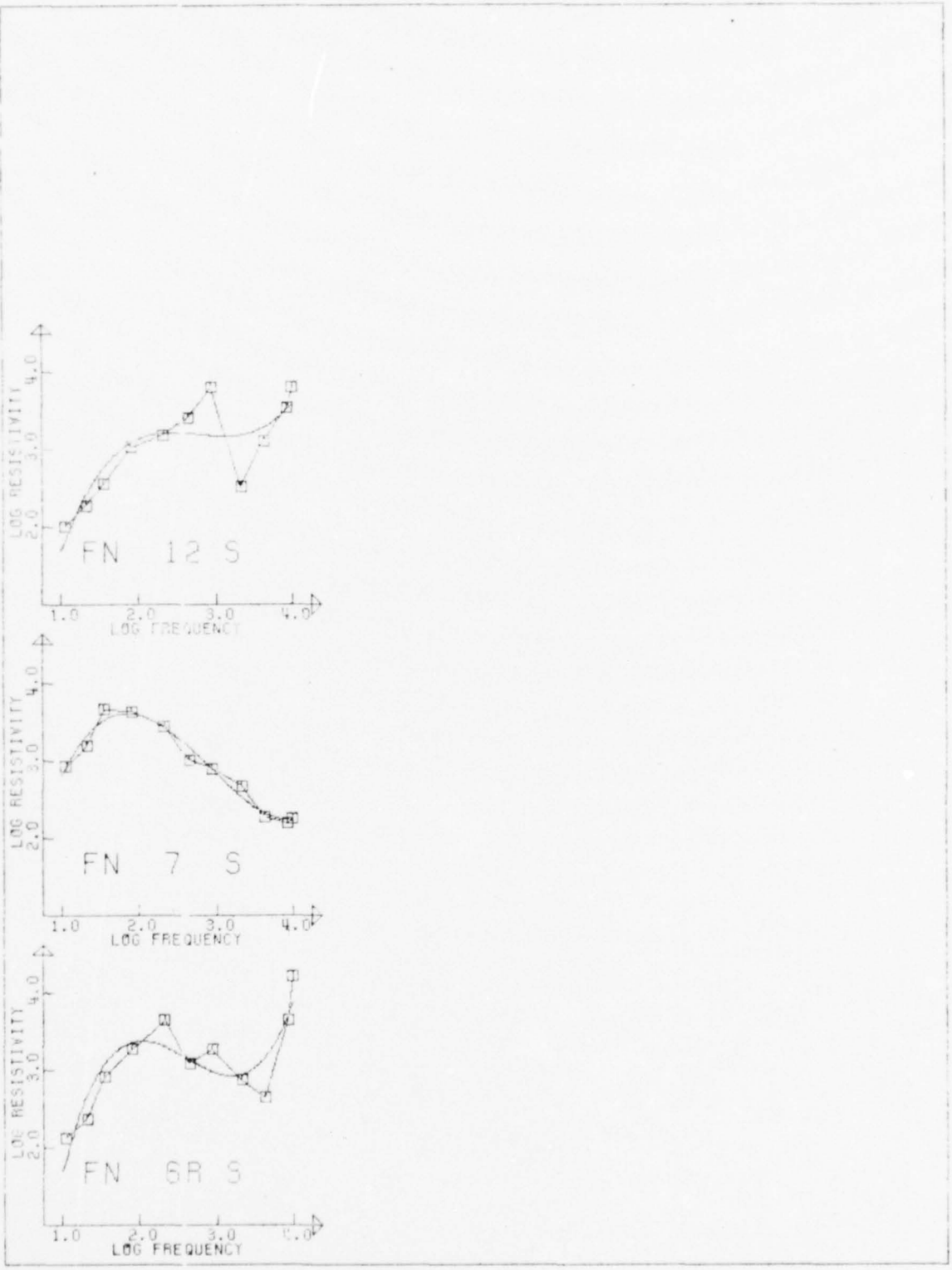
LOG RESISTIVITY
4.0
3.0
2.0
FN 12 S
1.0
2.0
3.0
4.0
LOG FREQUENCY
LOG RESISTIVITY
4.0
3.0
2.0
FN 7 S
1.0
2.0
3.0
4.0
LOG FREQUENCY
LOG RESISTIVITY
4.0
3.0
2.0
FN 6R S
1.0
2.0
3.0
LOG FREQUENCY

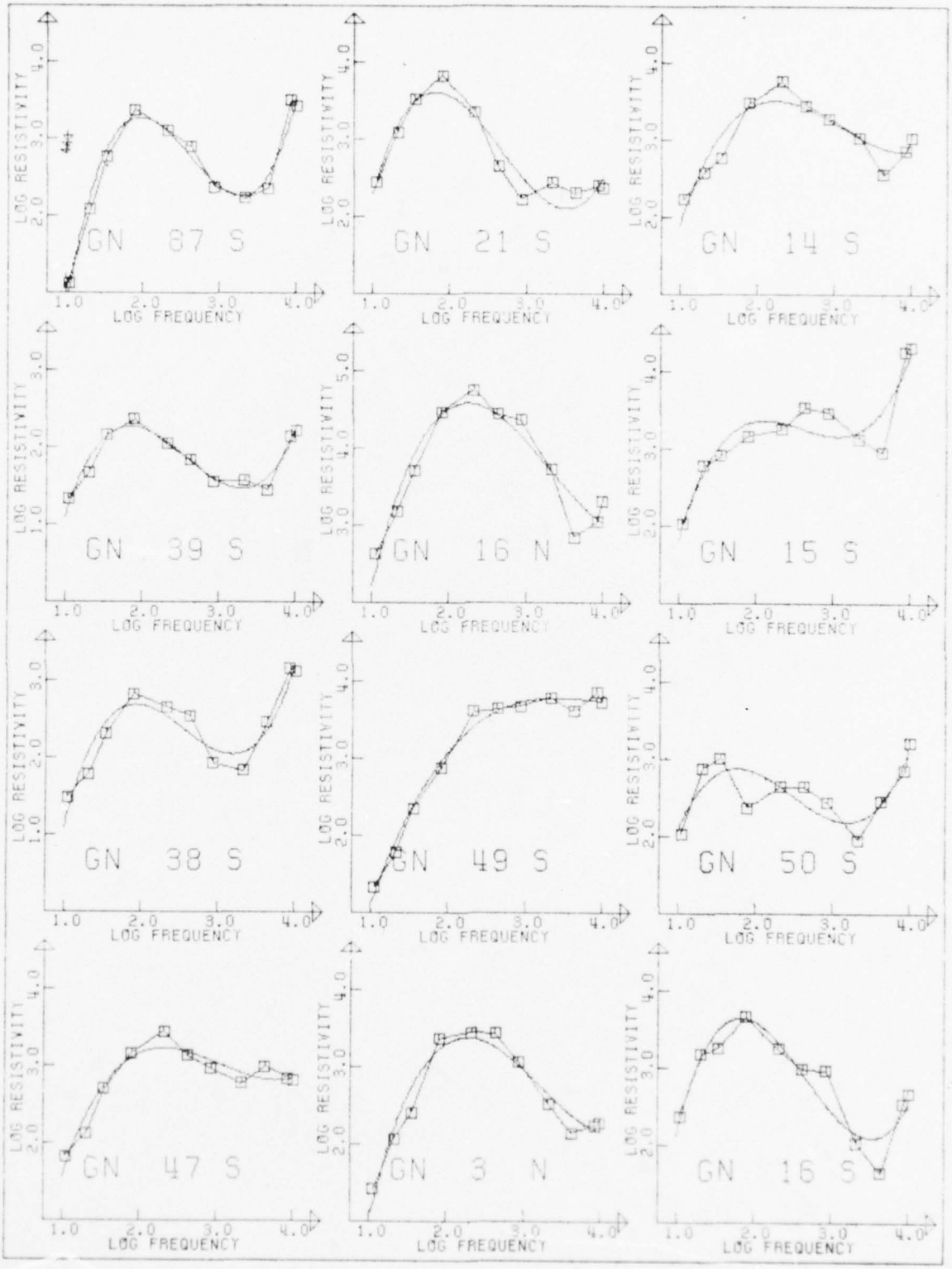
GN 87 S
GN 21 S
GN 14 S
GN 39 S
GN 16 N
GN 15 S
GN 38 S
GN 49 S
GN 50 S
GN 47 S
GN 3 N
GN 16 S
LOG RESISTIVITY
LOG FREQUENCY

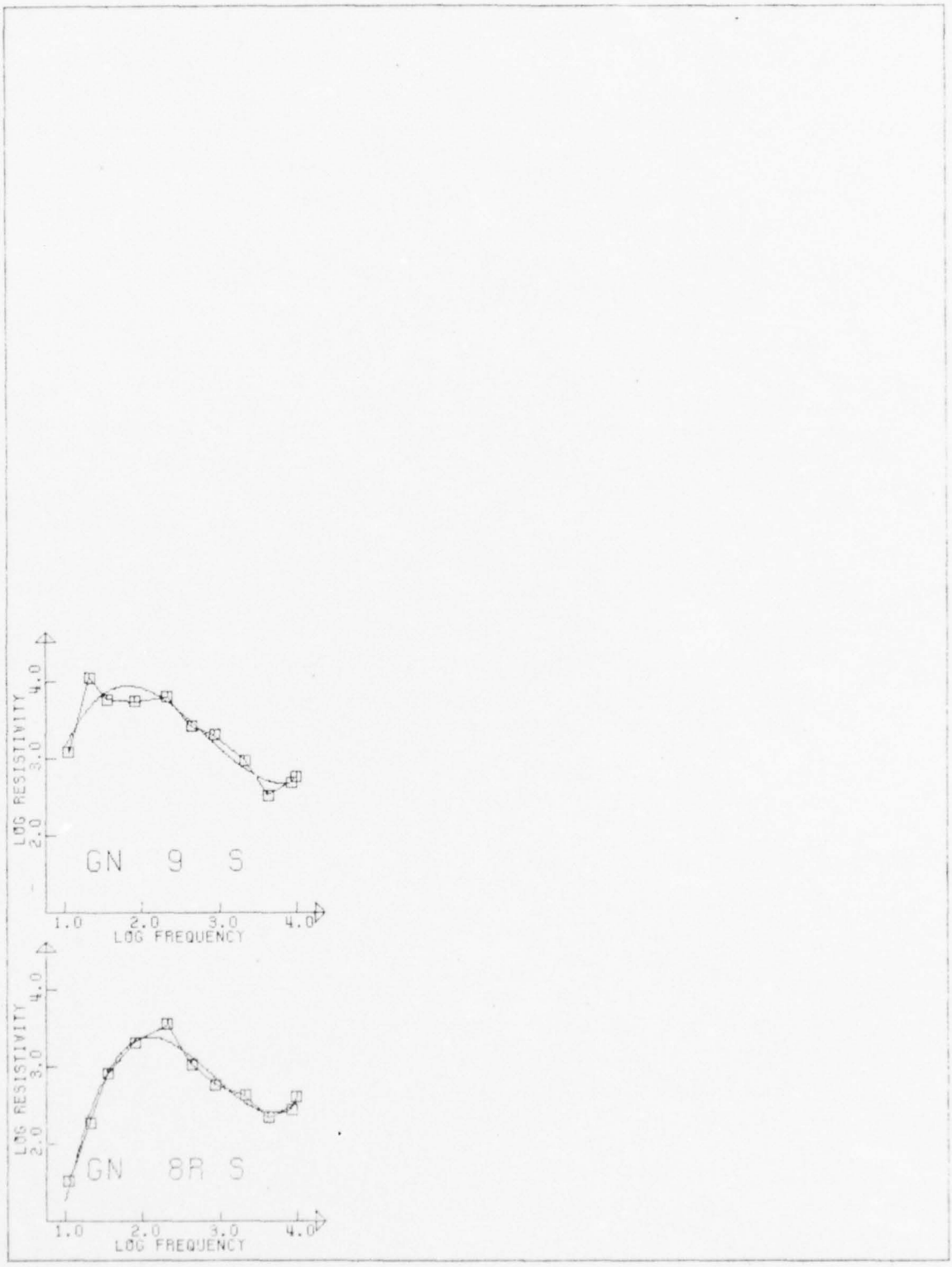
LOG RESISTIVITY
4.0
3.0
2.0
GN 9 S
1.0
2.0
3.0
4.0
LOG FREQUENCY
LOG RESISTIVITY
4.0
3.0
2.0
GN 8R S
1.0
2.0
3.0
4.0
LOG FREQUENCY

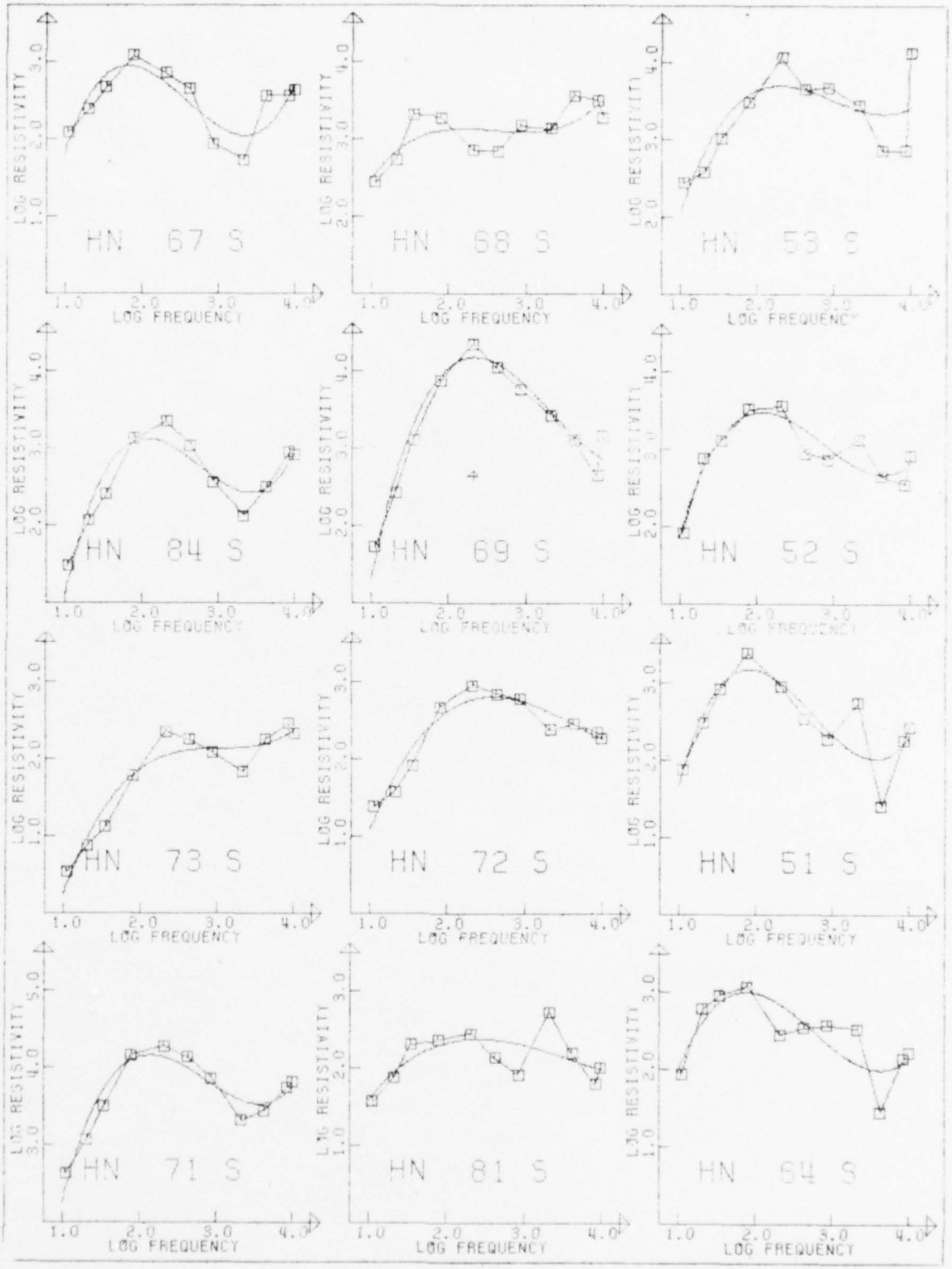
LOG RESISTIVITY
LOG FREQUENCY
HN 67 S
HN 68 S
HN 53 S
HN 84 S
HN 69 S
HN 52 S
HN 73 S
HN 72 S
HN 51 S
HN 71 S
HN 81 S
HN 64 S

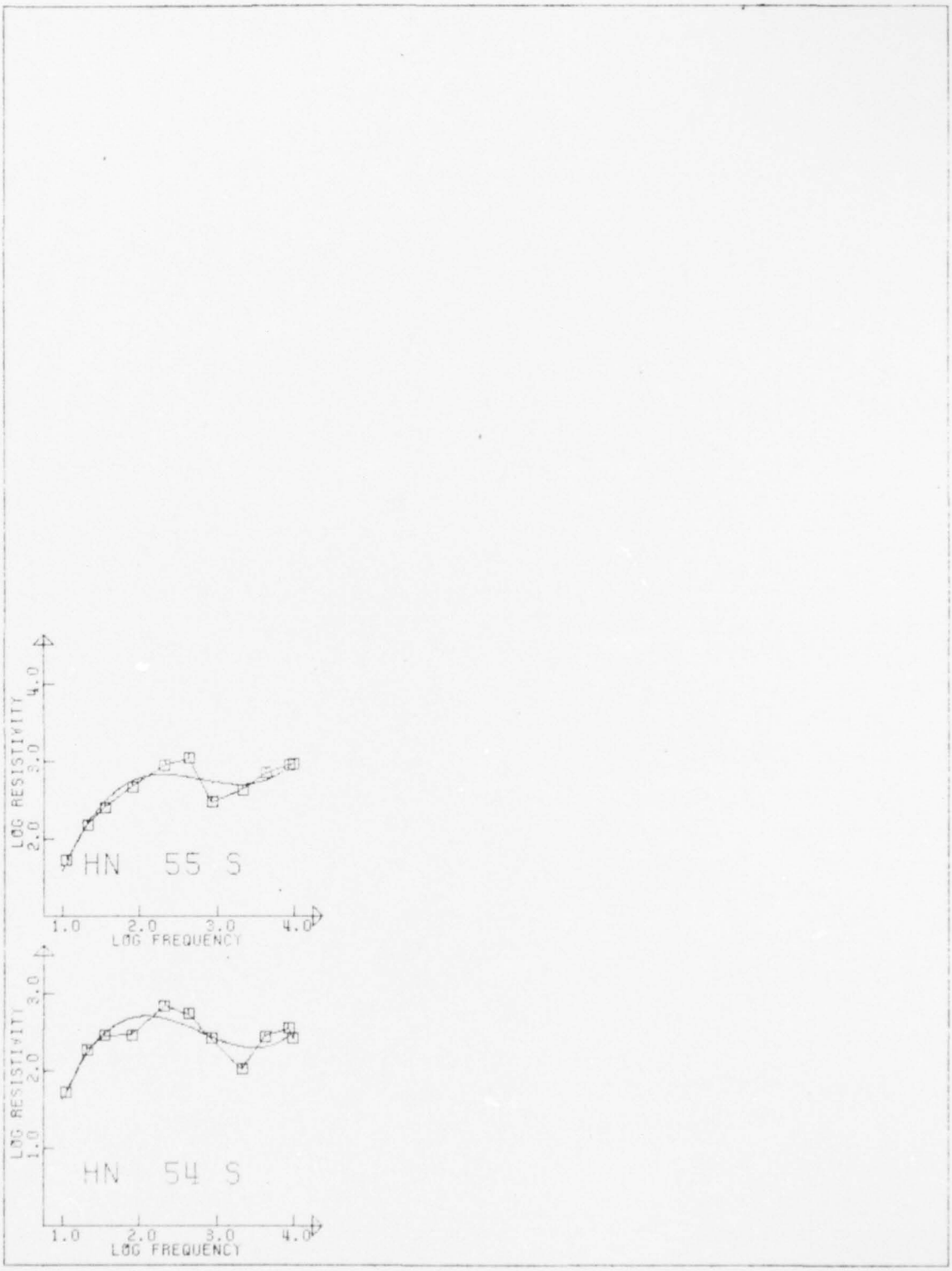
LOG RESISTIVITY
4.0
3.0
2.0
HN 55 S
1.0
2.0
3.0
4.0
LOG FREQUENCY
LOG RESISTIVITY
3.0
2.0
1.0
HN 54 S
1.0
2.0
3.0
4.0
LOG FREQUENCY

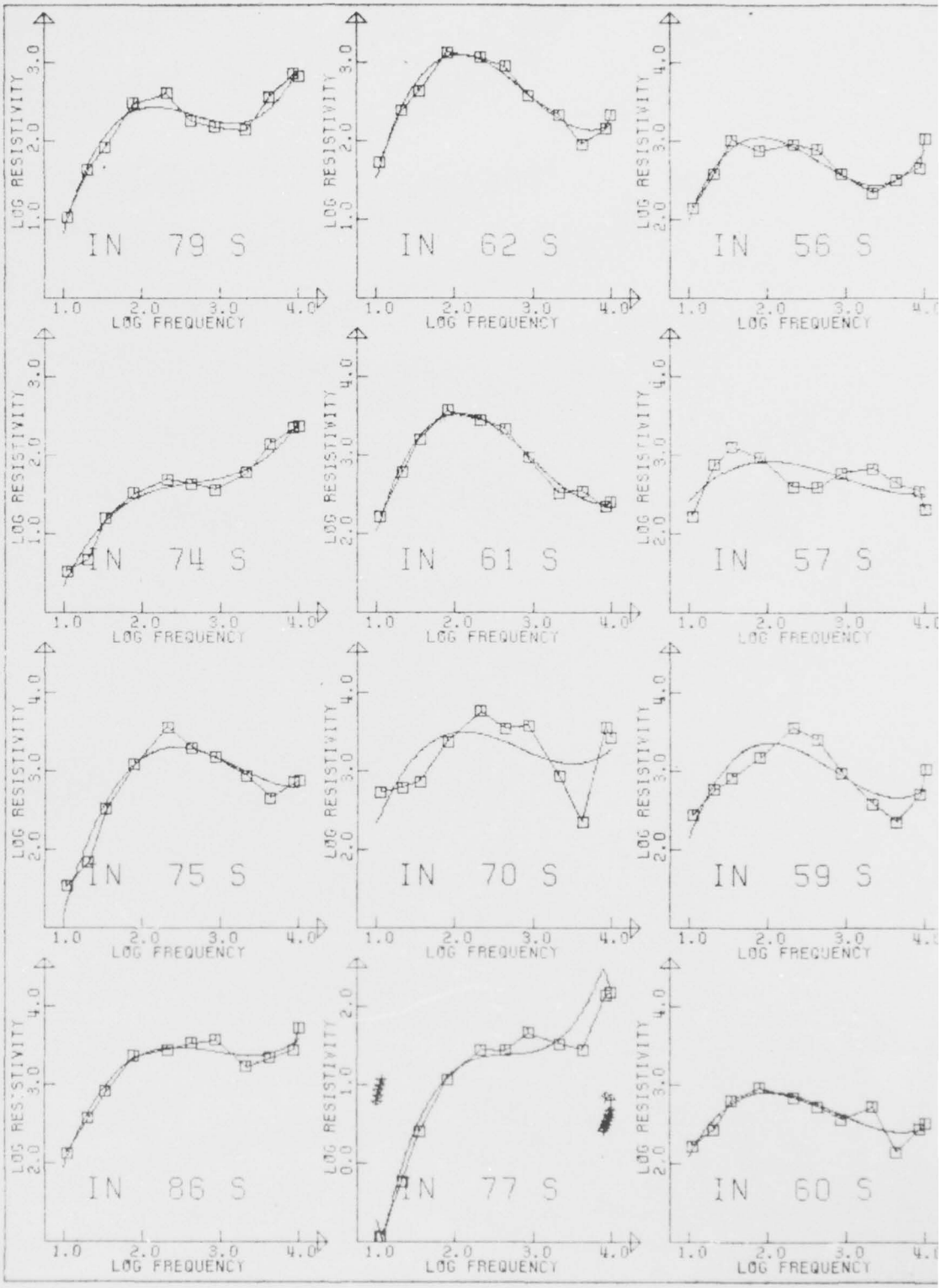
LOG RESISTIVITY
LOG FREQUENCY
IN 79 S
IN 62 S
IN 56 S
IN 74 S
IN 61 S
IN 57 S
IN 75 S
IN 70 S
IN 59 S
IN 86 S
IN 77 S
IN 60 S

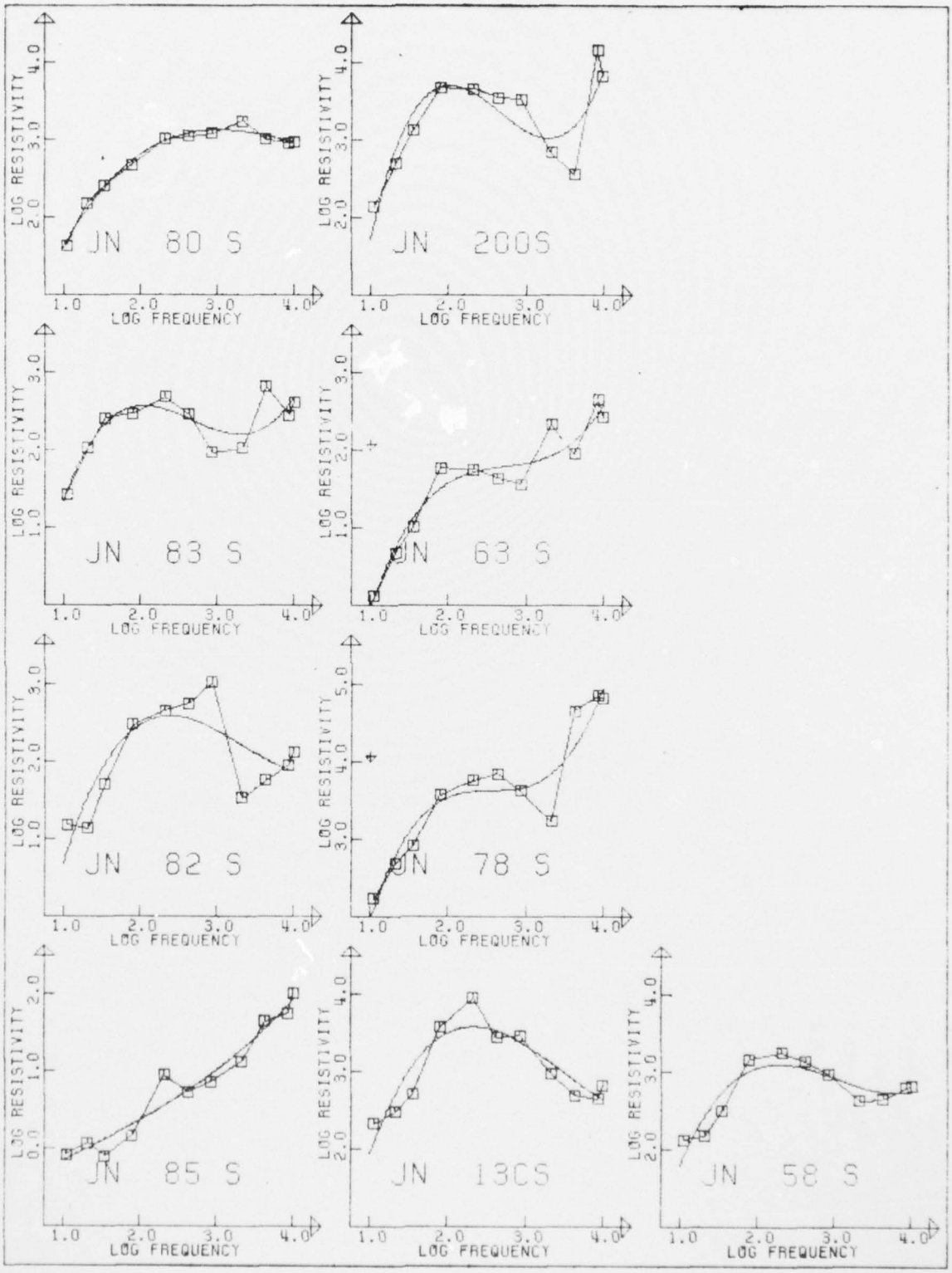
LOG RESISTIVITY
LOG FREQUENCY
JN 80 S
JN 200S
JN 83 S
JN 63 S
JN 82 S
JN 78 S
JN 85 S
JN 130S
JN 58 S

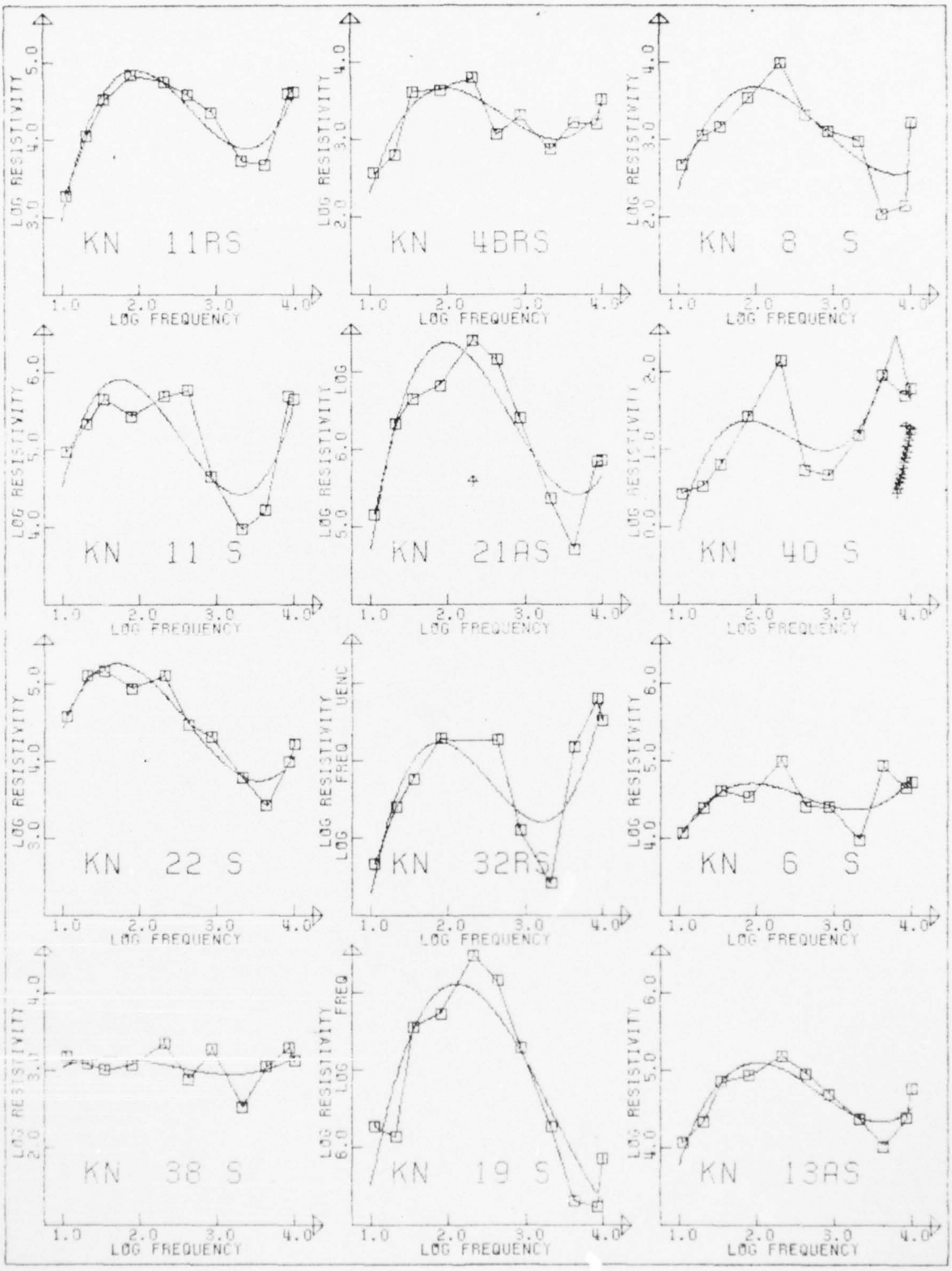
KN 11RS
KN 4BRS
KN 8 S
KN 11 S
KN 21AS
KN 40 S
KN 22 S
KN 32RS
KN 6 S
KN 38 S
KN 19 S
KN 13AS
LOG RESISTIVITY
LOG FREQUENCY

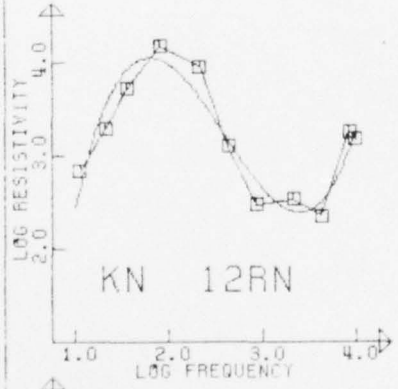
LOG RESISTIVITY
2.0
3.0
4.0
KN 12RN
1.0
2.0
3.0
4.0
LOG FREQUENCY

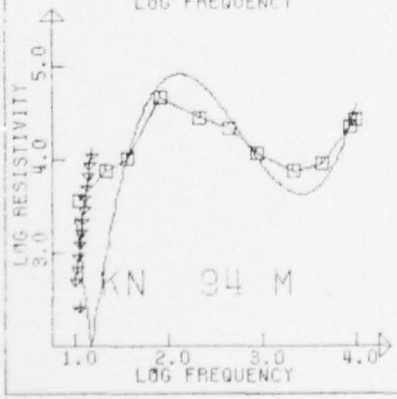
LOG RESISTIVITY
3.0
4.0
5.0
KN 34 M
1.0
2.0
3.0
4.0
LOG FREQUENCY

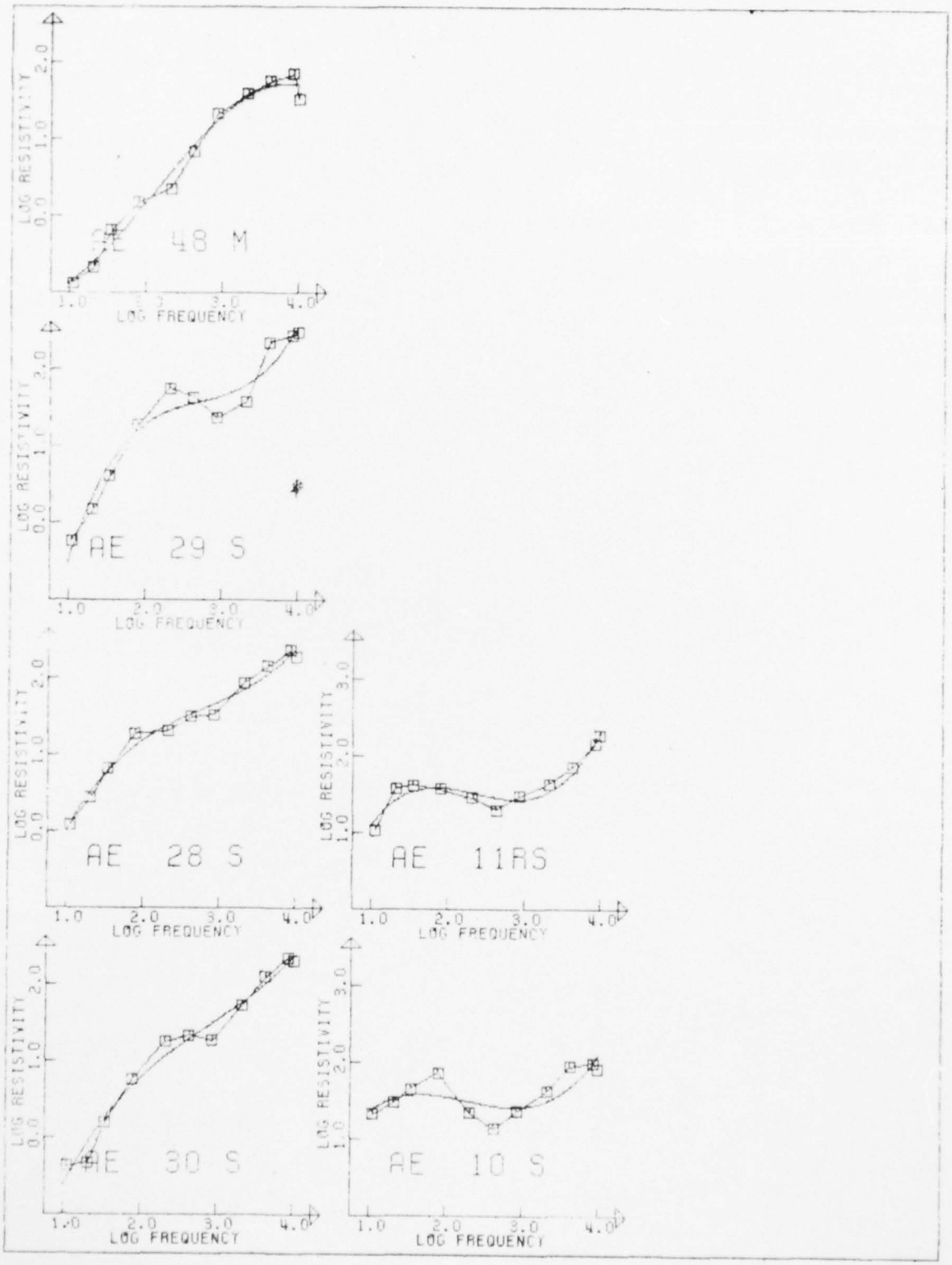
LOG RESISTIVITY
LOG FREQUENCY
AE 48 M
AE 29 S
AE 28 S
AE 11RS
AE 30 S
AE 10 S

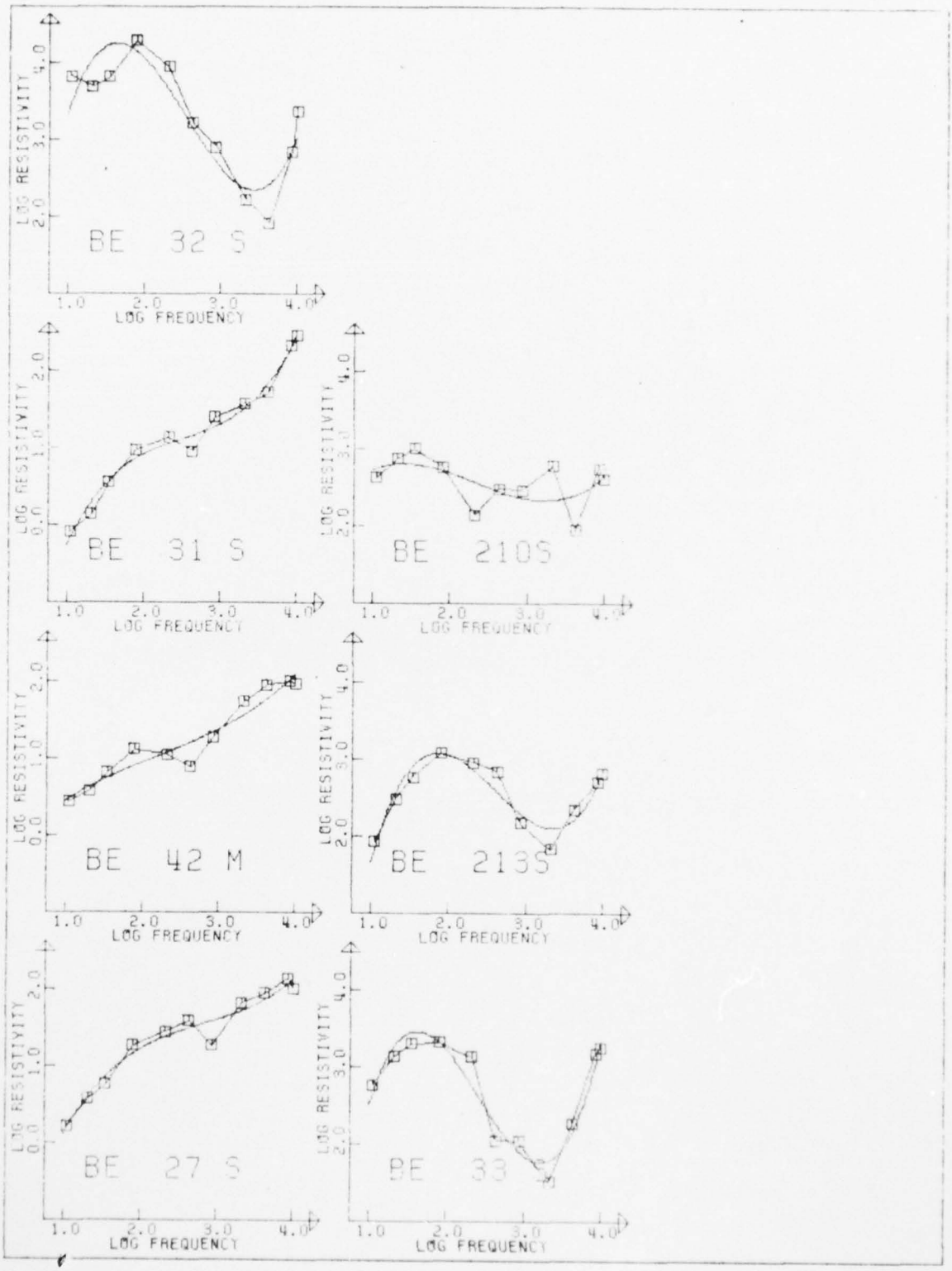
LOG RESISTIVITY
LOG FREQUENCY
BE 32 S
BE 31 S
BE 210S
BE 42 M
BE 213S
BE 27 S
BE 33

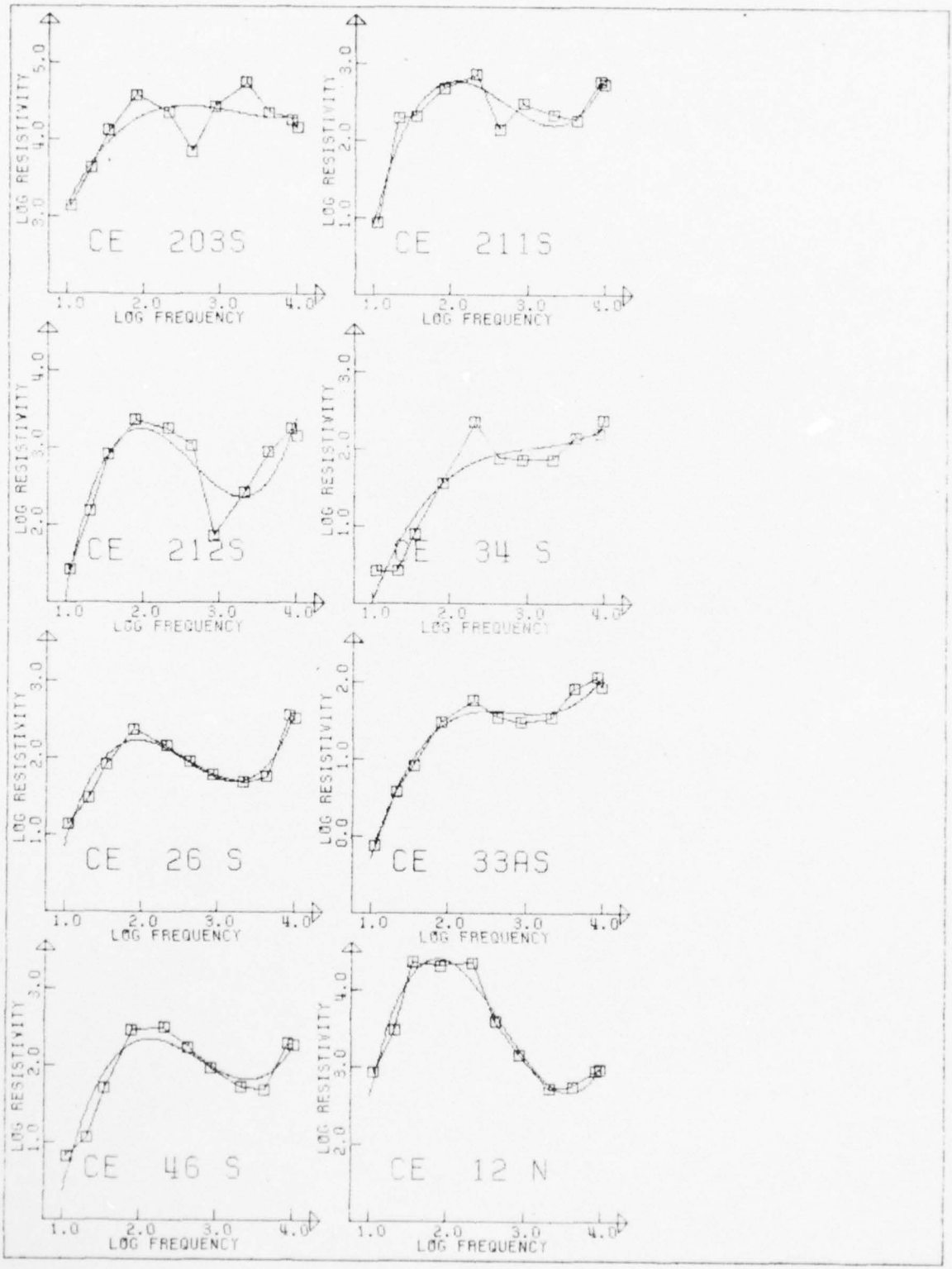
CE 203S
CE 211S
CE 212S
CE 34 S
CE 26 S
CE 33AS
CE 46 S
CE 12 N
LOG RESISTIVITY
LOG FREQUENCY

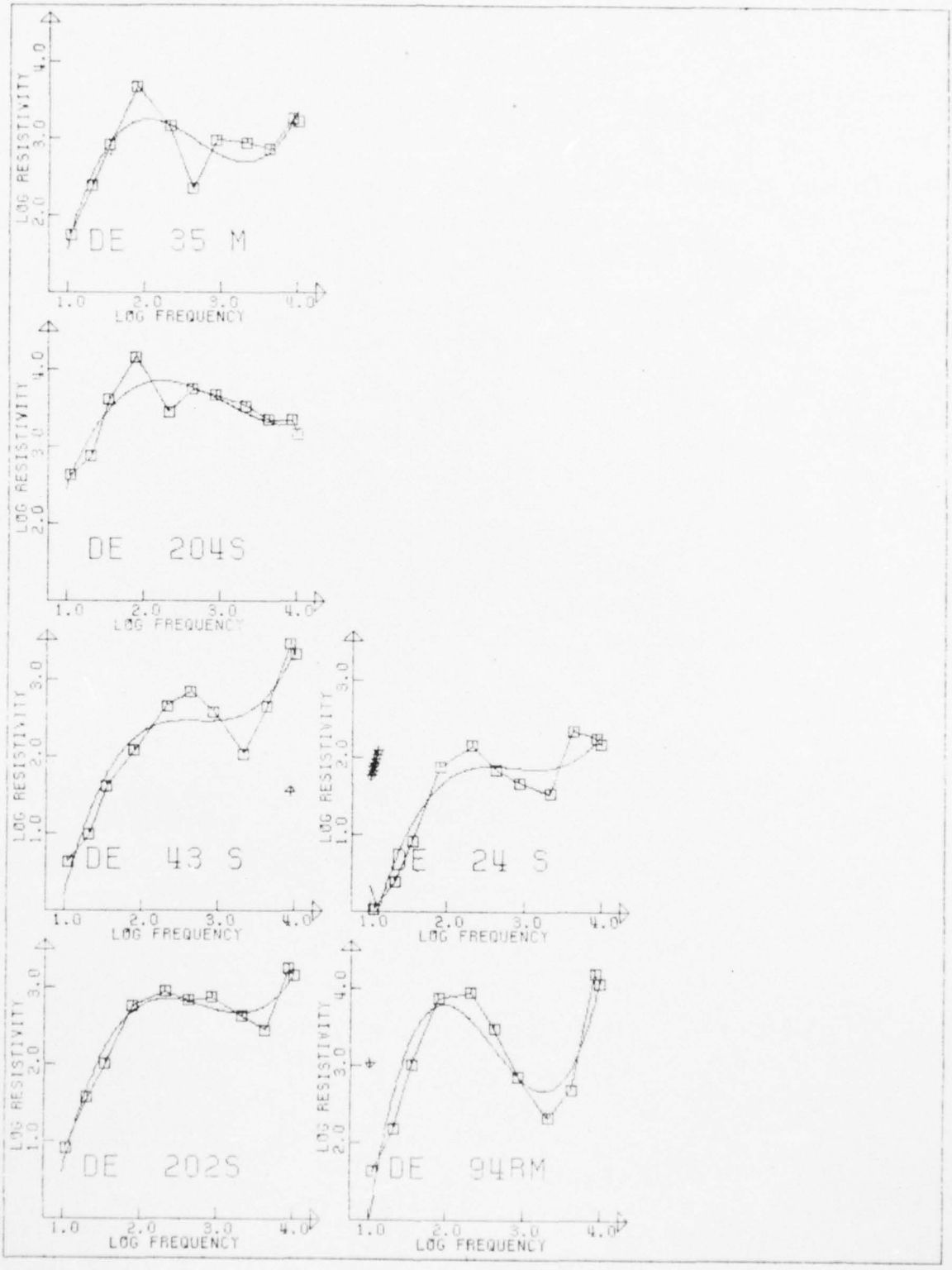
LOG RESISTIVITY
LOG FREQUENCY
DE 35 M
DE 204S
DE 43 S
DE 24 S
DE 202S
DE 94RM
1.0
2.0
3.0
4.0

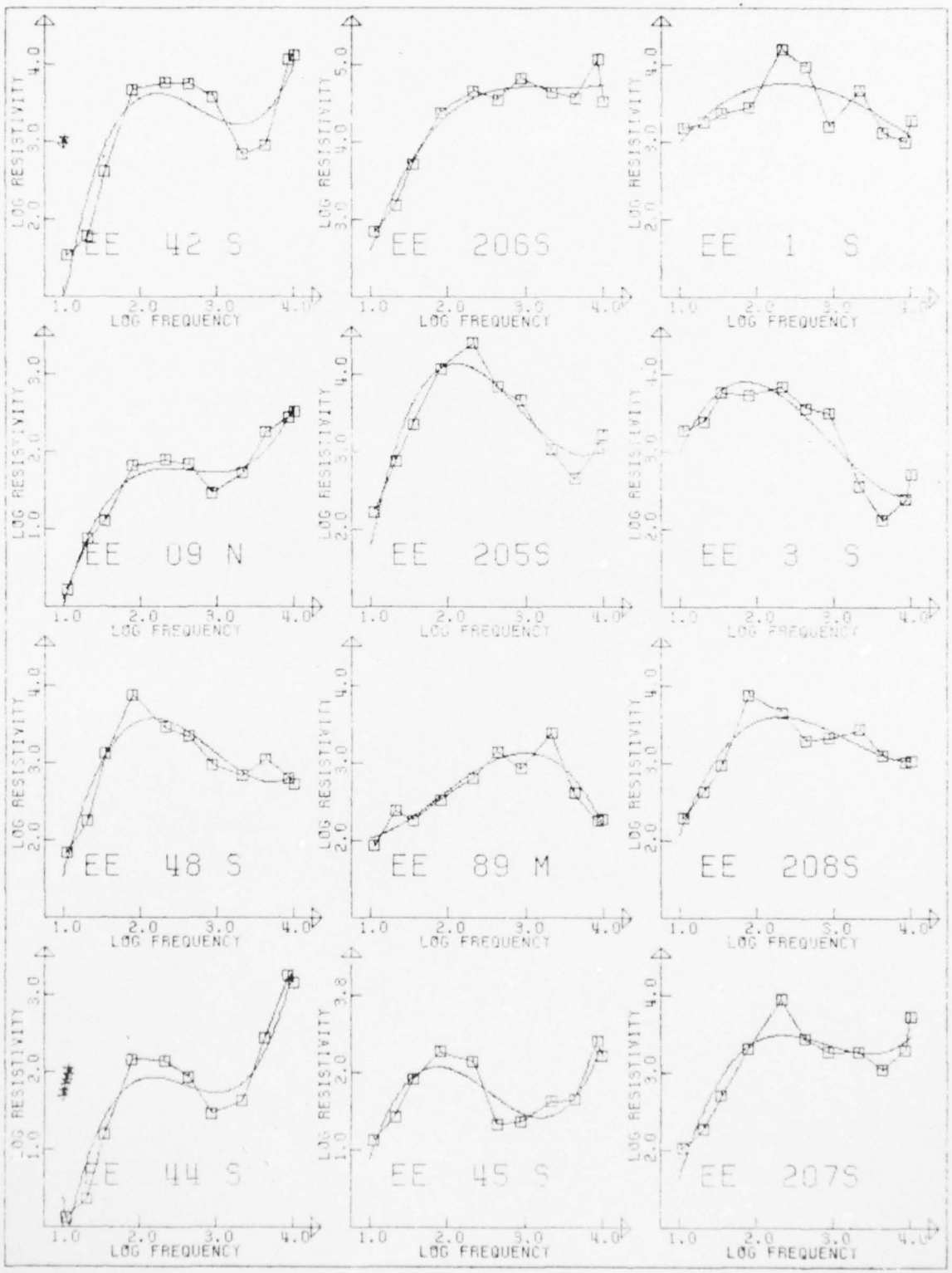
LOG RESISTIVITY
LOG FREQUENCY
EE 42 S
EE 206S
EE 1 S
EE 09 N
EE 205S
EE 3 S
EE 48 S
EE 89 M
EE 208S
EE 44 S
EE 45 S
EE 207S

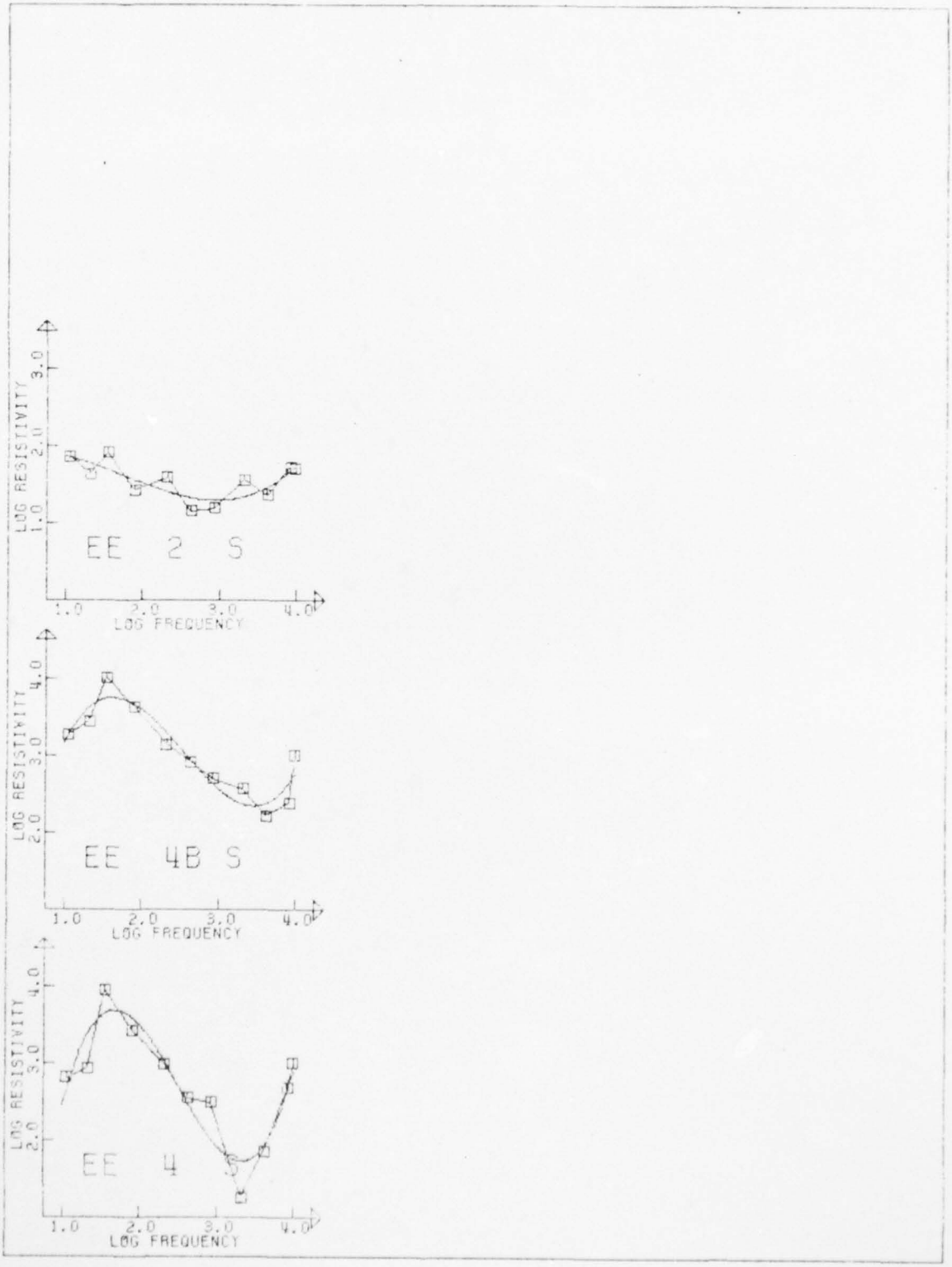
LOG RESISTIVITY
3.0
2.0
1.0
EE 2 S
1.0
2.0
3.0
4.0
LOG FREQUENCY
LOG RESISTIVITY
4.0
3.0
2.0
EE 4B S
1.0
2.0
3.0
4.0
LOG FREQUENCY
LOG RESISTIVITY
4.0
3.0
2.0
EE 4
1.0
2.0
3.0
4.0
LOG FREQUENCY

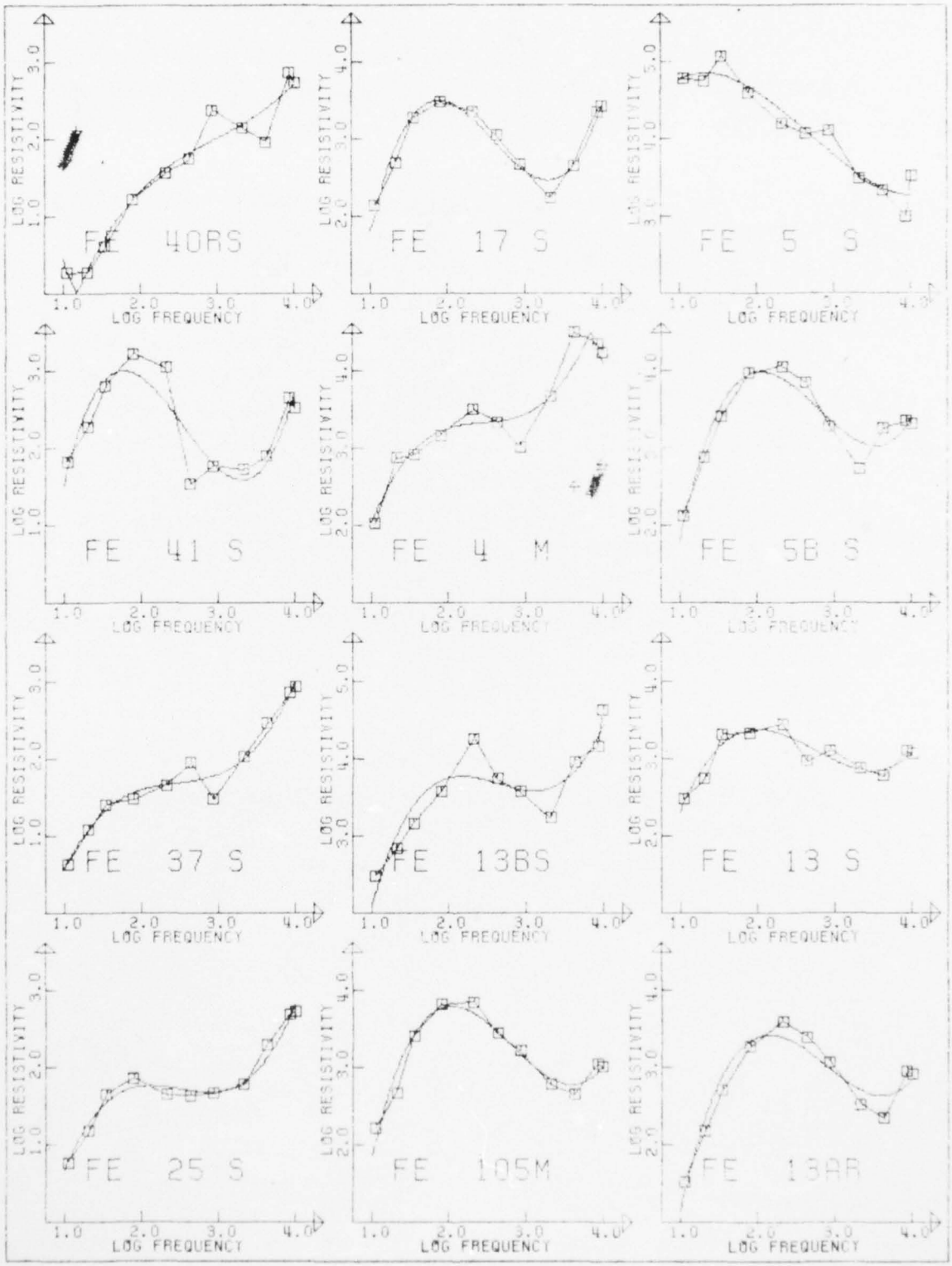
FE 40RS
FE 17 S
FE 5 S
FE 41 S
FE 4 M
FE 5B S
FE 37 S
FE 13BS
FE 13 S
FE 25 S
FE 105M
FE 13AR
LOG RESISTIVITY
LOG FREQUENCY

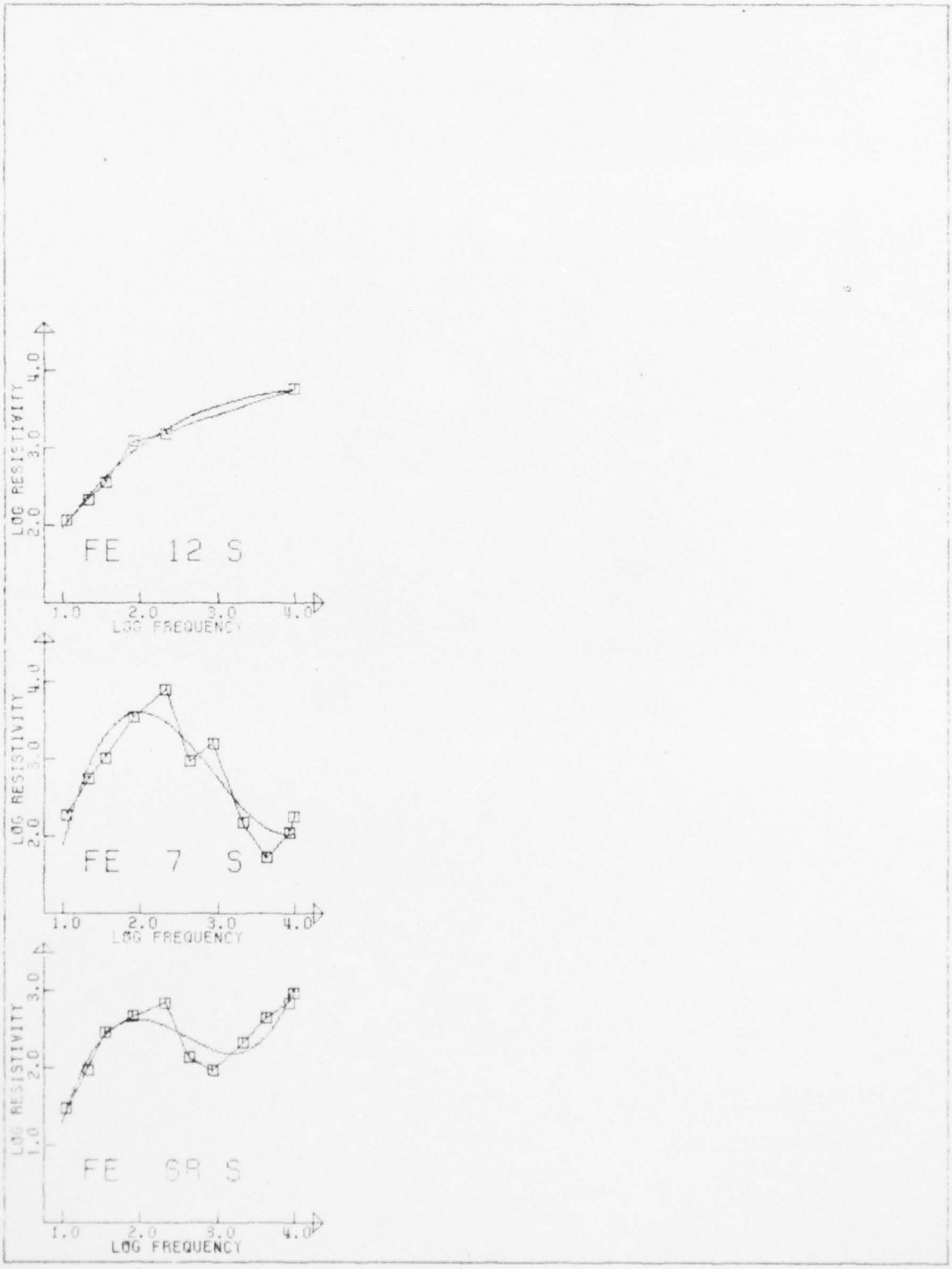
LOG RESISTIVITY
4.0
3.0
2.0
FE 12 S
1.0
2.0
3.0
4.0
LOG FREQUENCY
LOG RESISTIVITY
4.0
3.0
2.0
FE 7 S
1.0
2.0
3.0
4.0
LOG FREQUENCY
LOG RESISTIVITY
3.0
2.0
1.0
FE SR S
1.0
2.0
3.0
4.0
LOG FREQUENCY

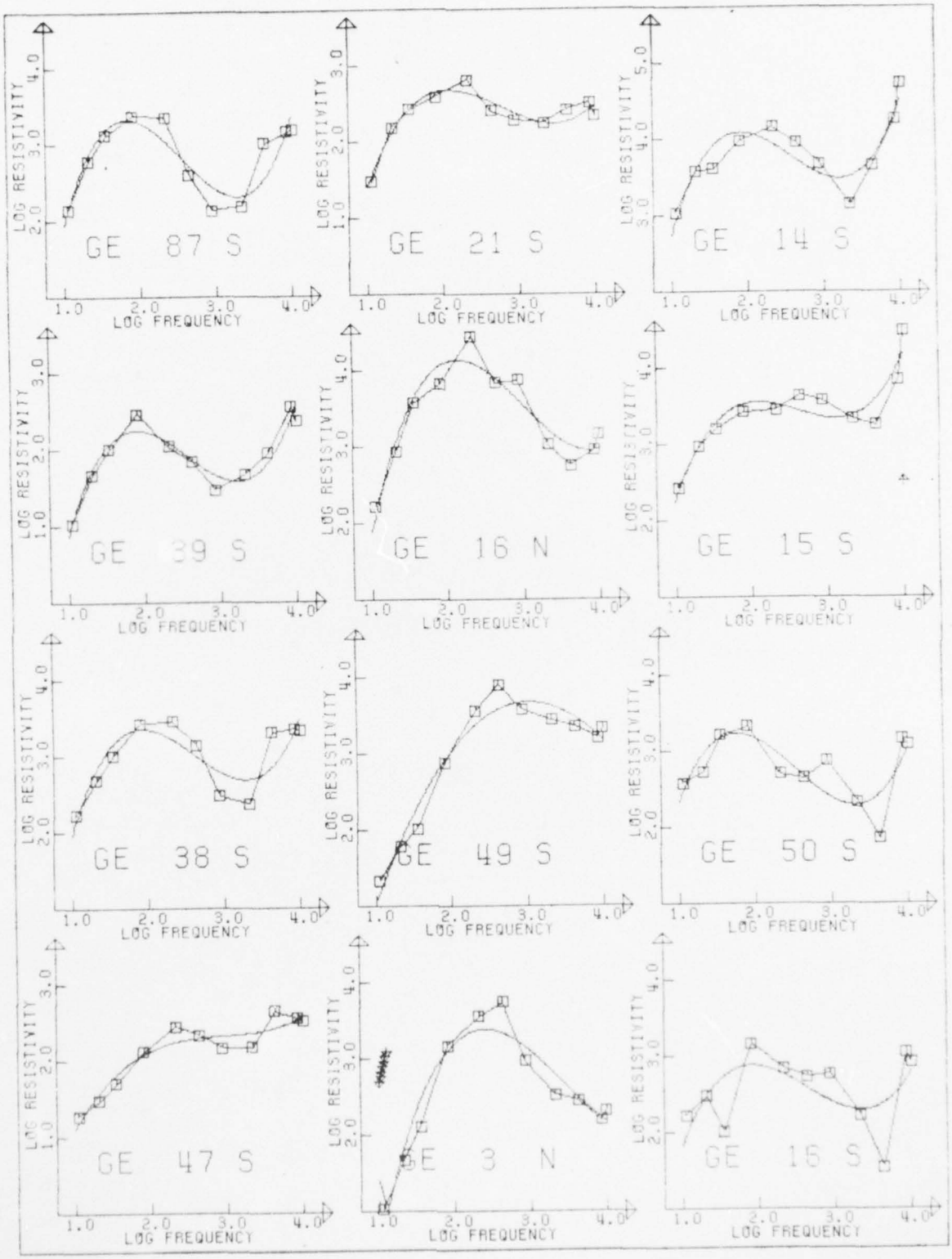
GE 87 S
GE 21 S
GE 14 S
GE 39 S
GE 16 N
GE 15 S
GE 38 S
GE 49 S
GE 50 S
GE 47 S
GE 3 N
GE 16 S
LOG RESISTIVITY
LOG FREQUENCY

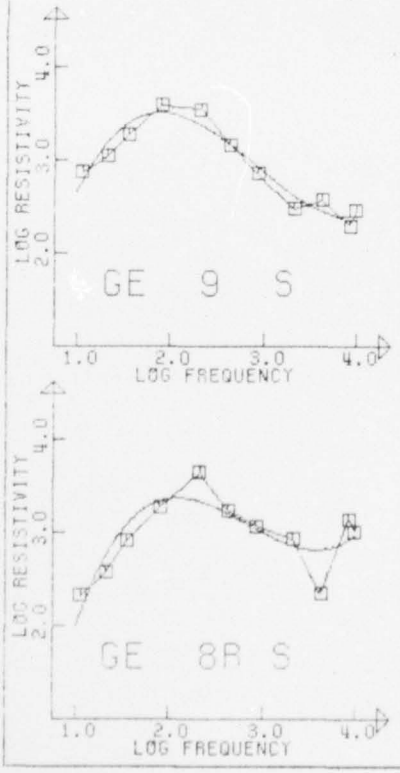
LOG RESISTIVITY
4.0
3.0
2.0
GE 9 S
1.0
2.0
3.0
4.0
LOG FREQUENCY
LOG RESISTIVITY
4.0
3.0
2.0
GE 8R S
1.0
2.0
3.0
4.0
LOG FREQUENCY

AD-A036 406 GTE SYLVANIA INC NEEDHAM HEIGHTS MASS COMMUNICATIONS--ETC F/G 17/2
ELF COMMUNICATIONS SEAFARER PROGRAM. SITE SURVEY, MICHIGAN REGI--ETC(U)
APR 76 N00093-75-C-0309

UNCLASSIFIED NL

2 OF 3
AD A036406

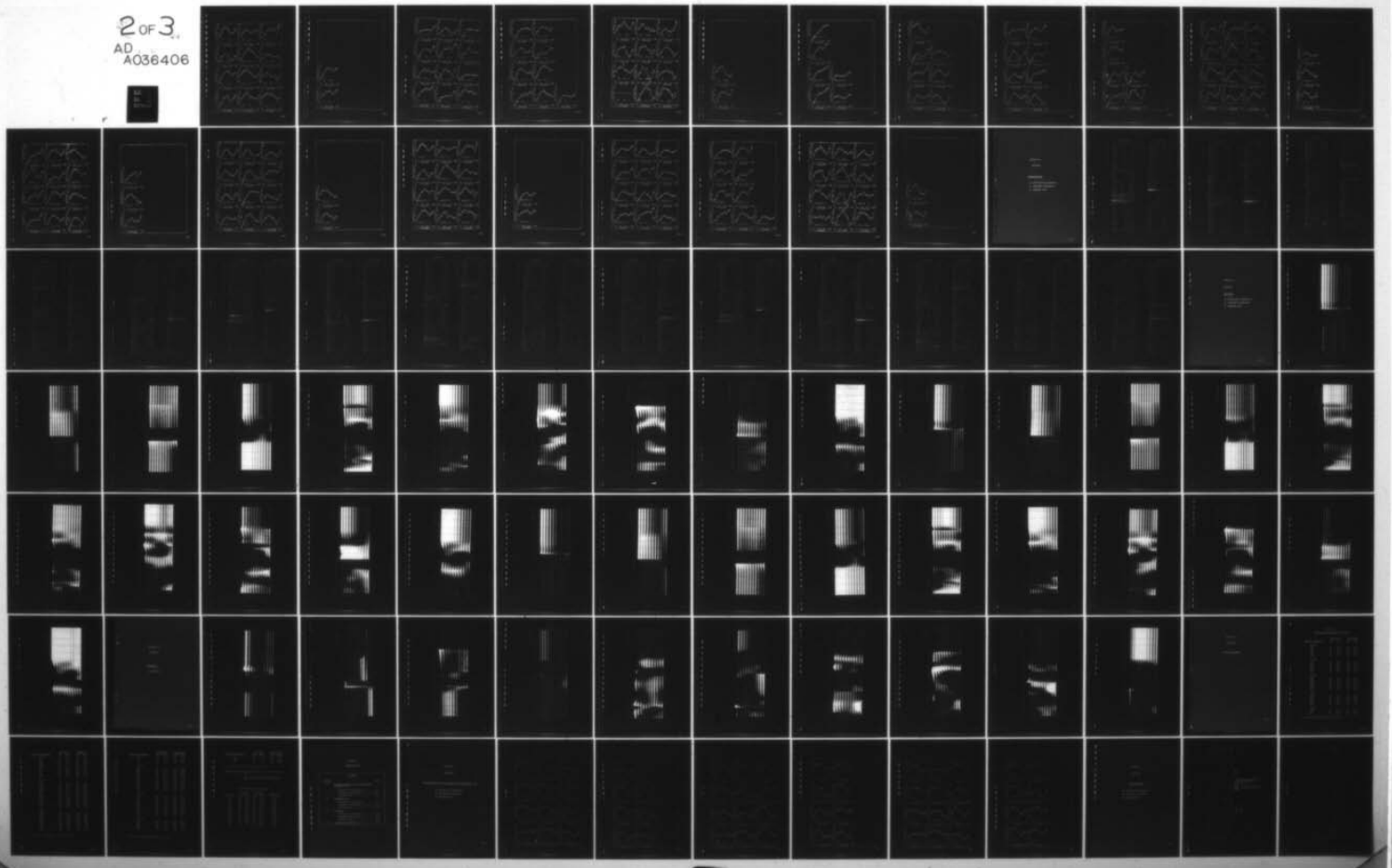

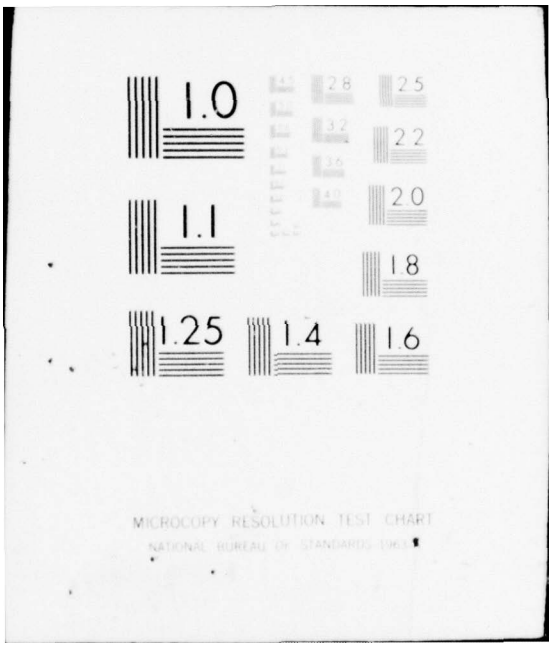
1.0
1.1
1.25
1.4
1.6
2.8
2.5
3.2
2.2
3.6
2.0
4.0
1.8
MICROCOPY RESOLUTION TEST CHART
NATIONAL BUREAU OF STANDARDS 1963

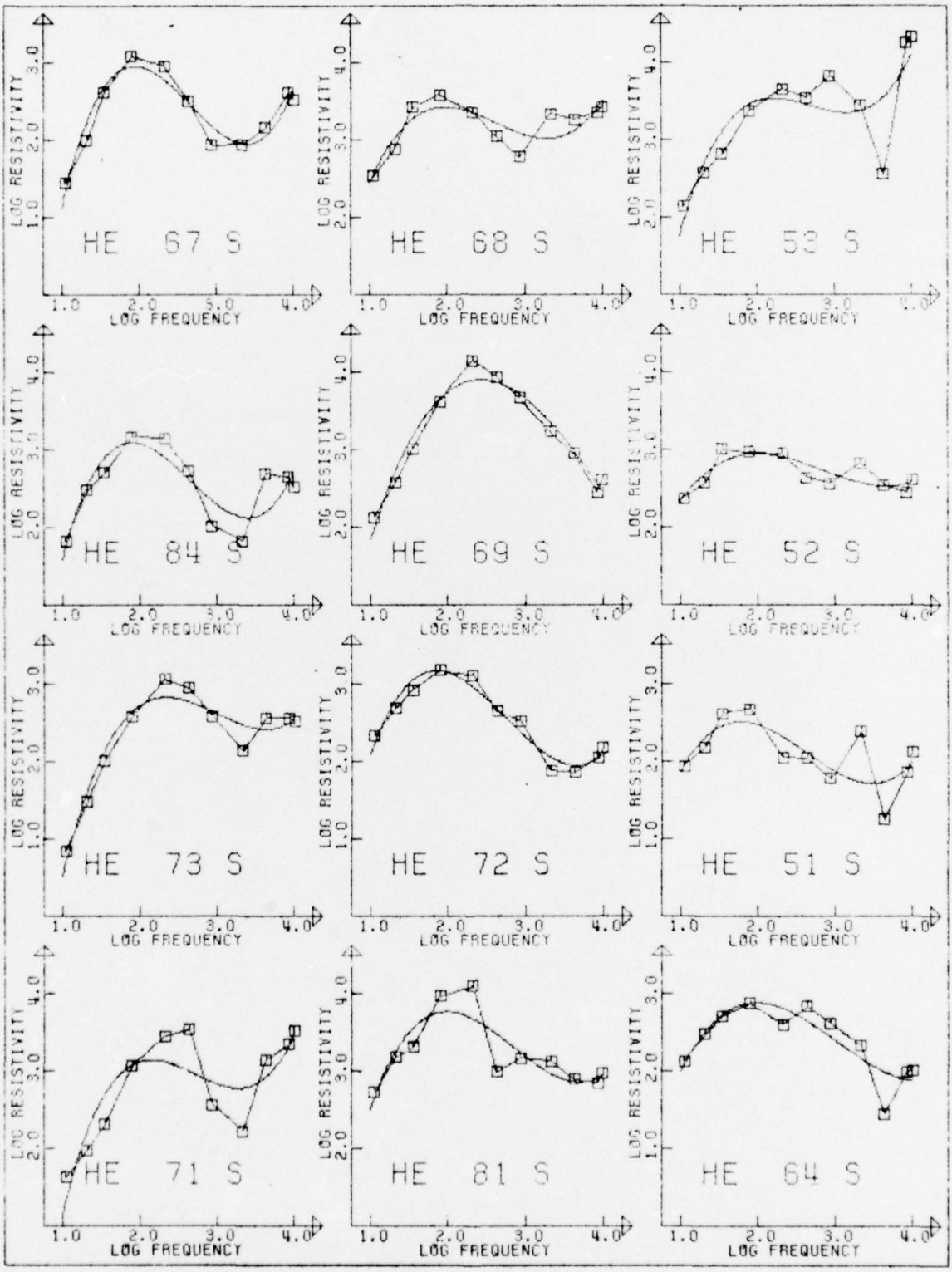
LOG RESISTIVITY
LOG FREQUENCY
HE 67 S
HE 68 S
HE 53 S
HE 84 S
HE 69 S
HE 52 S
HE 73 S
HE 72 S
HE 51 S
HE 71 S
HE 81 S
HE 64 S

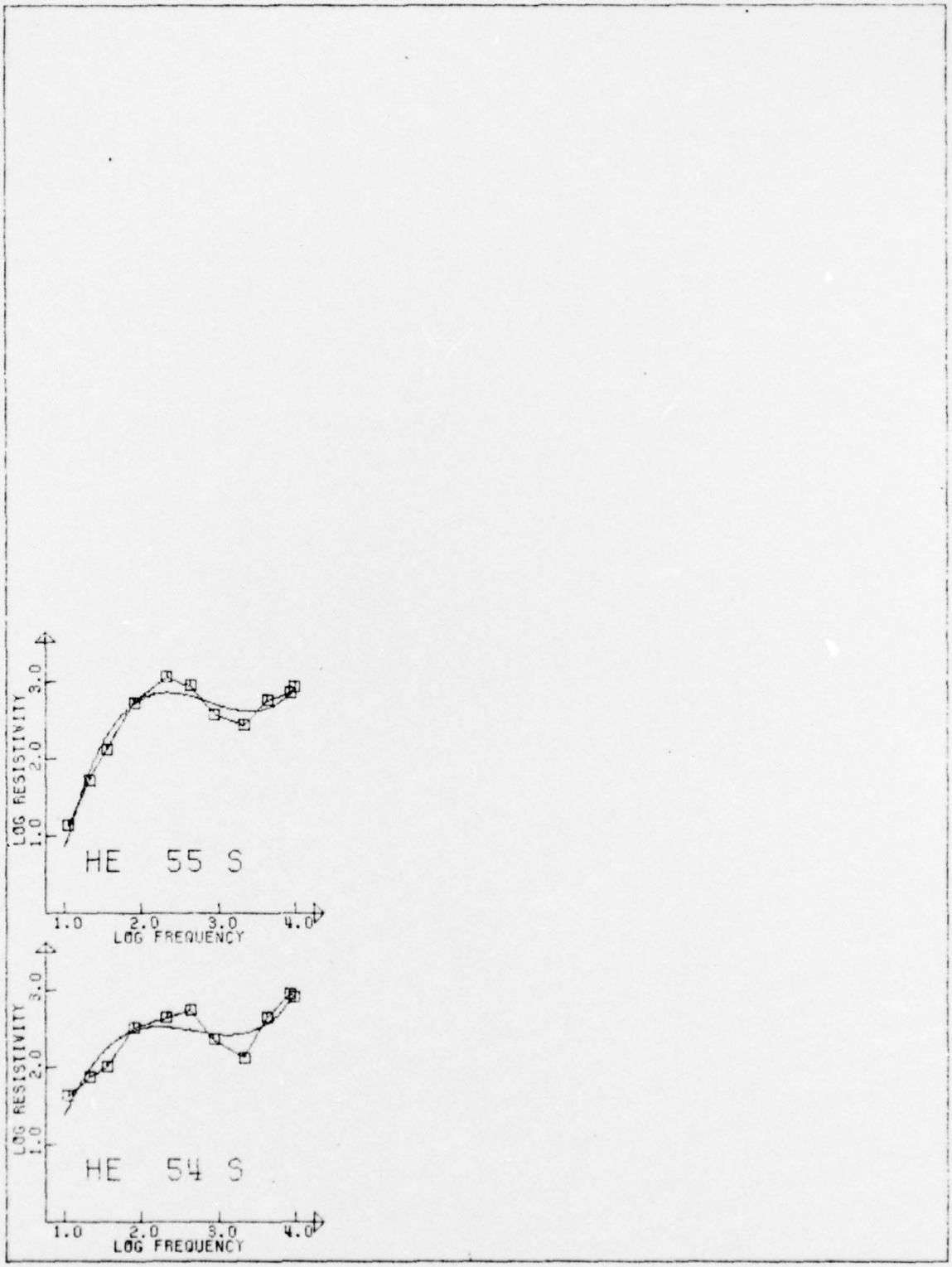
LOG RESISTIVITY
1.0
2.0
3.0
HE 55 S
1.0
2.0
3.0
4.0
LOG FREQUENCY
LOG RESISTIVITY
1.0
2.0
3.0
HE 54 S
1.0
2.0
3.0
4.0
LOG FREQUENCY

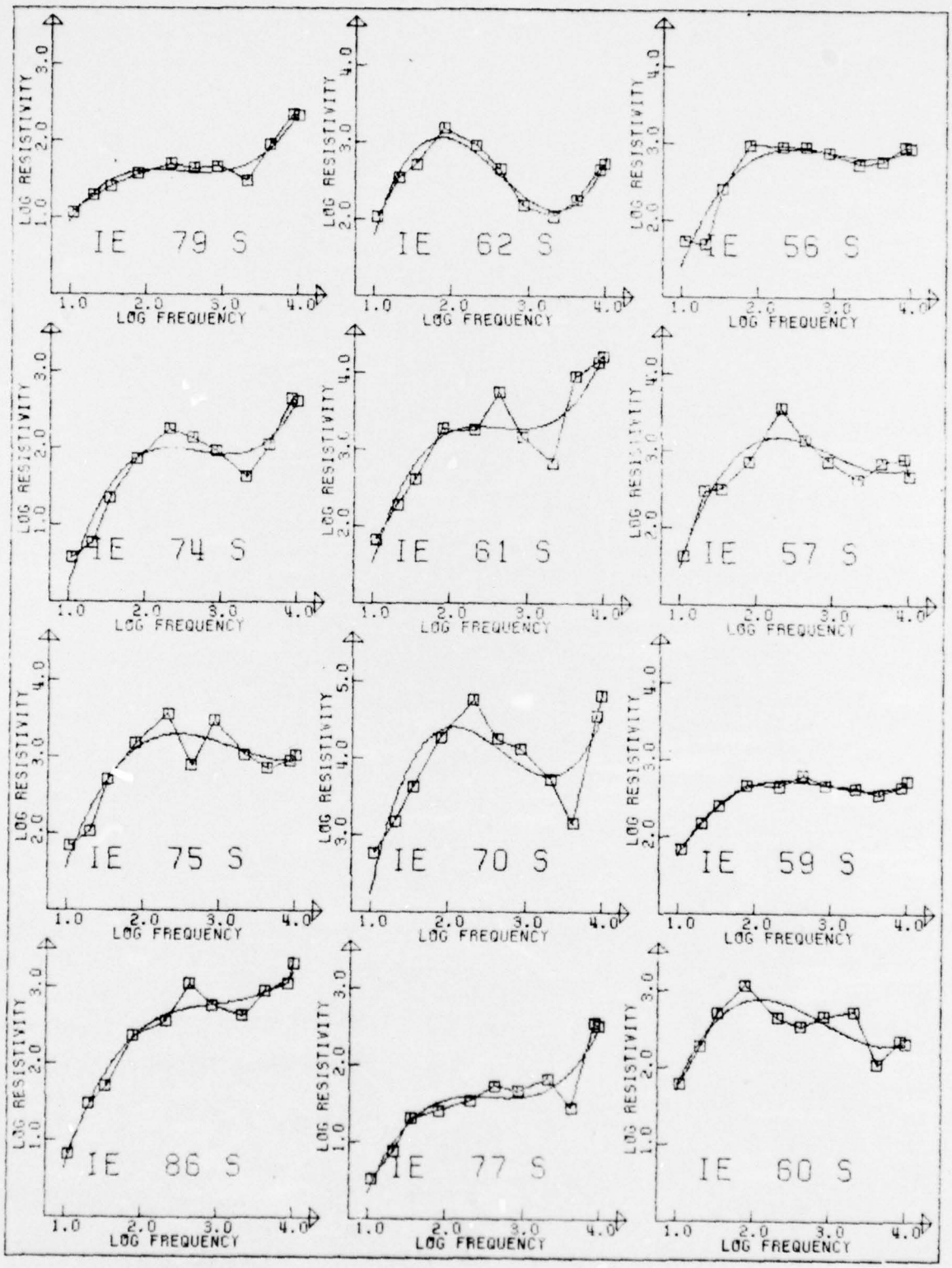
LOG RESISTIVITY
LOG FREQUENCY
IE 79 S
IE 62 S
IE 56 S
IE 74 S
IE 61 S
IE 57 S
IE 75 S
IE 70 S
IE 59 S
IE 86 S
IE 77 S
IE 60 S

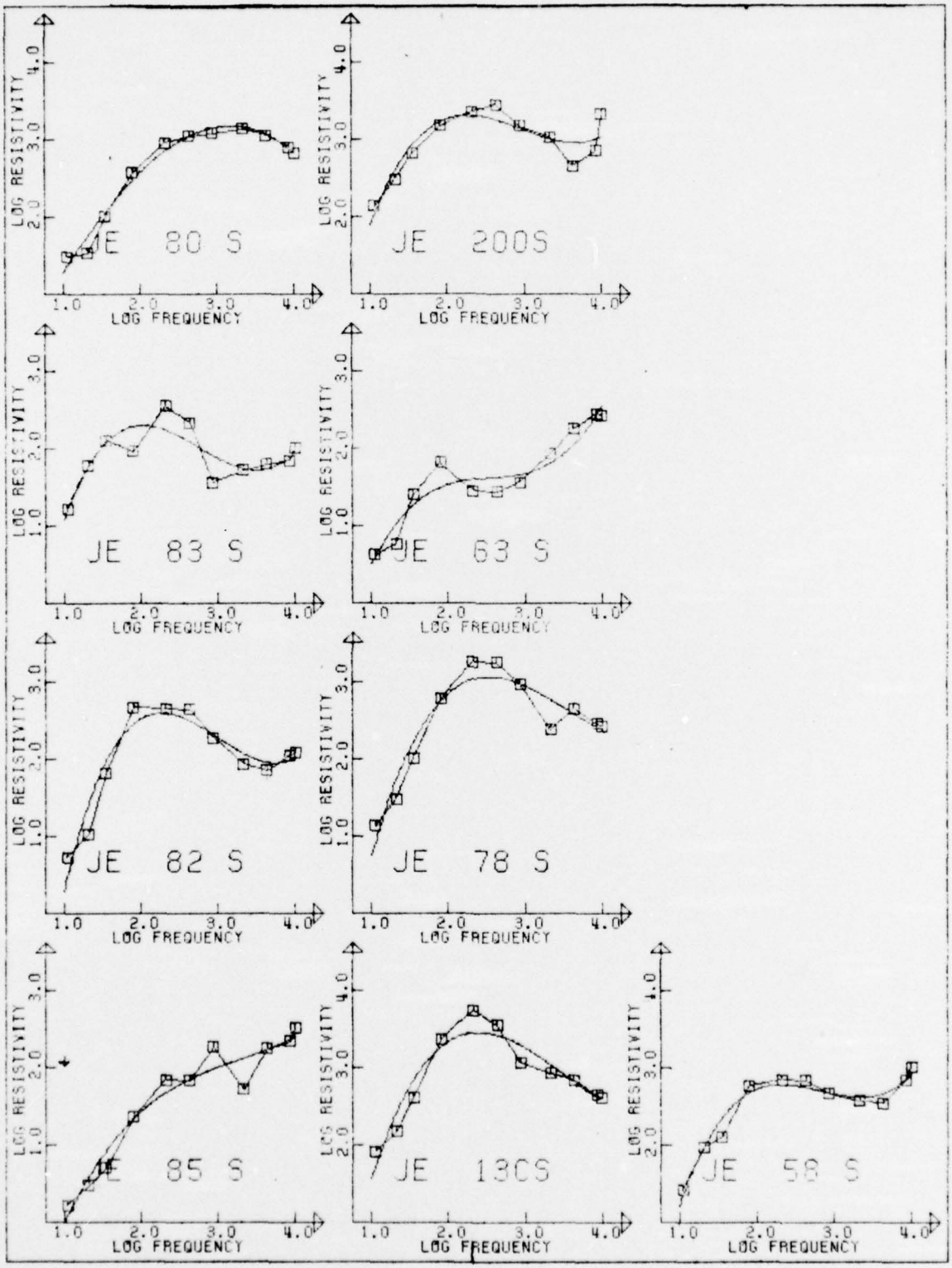
LOG RESISTIVITY
LOG FREQUENCY
JE 80 S
JE 200S
JE 83 S
JE 63 S
JE 82 S
JE 78 S
JE 85 S
JE 130S
JE 58 S

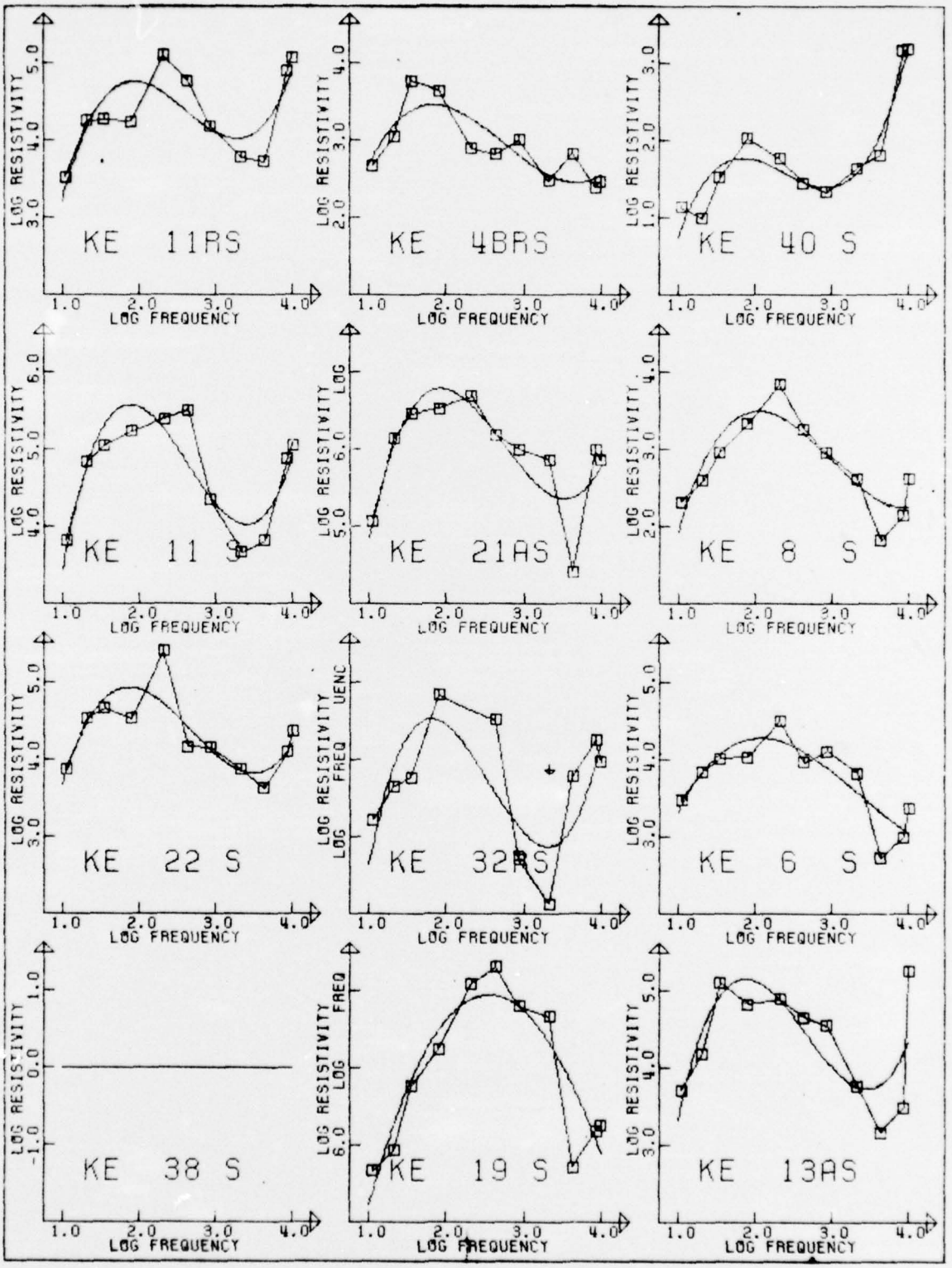
KE 11RS
KE 4BRS
KE 40 S
KE 11 S
KE 21AS
KE 8 S
KE 22 S
KE 32RS
KE 6 S
KE 38 S
KE 19 S
KE 13AS
LOG RESISTIVITY
LOG FREQUENCY

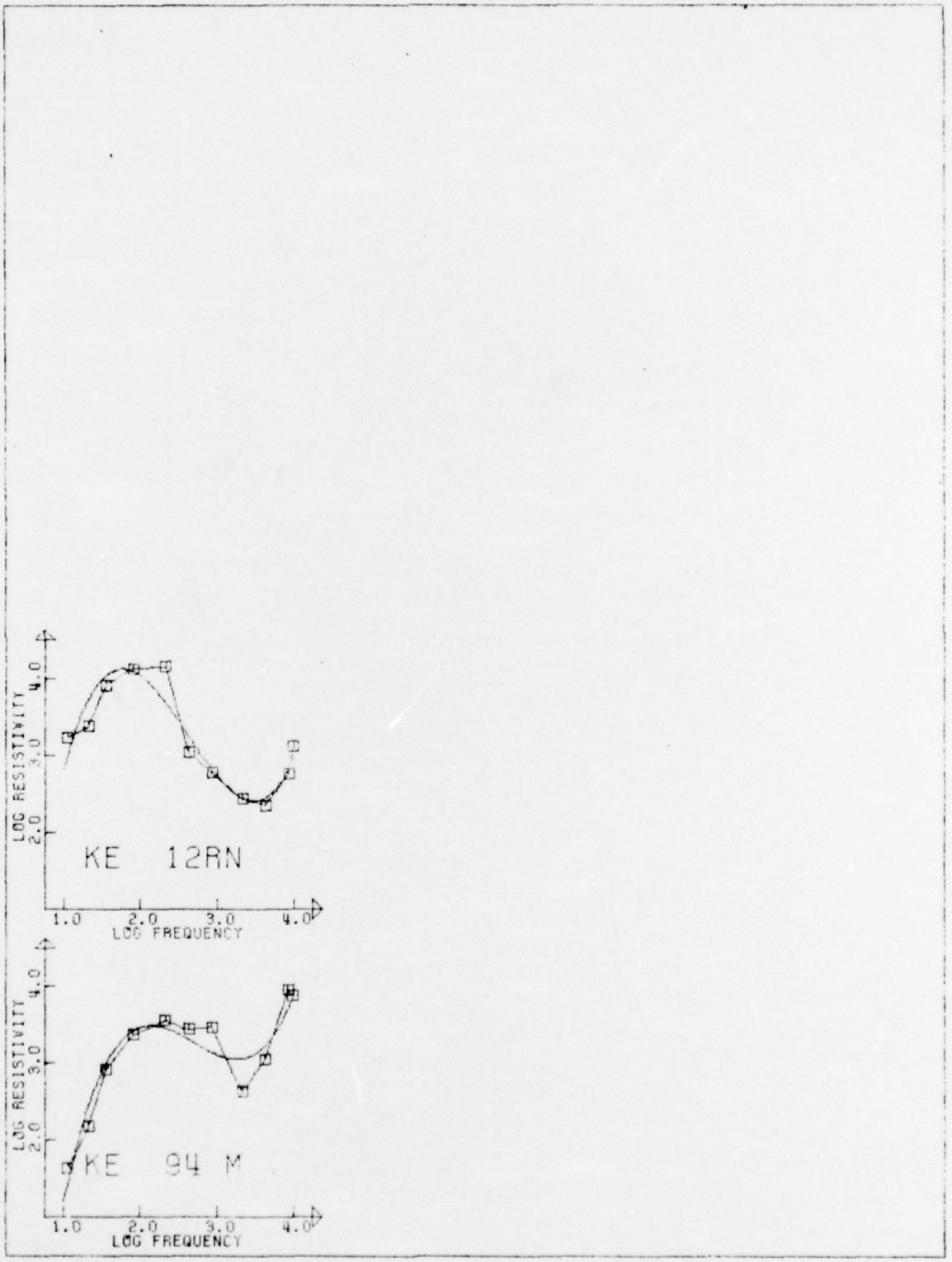
LOG RESISTIVITY
2.0
3.0
4.0
KE 12RN
1.0
2.0
3.0
4.0
LOG FREQUENCY
LOG RESISTIVITY
2.0
3.0
4.0
KE 94 M
1.0
2.0
3.0
4.0
LOG FREQUENCY

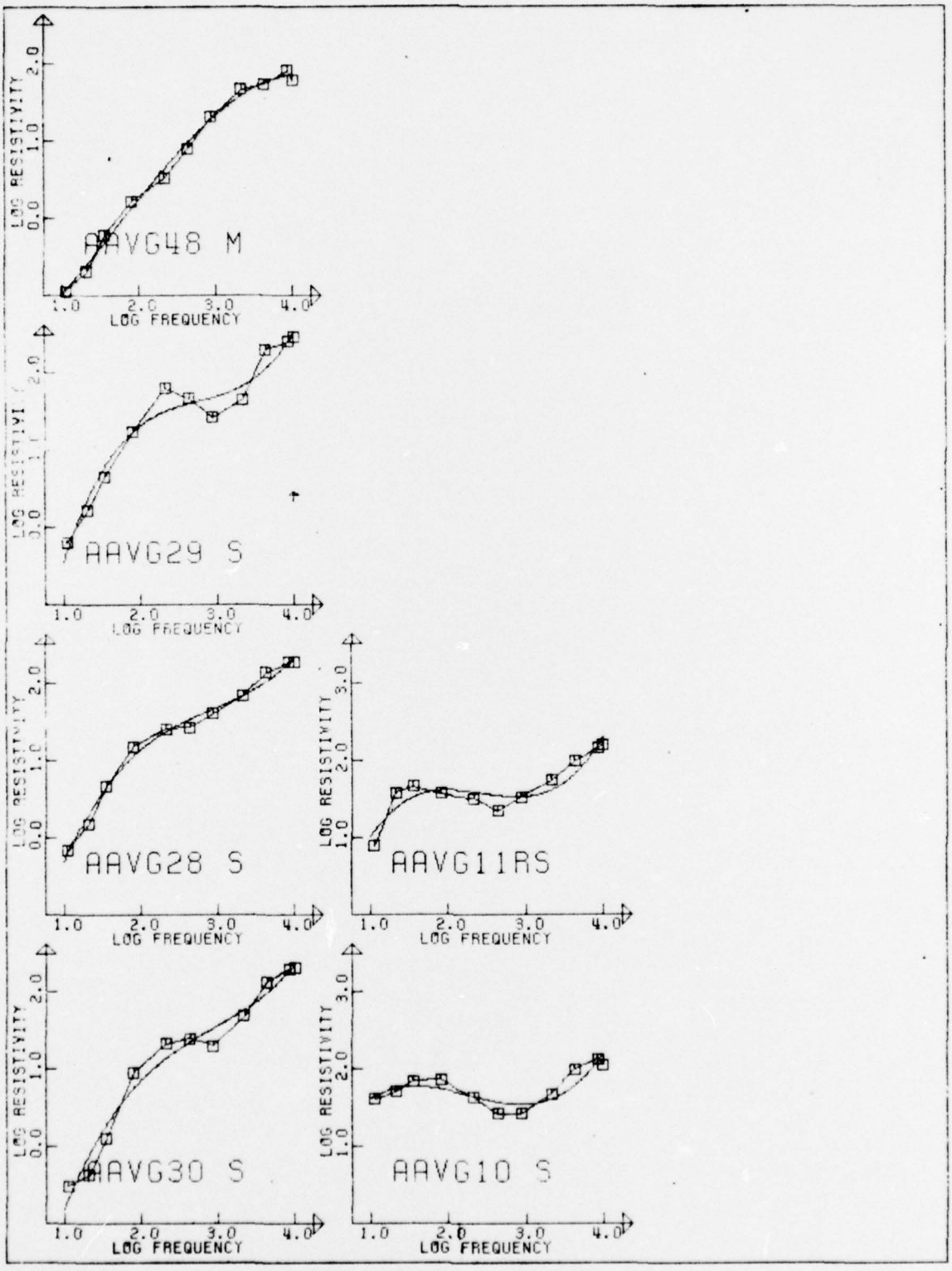
LOG RESISTIVITY
LOG FREQUENCY
AAVG48 M
AAVG29 S
AAVG28 S
AAVG11RS
AAVG30 S
AAVG10 S

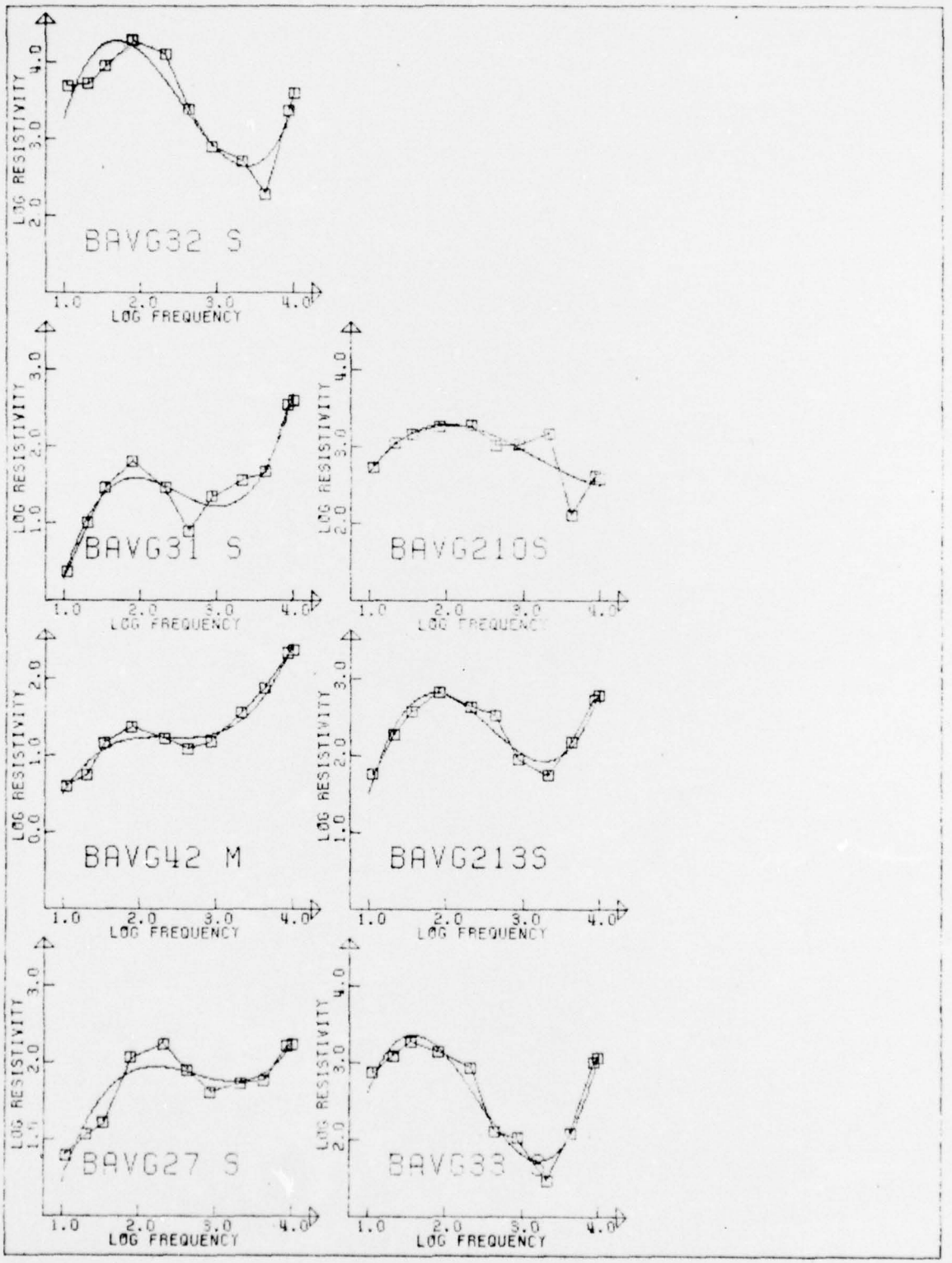
LOG RESISTIVITY
LOG FREQUENCY
BAVG32 S
BAVG31 S
BAVG210S
BAVG42 M
BAVG213S
BAVG27 S
BAVG33

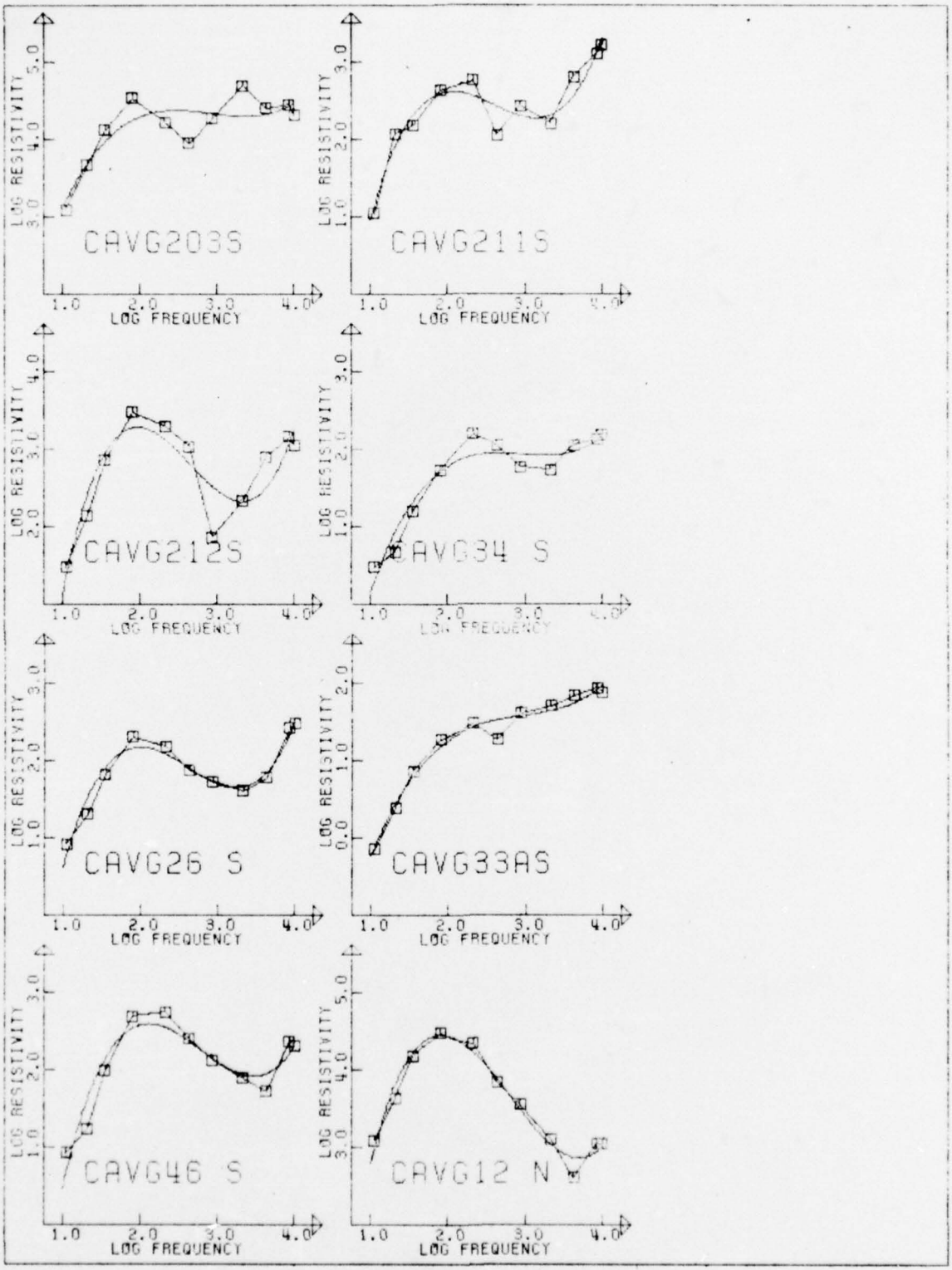
CAVG203S
CAVG211S
CAVG212S
CAVG34 S
CAVG26 S
CAVG33AS
CAVG46 S
CAVG12 N
LOG RESISTIVITY
LOG FREQUENCY

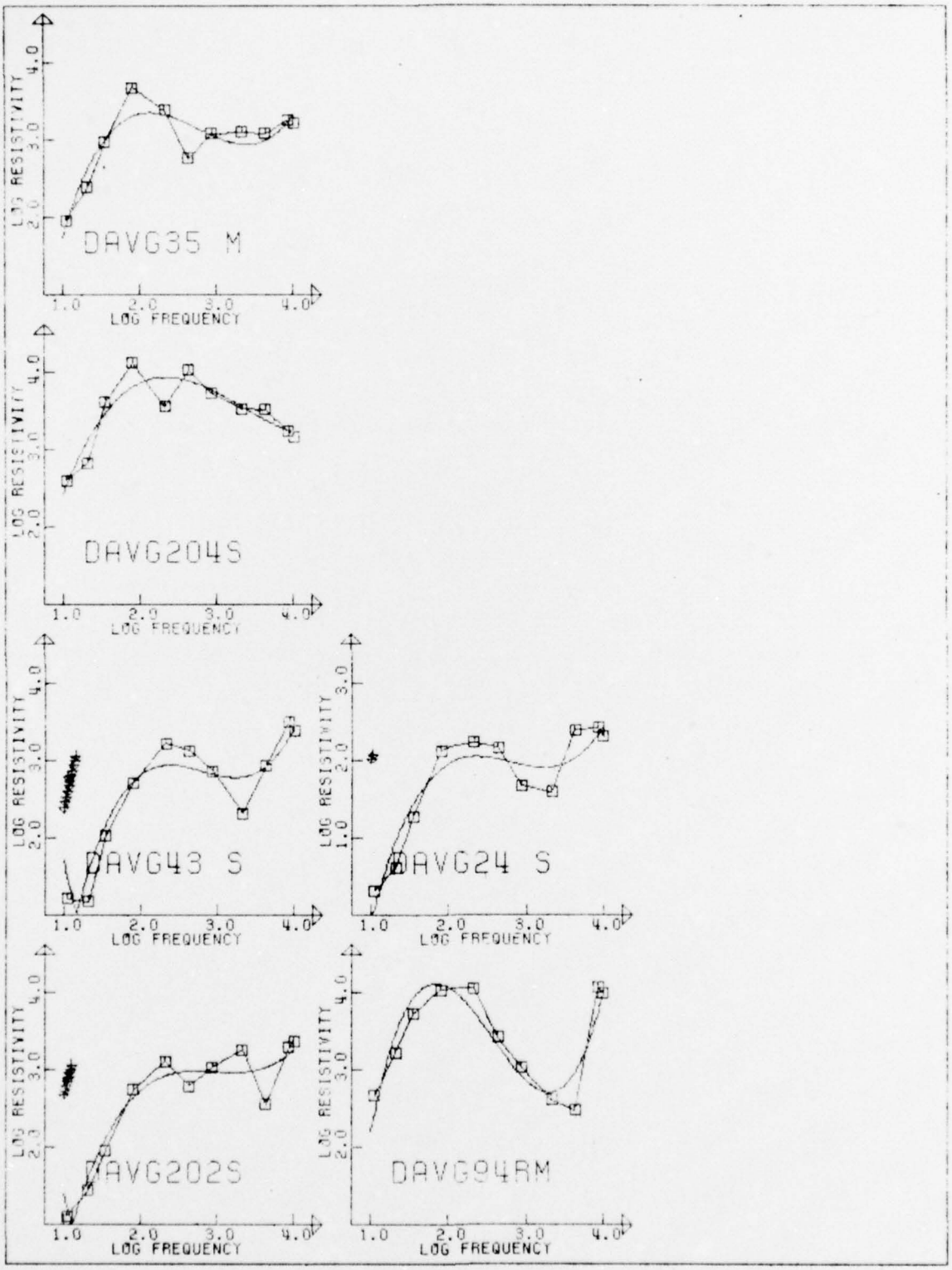
LOG RESISTIVITY
LOG FREQUENCY
DAVG35 M
DAVG204S
DAVG43 S
DAVG24 S
DAVG202S
DAVG94RM

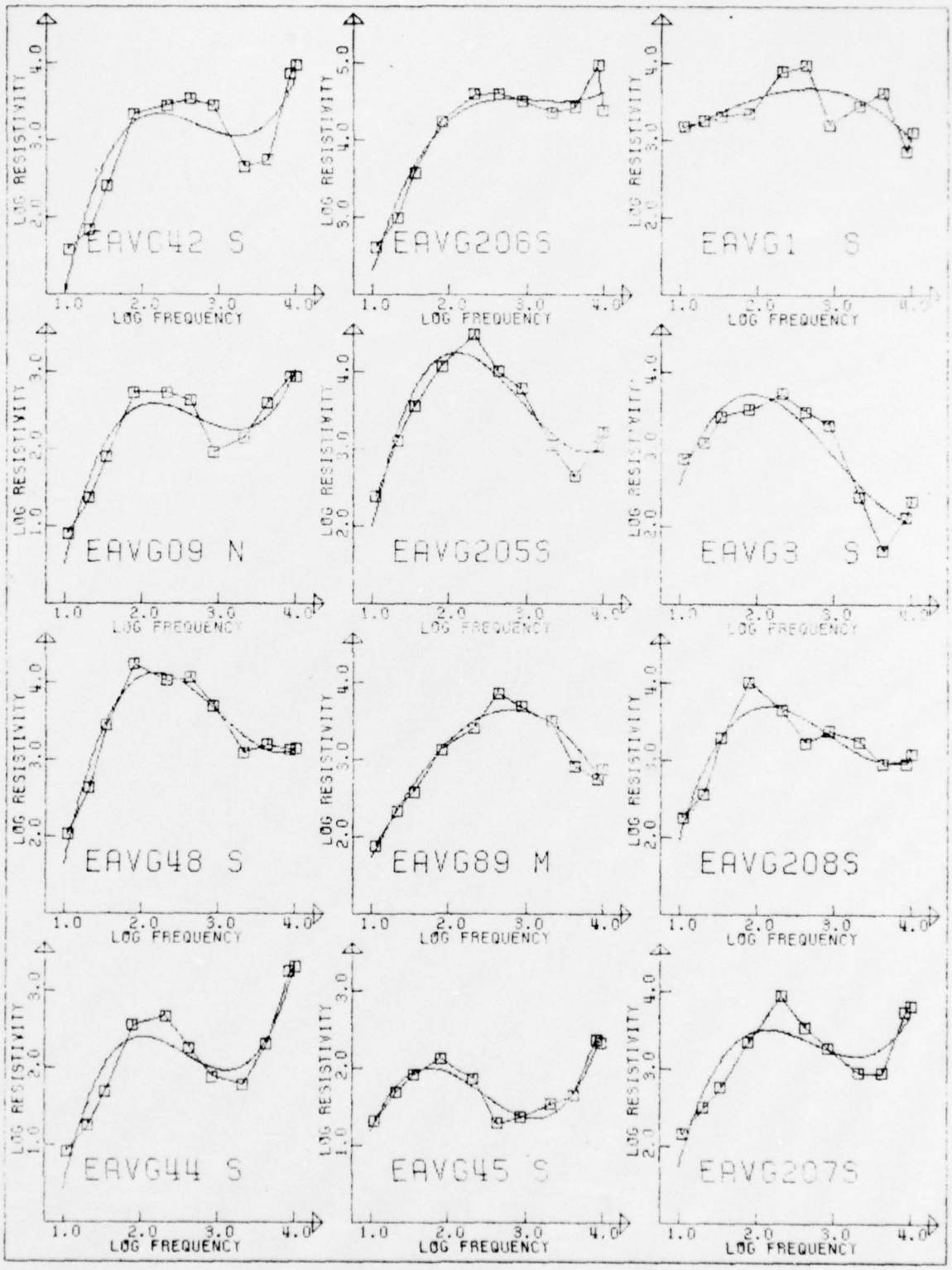
LOG RESISTIVITY
LOG FREQUENCY
EAVG42 S
EAVG206S
EAVG1 S
EAVG09 N
EAVG205S
EAVG3 S
EAVG48 S
EAVG89 M
EAVG208S
EAVG44 S
EAVG45 S
EAVG207S

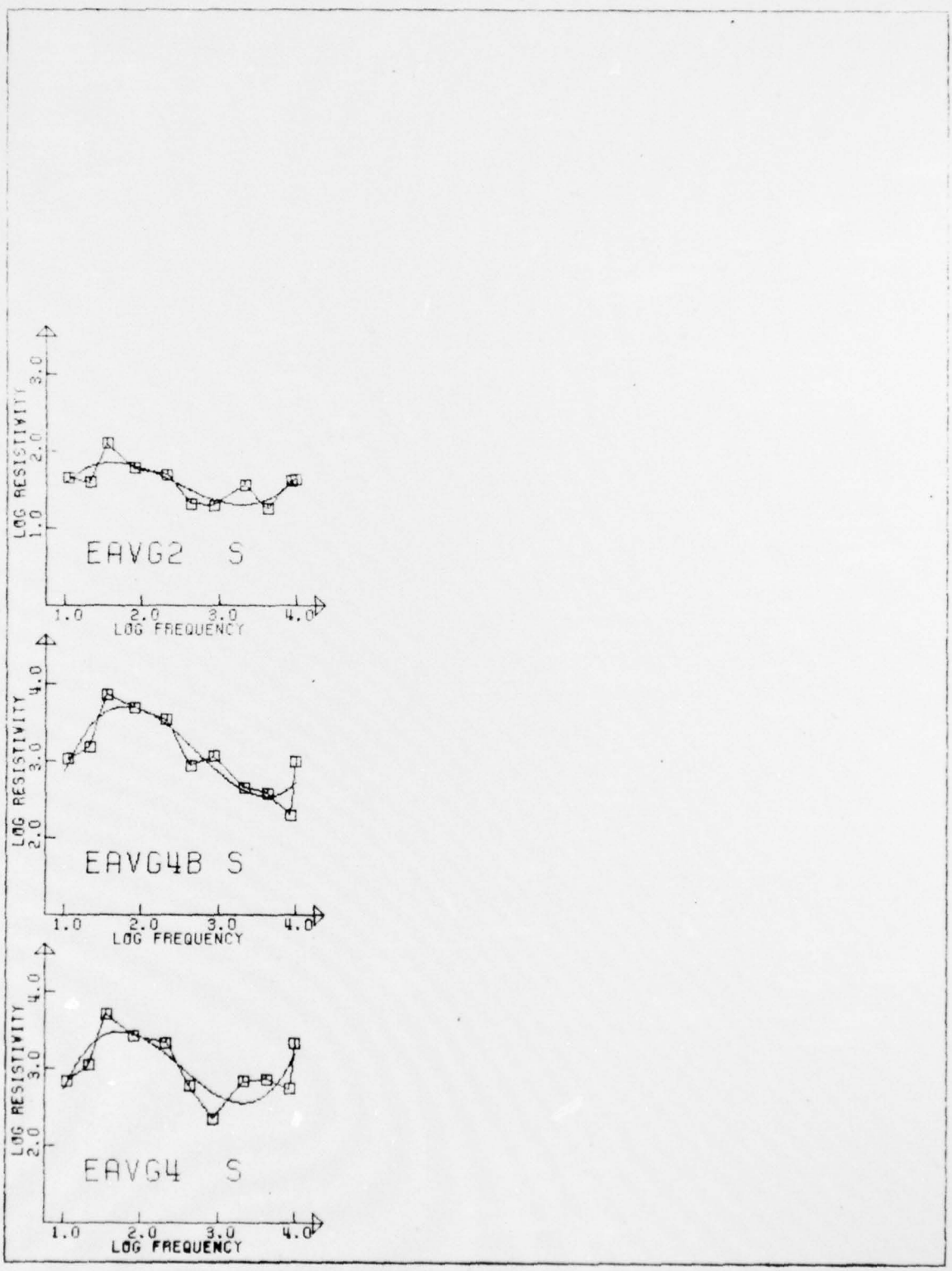
LOG RESISTIVITY
1.0
2.0
3.0
EAVG2 S
1.0
2.0
3.0
4.0
LOG FREQUENCY
LOG RESISTIVITY
2.0
3.0
4.0
EAVG4B S
1.0
2.0
3.0
4.0
LOG FREQUENCY
LOG RESISTIVITY
2.0
3.0
4.0
EAVG4 S
1.0
2.0
3.0
4.0
LOG FREQUENCY

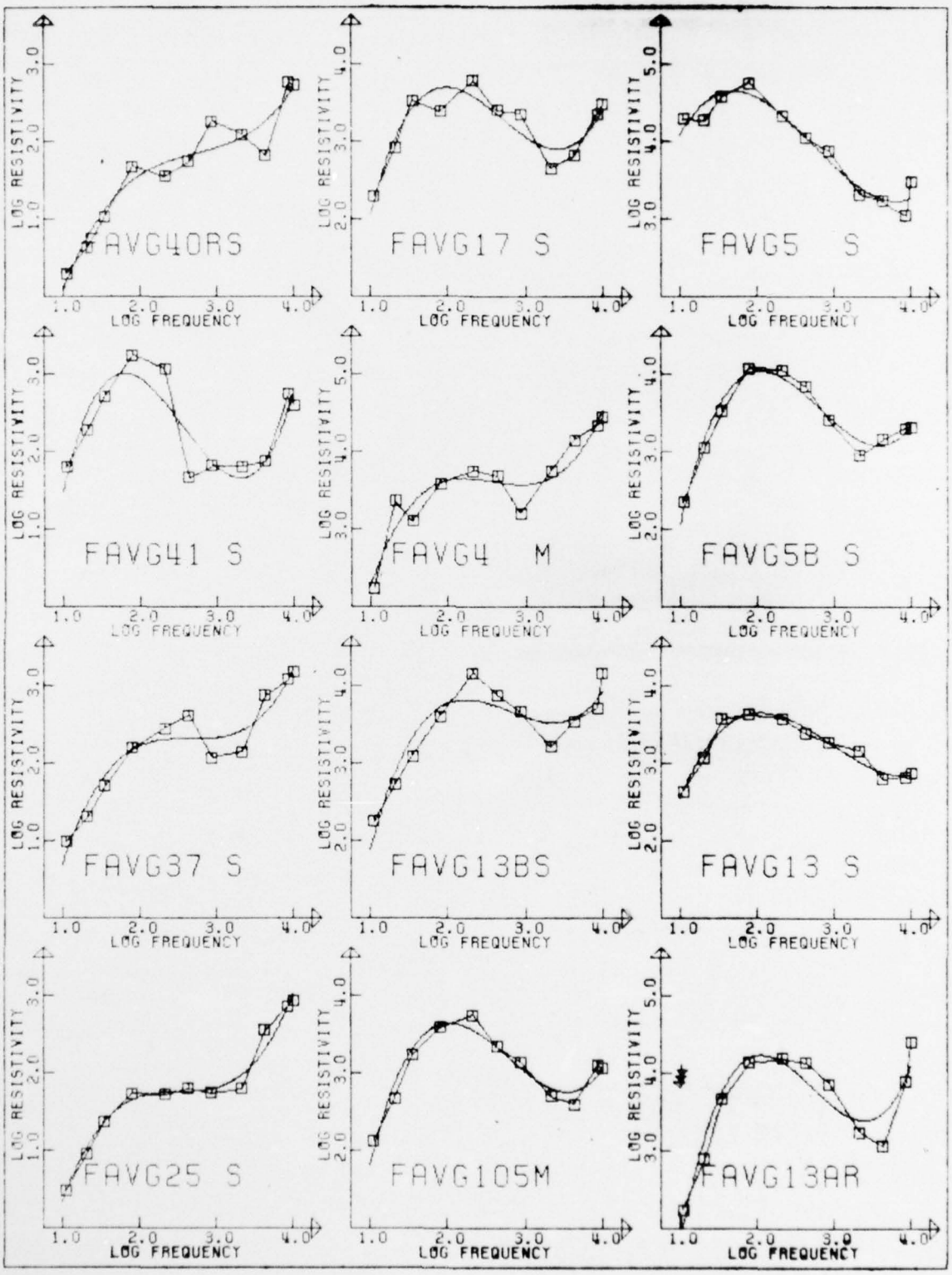
FAVG40RS
FAVG17 S
FAVG5 S
FAVG41 S
FAVG4 M
FAVG5B S
FAVG37 S
FAVG13BS
FAVG13 S
FAVG25 S
FAVG105M
FAVG13AR
LOG RESISTIVITY
LOG FREQUENCY

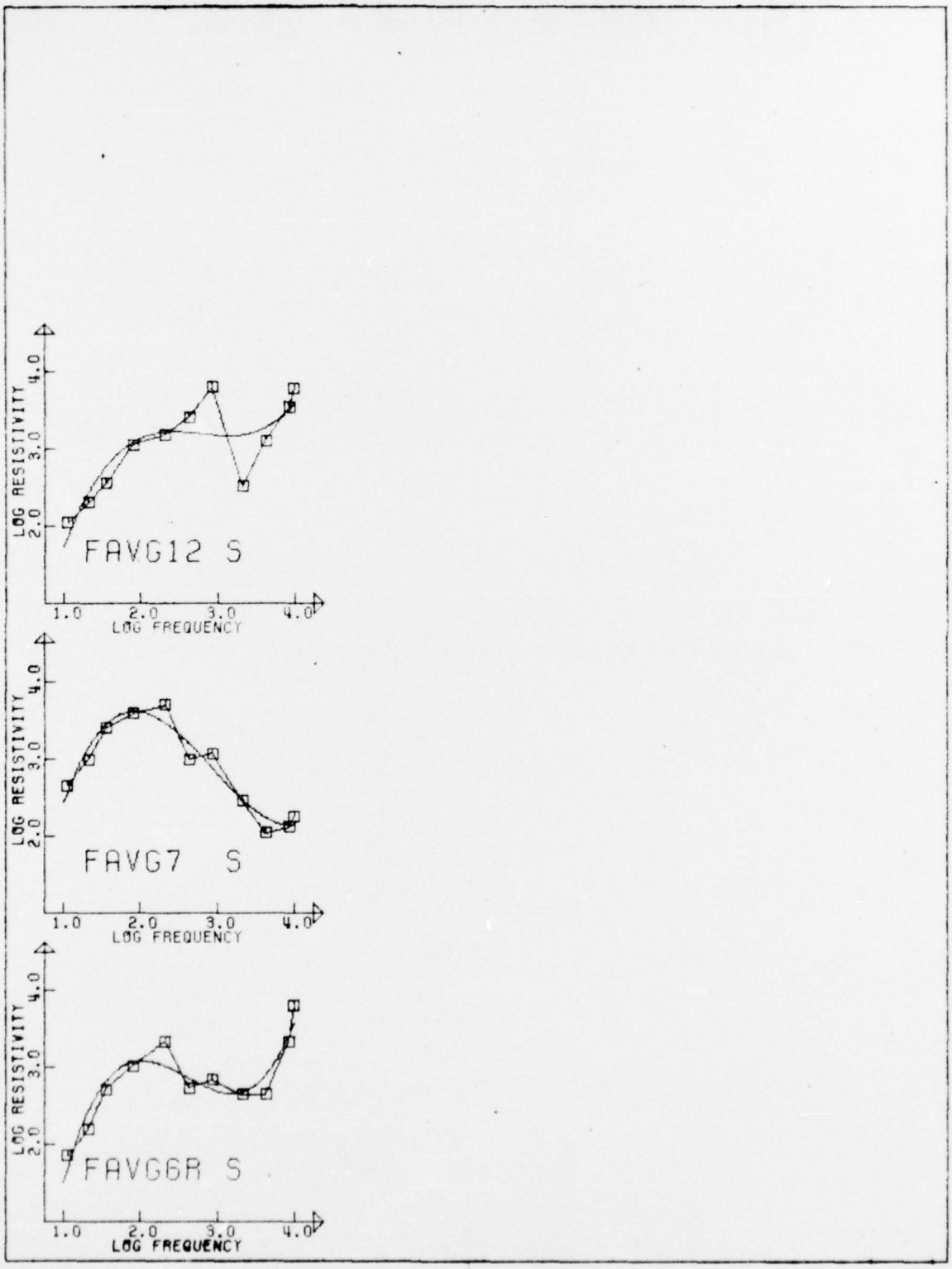
LOG RESISTIVITY
4.0
3.0
2.0
FAVG12 S
1.0
2.0
3.0
4.0
LOG FREQUENCY
LOG RESISTIVITY
4.0
3.0
2.0
FAVG7 S
1.0
2.0
3.0
4.0
LOG FREQUENCY
LOG RESISTIVITY
4.0
3.0
2.0
FAVG6R S
1.0
2.0
3.0
4.0
LOG FREQUENCY

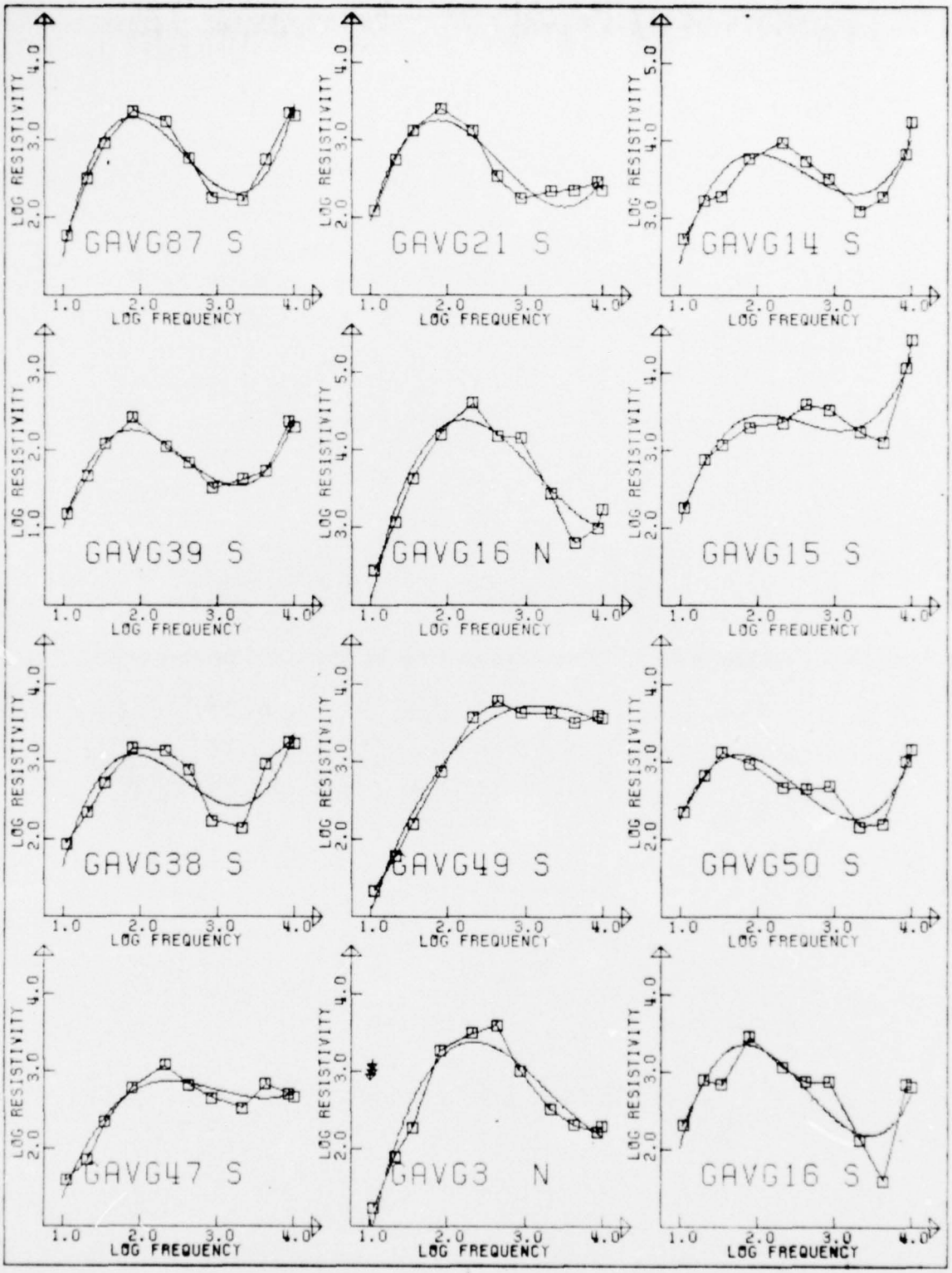
GAVG87 S
GAVG21 S
GAVG14 S
GAVG39 S
GAVG16 N
GAVG15 S
GAVG38 S
GAVG49 S
GAVG50 S
GAVG47 S
GAVG3 N
GAVG16 S
LOG RESISTIVITY
LOG FREQUENCY

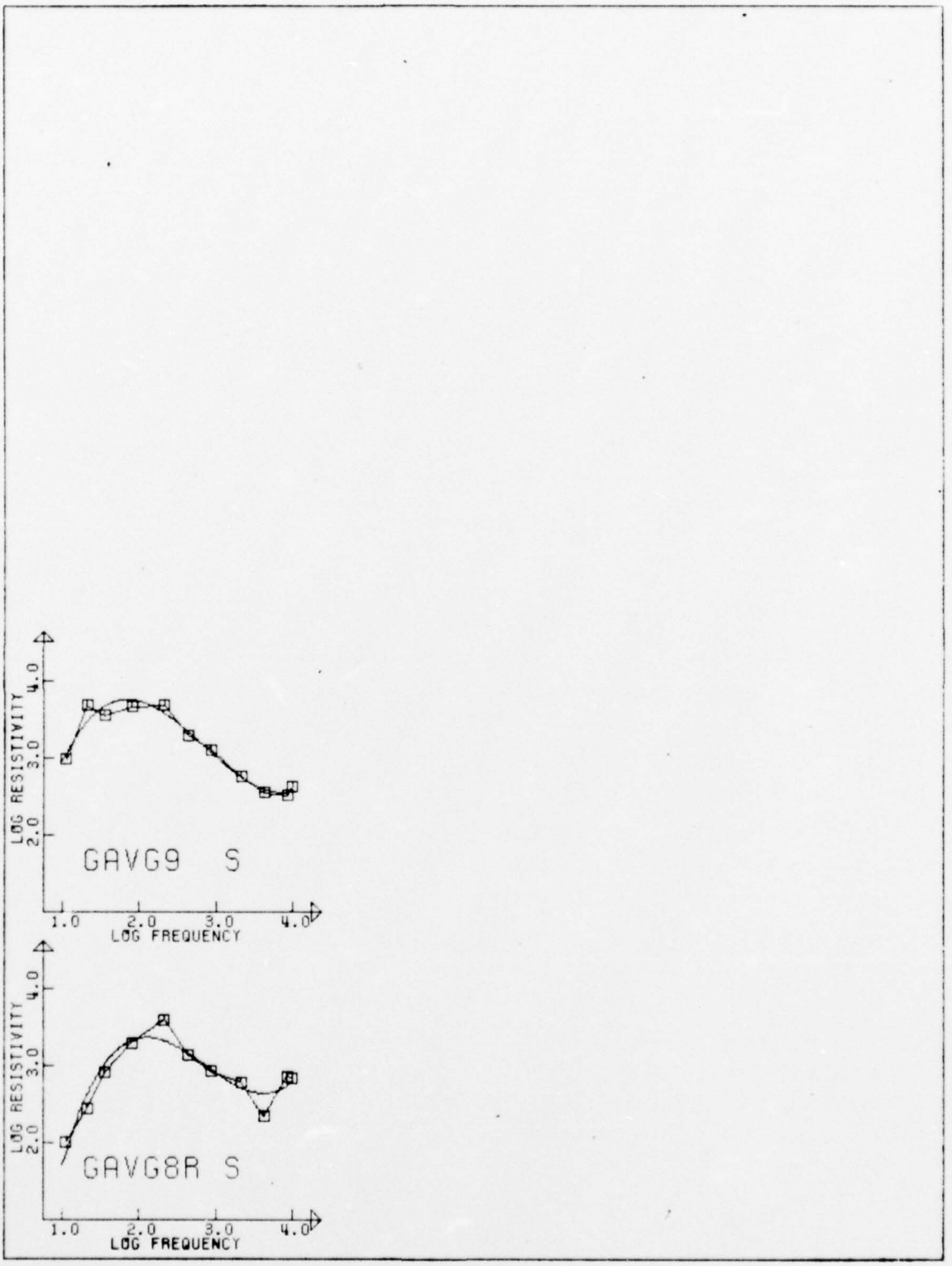
LOG RESISTIVITY
4.0
3.0
2.0
GAVG9 S
1.0
2.0
3.0
4.0
LOG FREQUENCY
LOG RESISTIVITY
4.0
3.0
2.0
GAVG8R S
1.0
2.0
3.0
4.0
LOG FREQUENCY

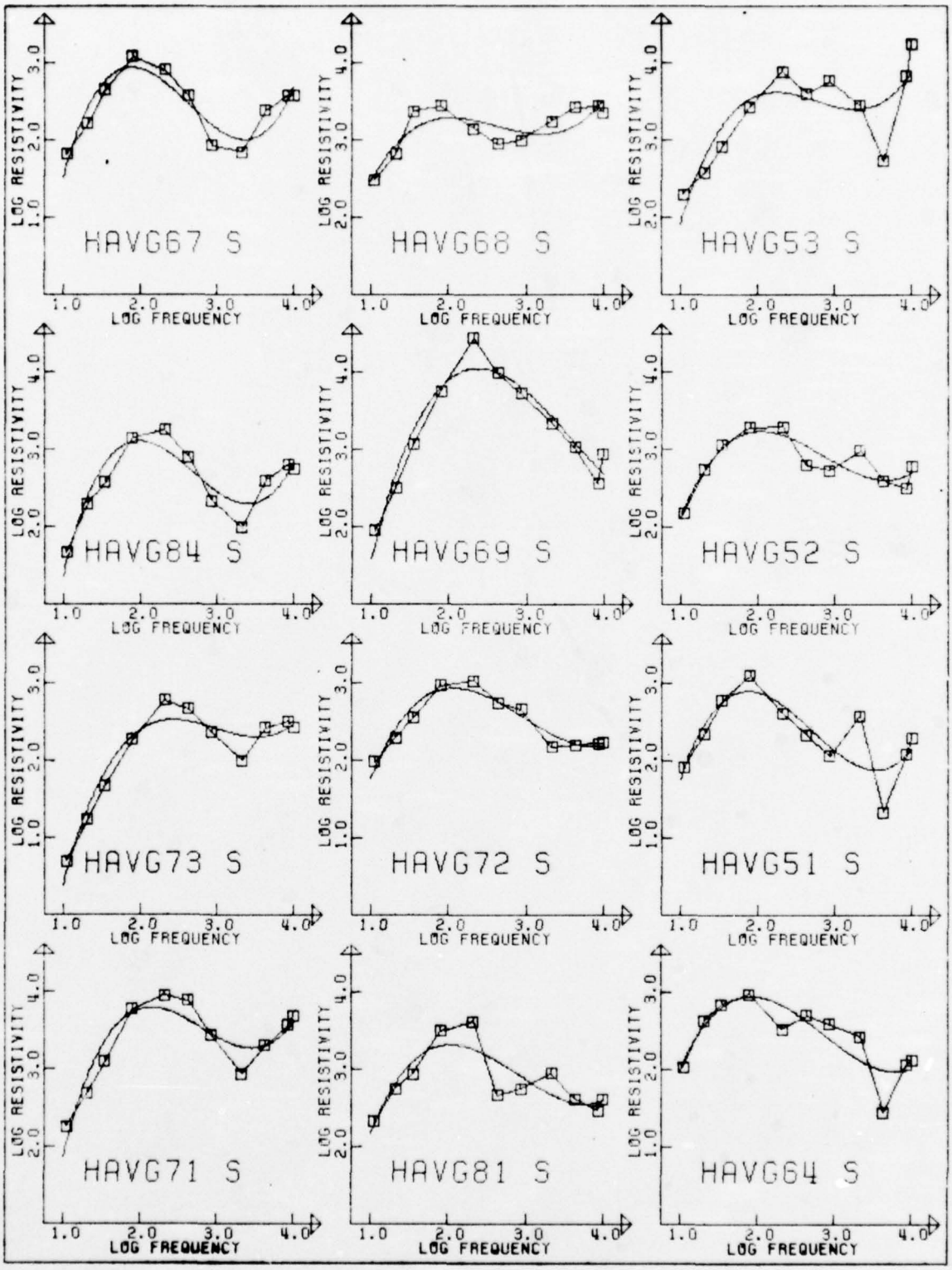
HAVG67 S
HAVG68 S
HAVG53 S
HAVG84 S
HAVG69 S
HAVG52 S
HAVG73 S
HAVG72 S
HAVG51 S
HAVG71 S
HAVG81 S
HAVG64 S
LOG RESISTIVITY
LOG FREQUENCY
1.0
2.0
3.0
4.0

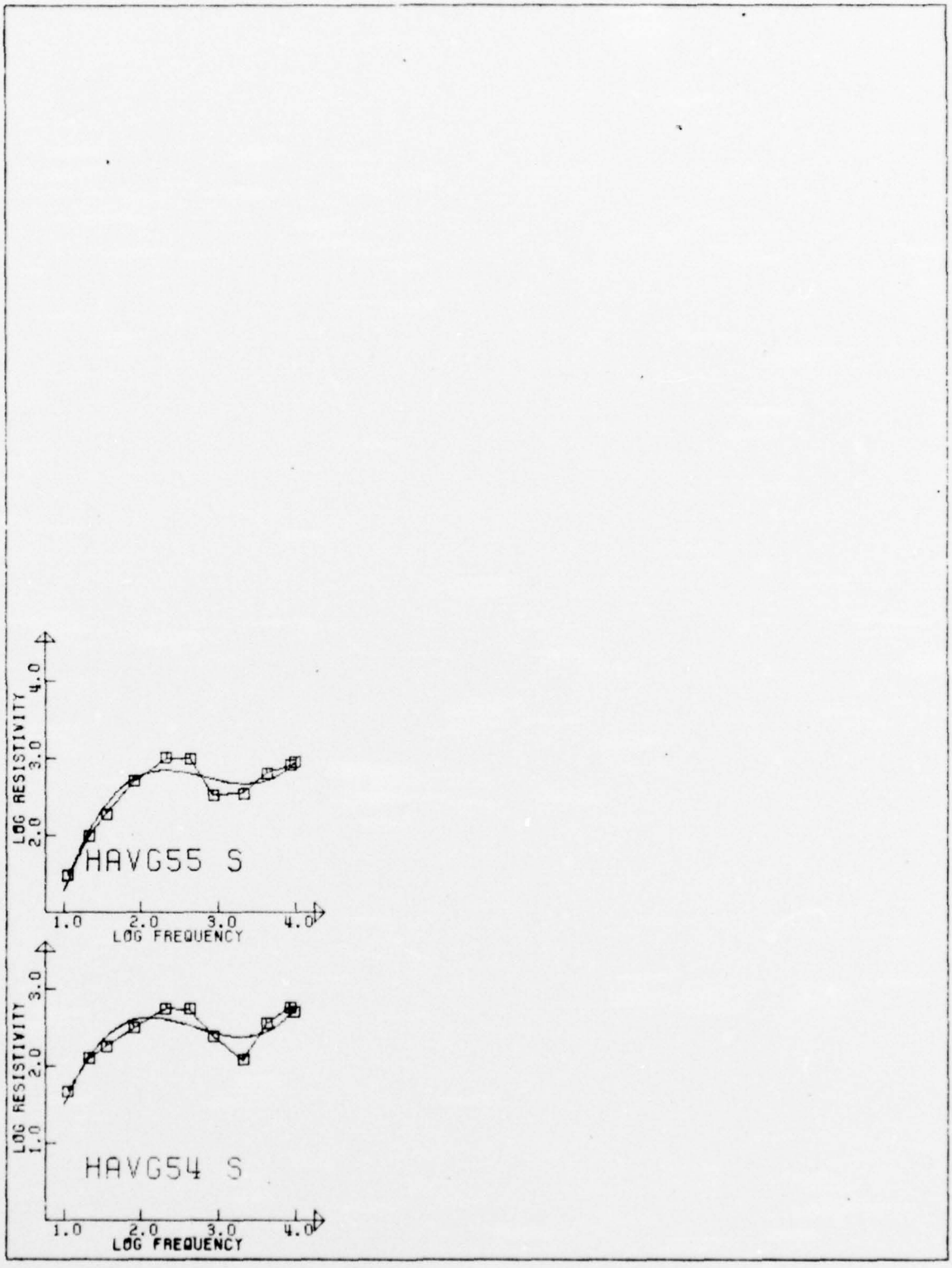
LOG RESISTIVITY
4.0
3.0
2.0
HAVG55 S
1.0
2.0
3.0
4.0
LOG FREQUENCY
LOG RESISTIVITY
3.0
2.0
1.0
HAVG54 S
1.0
2.0
3.0
4.0
LOG FREQUENCY

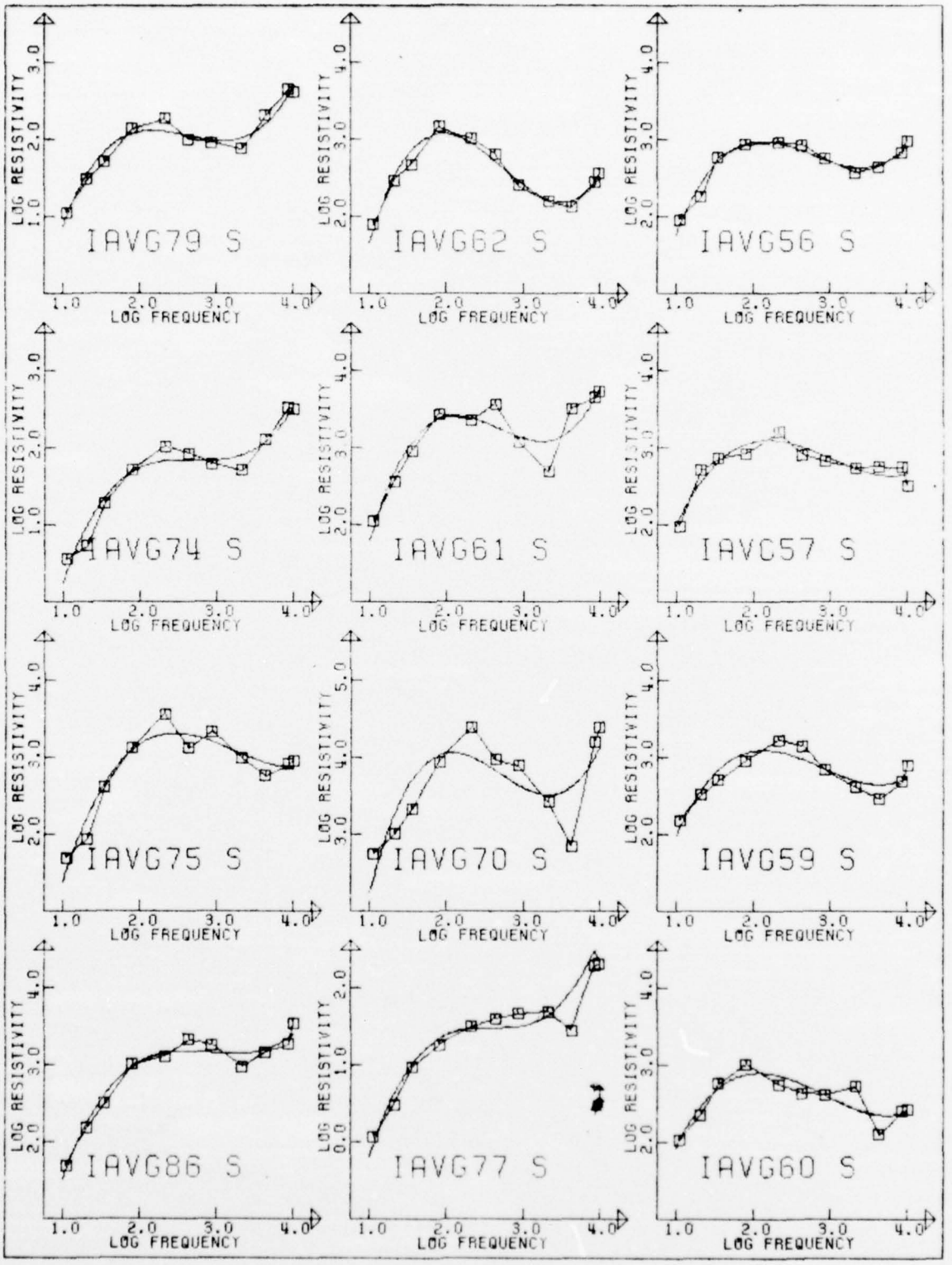
IAVG79 S
IAVG62 S
IAVG56 S
IAVG74 S
IAVG61 S
IAVG57 S
IAVG75 S
IAVG70 S
IAVG59 S
IAVG86 S
IAVG77 S
IAVG60 S
LOG RESISTIVITY
LOG FREQUENCY

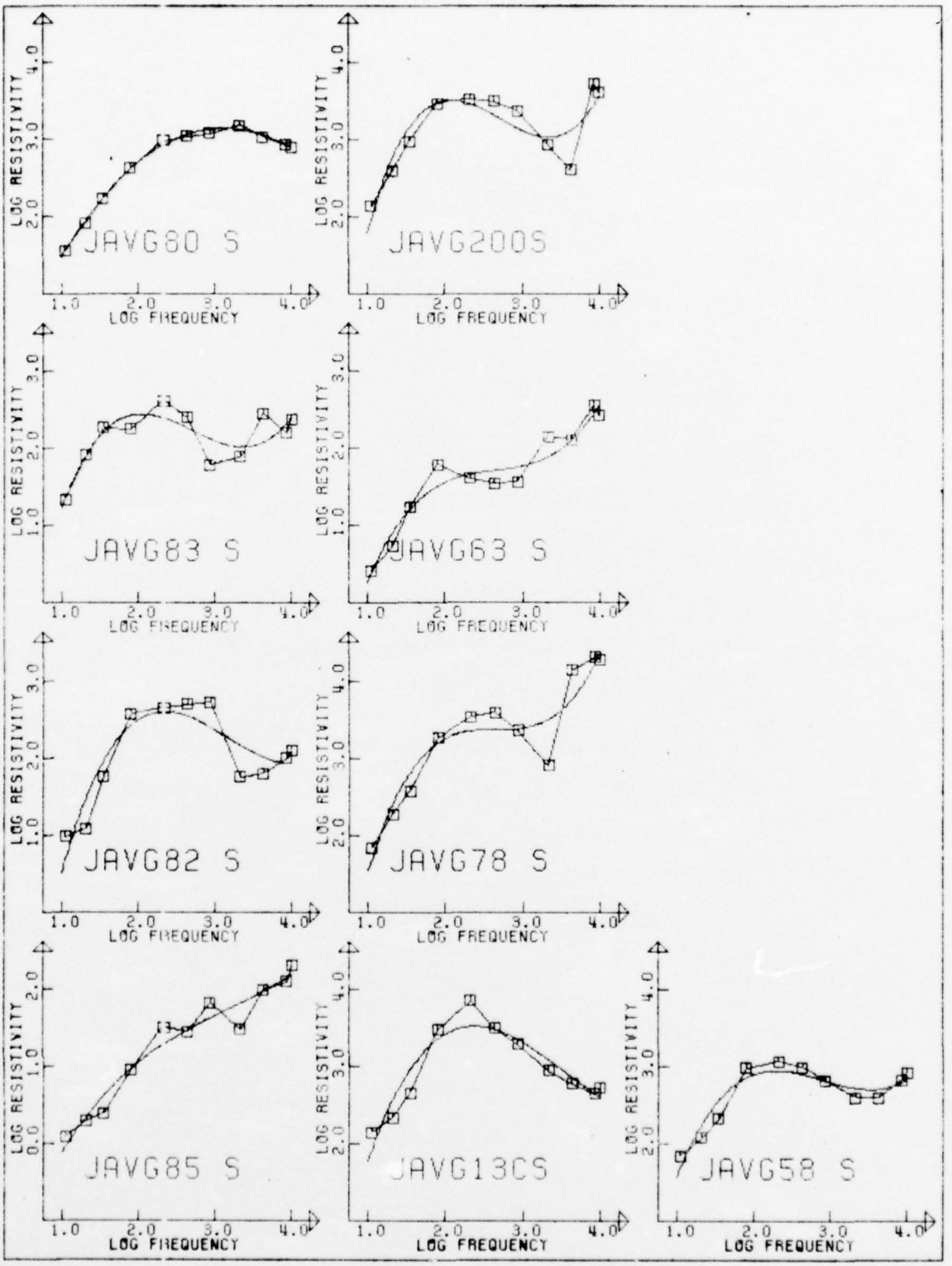
LOG RESISTIVITY
LOG FREQUENCY
JAVG80 S
JAVG200S
JAVG83 S
JAVG63 S
JAVG82 S
JAVG78 S
JAVG85 S
JAVG130S
JAVG58 S

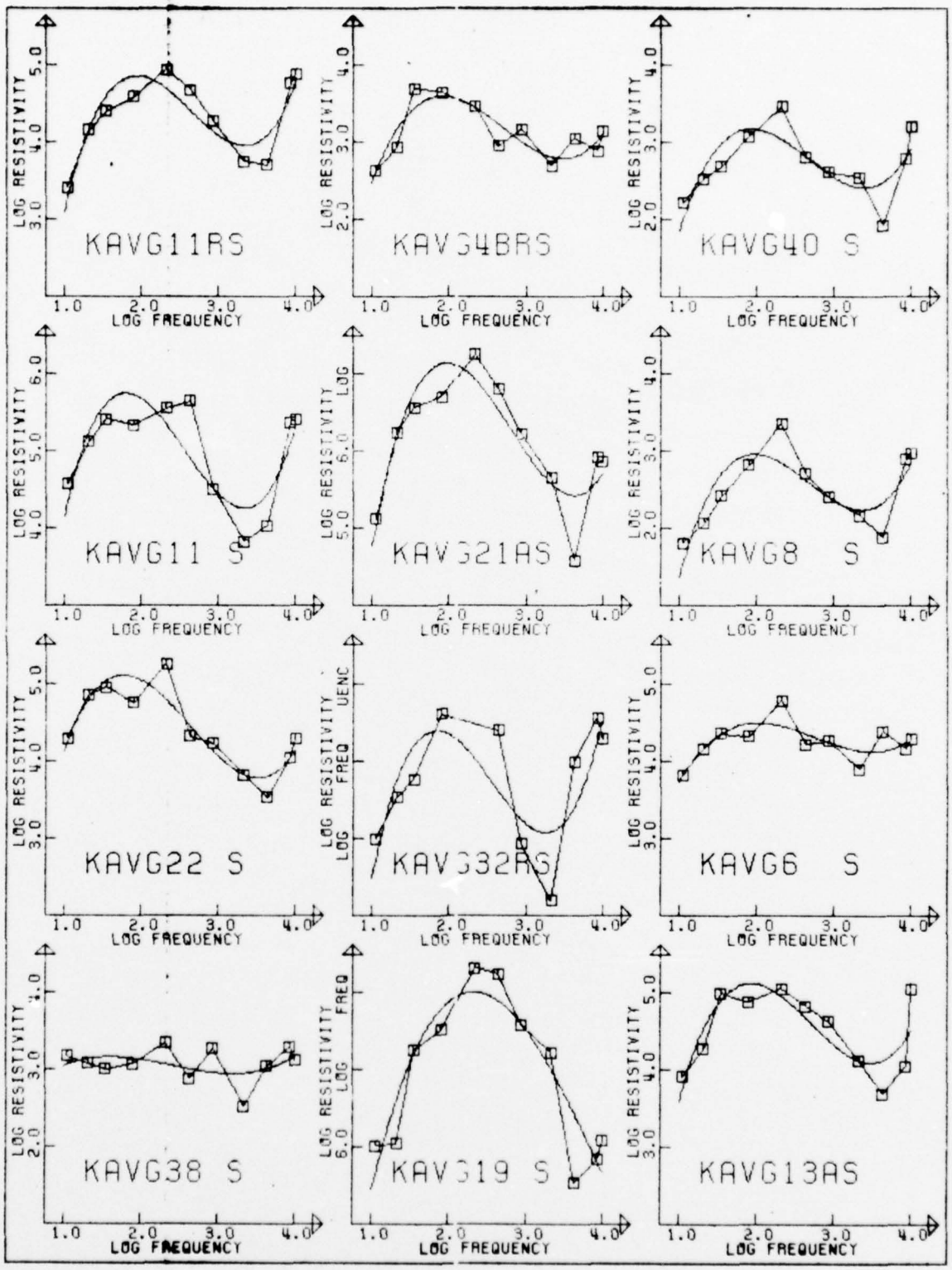
KAVG11RS
KAVG34BRS
KAVG40 S
KAVG11 S
KAVG21AS
KAVG8 S
KAVG22 S
KAVG32RS
KAVG6 S
KAVG38 S
KAVG19 S
KAVG13AS
LOG RESISTIVITY
LOG FREQUENCY
LOG FREQ UENC
LOG FREQ

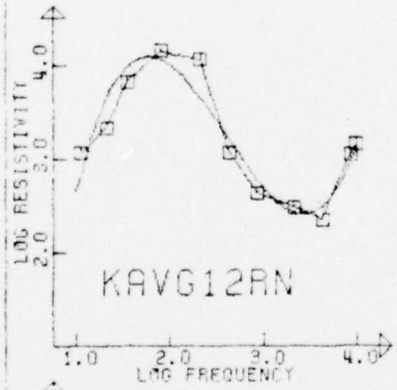
LOG RESISTIVITY
4.0
3.0
2.0
KAVG12RN
1.0
2.0
3.0
4.0
LOG FREQUENCY

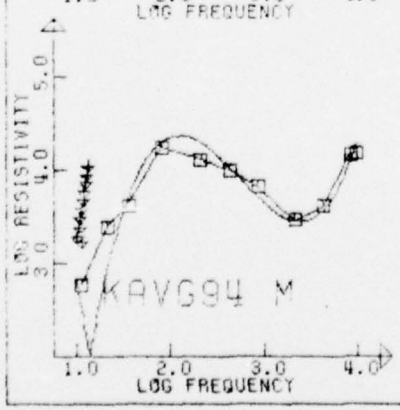
LOG RESISTIVITY
5.0
4.0
3.0
KAVG94 M
1.0
2.0
3.0
4.0
LOG FREQUENCY

SECTION A.2

MICHIGAN

PSEUDOSECTIONS

- NORTH-SOUTH ORIENTATION
- EAST-WEST ORIENTATION
- AVERAGED DATA

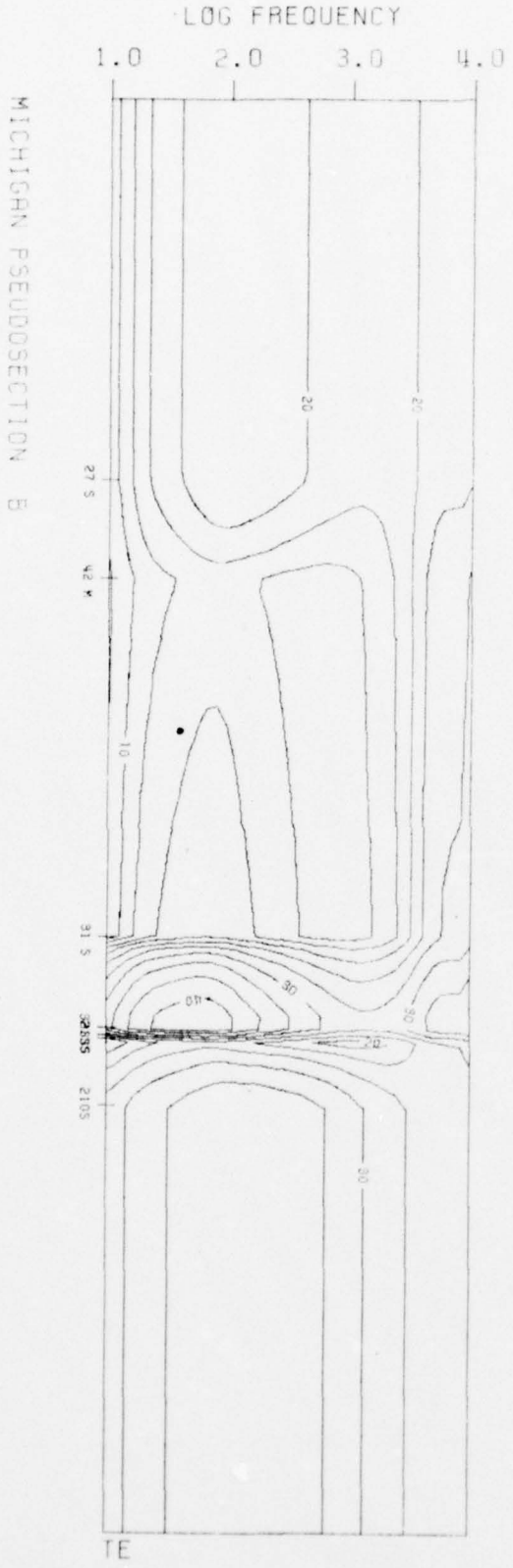
LOG FREQUENCY
1.0
2.0
3.0
4.0
MICHIGAN PSEUDOSECTION B
TE

LOG FREQUENCY
1.0
2.0
3.0
4.0
MICHIGAN PSEUDOSECTION B
TE

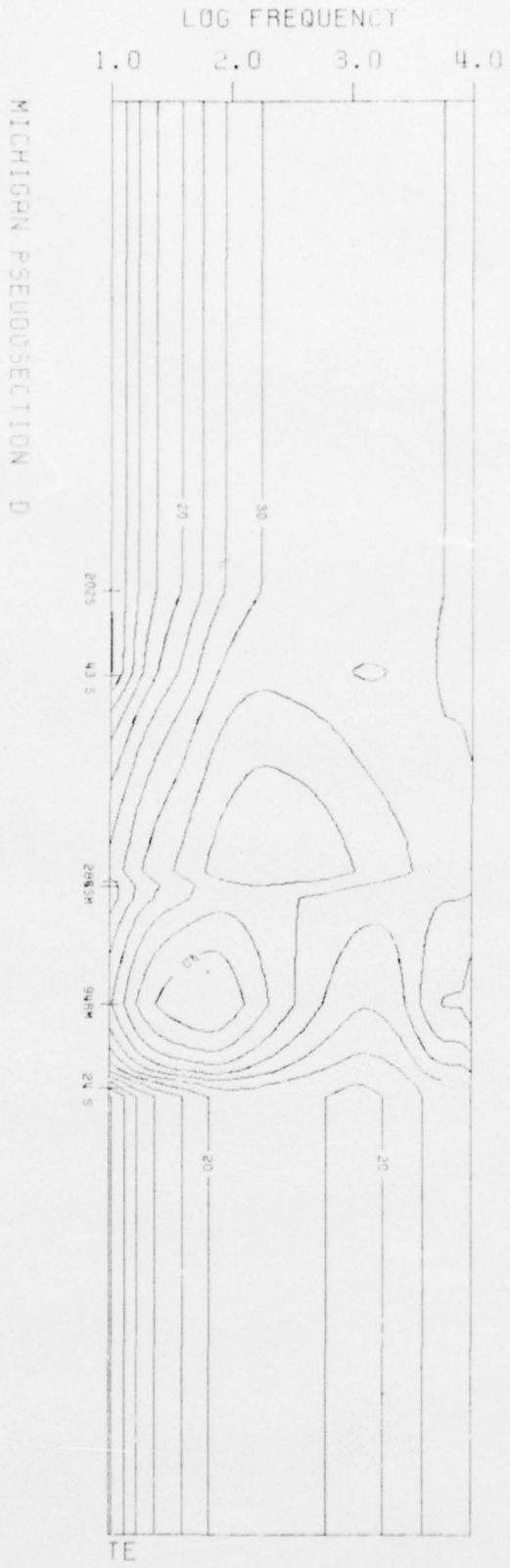
LOG FREQUENCY
1.0
2.0
3.0
4.0
MICHIGAN PSEUDOSECTION D
20
30
20
20
TE

LOG FREQUENCY
1.0
2.0
3.0
4.0
20
20
20
TE

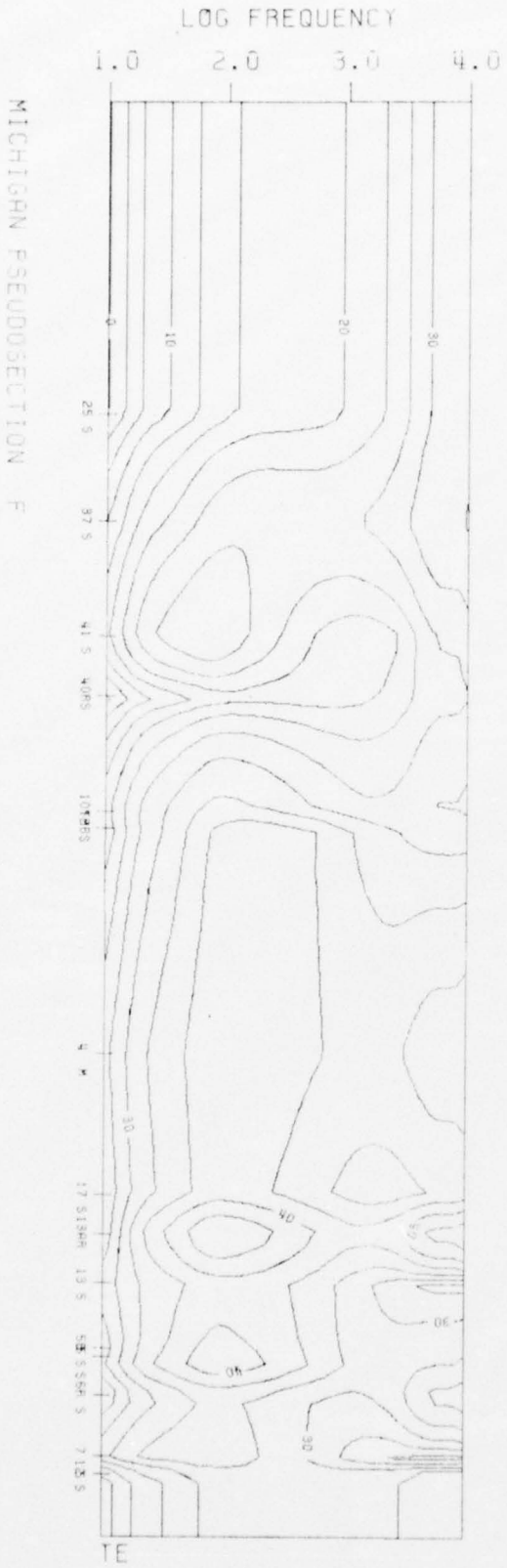
LOG FREQUENCY
1.0
2.0
3.0
4.0
MICHIGAN PSEUDOSECTION F
TE

LOG FREQUENCY
1.0
2.0
3.0
4.0
MICHIGAN PSEUDOSECTION E
TE

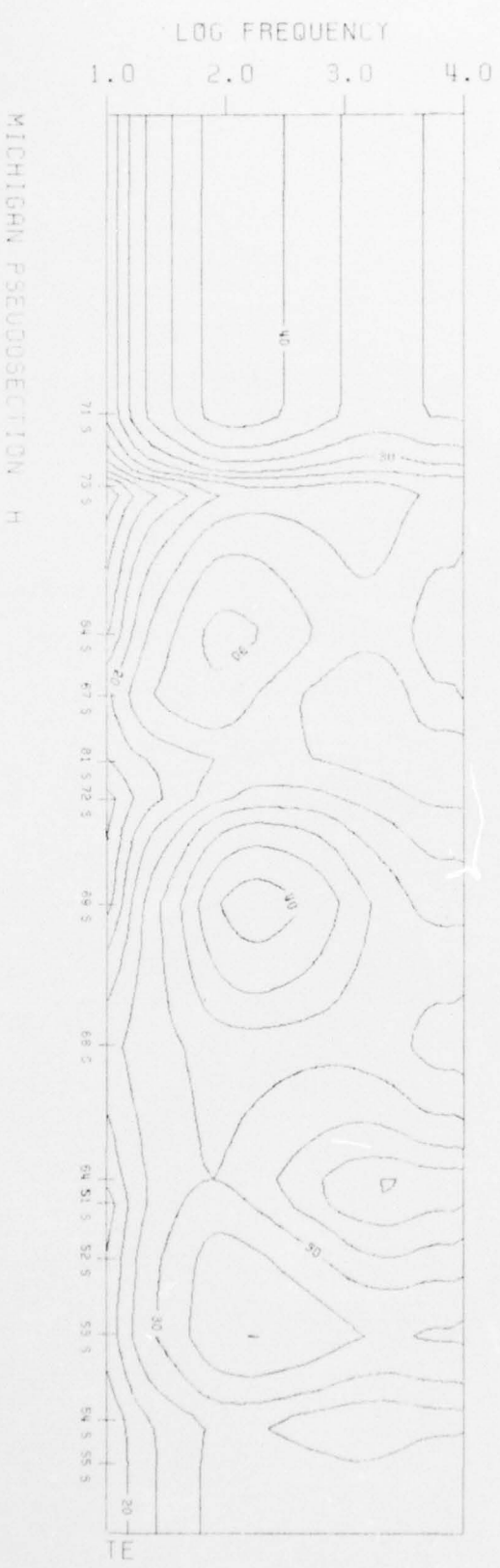
LOG FREQUENCY
1.0
2.0
3.0
4.0
MICHIGAN PSEUDOSECTION H
TE

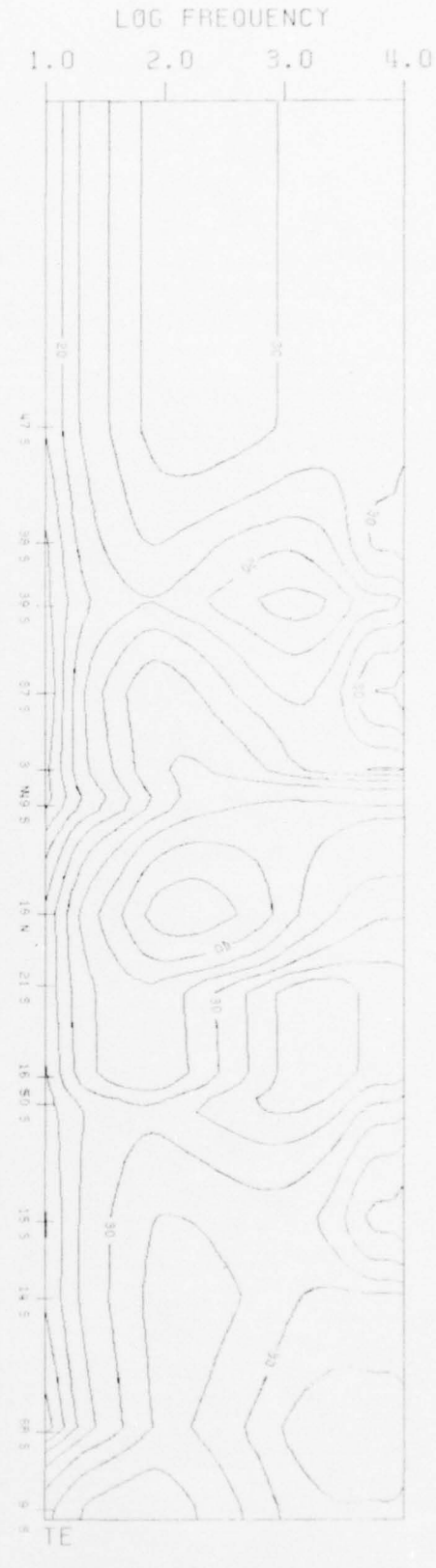
LOG FREQUENCY
1.0
2.0
3.0
4.0
MICHIGAN PSEUDOSECTION G
TE

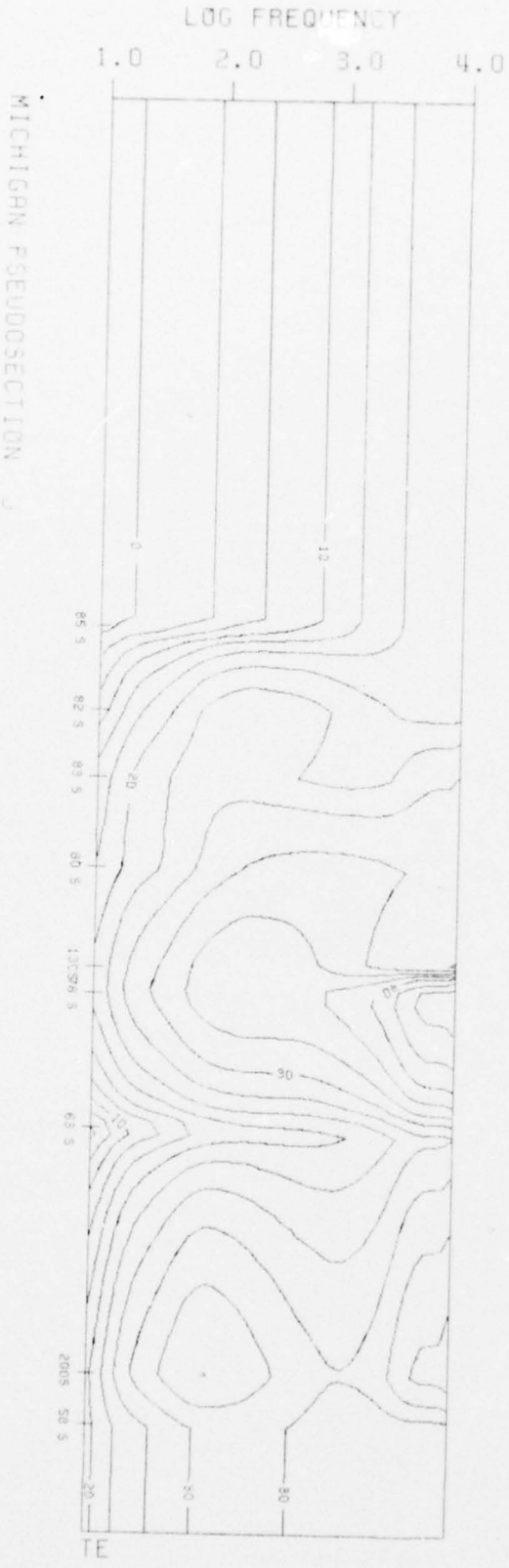
LOG FREQUENCY
1.0
2.0
3.0
4.0
MICHIGAN PSEUDOSECTION J
TE

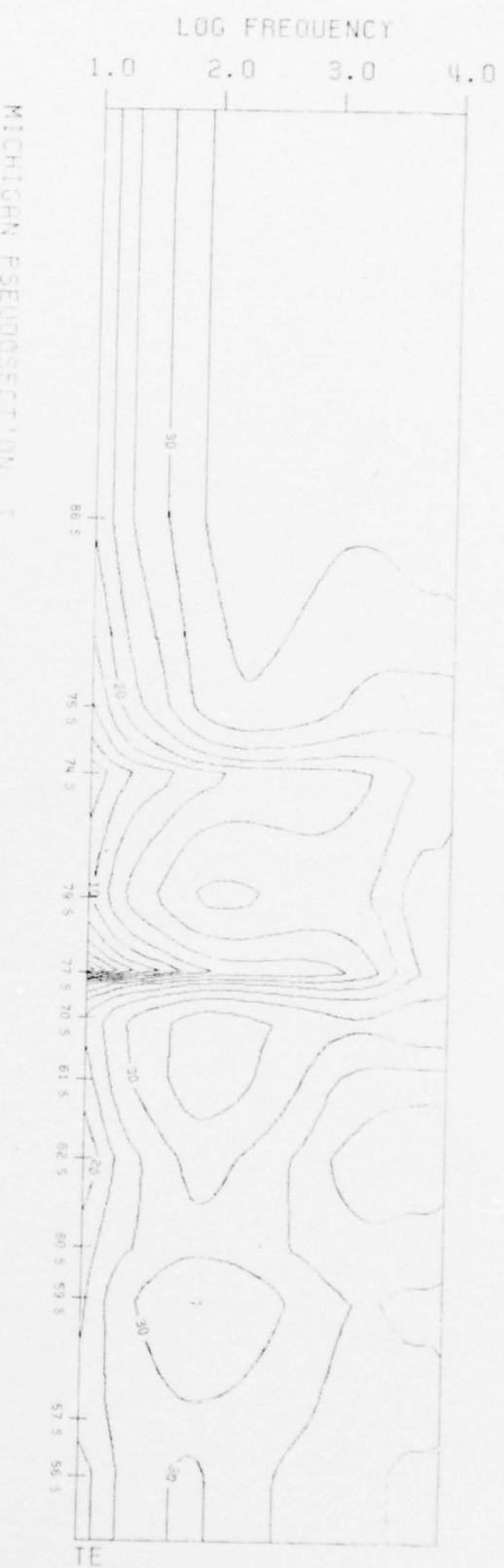
LOG FREQUENCY
1.0
2.0
3.0
4.0
MICHIGAN PSEUDOSECTION I
TE

LOG FREQUENCY
1.0
2.0
3.0
4.0
MICHIGAN PSEUDOSECTION B
10
20
27 S
42 M
31 S
40
30
210S
TM

LOG FREQUENCY
1.0
2.0
3.0
4.0
MICHIGAN PSEUDOSECTION A
0
10
30 S
28 S
29 S
11RS
TM

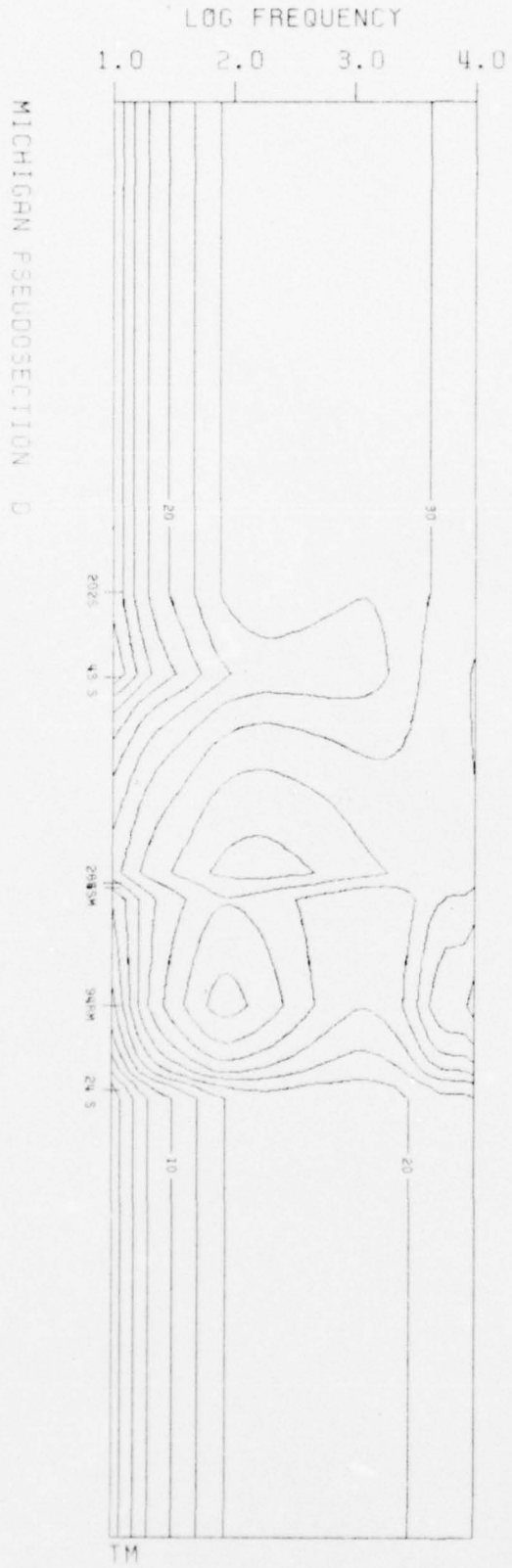
LOG FREQUENCY
1.0
2.0
3.0
4.0
MICHIGAN PSEUDOSECTION D
20
30
10
20
TM

LOG FREQUENCY
1.0
2.0
3.0
4.0
MICHIGAN PSEUDOSECTION C
20
20
TM

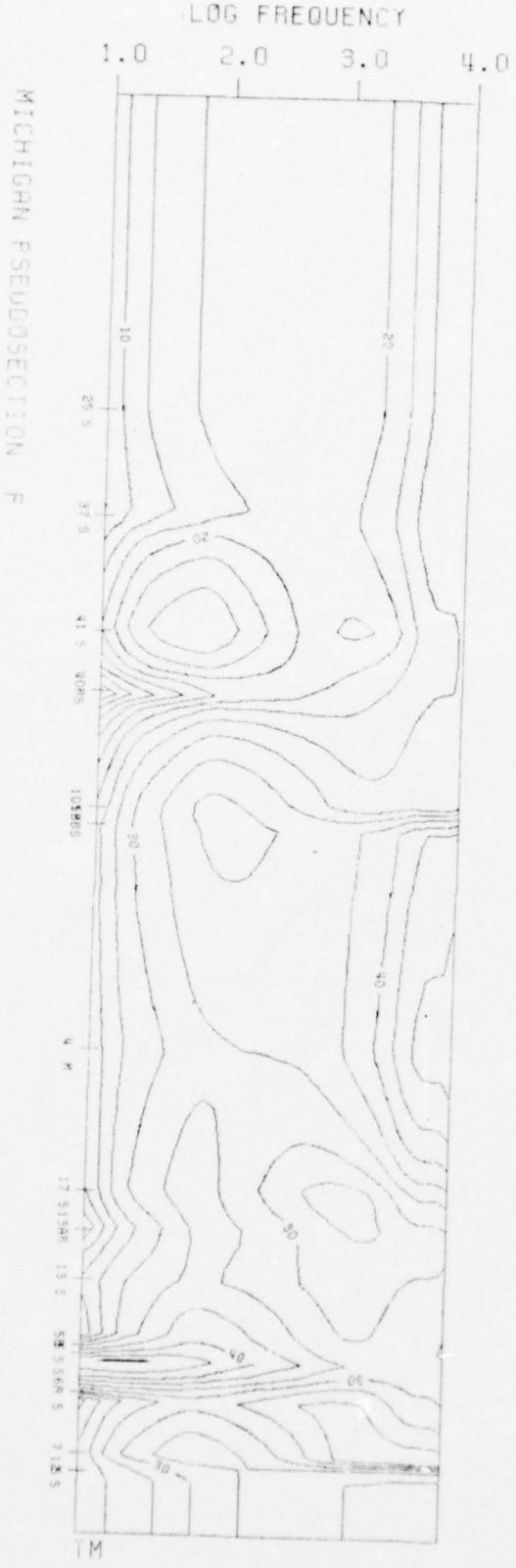
LOG FREQUENCY
1.0
2.0
3.0
4.0
MICHIGAN PSEUDOSECTION F
TM

LOG FREQUENCY
1.0
2.0
3.0
4.0
MICHIGAN PSEUDOSECTION E
TM

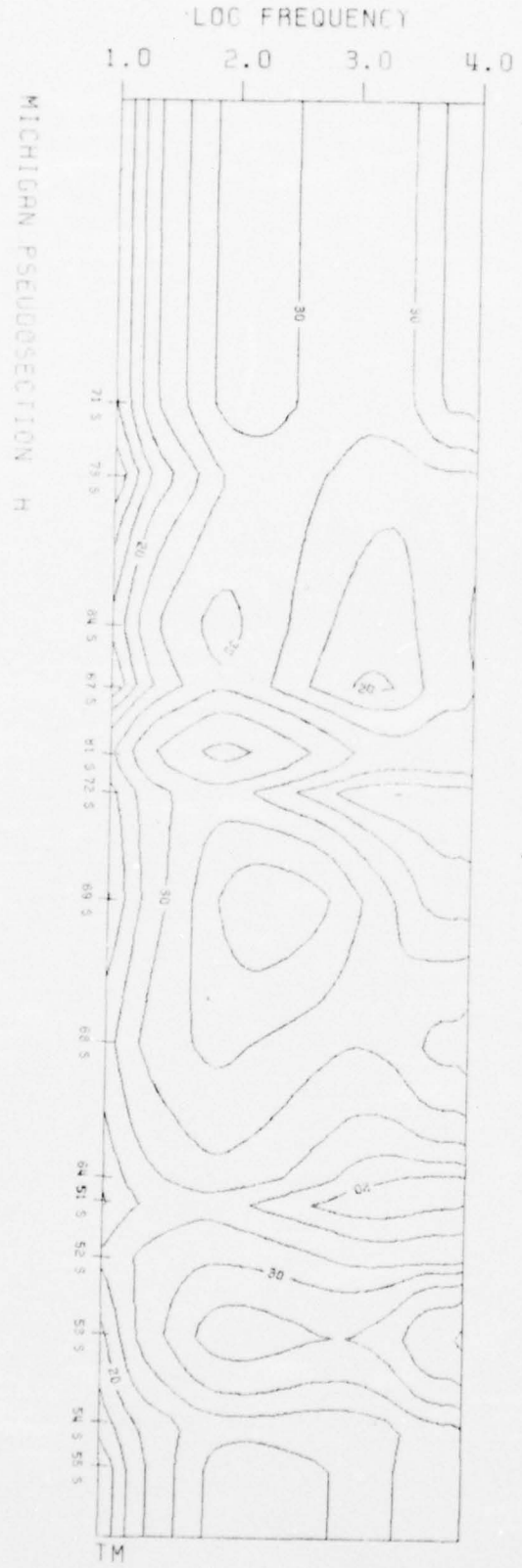
LOG FREQUENCY
1.0
2.0
3.0
4.0
MICHIGAN PSEUDOSECTION H
TM

LOG FREQUENCY
1.0
2.0
3.0
4.0
MICHIGAN PSEUDOSECTION G
TM

LOG FREQUENCY
1.0
2.0
3.0
4.0
MICHIGAN PSEUDOSECTION J
TM

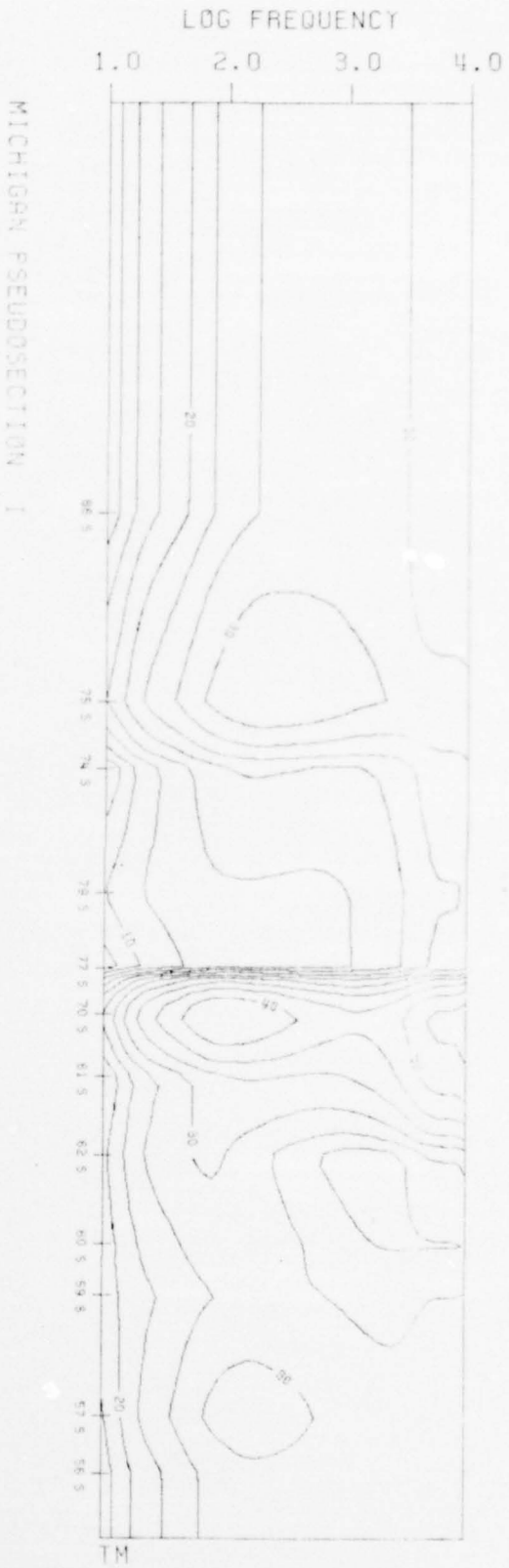
LOG FREQUENCY
1.0
2.0
3.0
4.0
MICHIGAN PSEUDOSECTION I
TM

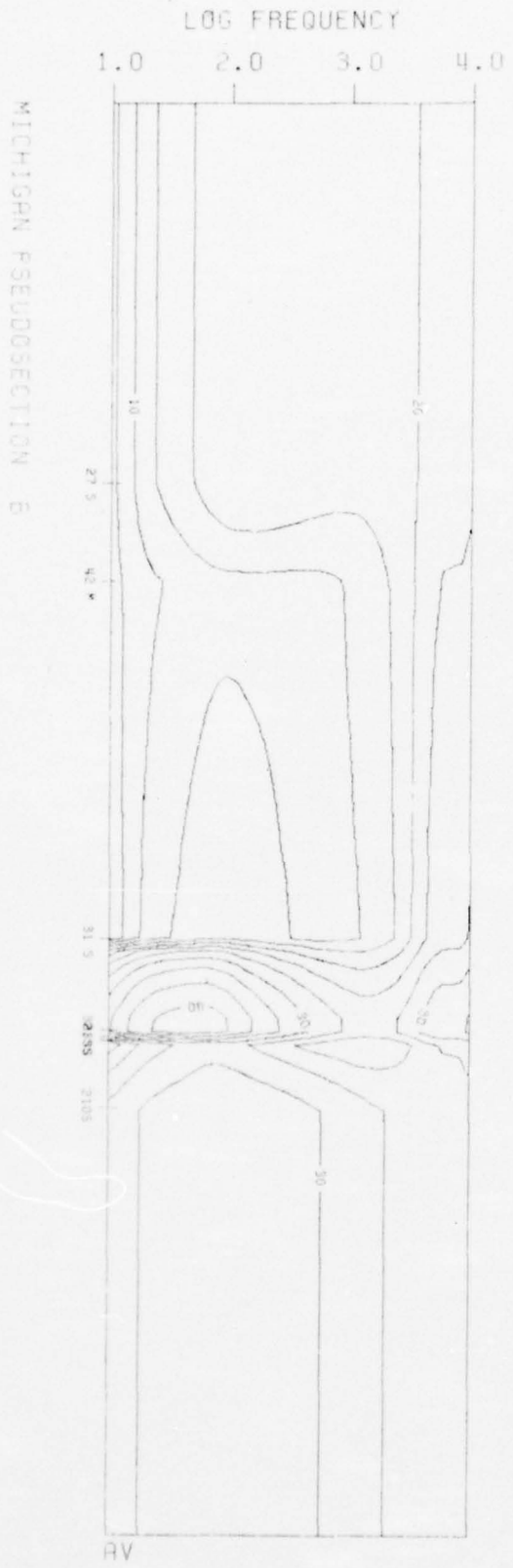
LOG FREQUENCY
1.0
2.0
3.0
4.0
MICHIGAN PSEUDOSECTION B
AV

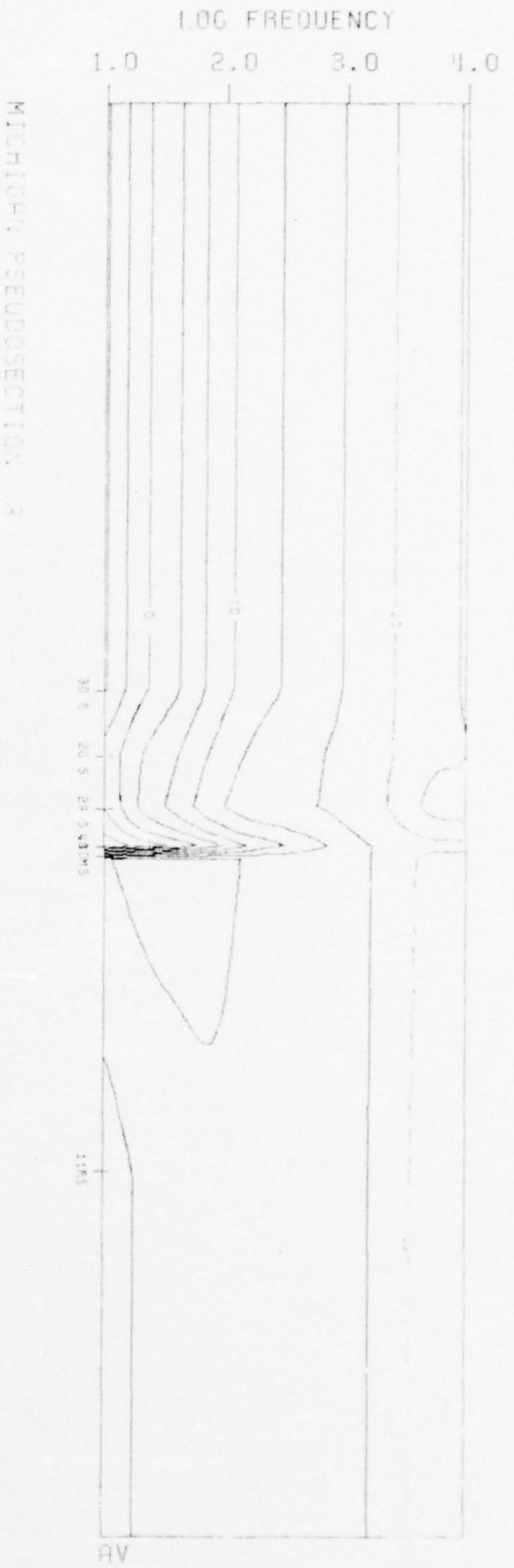
LOG FREQUENCY
1.0
2.0
3.0
4.0
MICHIGAN PSEUDOSECTION A
AV

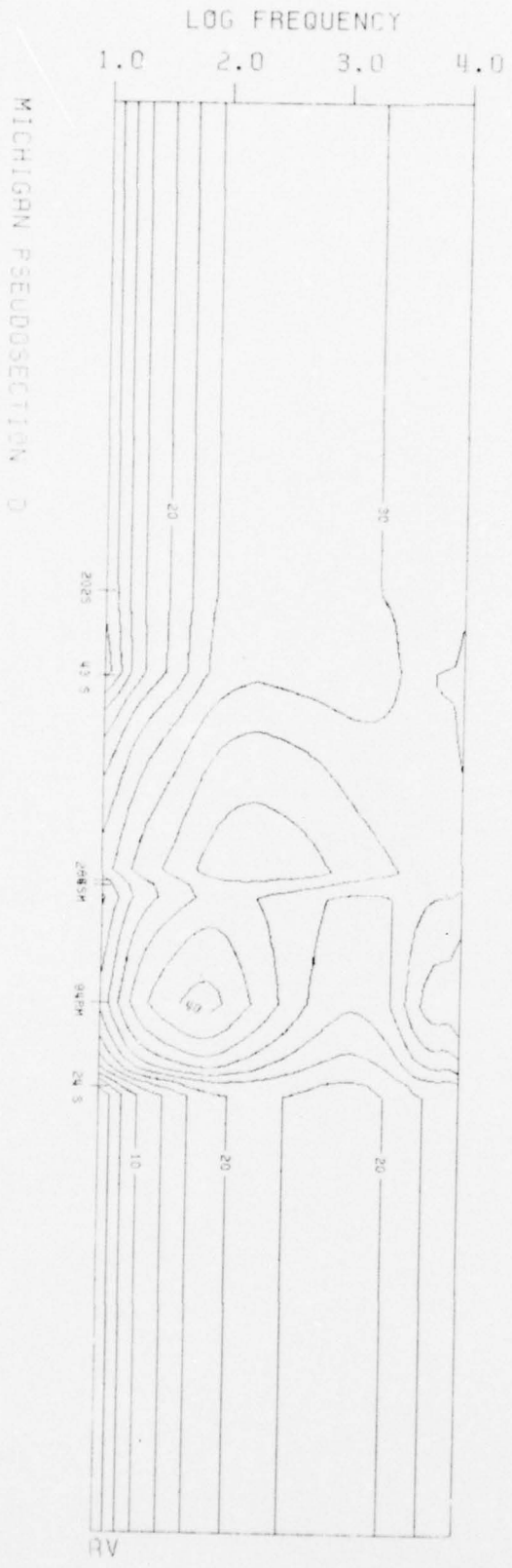
LOG FREQUENCY
1.0
2.0
3.0
4.0
MICHIGAN PSEUDOSECTION D
20
30
10
20
20
RV

LOG FREQUENCY
1.0
2.0
3.0
4.0
MICHIGAN PSEUDOSECTION C
20
40
20
RV

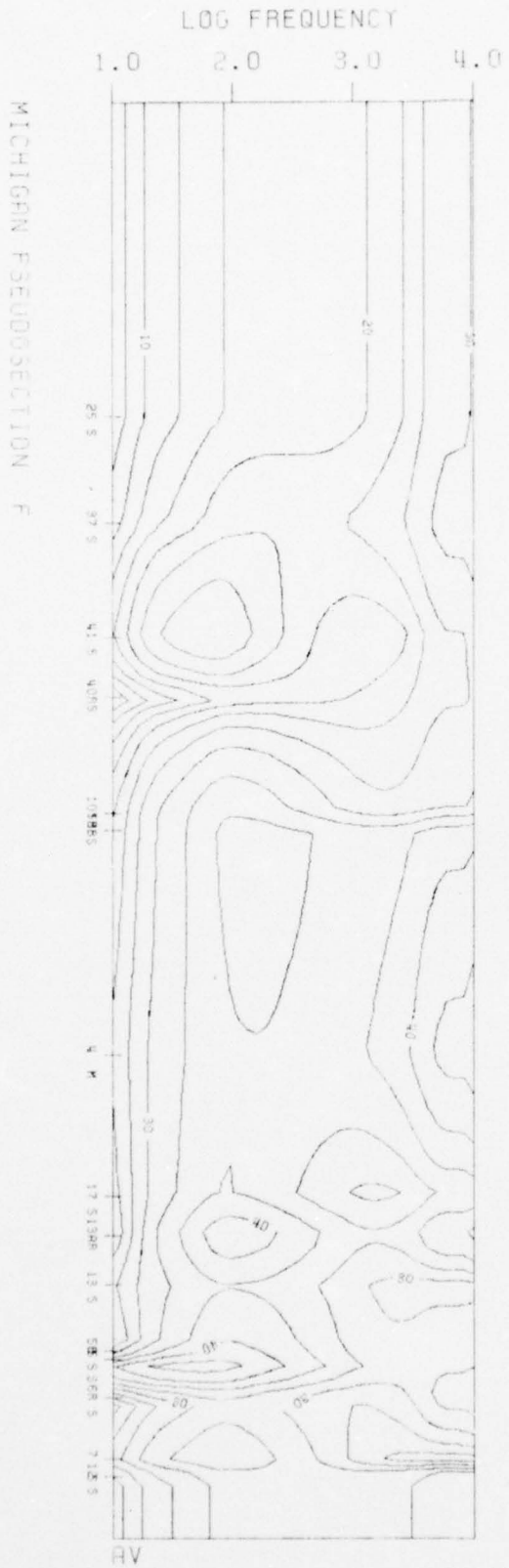
LOG FREQUENCY
1.0
2.0
3.0
4.0
MICHIGAN PSEUDOSECTION F
AV

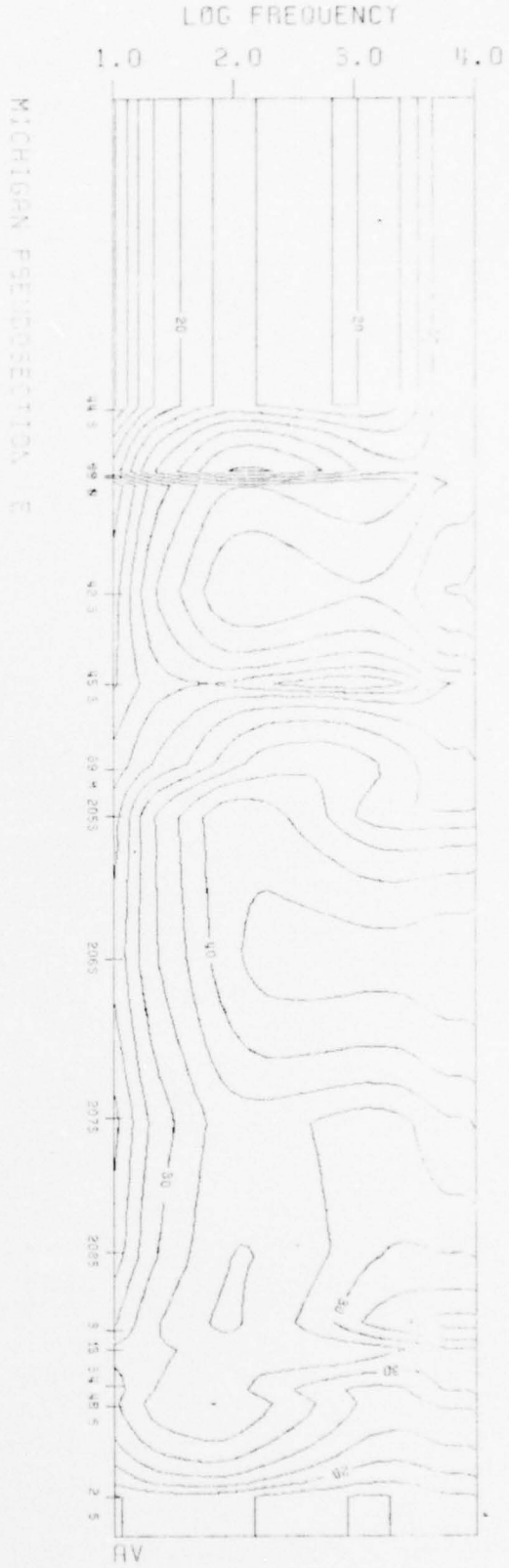
LOG FREQUENCY
1.0
2.0
3.0
4.0
MICHIGAN PSEUDOSECTION E
AV

LOG FREQUENCY
1.0
2.0
3.0
4.0
MICHIGAN PSEUDOSECTION A
AV

LOG FREQUENCY
1.0
2.0
3.0
4.0
MICHIGAN PSEUDOSECTION B
AV

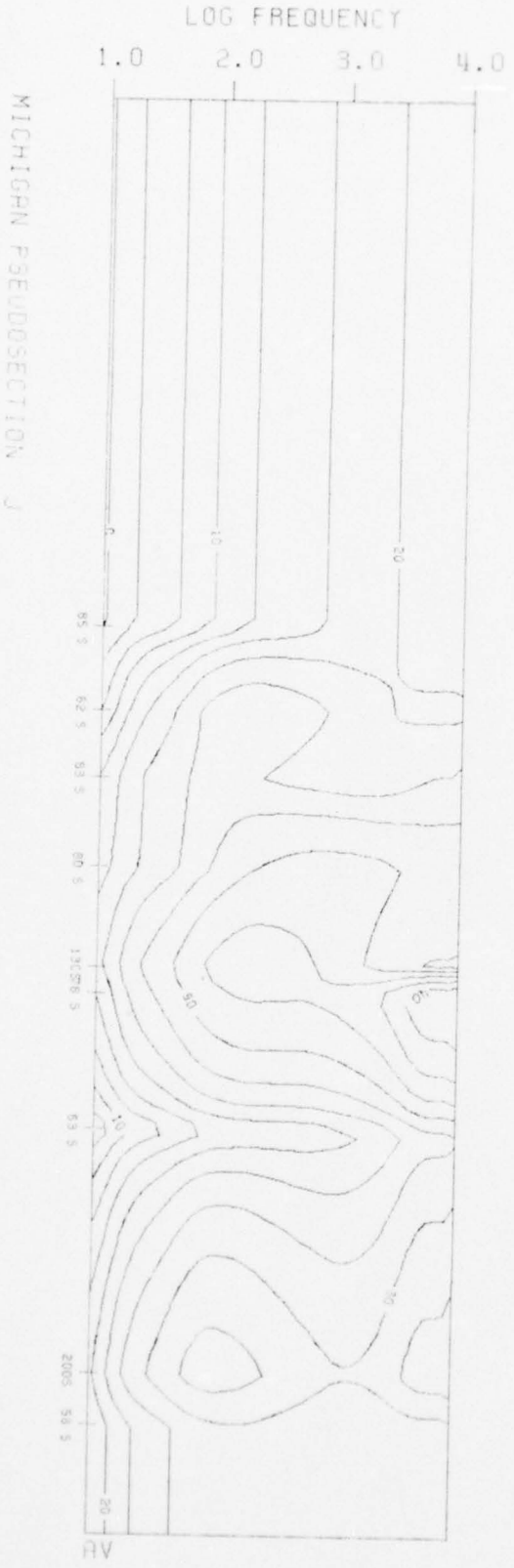
LOG FREQUENCY
1.0
2.0
3.0
4.0
MICHIGAN PSEUDOSECTION J
AV

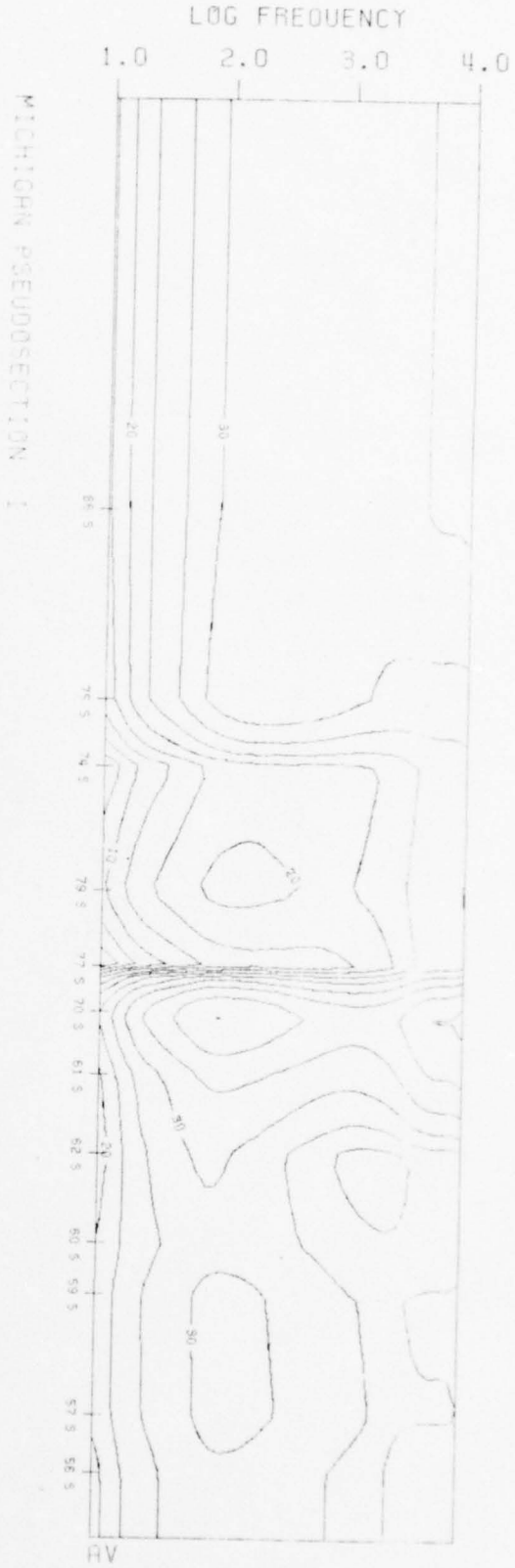
LOG FREQUENCY
1.0
2.0
3.0
4.0
MICHIGAN PSEUDOSECTION I
AV

SECTION A.3

MICHIGAN

RESIDUALS

- NORTH-SOUTH ORIENTATION
- EAST-WEST ORIENTATION
- AVERAGED DATA

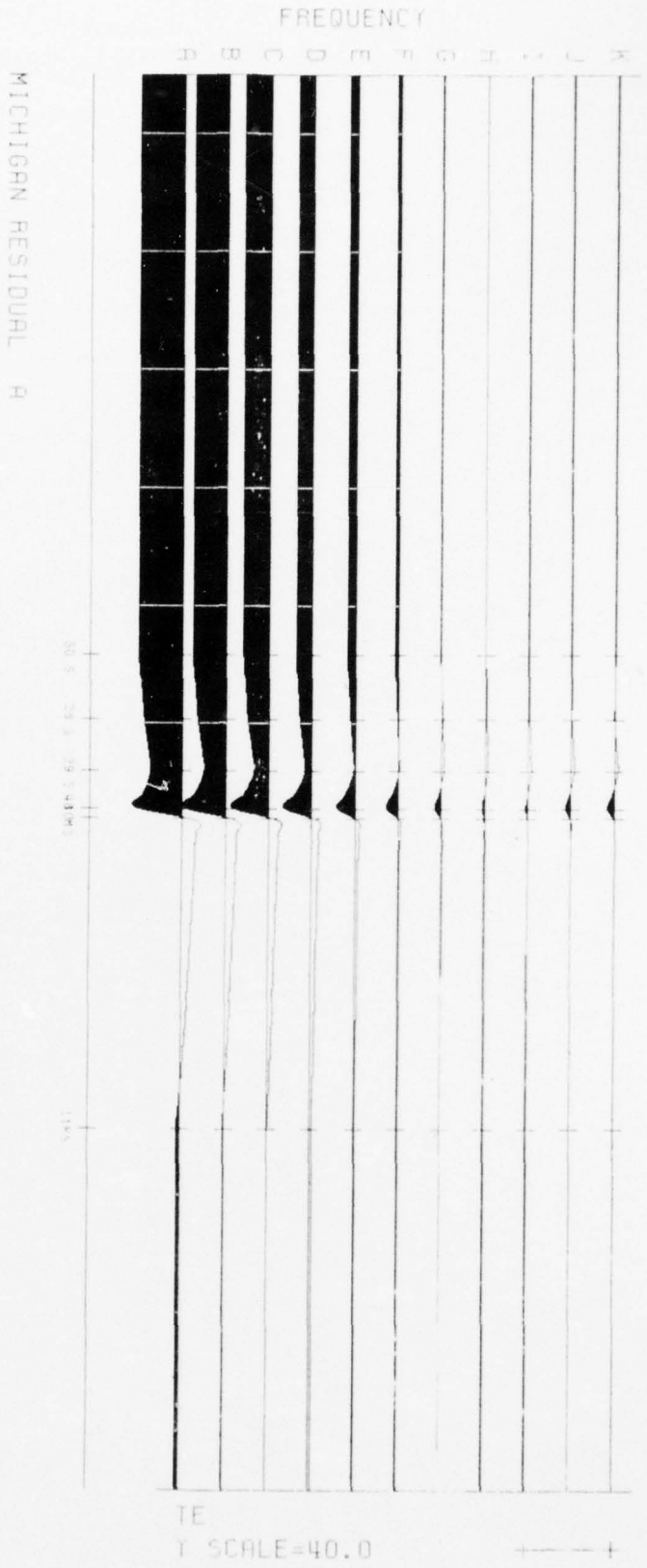
FREQUENCY
MICHIGAN RESIDUAL A
TE
Y SCALE=40.0

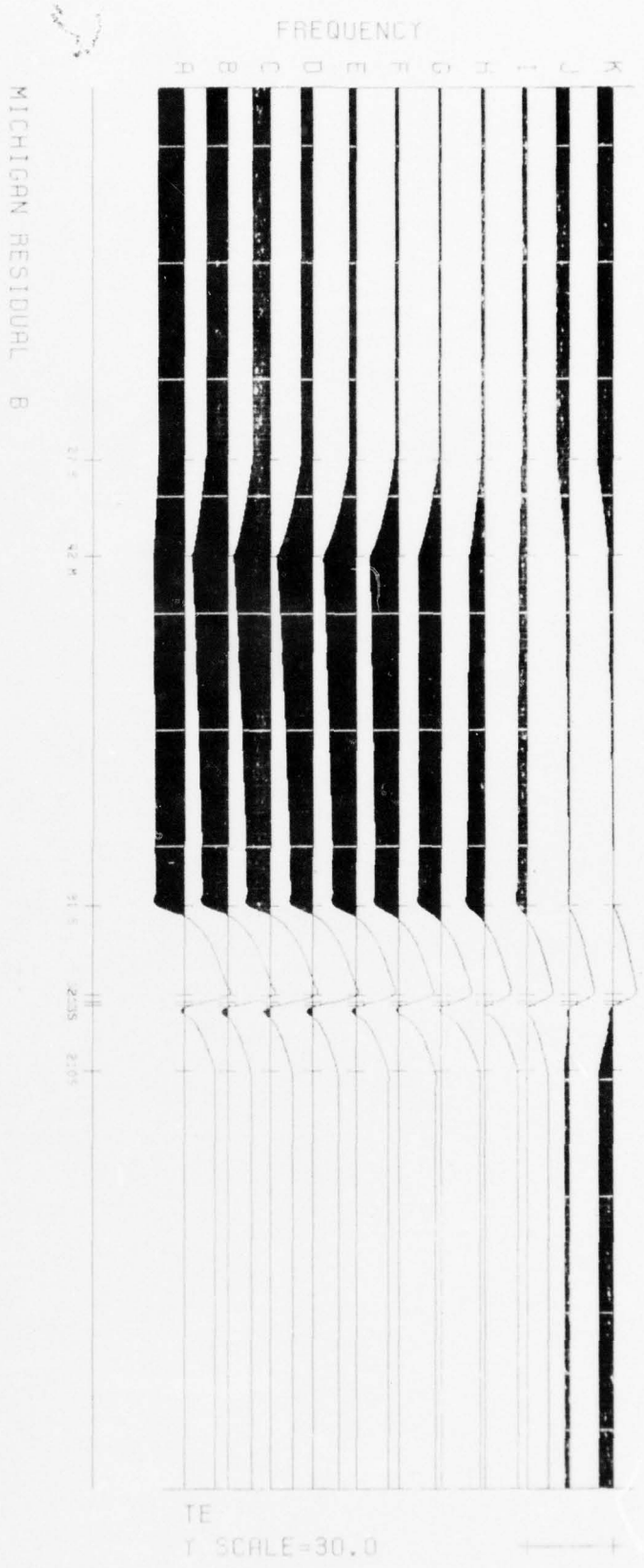
FREQUENCY
MICHIGAN RESIDUAL B
TE
Y SCALE=30.0

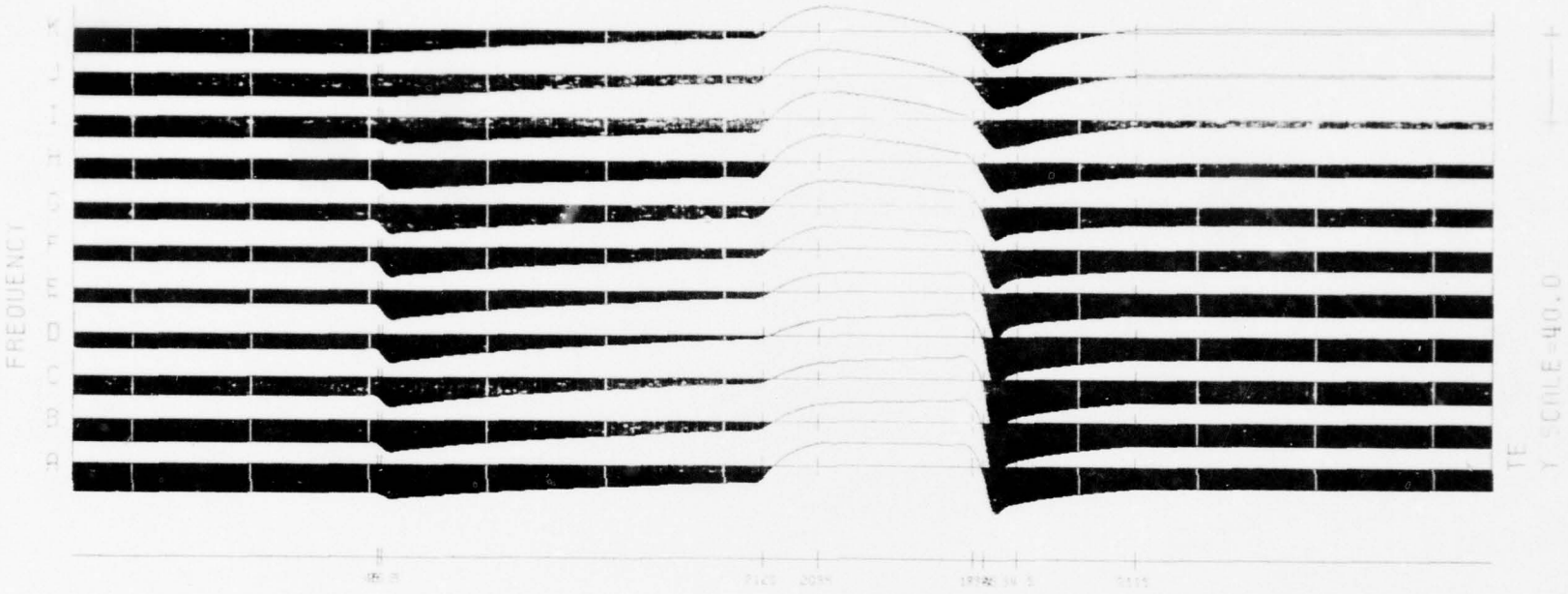

MICHIGAN RESIDUAL C

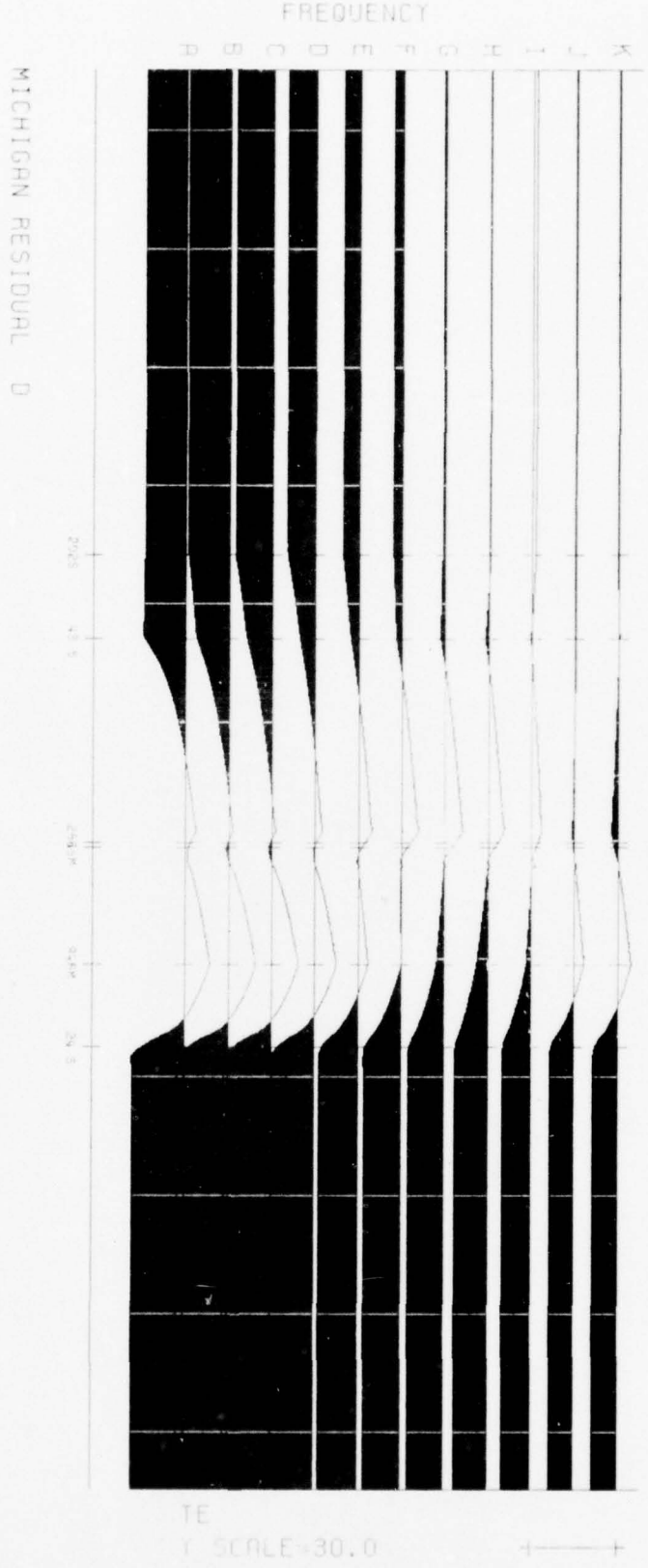
FREQUENCY
MICHIGAN RESIDUAL 0
TE
Y SCALE=30.0

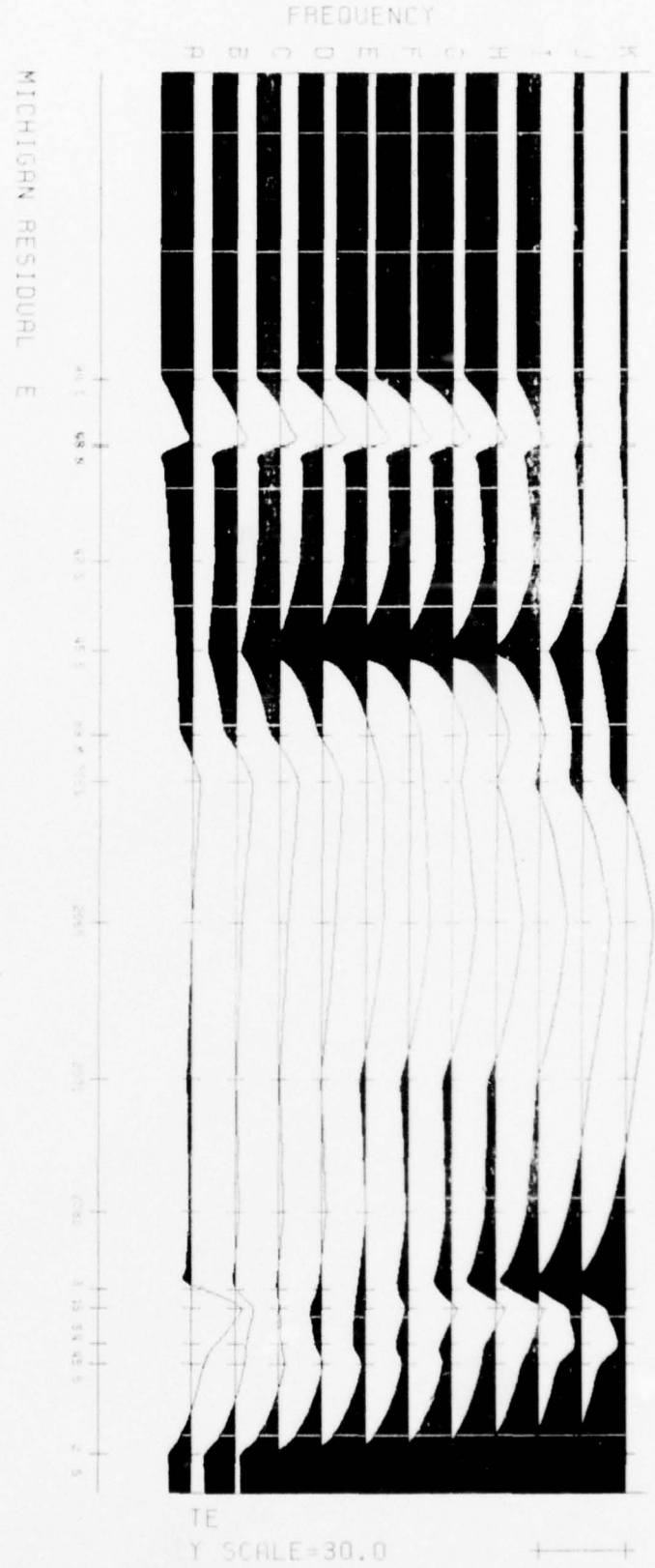
FREQUENCY
MICHIGAN RESIDUAL E
TE
Y SCALE=30.0

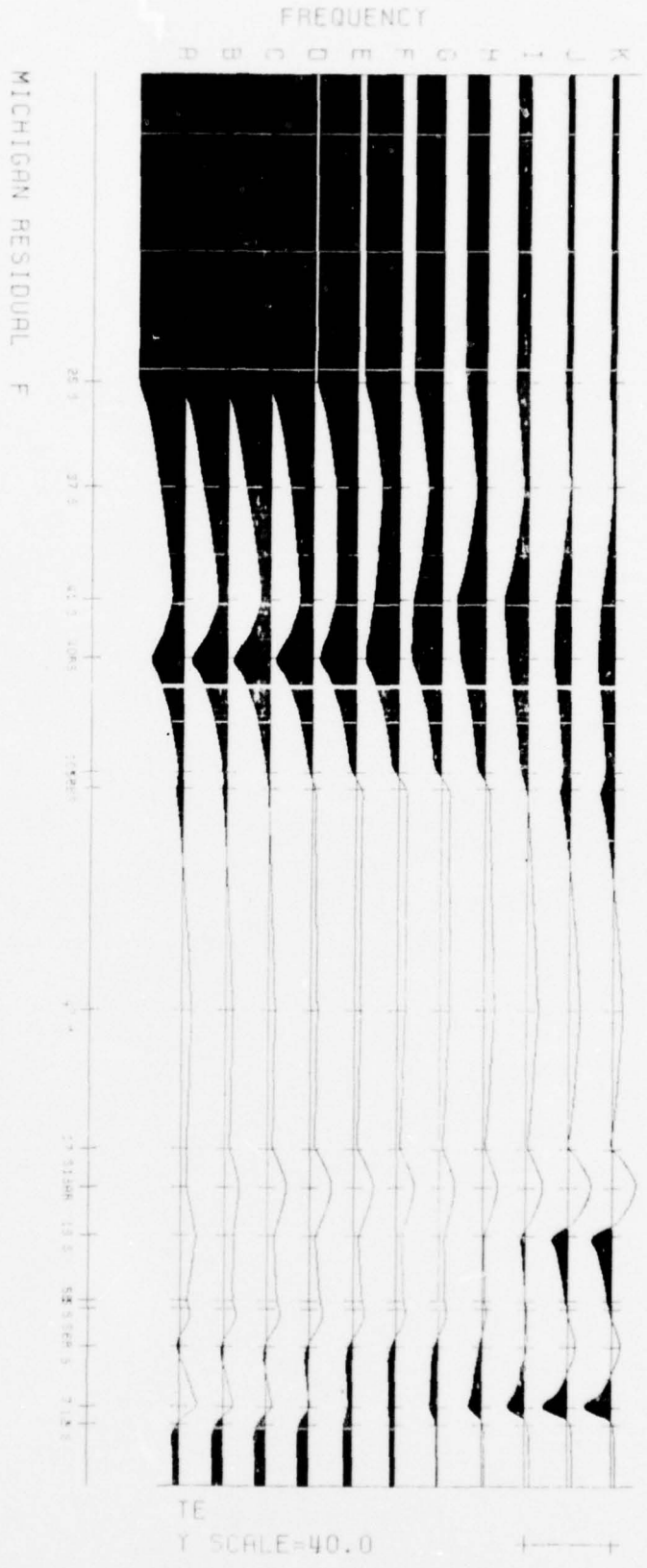
FREQUENCY
MICHIGAN RESIDUAL F
TE
Y SCALE=40.0

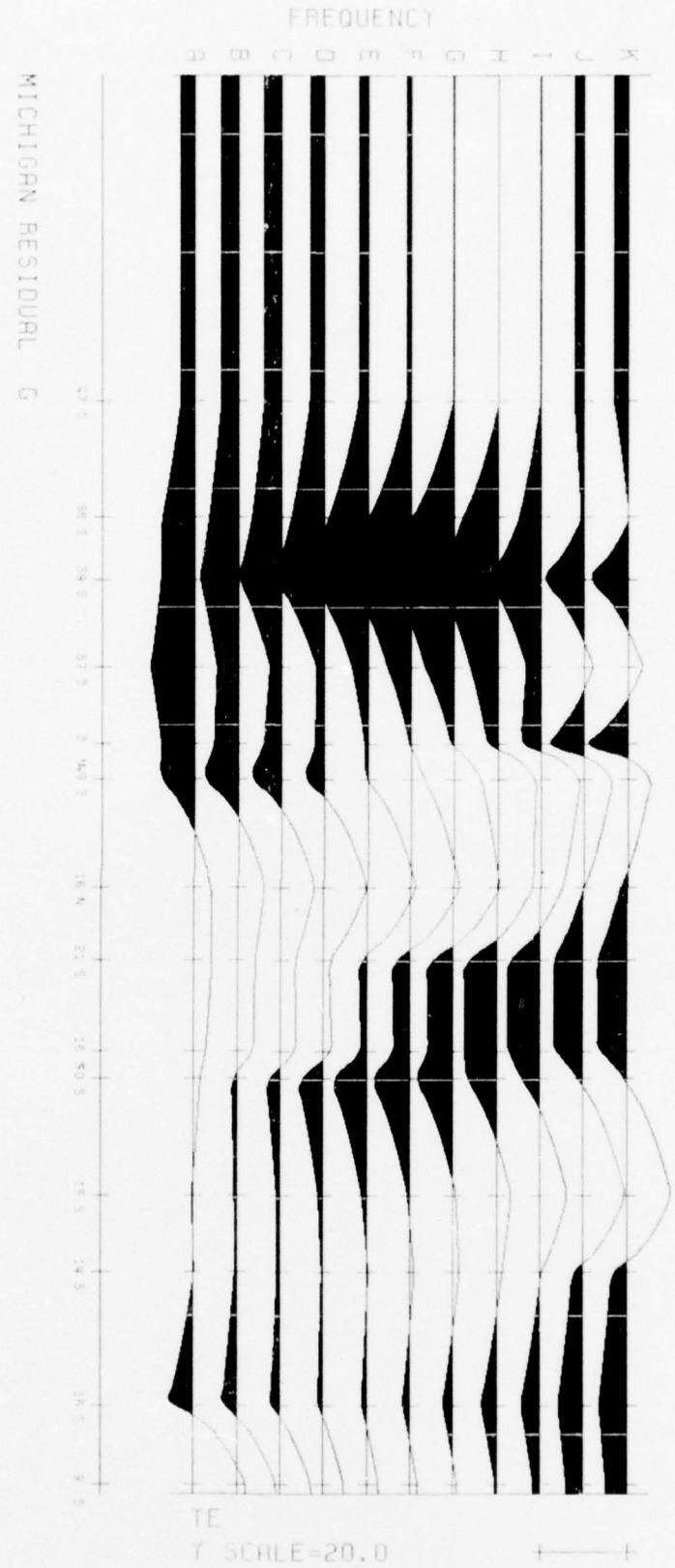
FREQUENCY
MICHIGAN RESIDUAL G
TE
Y SCALE=20.0

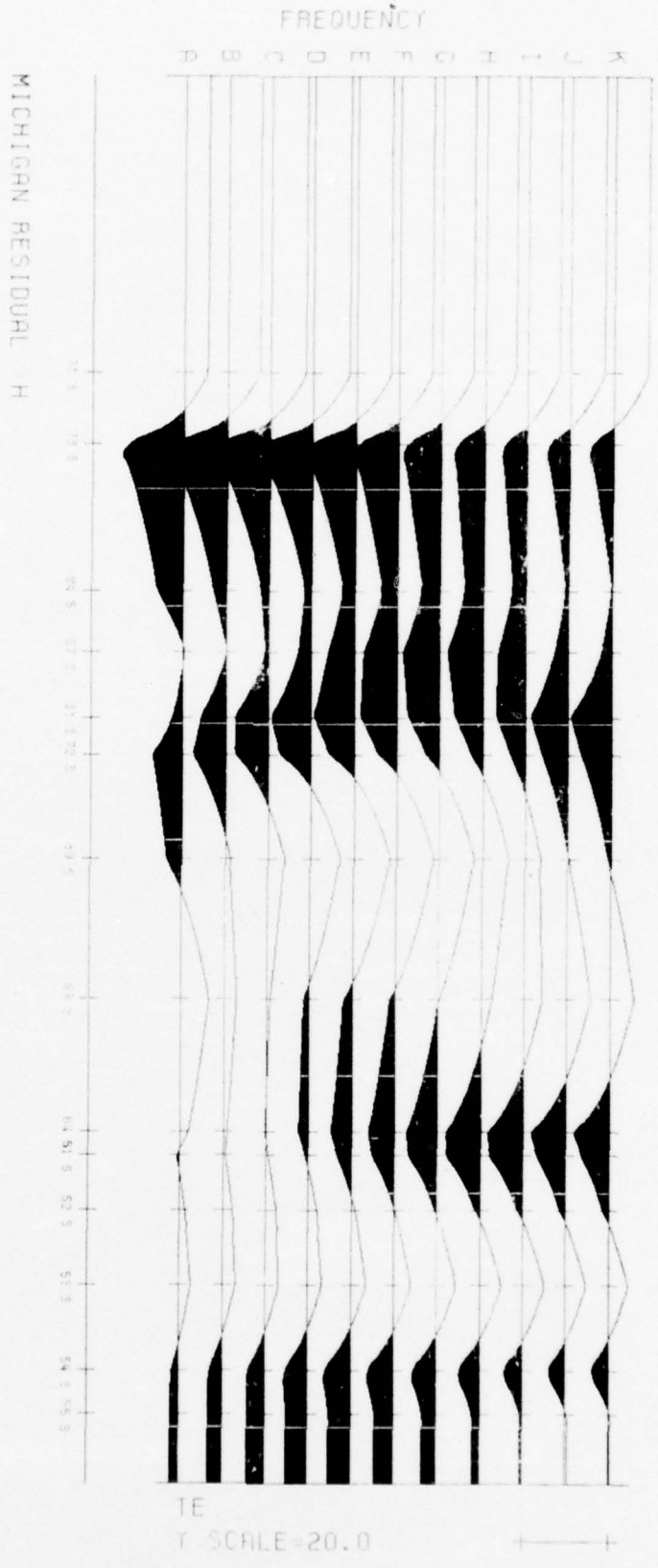
FREQUENCY
MICHIGAN RESIDUAL H
TE
Y SCALE=20.0

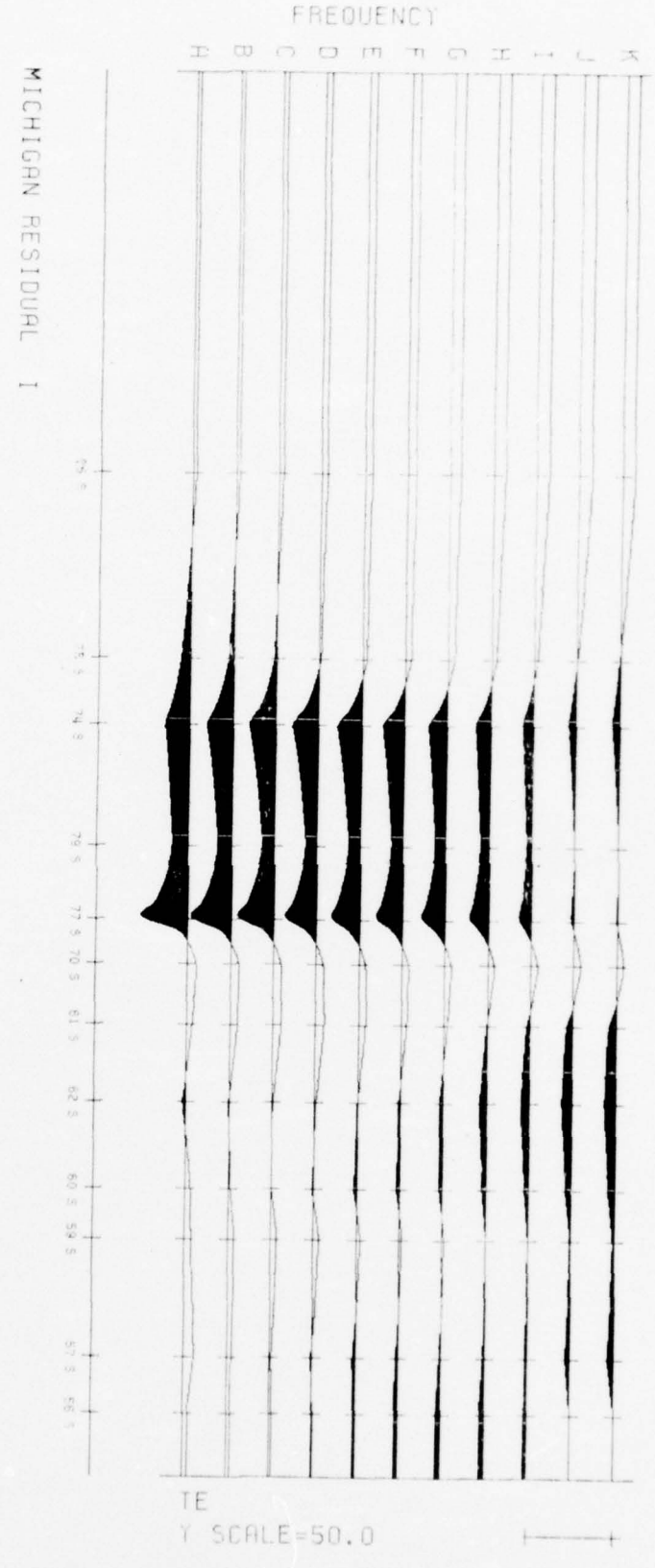
FREQUENCY
A B C D E F G H I J K L M
MICHIGAN RESIDUAL I
TE
Y SCALE=50.0

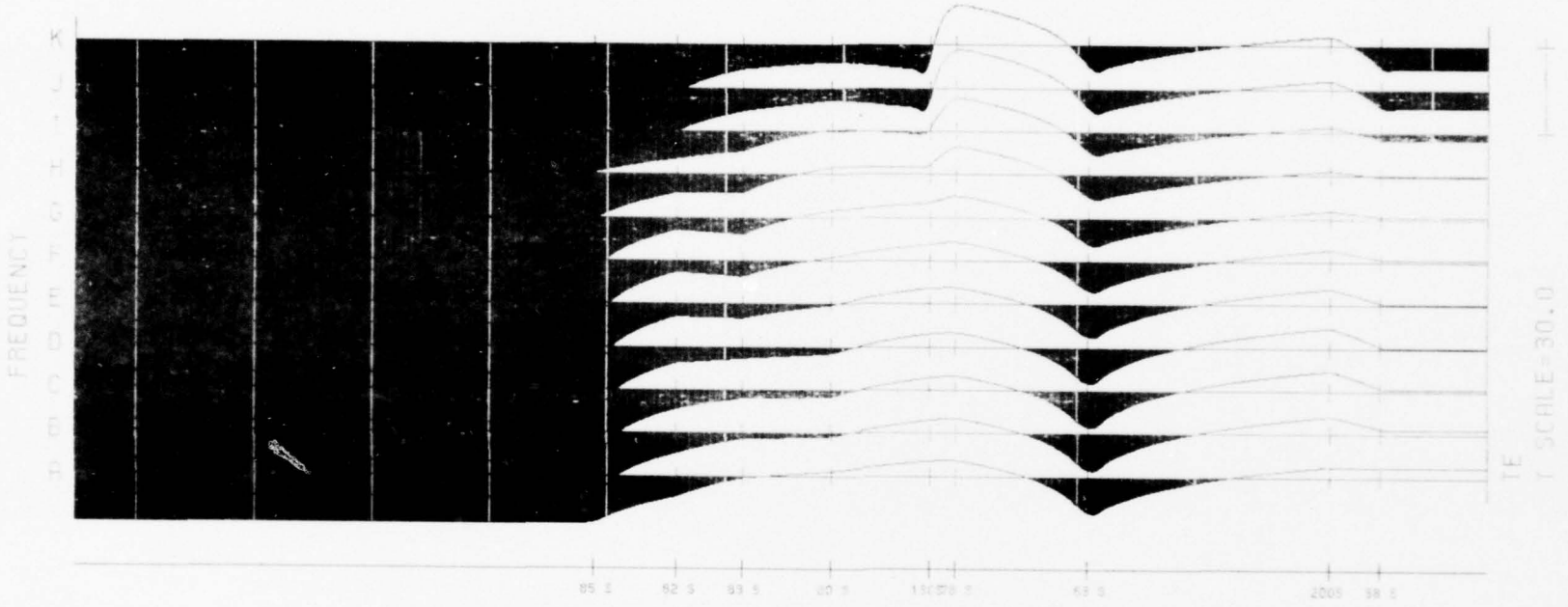

MICHIGAN RESIDUAL J

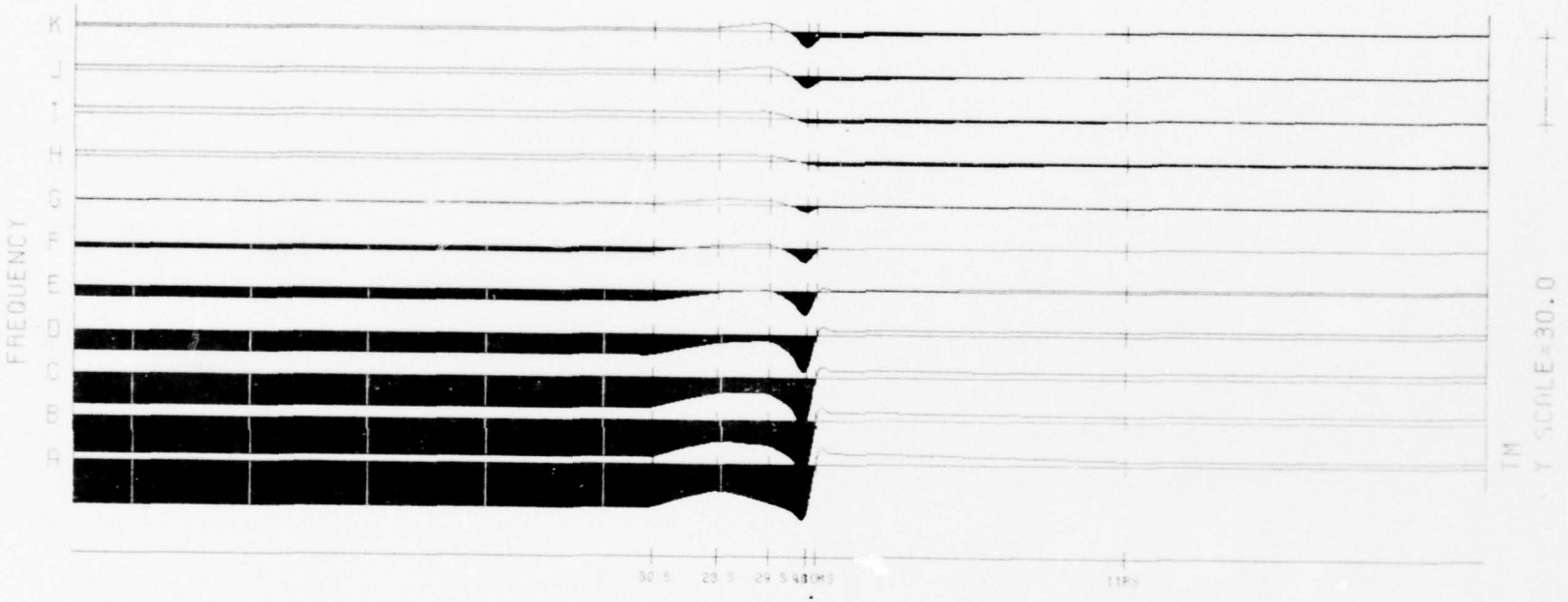

MICHIGAN RESIDUAL A

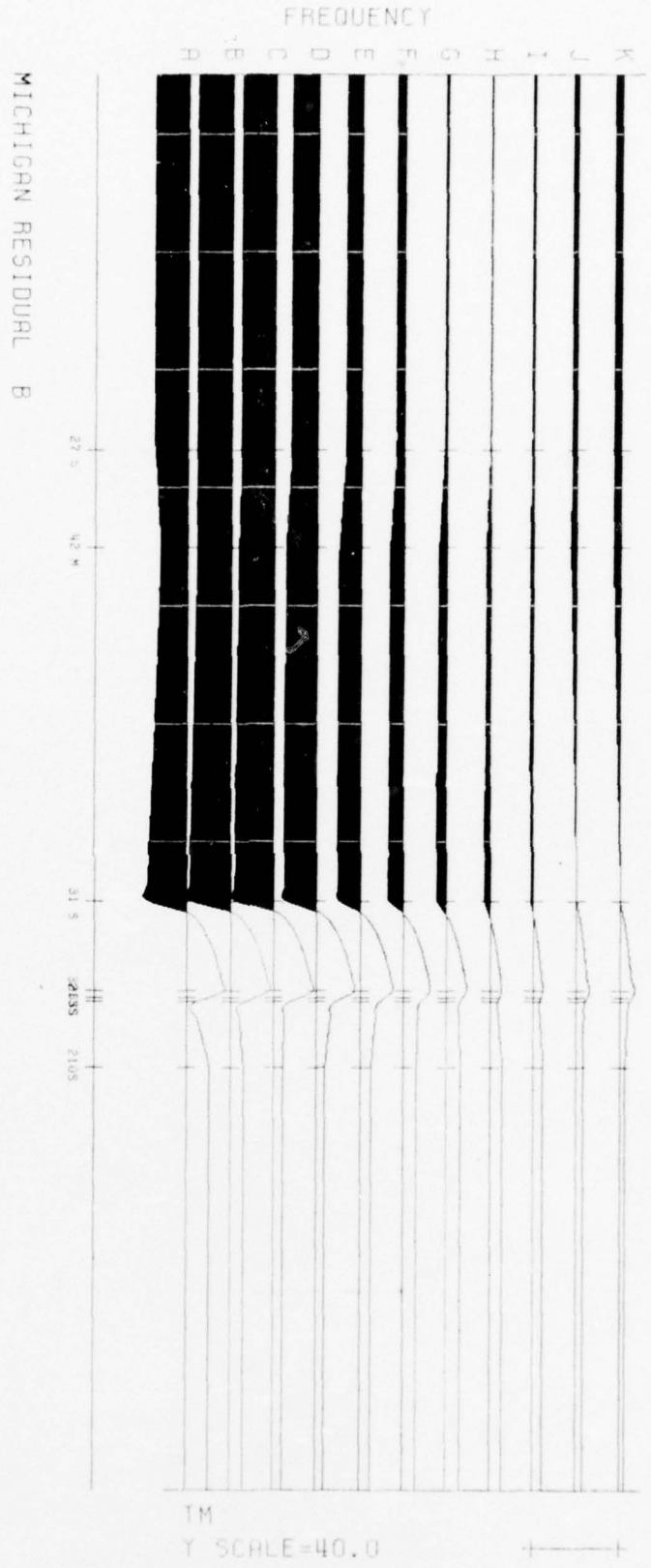
FREQUENCY
MICHIGAN RESIDUAL B
27 S
42 M
31 S
TM
Y SCALE=40.0

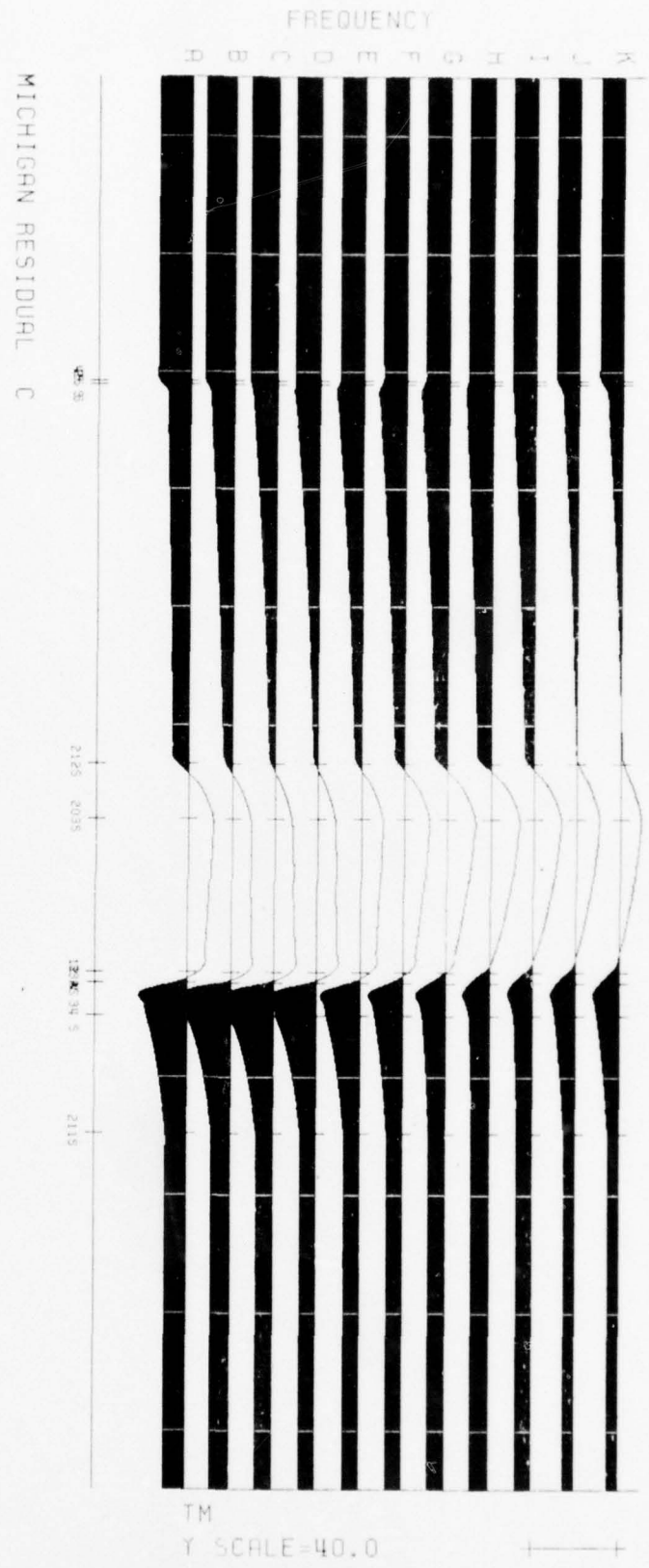
FREQUENCY
MICHIGAN RESIDUAL C
TM
Y SCALE=40.0

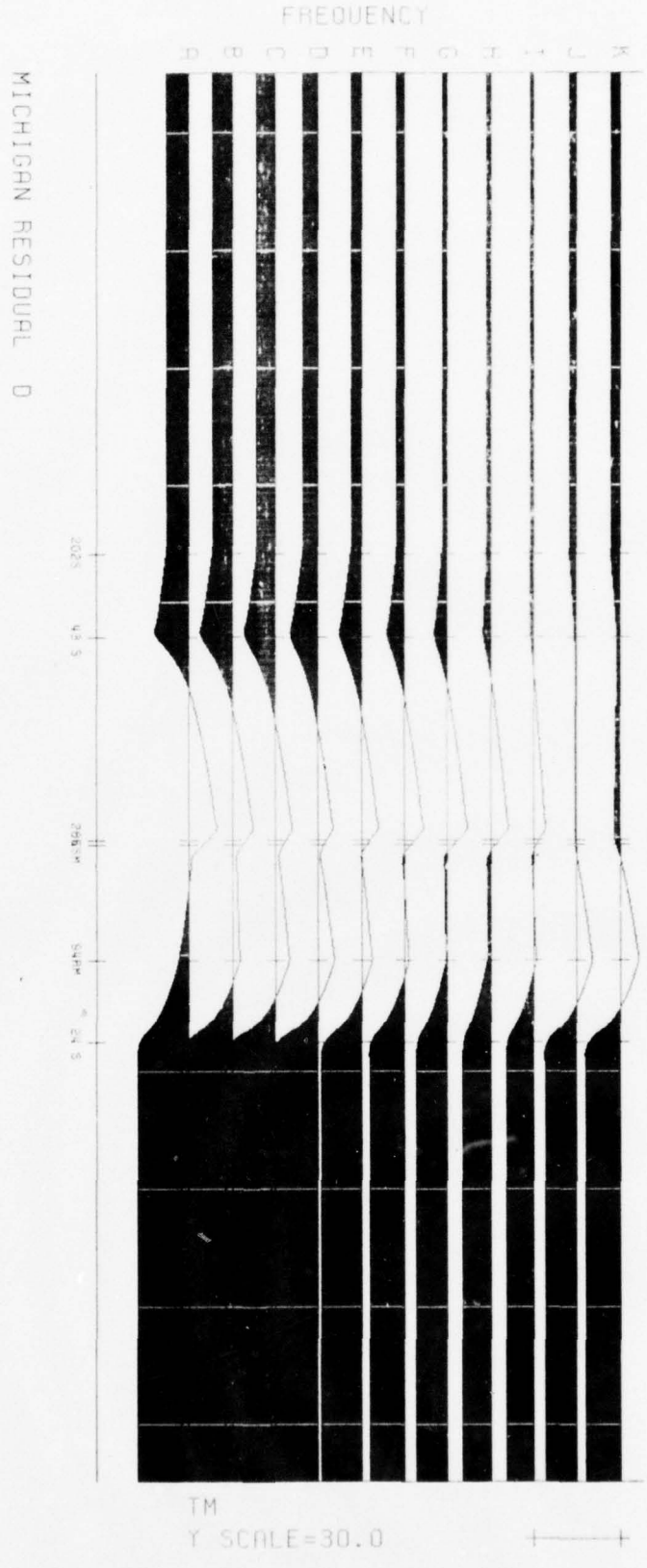
FREQUENCY
MICHIGAN RESIDUAL 0
TM
Y SCALE=30.0

FREQUENCY
MICHIGAN RESIDUAL E
TM
Y SCALE=40.0

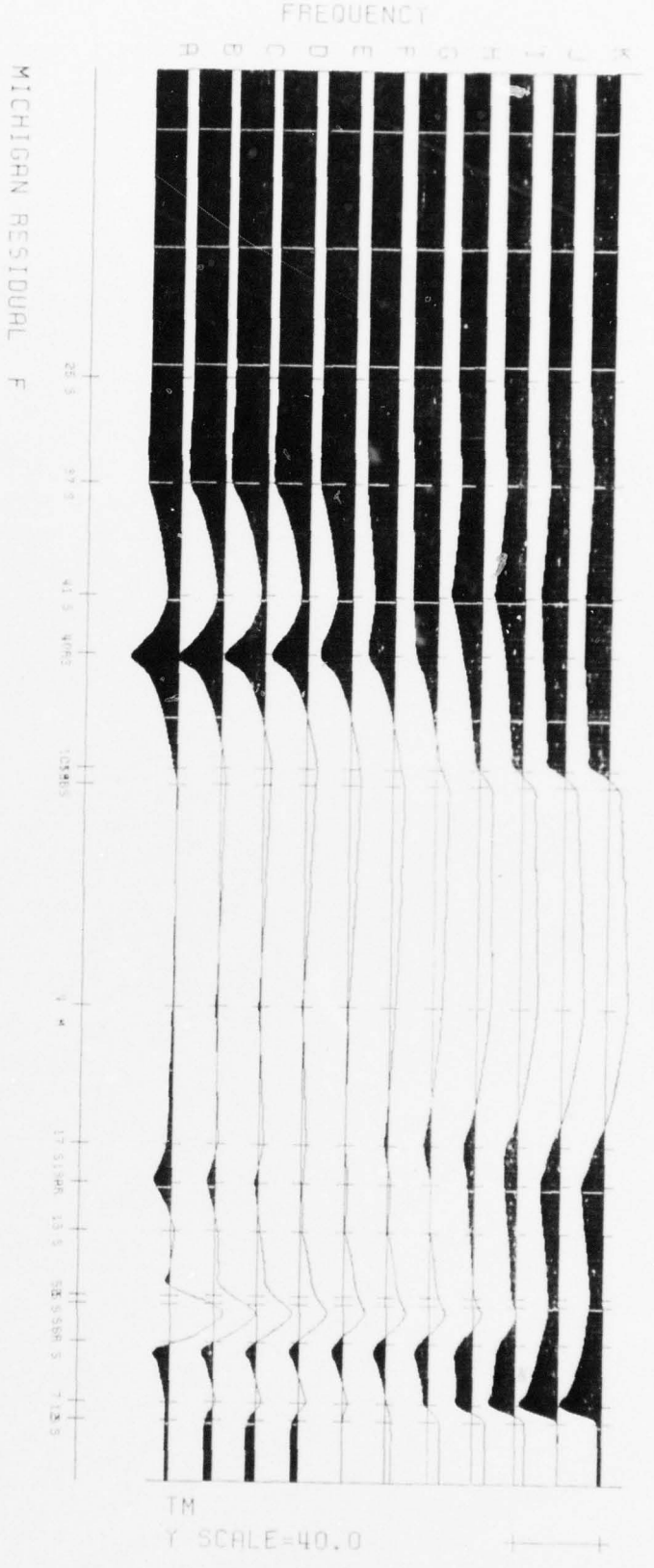
FREQUENCY
MICHIGAN RESIDUAL F
TM
Y SCALE=40.0

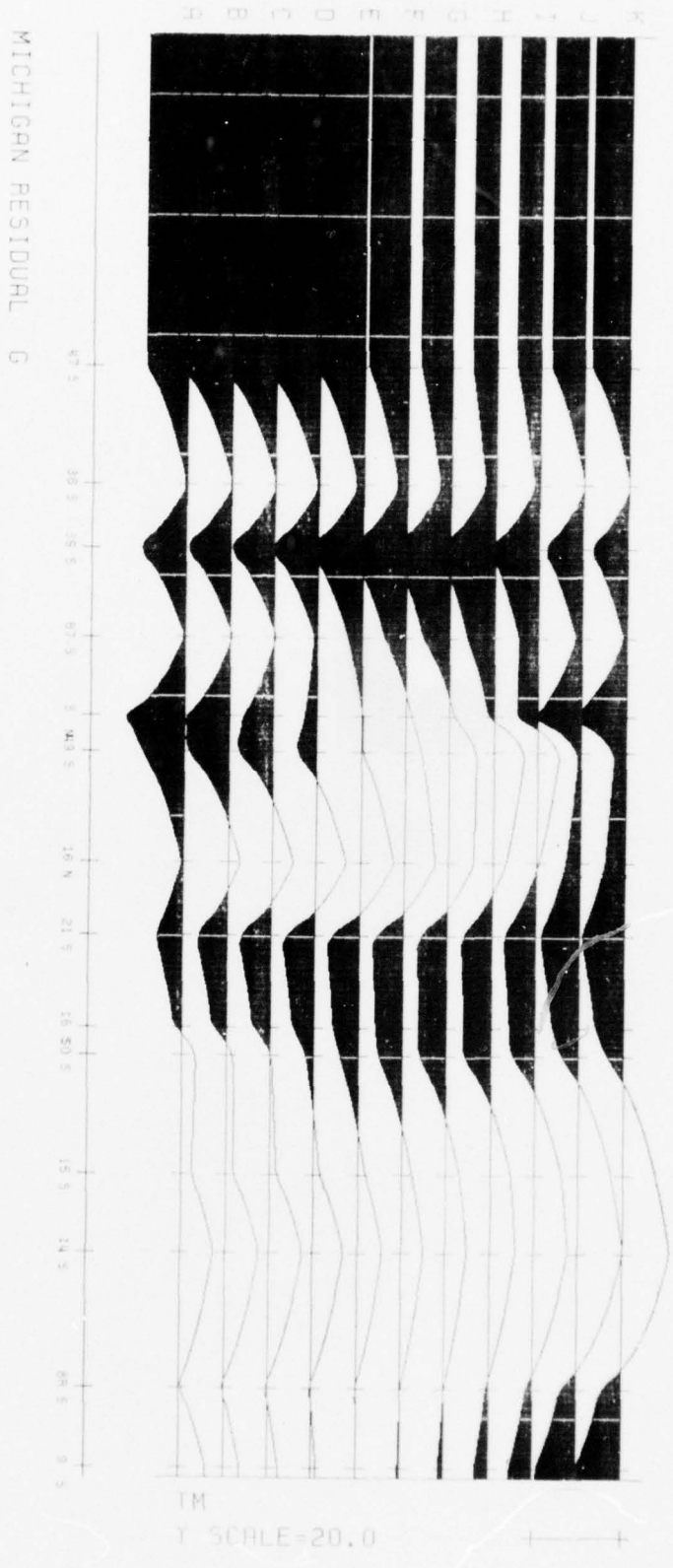
FREQUENCY
MICHIGAN RESIDUAL G
TM
Y SCALE=20.0

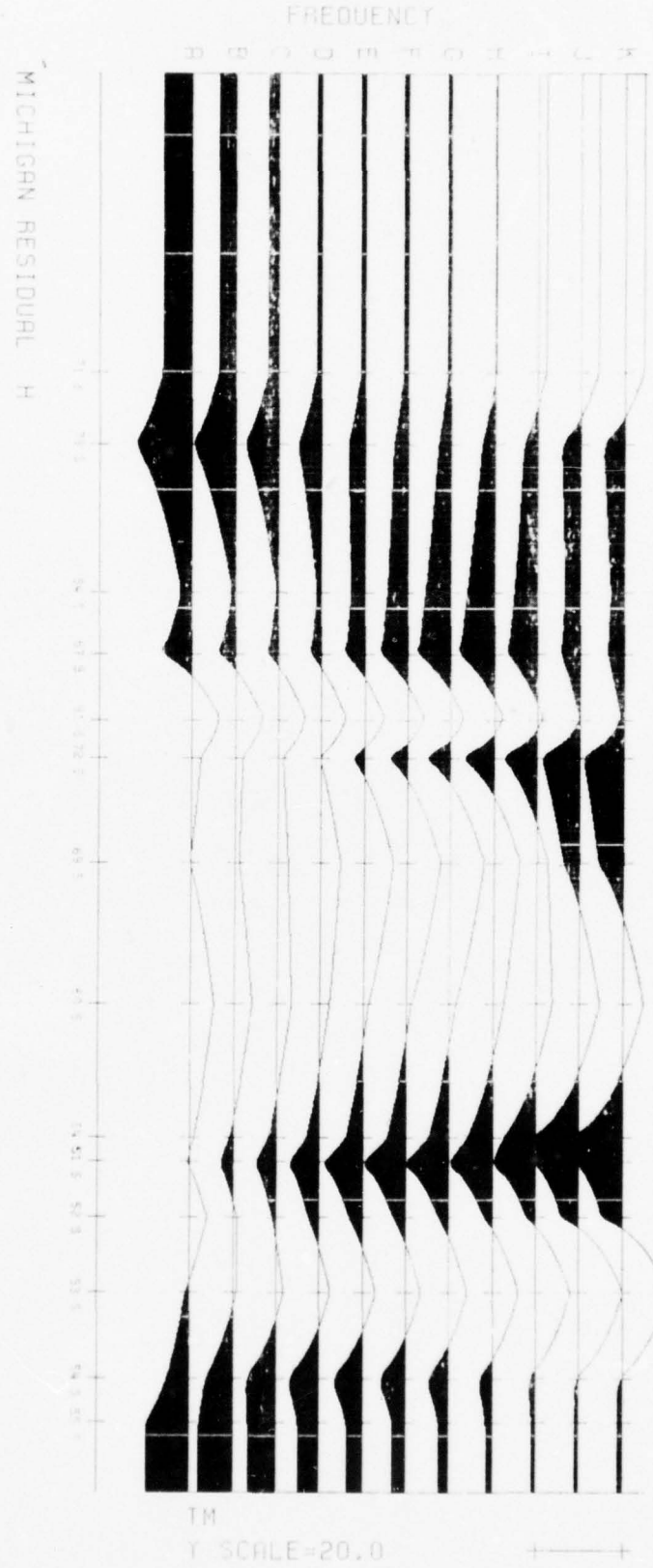
FREQUENCY
MICHIGAN RESIDUAL H
TM
Y SCALE=20.0

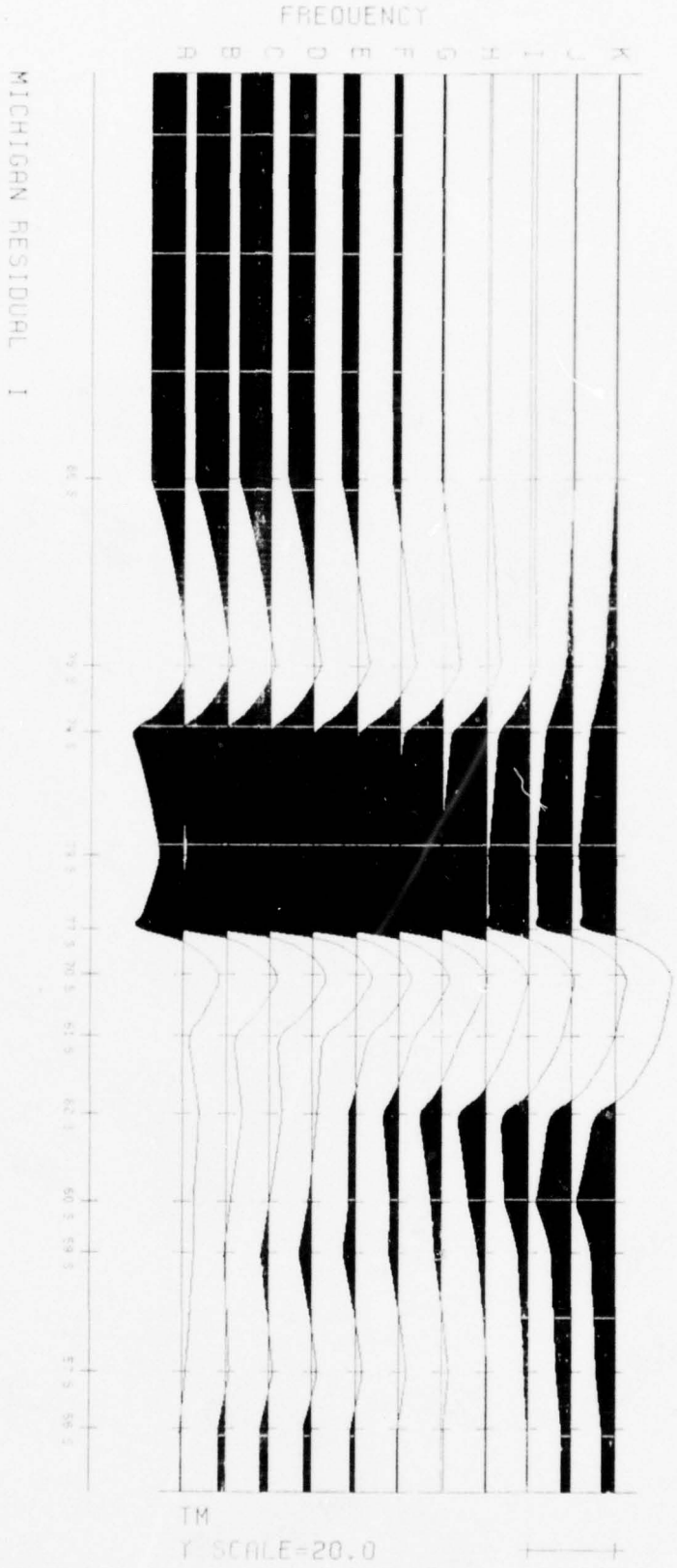
FREQUENCY
MICHIGAN RESIDUAL I
TM
Y SCALE=20.0

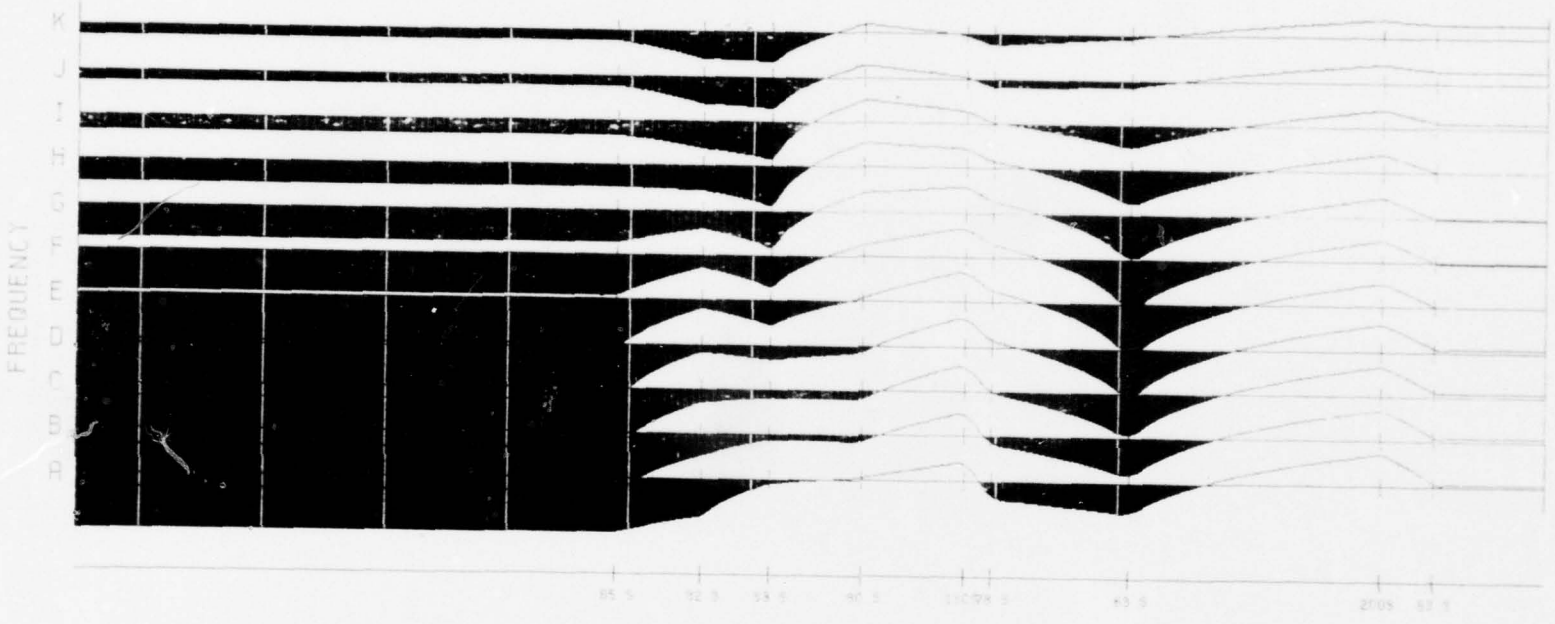

MICHIGAN RESIDUAL J

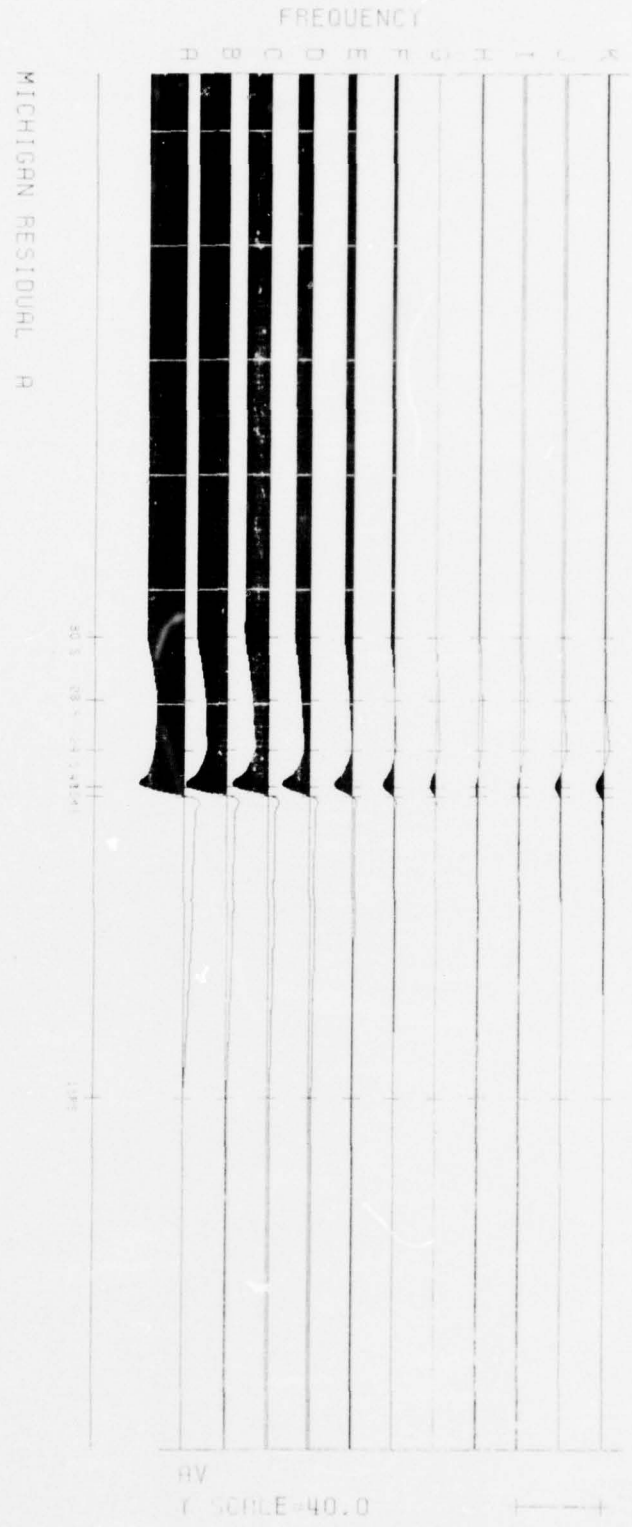
FREQUENCY
MICHIGAN RESIDUAL A
AV
Y SCALE=40.0

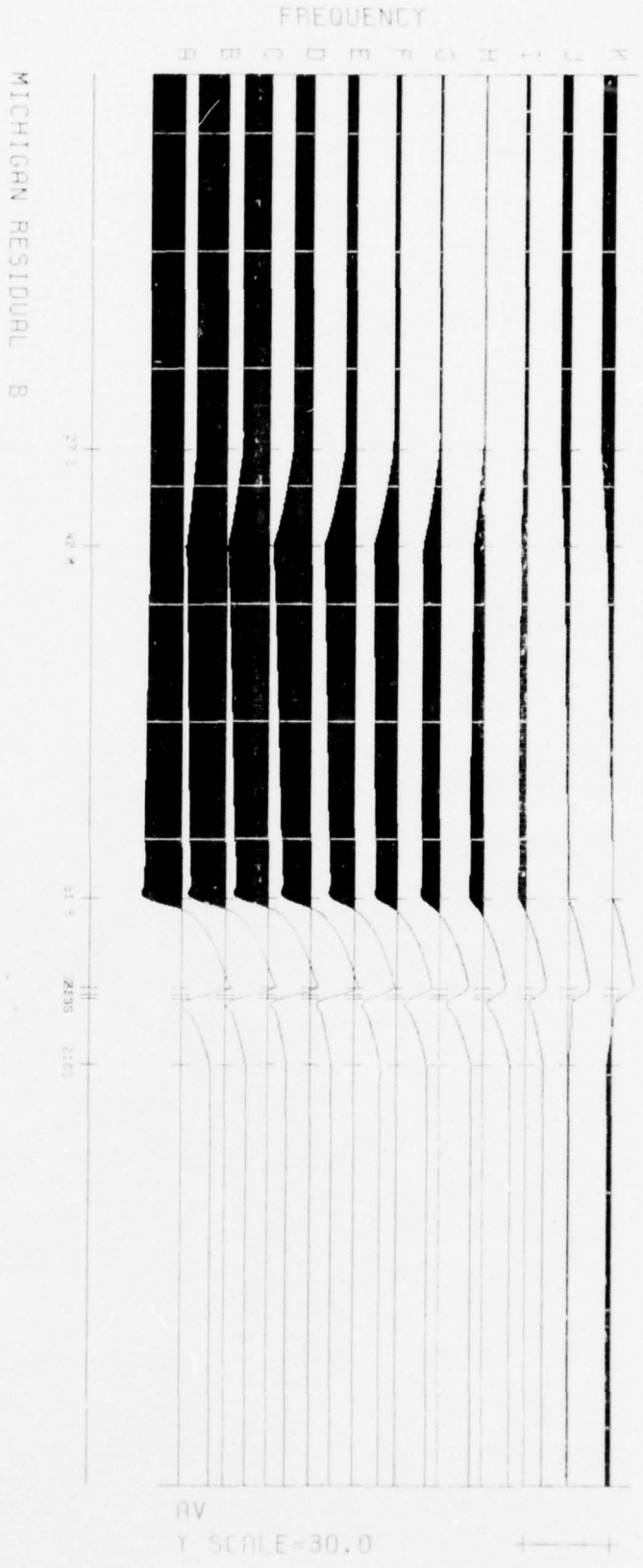
FREQUENCY
MICHIGAN RESIDUAL B
AV
Y SCALE=30.0

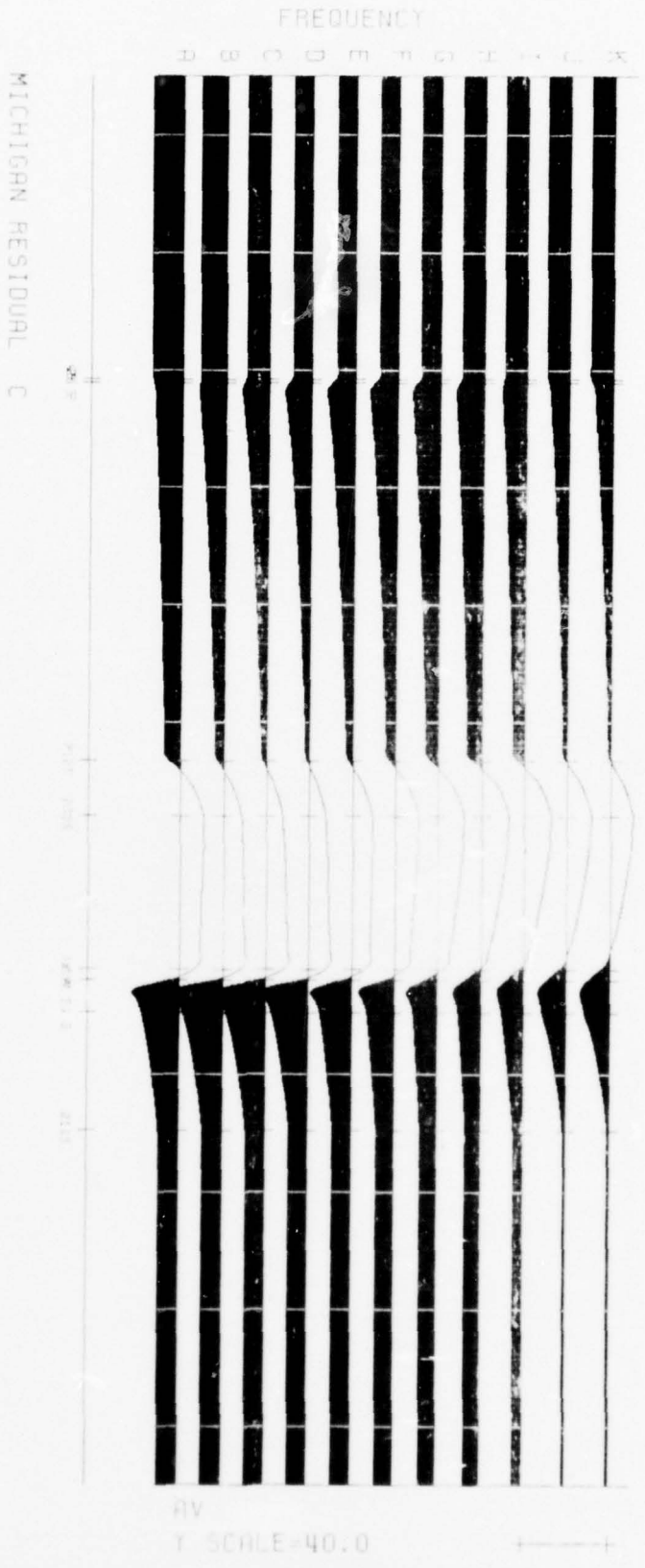
FREQUENCY
MICHIGAN RESIDUAL C
AV
Y SCALE=40.0

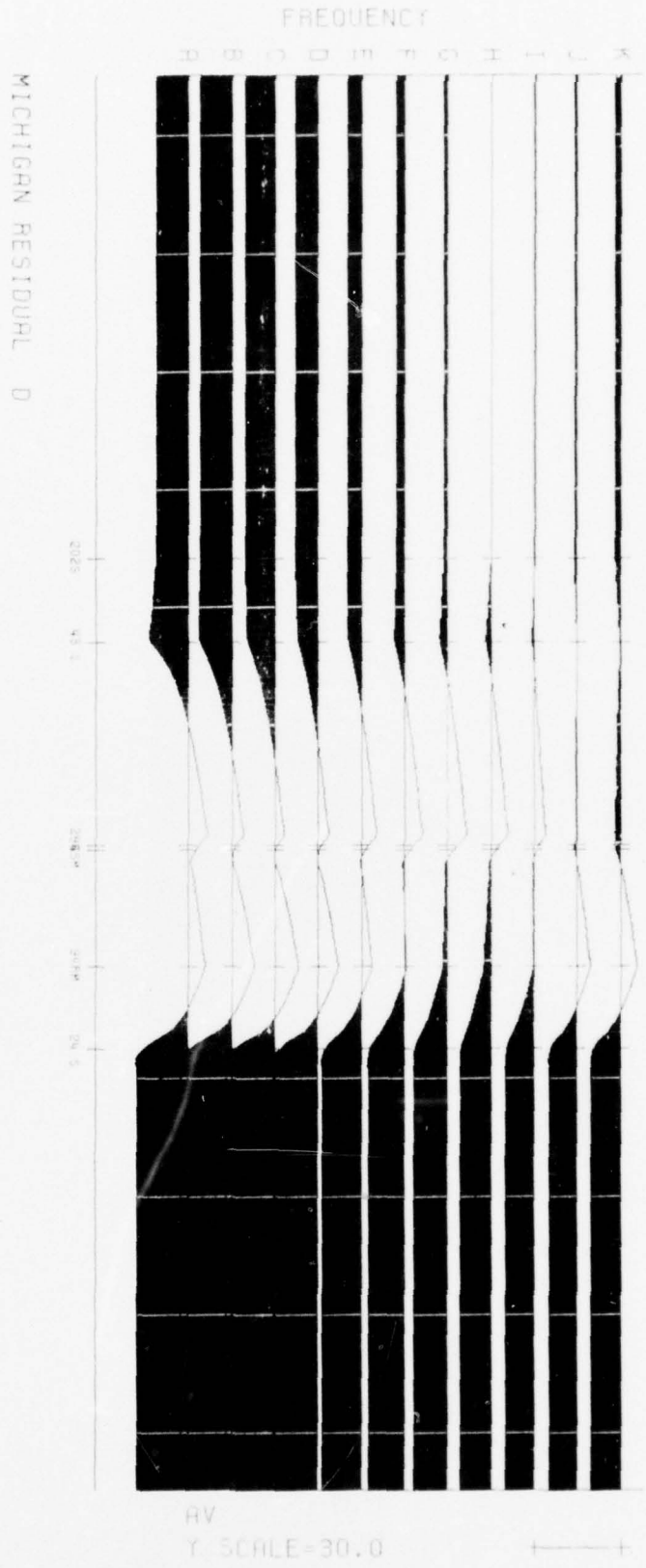
FREQUENCY
MICHIGAN RESIDUAL 0
AV
Y SCALE=30.0

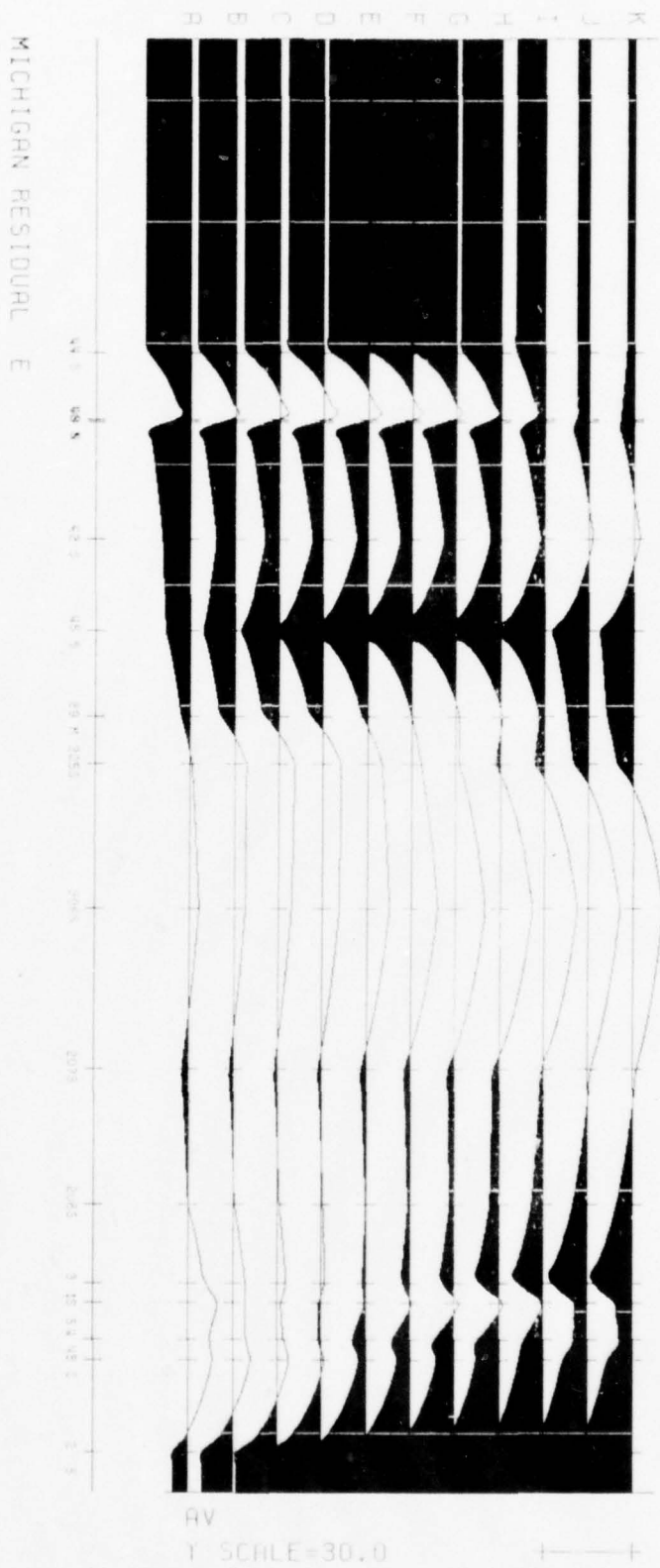
FREQUENCY
MICHIGAN RESIDUAL E
AV
Y SCALE=30.0

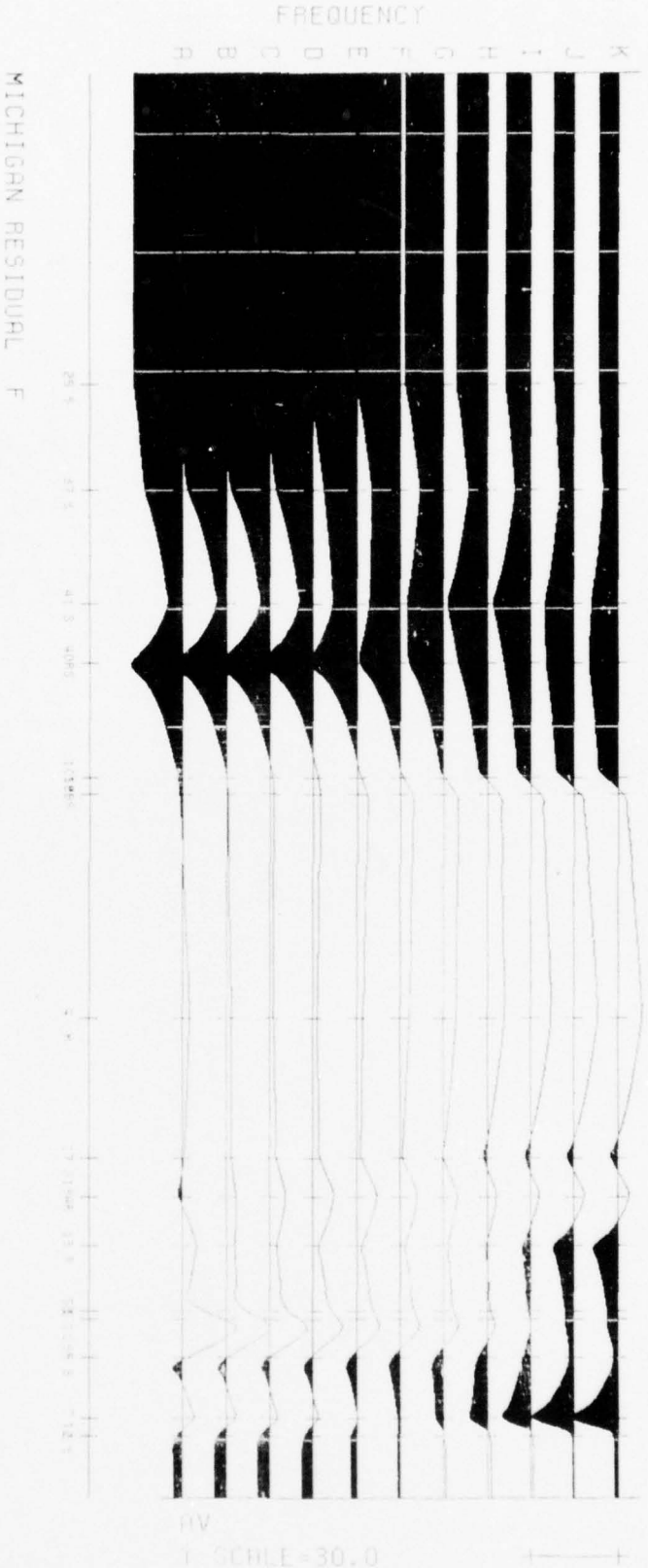
FREQUENCY
MICHIGAN RESIDUAL F
AV
1 SCALE=30.0

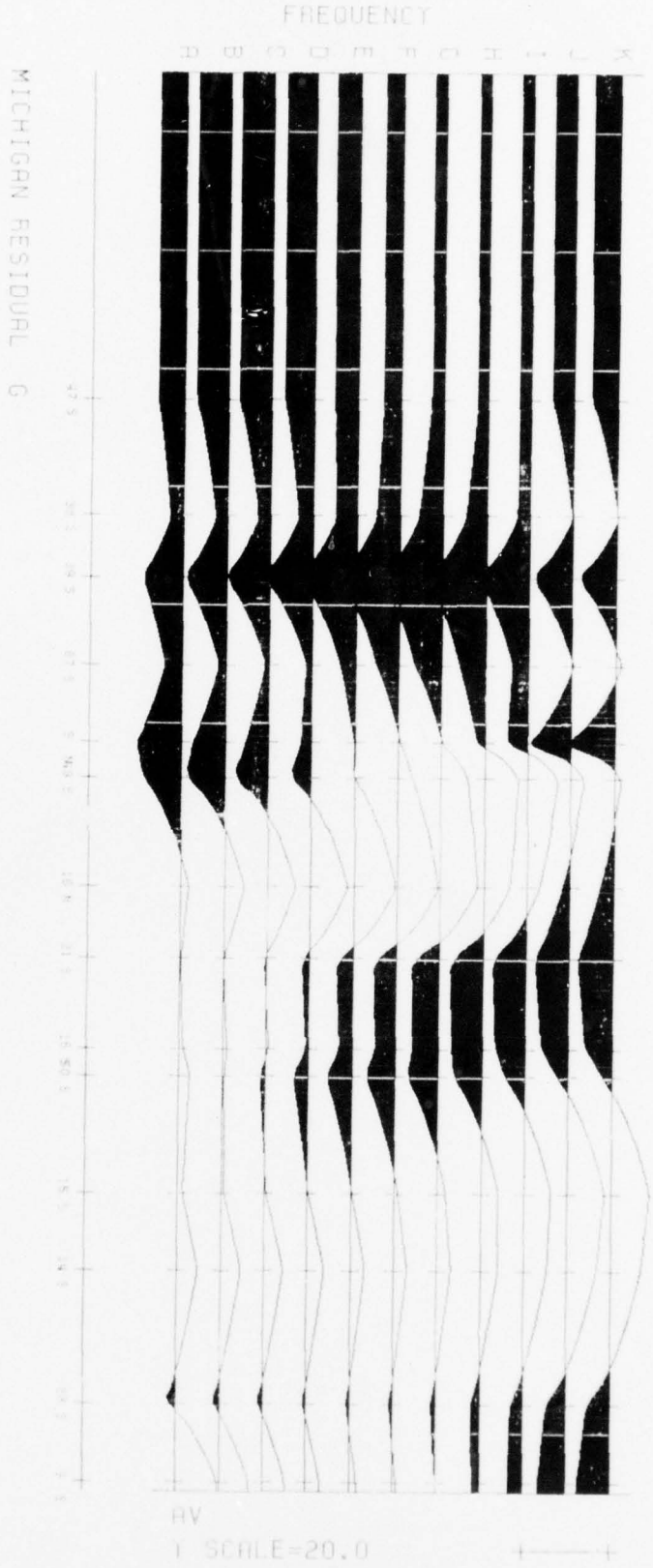
FREQUENCY
MICHIGAN RESIDUAL G
AV
SCALE=20.0

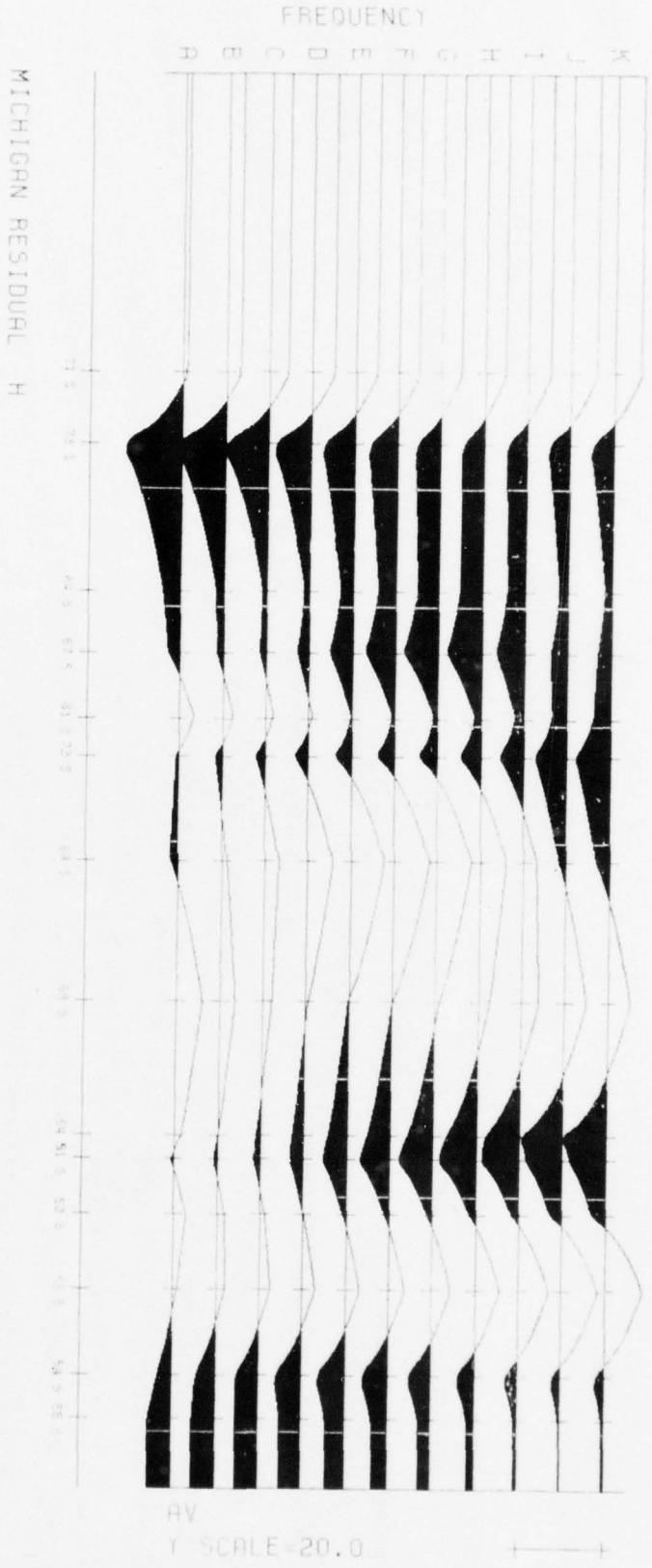
FREQUENCY
MICHIGAN RESIDUAL H
AV
Y SCALE=20.0

FREQUENCY
MICHIGAN RESIDUAL 1
AV
Y SCALE=30.0

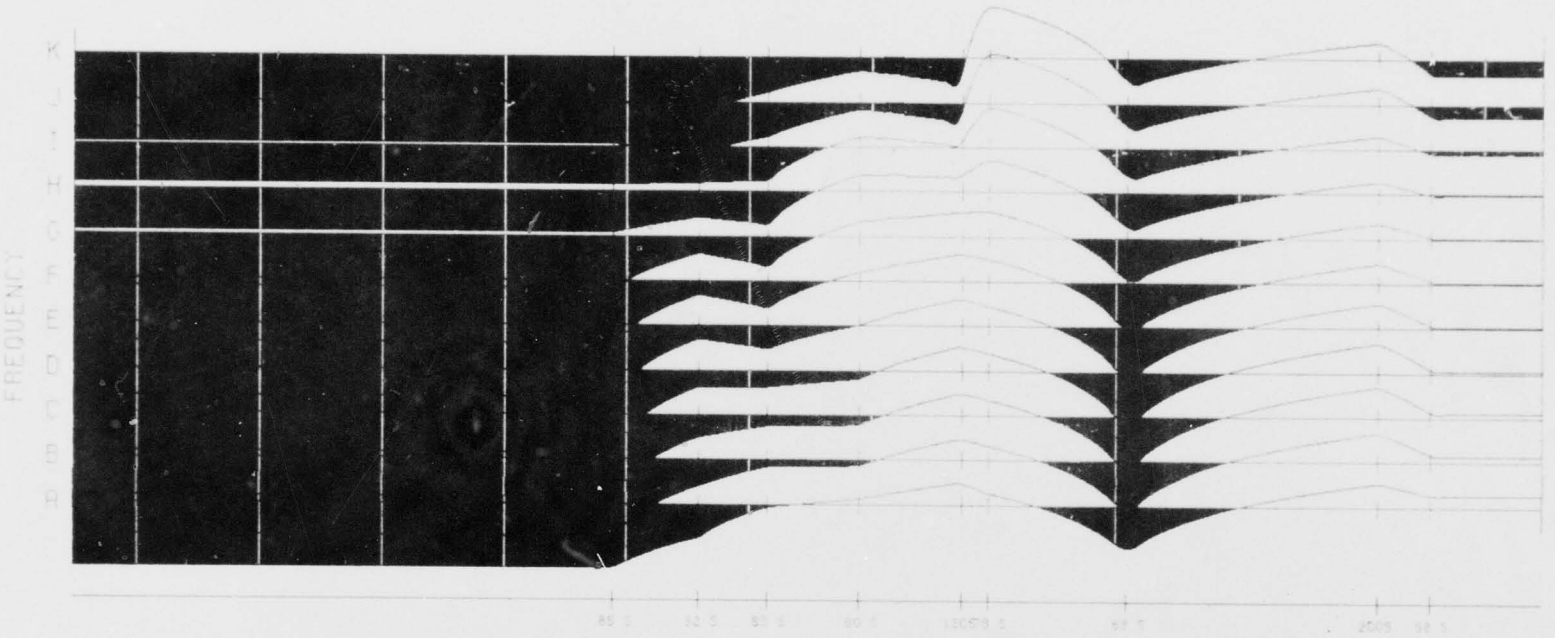

MICHIGAN RESIDUAL J

SECTION A.4

MICHIGAN

ANISOTROPY

TE/TM RATIO

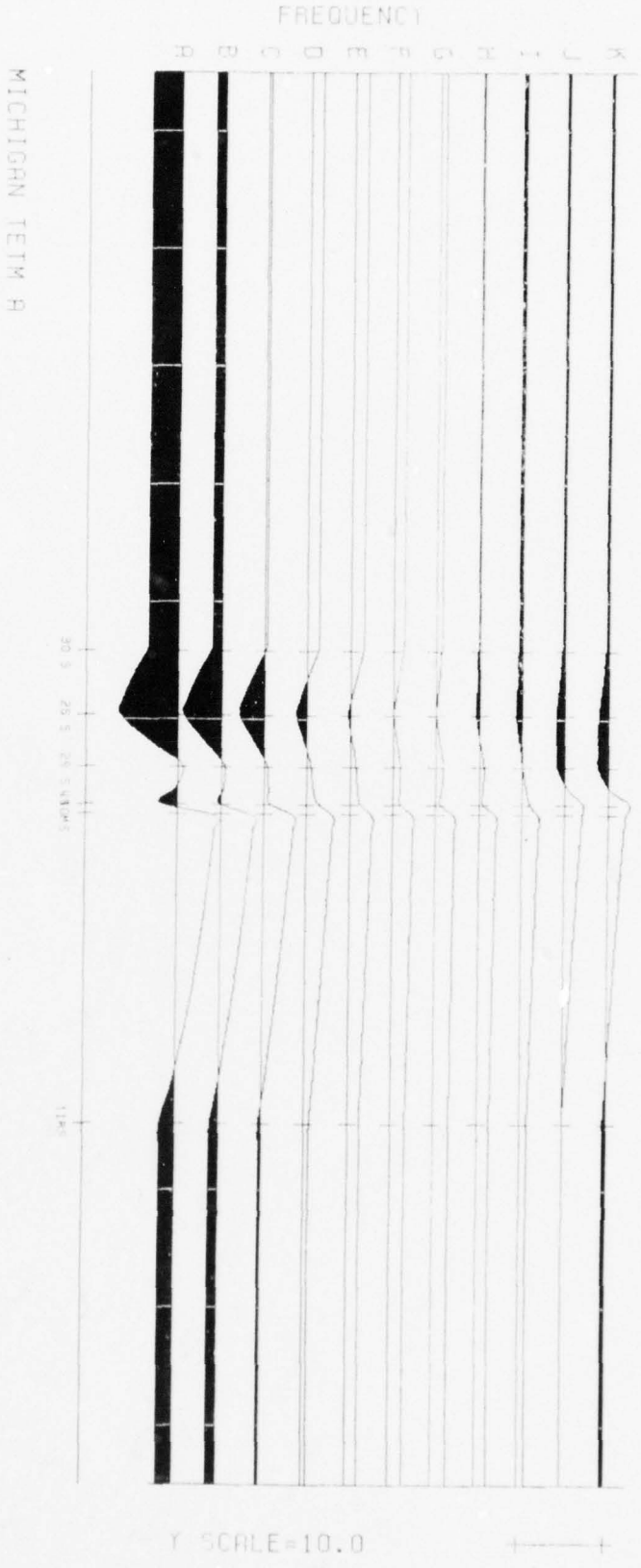
FREQUENCY
MICHIGAN TETM A
Y SCALE=10.0

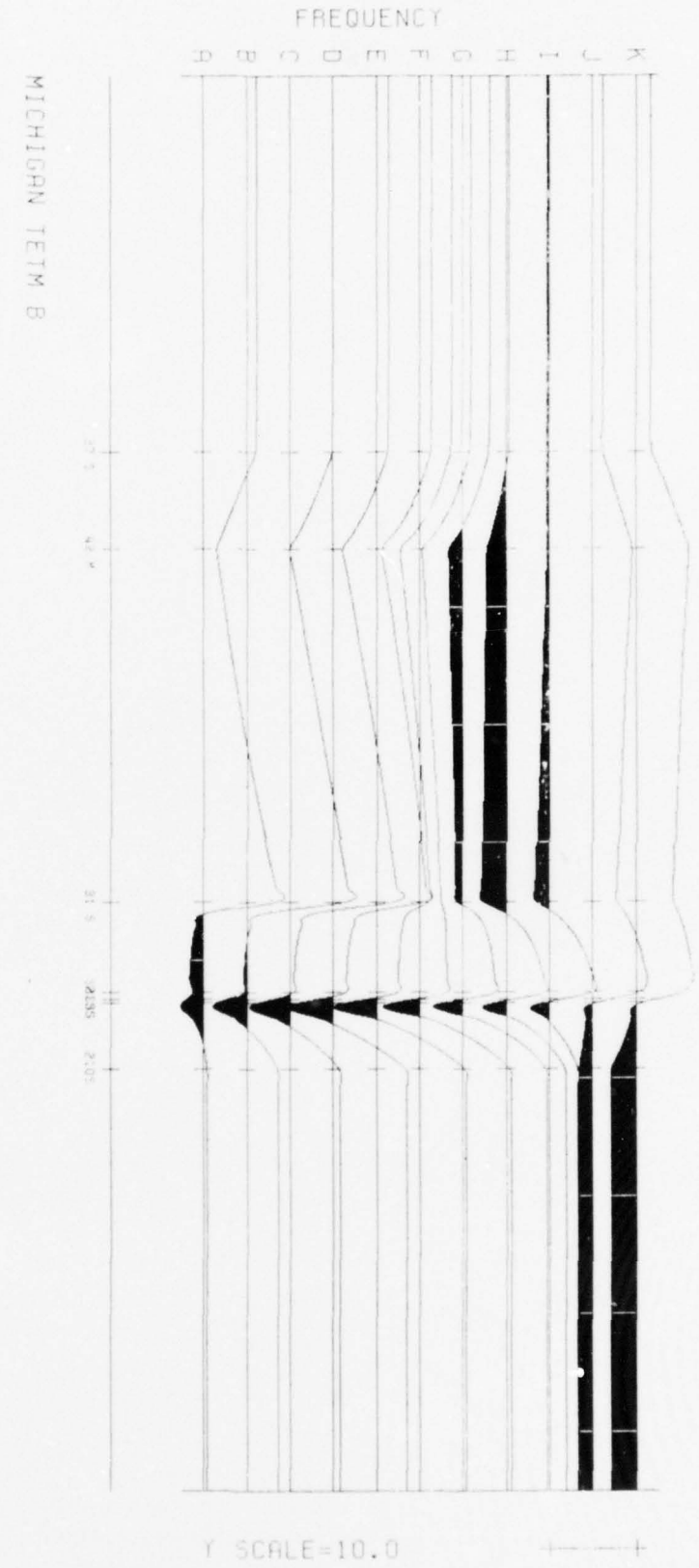
FREQUENCY
A B C D E F G H I J K
MICHIGAN TETM B
Y SCALE=10.0

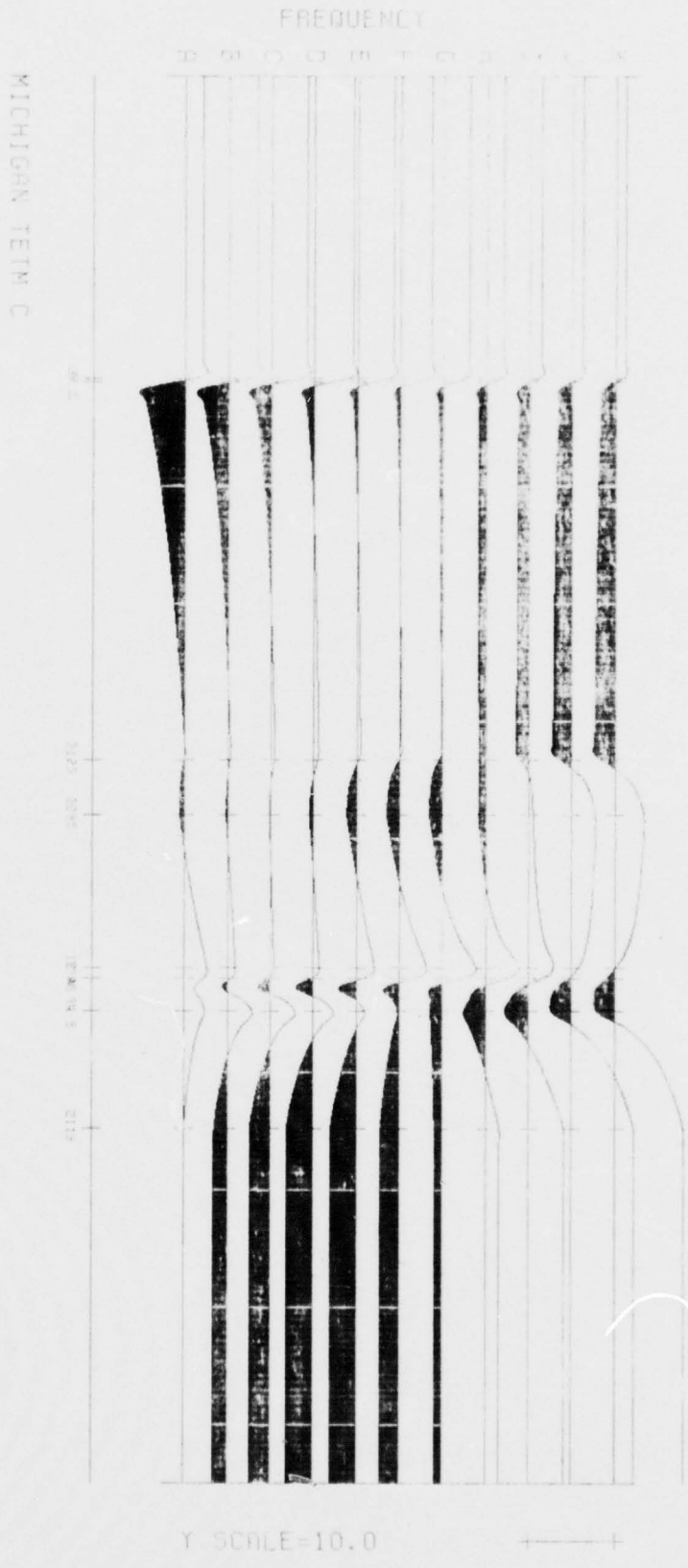
FREQUENCY
MICHIGAN TETN C
Y SCALE=10.0

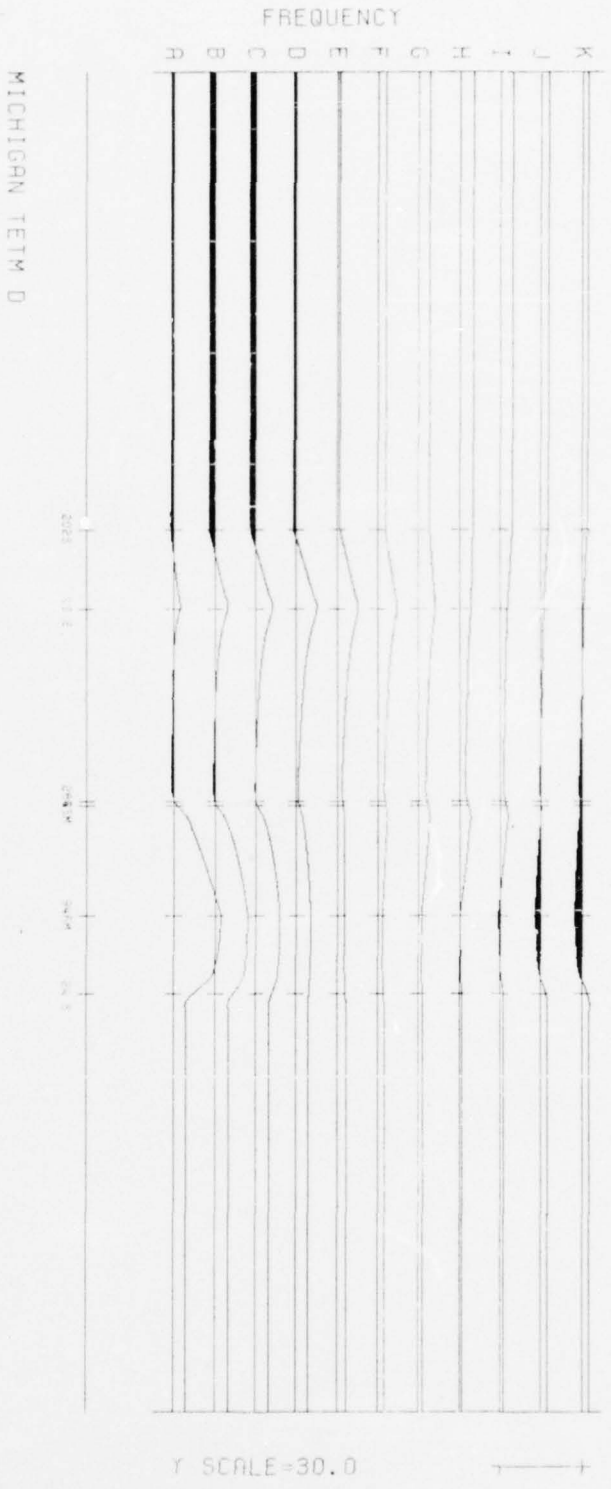
FREQUENCY
MICHIGAN TETM D
Y SCALE=30.0

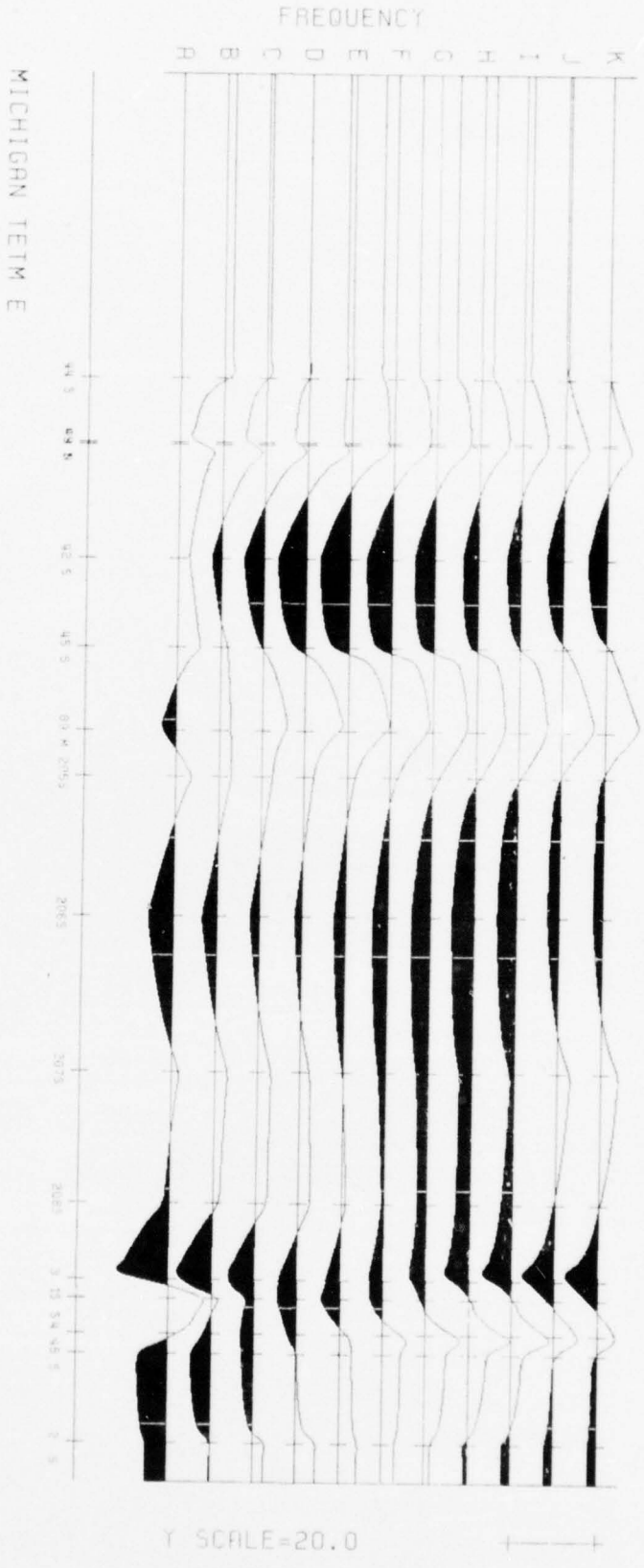
FREQUENCY
MICHIGAN TETM E
Y SCALE=20.0

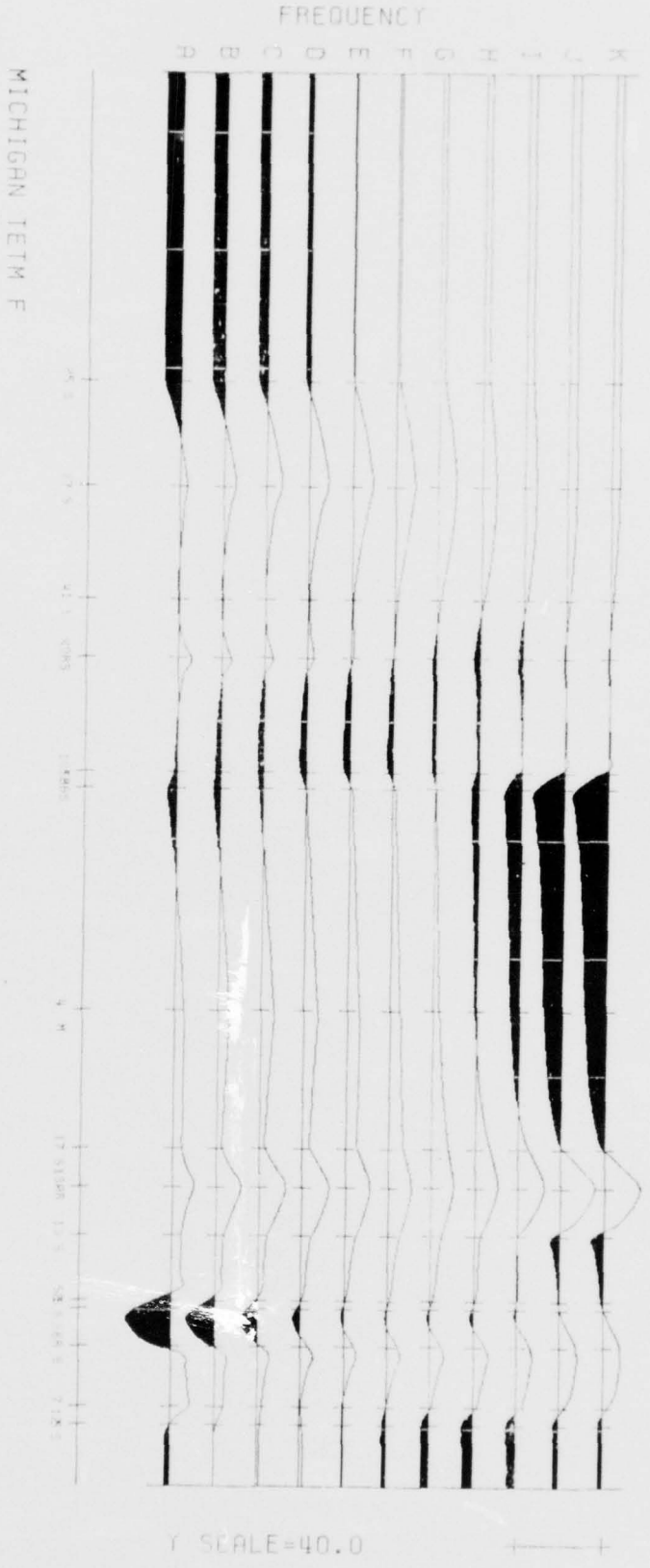
FREQUENCY
MICHIGAN TETM F
Y SCALE=40.0

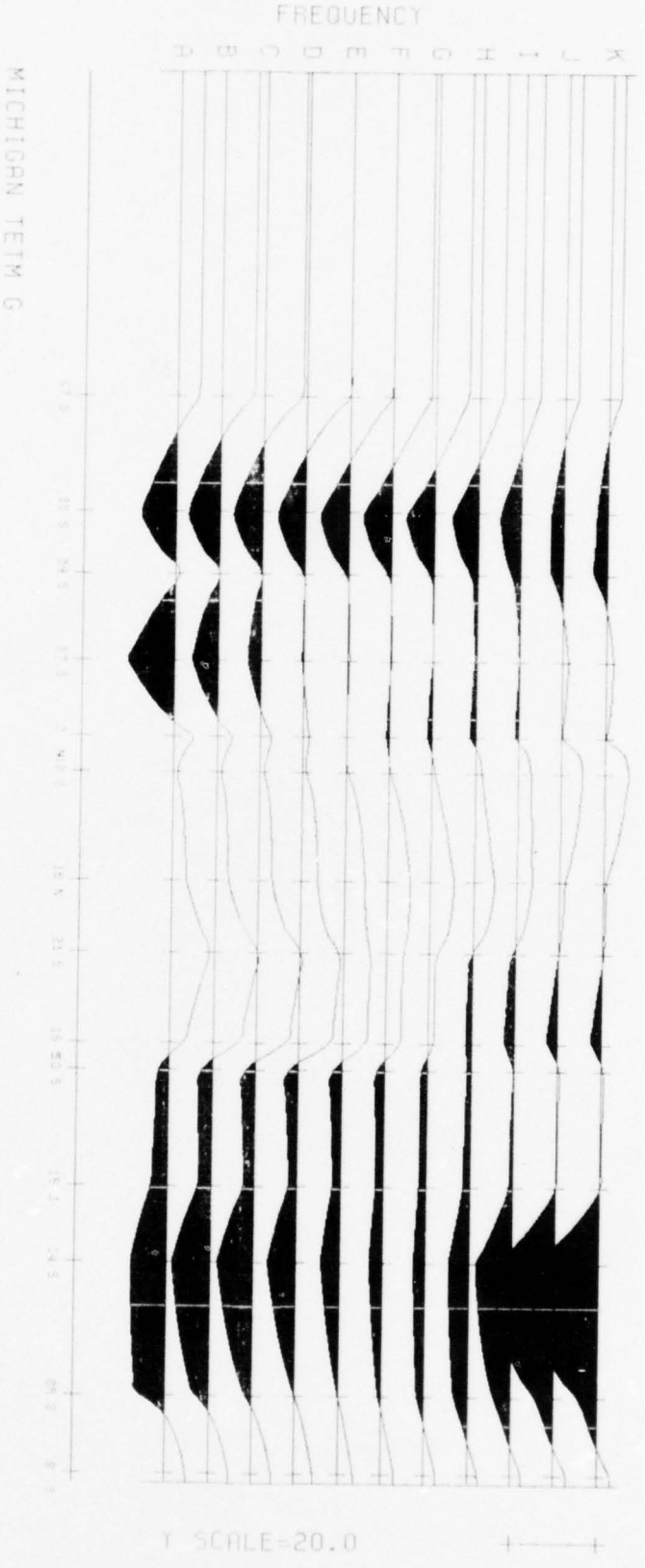
FREQUENCY
MICHIGAN TETM G
Y SCALE=20.0

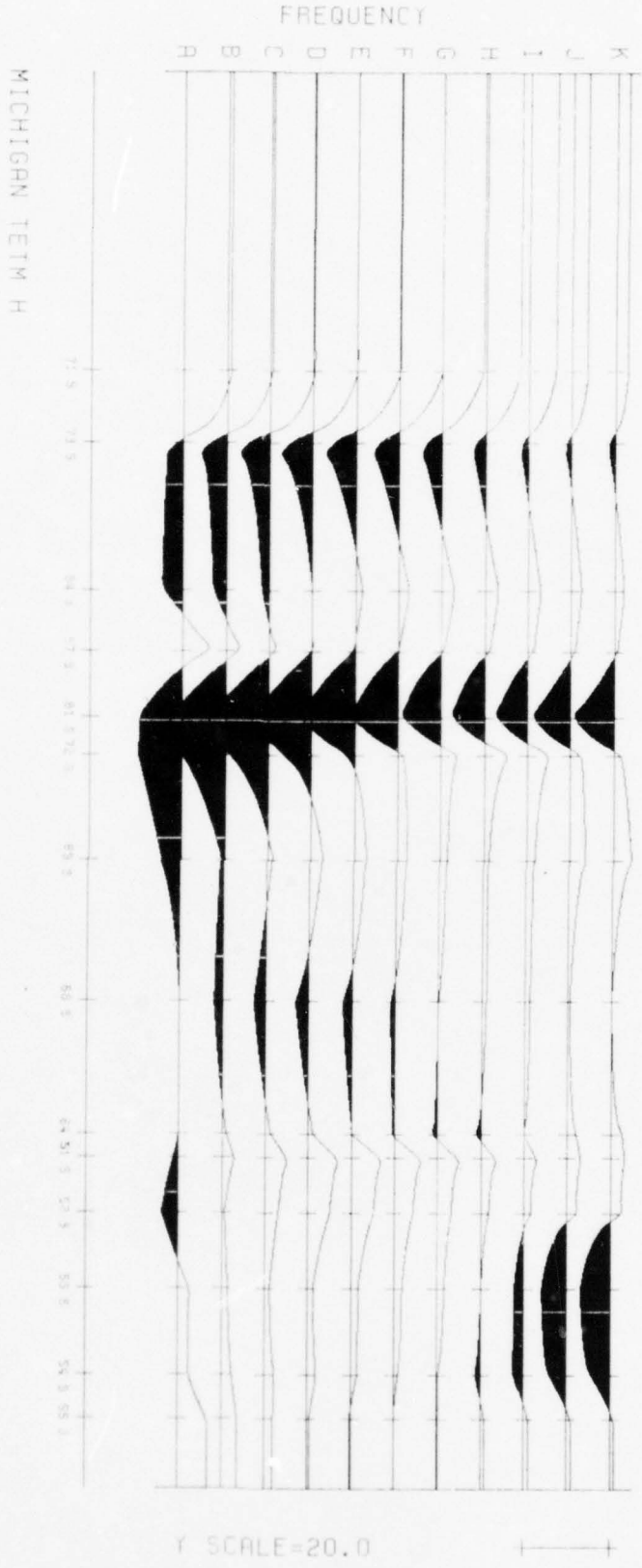
FREQUENCY
MICHIGAN TETM H
Y SCALE=20.0

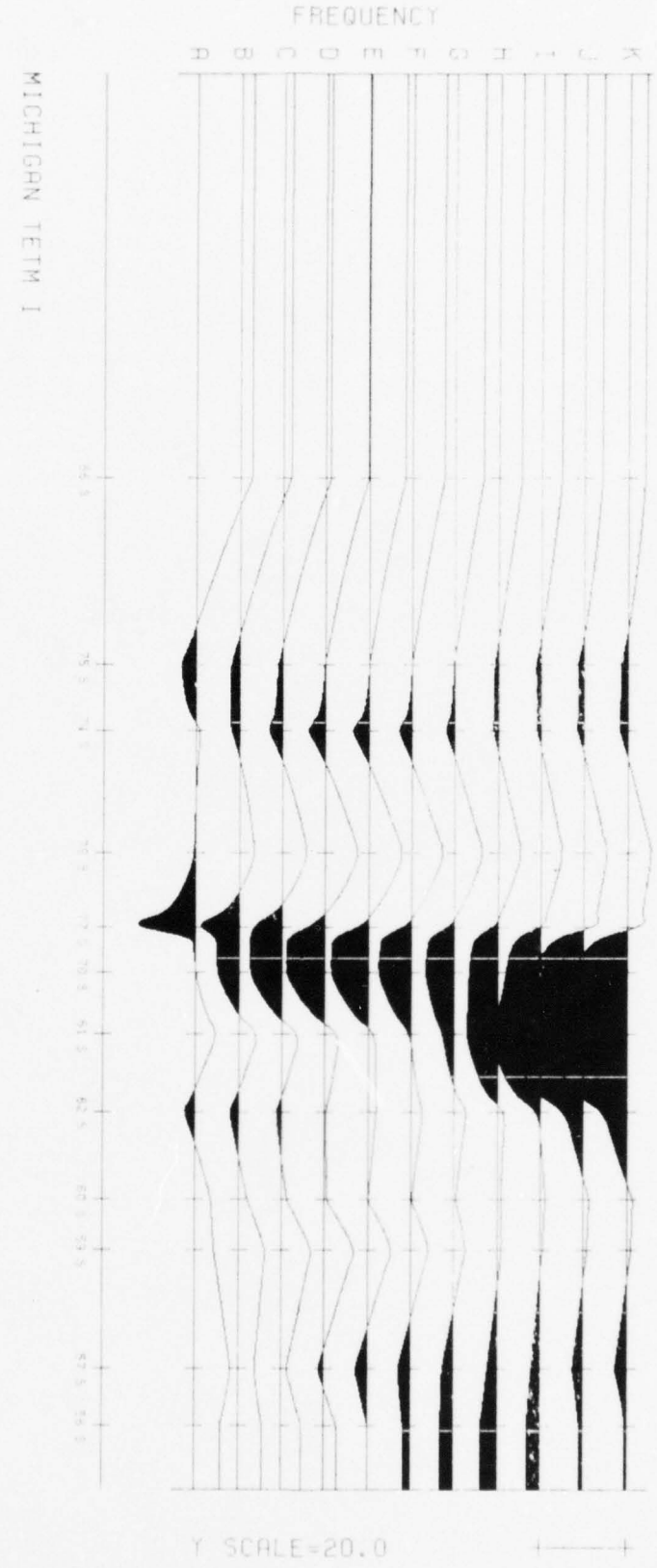
FREQUENCY
MICHIGAN TETM I
Y SCALE=20.0

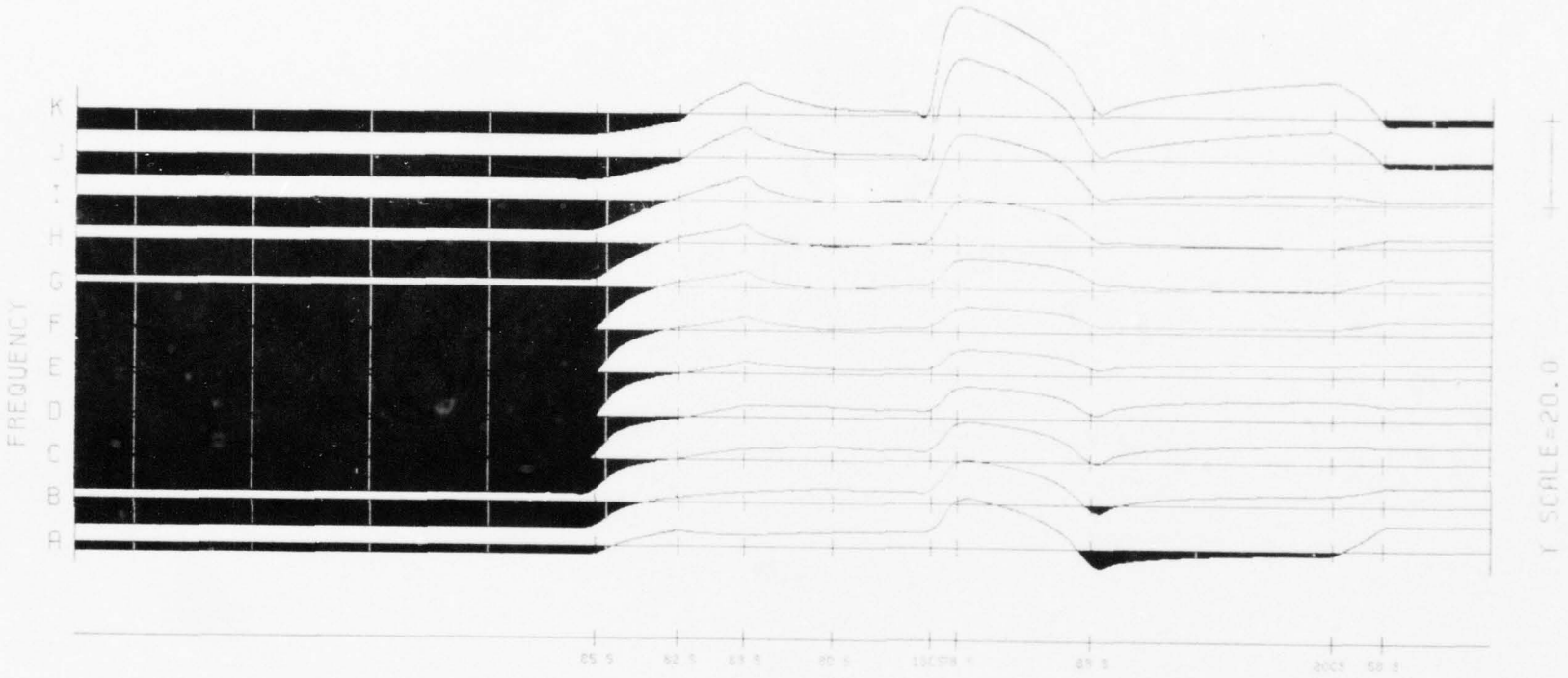

MICHIGAN TETM J

SECTION A.5

MICHIGAN

STATION LOCATIONS

SECTION A.5

MICHIGAN REGION STATION LOCATIONS

STATION DESIGNATION	LATITUDES DEG	LATITUDES MINS	LONGITUDES* DEG	LONGITUDES* MINS
Line A				
S30	46	49.2	271	45.3
S28	46	50.5	271	50.2
S29	46	49.2	271	54.2
M48	46	50.2	271	57.1
S10	46	54.1	271	57.8
S11R	46	47.7	272	21.5
Line B				
S27	46	44.4	271	29.7
M42	46	44.6	271	37.1
S31	46	44.7	272	4.1
S32	46	45.6	272	10.9
S33	46	44.2	272	11.5
S213	46	45.6	272	11.7
S210	46	43.8	272	16.8
Line C				
S46	46	38.9	271	24.2
S26	46	39.1	271	24.5
S212	46	39.7	271	53.5
S203	46	37.5	271	57.7
N12	46	35.2	272	9.5
S33A	46	37.3	272	10.3
S34	46	37.3	272	12.8
S211	46	36.8	272	21.8
Line D				
S202	46	33.1	271	37.9
S43	46	32.5	271	44.3
S204	46	32.5	271	59.8
M35	46	34.9	272	0.1
M94R	46	33.3	272	9.0
S24	46	34.2	272	15.3
Line E				
S44	46	28.2	271	24.3
S48	46	28.5	271	29.3
N9	46	25.7	271	29.4

* For true longitude, subtract from 360°.

STATION DESIGNATION	LATITUDES		LONGITUDES*	
	DEG	MINS	DEG	MINS
S42	46	28.7	271	38.2
S45	46	25.0	271	45.0
M89	46	29.7	271	51.4
S205	45	27.5	271	54.9
S206	46	27.7	272	5.6
S207	46	27.2	272	17.6
S208	46	28.2	272	27.7
S3	46	26.7	272	33.5
S1	46	27.0	272	35.0
S4	46	25.7	272	37.7
S4B	46	25.3	272	39.2
S2	46	27.0	272	46.0
Line F				
S25	46	21.0	271	24.6
S37	46	21.4	271	32.6
S41	46	21.2	271	41.2
S40R	46	21.3	271	45.7
M105	46	22.7	271	54.5
S13B	46	21.0	271	55.7
M4	46	20.7	272	12.6
S17	46	20.9	272	23.3
S13AR	46	24.1	272	26.2
S13	46	22.1	272	29.9
S5B	46	21.2	272	34.9
S5	46	22.8	272	35.5
S6R	46	19.3	272	38.4
S7	46	20.2	272	43.0
S12	46	21.2	272	44.3
Line G				
S47	46	16.1	271	25.8
S38	46	16.2	271	34.7
S39	46	16.2	271	39.4
S87	46	16.1	271	46.1
N3	46	16.8	271	51.9
S49	46	17.2	271	54.6
N16	46	15.3	272	2.9
S21	46	16.2	272	8.4
S16	46	16.7	272	15.3
S50	46	15.8	272	17.4
S15	46	15.5	272	26.3

* For true longitude, subtract from 360°.

STATION DESIGNATION	LATITUDES		LONGITUDES*	
	DEG	MINS	DEG	MINS
S14	46	15.6	272	32.2
S8R	46	16.8	272	42.3
S9	46	16.7	272	48.3
Line H				
S71	46	11.2	271	23.8
S73	46	10.9	271	29.3
S84	46	10.8	271	40.5
S67	46	11.5	271	45.2
S81	46	10.7	271	50.2
S72	46	11.0	271	53.1
S69	46	11.1	272	1.1
S68	46	10.0	272	11.8
S64	46	11.4	272	22.0
S51	46	12.4	272	23.8
S52	46	11.5	272	28.0
S53	46	12.2	272	33.8
S54	46	10.3	272	40.4
S55	46	8.5	272	43.7
Line I				
S86	46	7.1	271	31.9
S75	46	5.9	271	46.1
S74	46	7.1	271	51.1
S79	46	5.7	272	0.5
S77	46	5.9	272	6.2
S70	46	6.9	272	9.6
S61	46	6.7	272	14.3
S62	46	6.7	272	20.2
S60	46	6.5	272	26.9
S59	46	6.1	272	30.7
S57	46	5.8	272	39.8
S56	46	5.7	272	44.1
Line J				
S85	46	1.4	271	40.7
S82	46	1.8	271	47.0
S83	46	1.7	271	52.0
S80	46	0.9	271	58.8
S130	46	1.8	272	6.3
S78	46	1.4	272	8.8

* For true longitude, subtract from 360°.

STATION DESIGNATION	LATITUDES DEG	LATITUDES MINS	LONGITUDES* DEG	LONGITUDES* MINS
S63	46	1.3	272	18.5
S200	46	1.6	272	36.9
S58	46	1.5	272	40.8

* For true longitude, subtract from 360°.

Stations not used (either repeats or bad station measurements):

S38, S22, S11, S11R, S19, S32R, S21A, S4BR, S13A, S6, S8, S40, M94, N12R

NUSC-SELECTED SITE LOCATIONS

NUSC SITES	LATITUDES DEG	LATITUDES MINS	LONGITUDES DEG	LONGITUDES MINS	AVERAGE LOG ρ (75 Hz)
N2	46	36.9	87	36.1	3.25
N3	46	18.1	88	8.8	2.95
N4	46	11.5	87	58.9	3.10
N5	46	23.2	87	8.4	1.77
N6	46	14.3	87	15.7	3.68
N7	46	12.1	87	28.8	3.64
N8	46	13.5	88	21.1	3.11
N9	46	25.7	88	30.5	2.54
N10	46	39.0	88	17.8	3.28
N11	46	54.2	88	5.0	2.46
N12	46	34.3	87	50.4	4.44
N14	46	20.3	88	19.1	3.55
N15	46	30.5	88	16.7	3.77
N16	46	14.8	87	54.4	3.70
N28	46	23.2	88	39.2	2.39
N32	46	2.4	87	41.9	2.36
N33	46	7.1	87	48.5	3.77

APPENDIX B

WISCONSIN DATA

CONTENTS

SECTION		PAGE
B.1	Log Resistivity vs Log Frequency with Polynomial Fits	
	North-South Orientation.....	B-3
	East-West Orientation.....	B-5
	Averaged Data.....	B-7
B.2	Pseudosections	
	North-South Orientation.....	B-10
	East-West Orientation.....	B-11
	Averaged Data.....	B-12
B.3	Residuals	
	North-South Orientation.....	B-14
	East-West Orientation.....	B-15
	Averaged Data.....	B-16
B.4	Anisotropy (TE/TM Ratio).....	B-18

SECTION B.1

WISCONSIN

LOG RESISTIVITY VS LOG FREQUENCY WITH POLYNOMIAL FITS

- North-South Orientation
- East-West Orientation
- Averaged Data

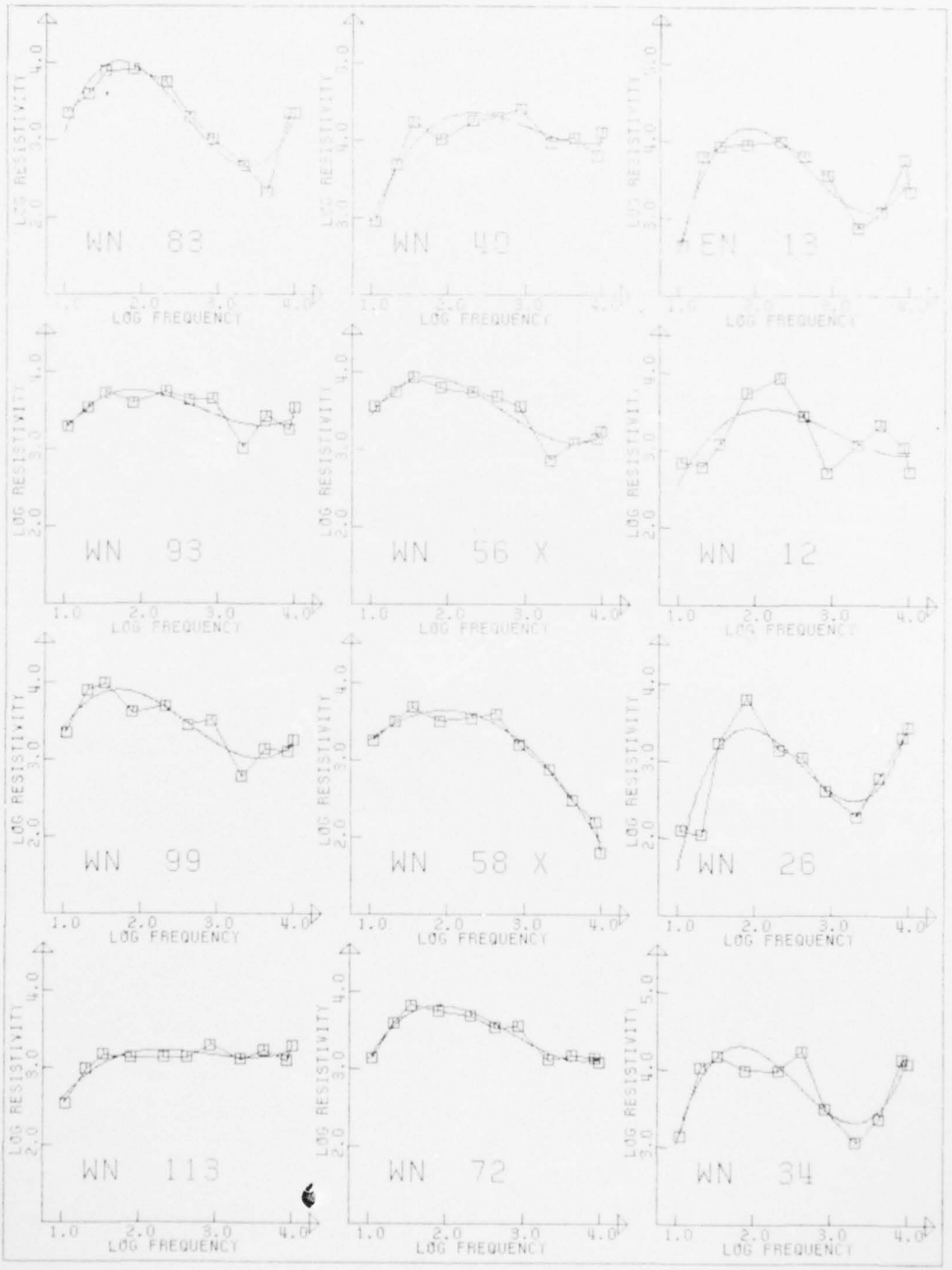
WN 83
WN 40
WEN 13
WN 93
WN 56 X
WN 12
WN 99
WN 58 X
WN 26
WN 113
WN 72
WN 34
LOG RESISTIVITY
LOG FREQUENCY

B-3

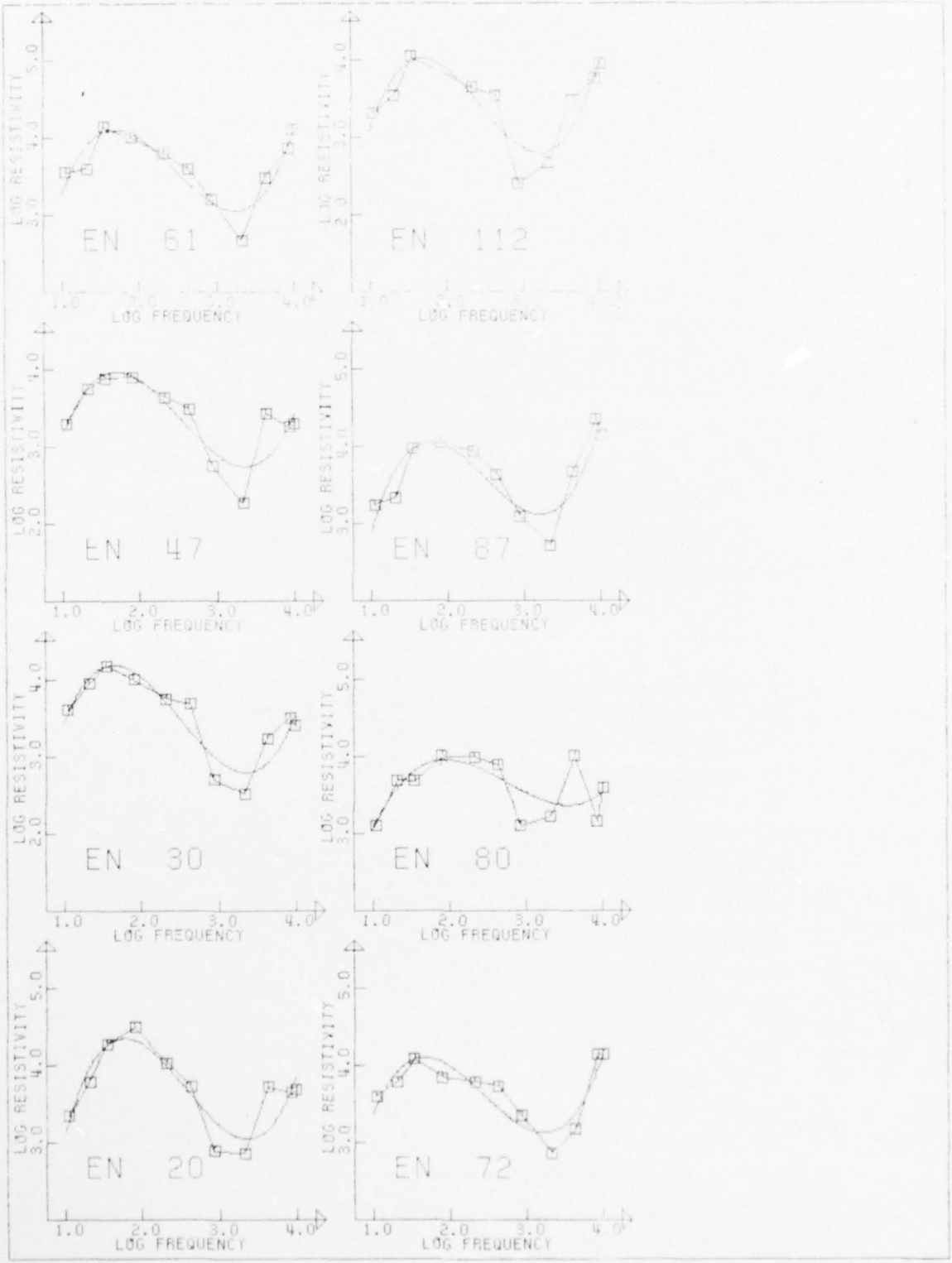
EN 61
EN 112
EN 47
EN 87
EN 30
EN 80
EN 20
EN 72
LOG RESISTIVITY
LOG FREQUENCY
1.0
2.0
3.0
4.0
5.0

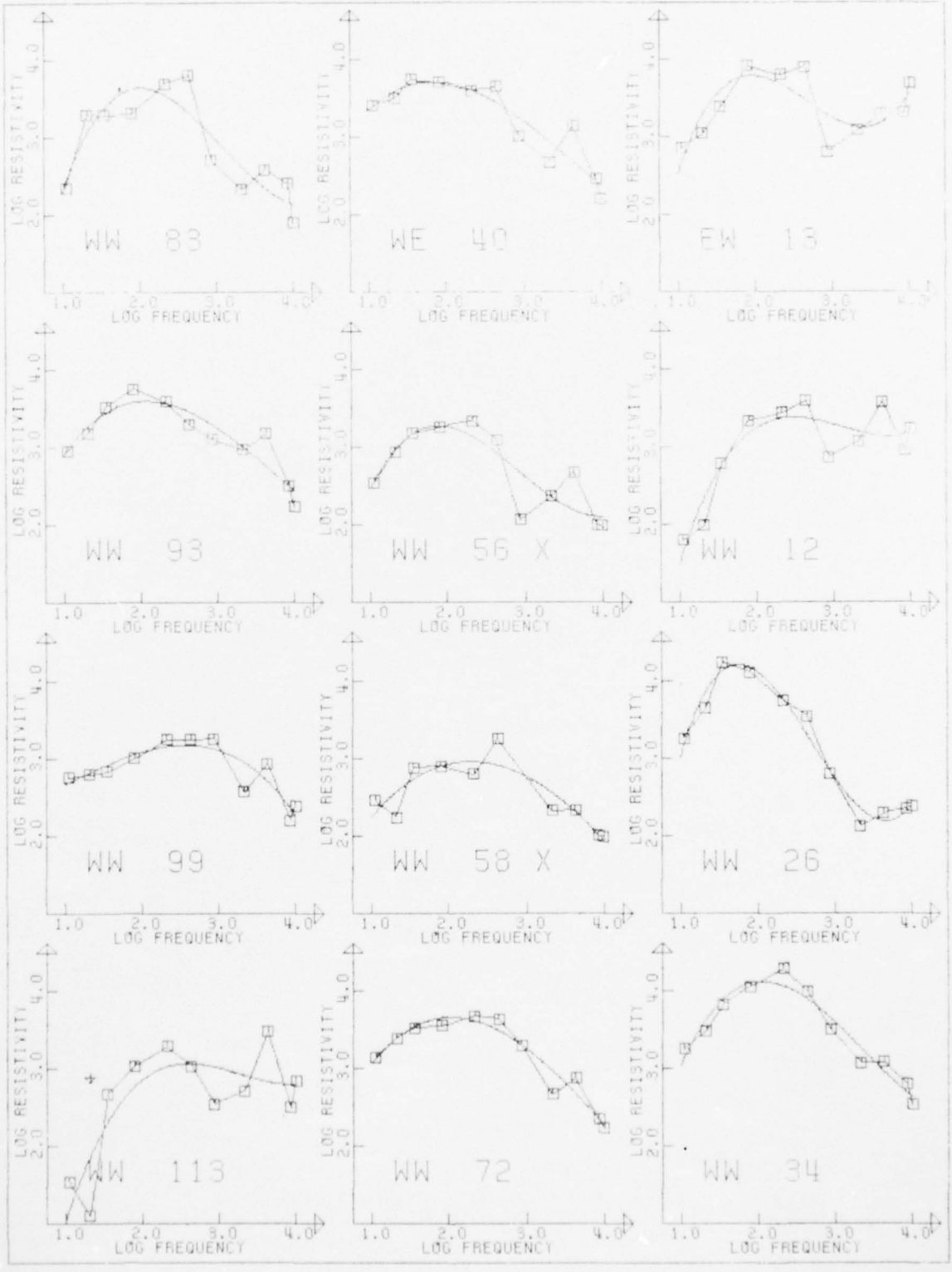
WW 83
WE 40
EW 13
WW 93
WW 56 X
WW 12
WW 99
WW 58 X
WW 26
WW 113
WW 72
WW 34
LOG RESISTIVITY
LOG FREQUENCY
1.0
2.0
3.0
4.0

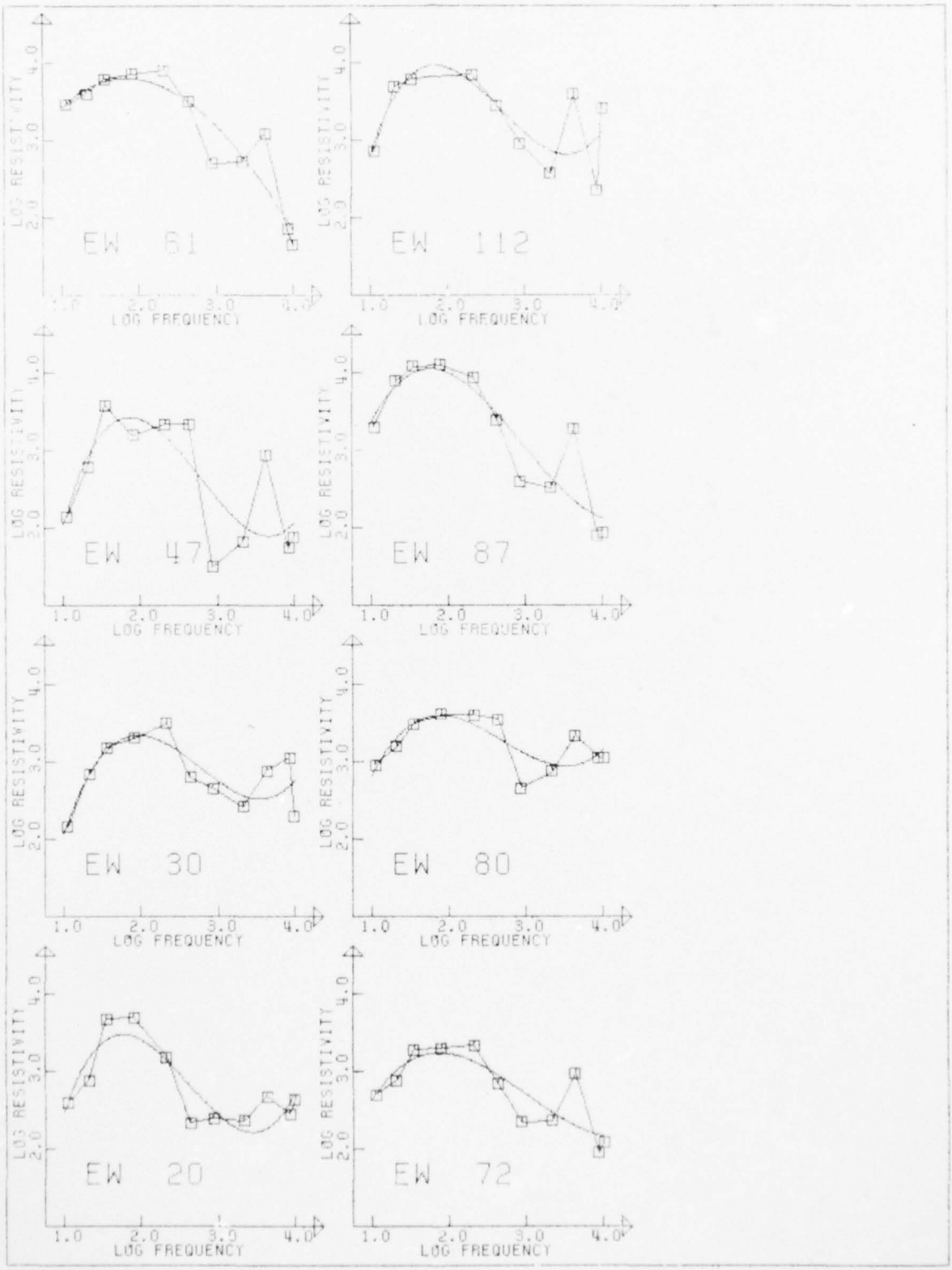
EW 61
EW 112
EW 47
EW 87
EW 30
EW 80
EW 20
EW 72
LOG RESISTIVITY
LOG FREQUENCY
1.0
2.0
3.0
4.0

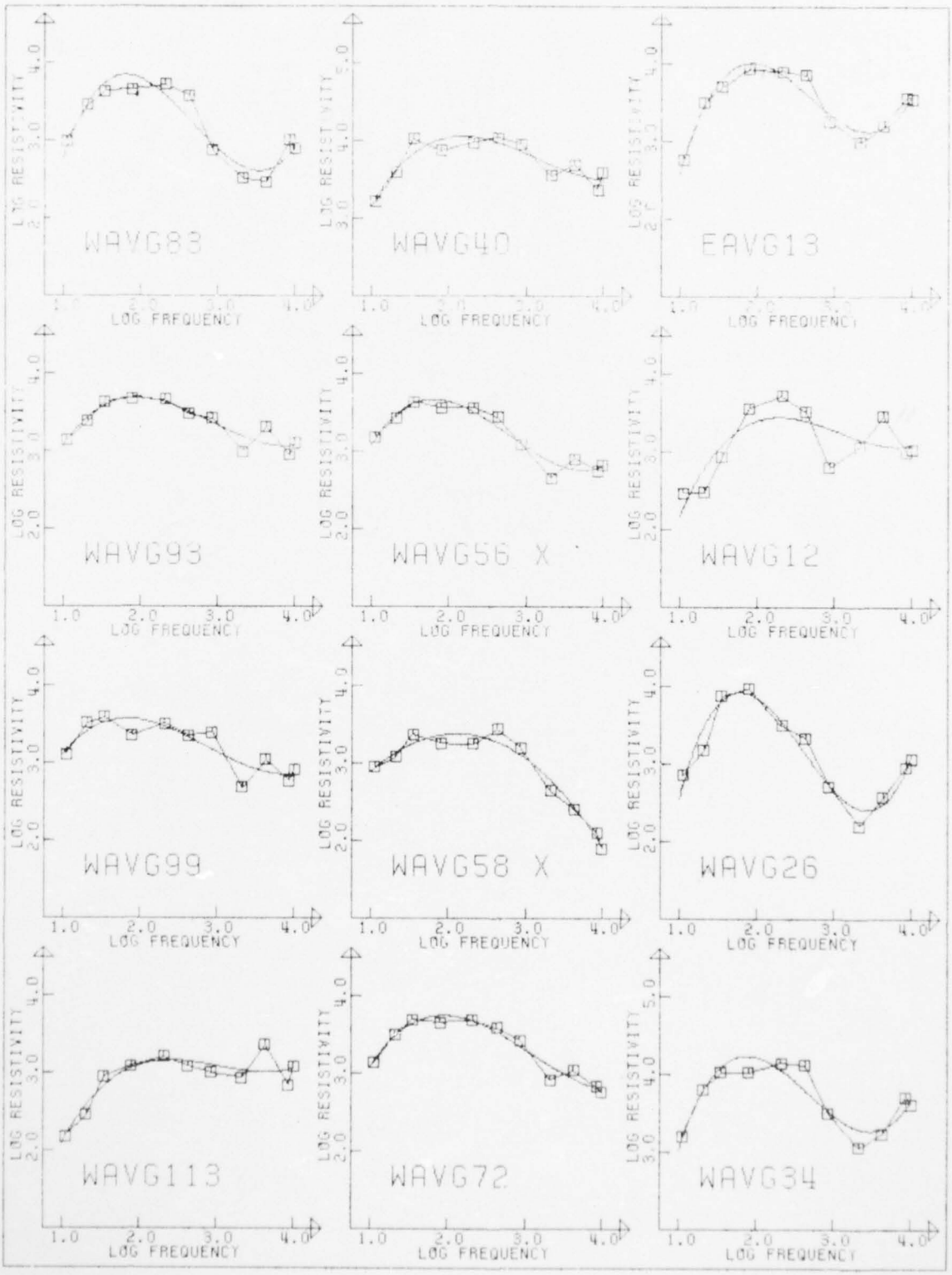
WAVG83
WAVG40
EAVG13
WAVG93
WAVG56 X
WAVG12
WAVG99
WAVG58 X
WAVG26
WAVG113
WAVG72
WAVG34
LOG RESISTIVITY
LOG FREQUENCY

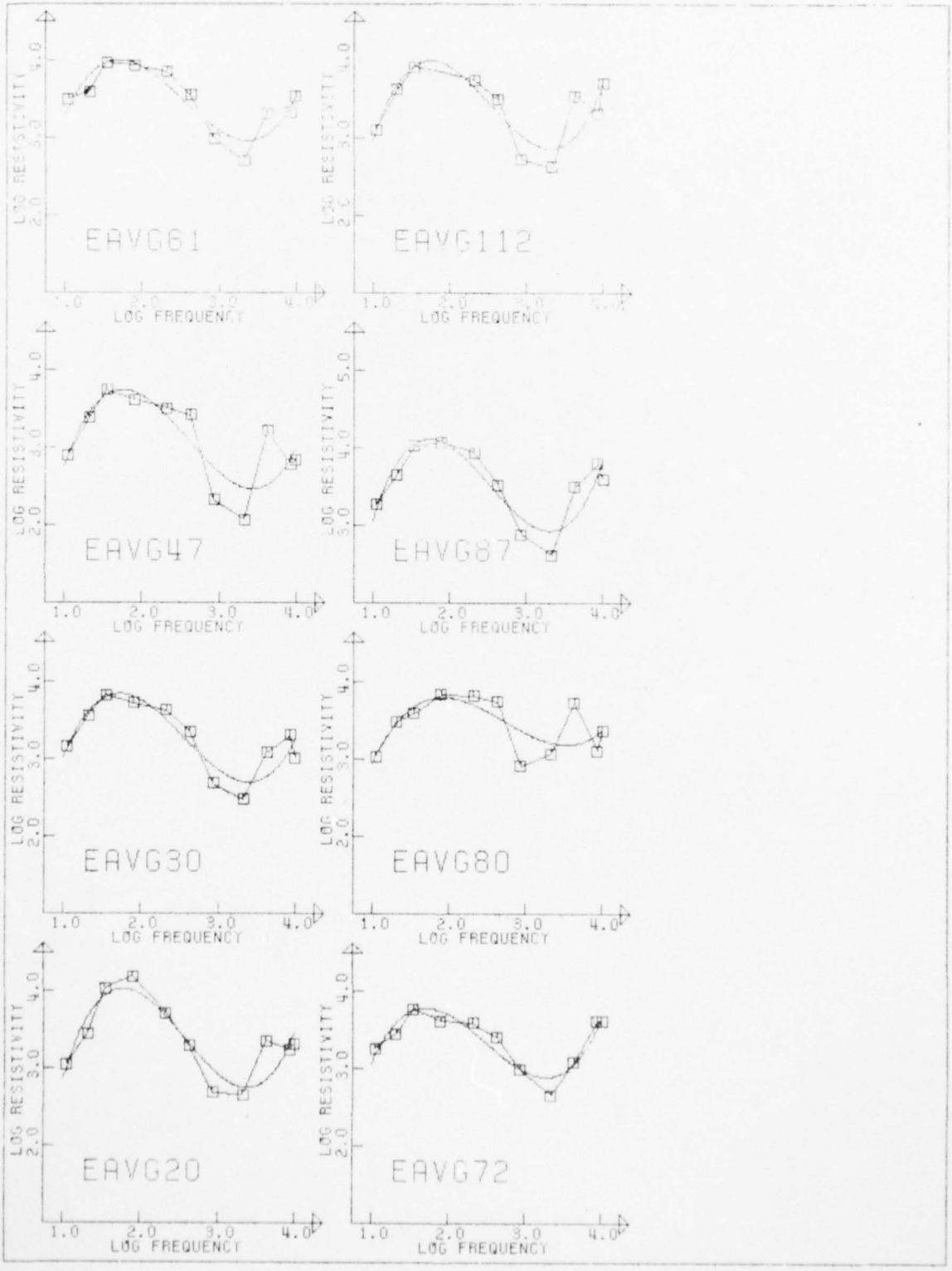
LOG RESISTIVITY
LOG FREQUENCY
EAVG61
EAVG112
EAVG47
EAVG87
EAVG30
EAVG80
EAVG20
EAVG72

SECTION B.2

WISCONSIN

PSEUDOSECTIONS

- North-South Orientation
- East-West Orientation
- Averaged Data

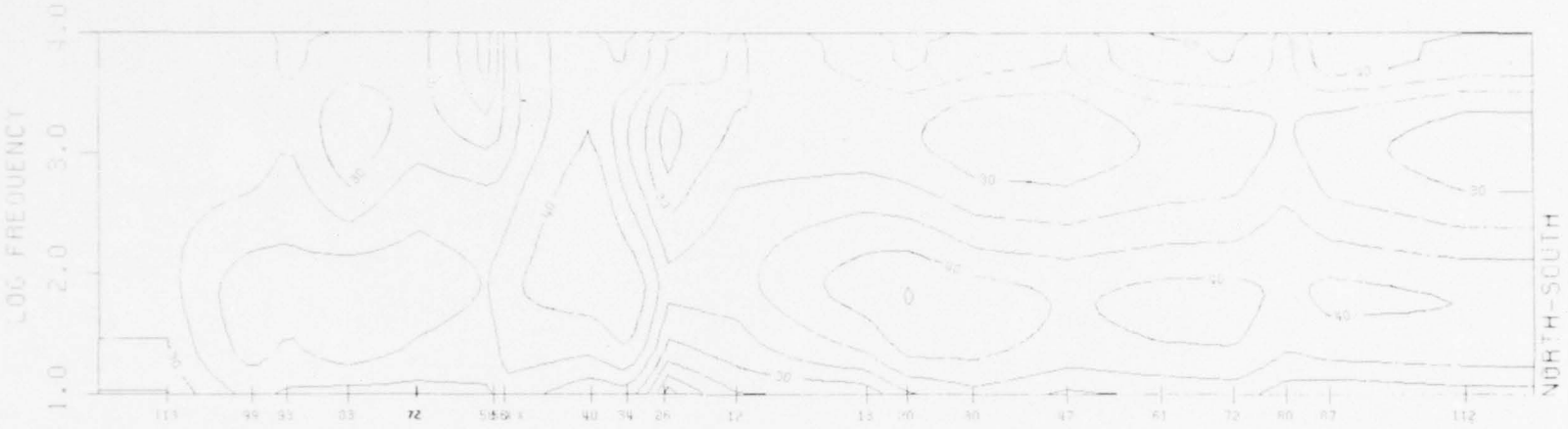

WIS

0 1 2

SCALE - KM

CONTOUR UNITS - 10 LOG ρ

COUNTOUR INTERVAL x 3.33

	ρ-Ω-M
43.3	21,400
40.0	10,000
36.7	4,680
33.3	2,140
30.0	1,000
26.7	468
23.3	214
20.0	100
16.7	46.8
13.3	21.4
10.0	10

LOG FREQUENCY
1.0
2.0
3.0
4.0
EAST-WEST

AD-A036 406 GTE SYLVANIA INC NEEDHAM HEIGHTS MASS COMMUNICATIONS--ETC F/G 17/2
ELF COMMUNICATIONS SEAFARER PROGRAM. SITE SURVEY, MICHIGAN REGI--ETC(U)
APR 76 N00093-75-C-0309

UNCLASSIFIED NL

3 OF 3
AD
A036406

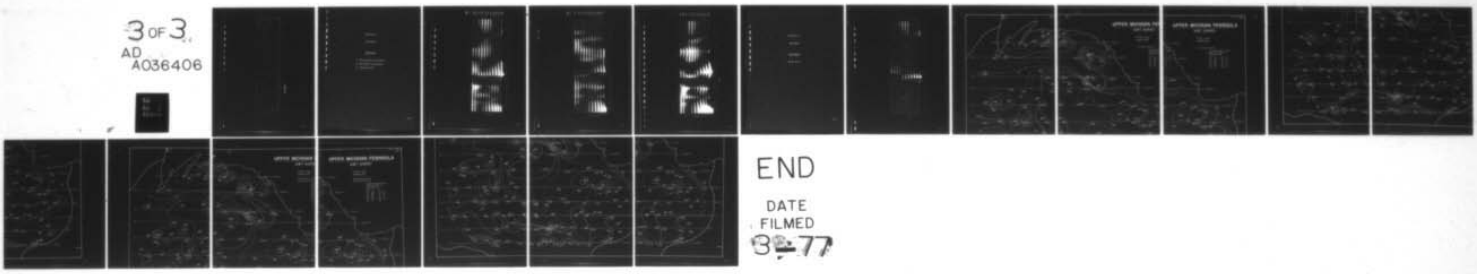

END

DATE
FILMED
3-77

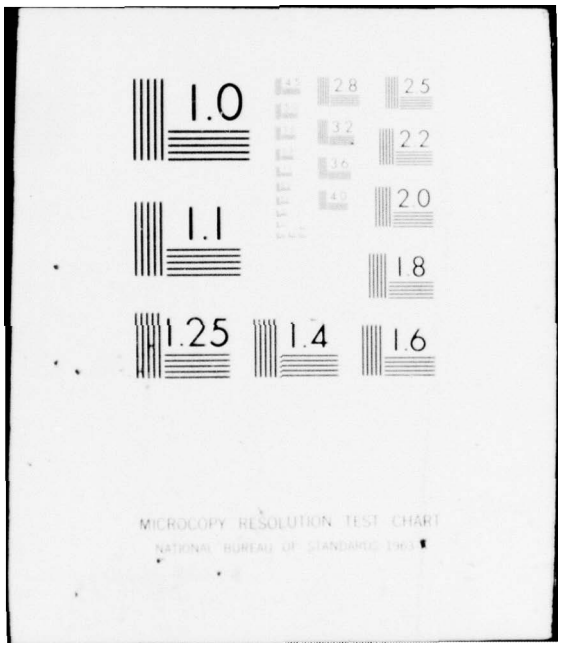
1.0
1.1
1.25
1.4
1.6
2.8
2.5
3.2
2.2
3.6
2.0
4.0
1.8
MICROCOPY RESOLUTION TEST CHART
NATIONAL BUREAU OF STANDARDS 1963

WIG

5. XI.75

SECTION B.3

WISCONSIN

RESIDUALS

- North-South Orientation
- East-West Orientation
- Averaged Data

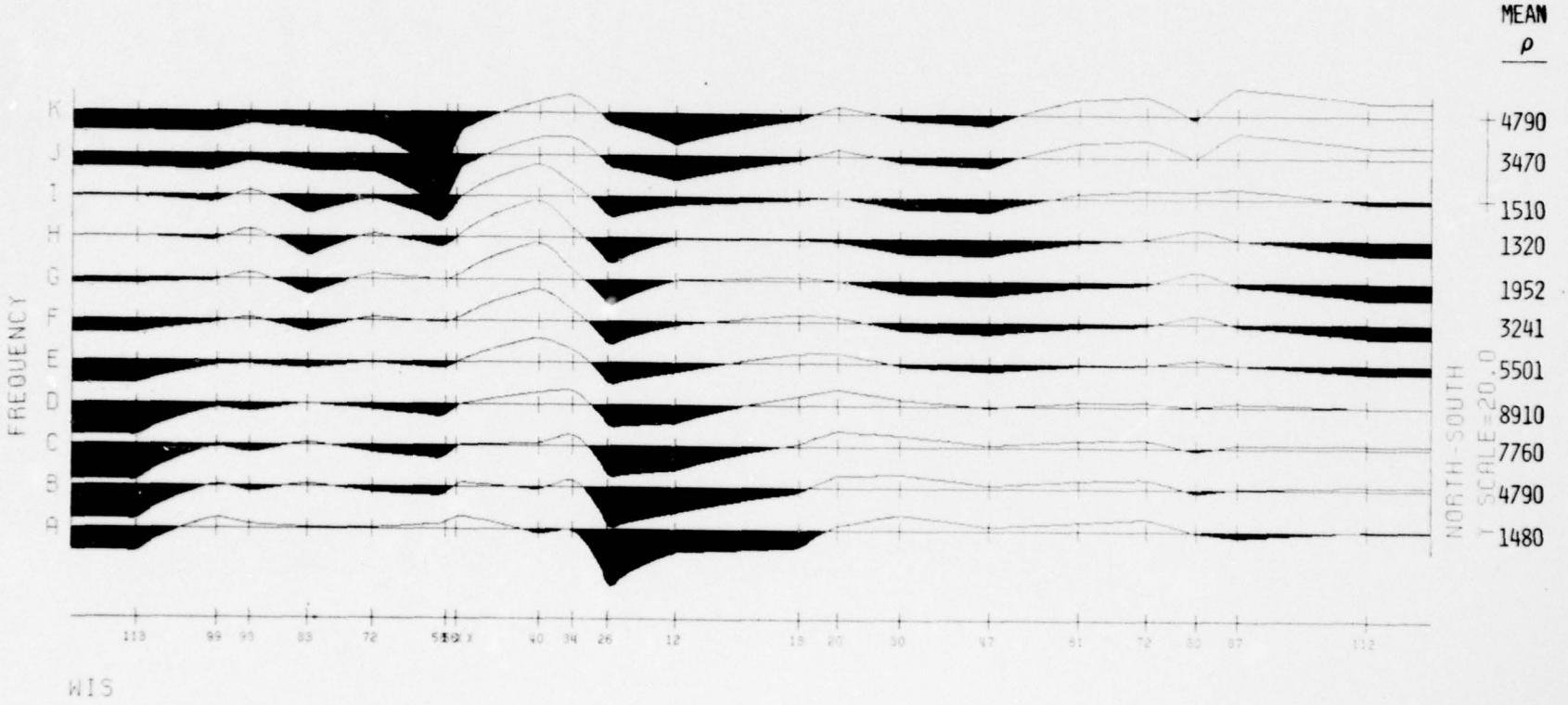
MEAN
ρ
4790
3470
1510
1320
1952
3241
5501
8910
7760
4790
1480
FREQUENCY
K
J
I
H
G
F
E
D
C
B
A
NORTH-SOUTH
Y SCALE=20.0
WIS

MEAN ρ
467
437
447
617
1200
2000
3090
4170
3090
1860
676
EAST-WEST
↑ SCALE=30.0
FREQUENCY
A B C D E F G H I J K
W15

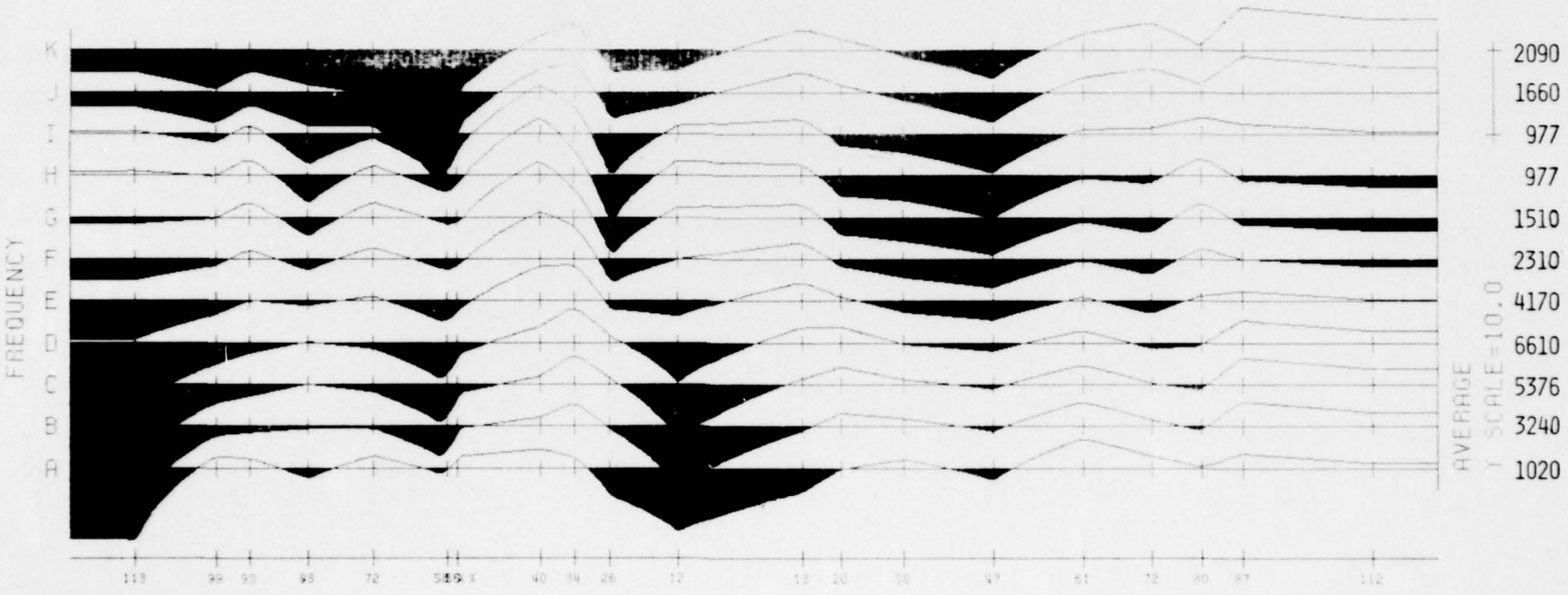
FREQUENCY
K
J
I
H
G
F
E
D
C
B
A
2090
1660
977
977
1510
2310
4170
6610
5376
3240
1020
AVERAGE
Y SCALE=10.0
WIS
5.XI.75

SECTION B.4

WISCONSIN

ANISOTROPY

TE/TM Ratio

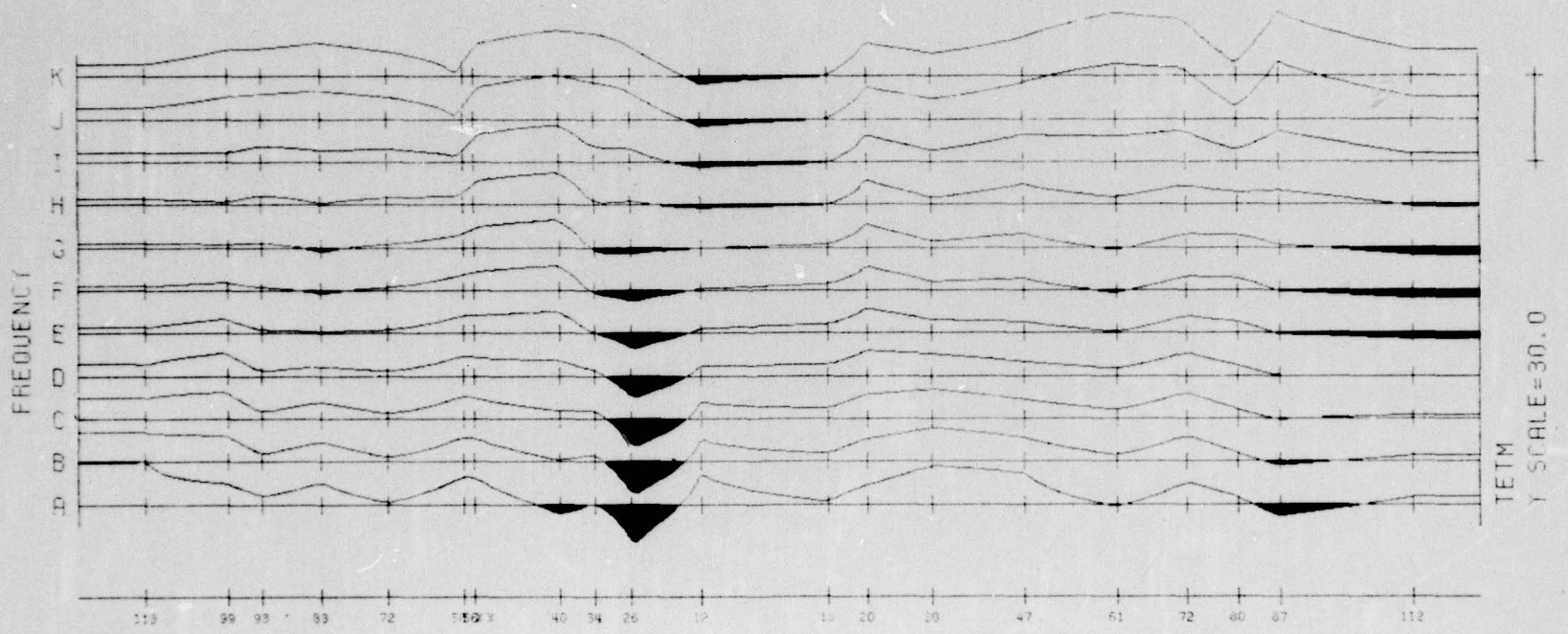
FREQUENCY
K
J
I
H
G
F
E
D
C
B
A
TEIM
Y SCALE=30.0
WIS

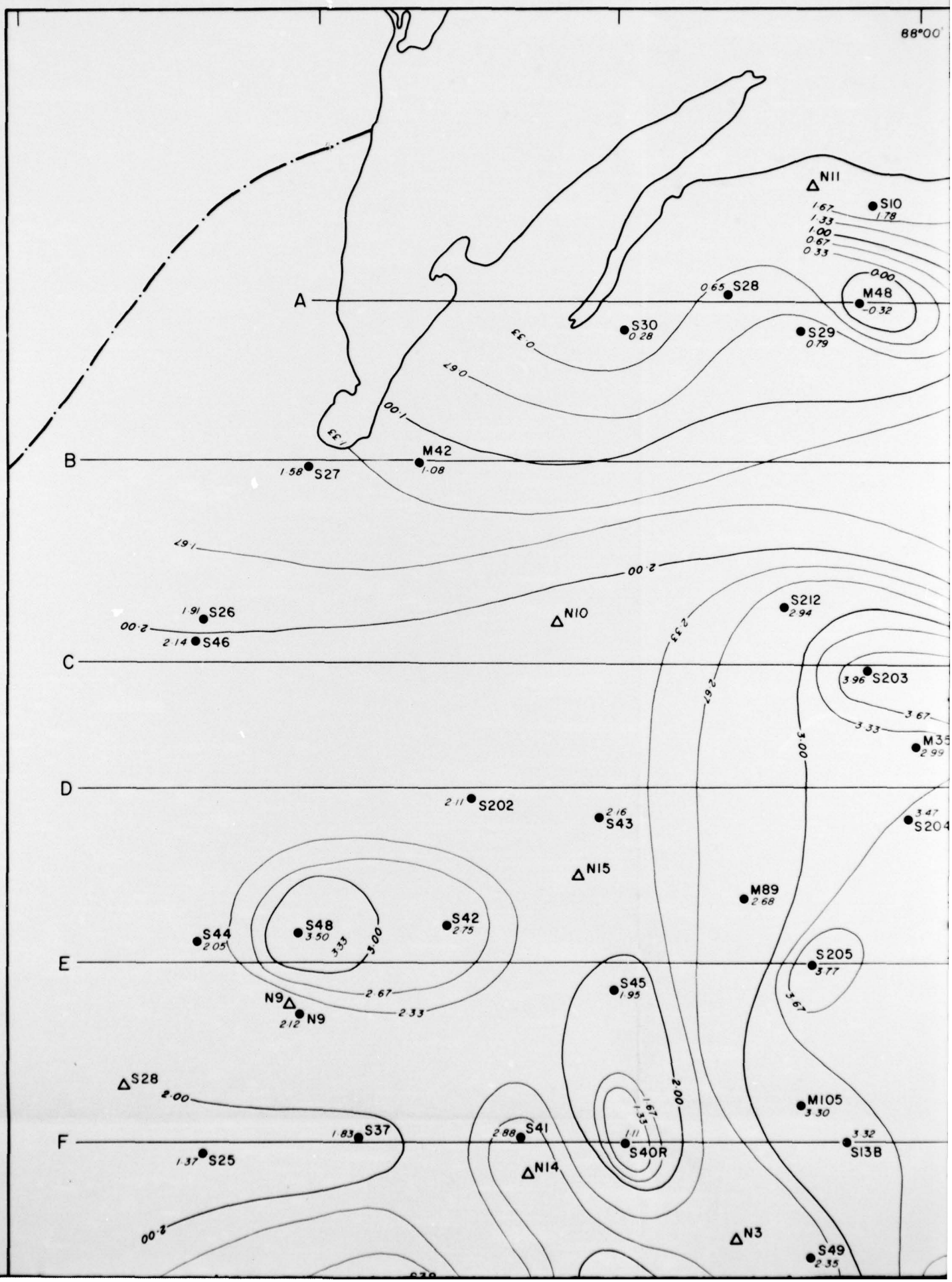
88°00'
A
B
C
D
E
F
N11
S10
1.78
1.67
1.33
1.00
0.67
0.33
0.00
0.65 S28
M48
-0.32
S30
0.28
S29
0.79
0.33
0.67
1.00
1.33
M42
1.08
1.58 S27
1.67
2.00
1.91 S26
2.00
2.14 S46
N10
S212
2.94
2.33
2.67
3.00
3.96 S203
3.67
3.33
M35
2.99
2.11 S202
2.16
S43
3.47
S204
N15
M89
2.68
S44
2.05
S48
3.50
3.33
3.00
S42
2.75
S205
3.77
3.67
2.67
2.33
N9
2.12 N9
S45
1.95
S28
2.00
1.83 S37
1.37 S25
2.88 S41
1.67
1.33
1.11
S40R
2.00
M105
3.30
3.32
S13B
N14
N3
S49
2.35

12

88°00'

UPPER MICHIGAN PEN

A.M.T. SURVEY

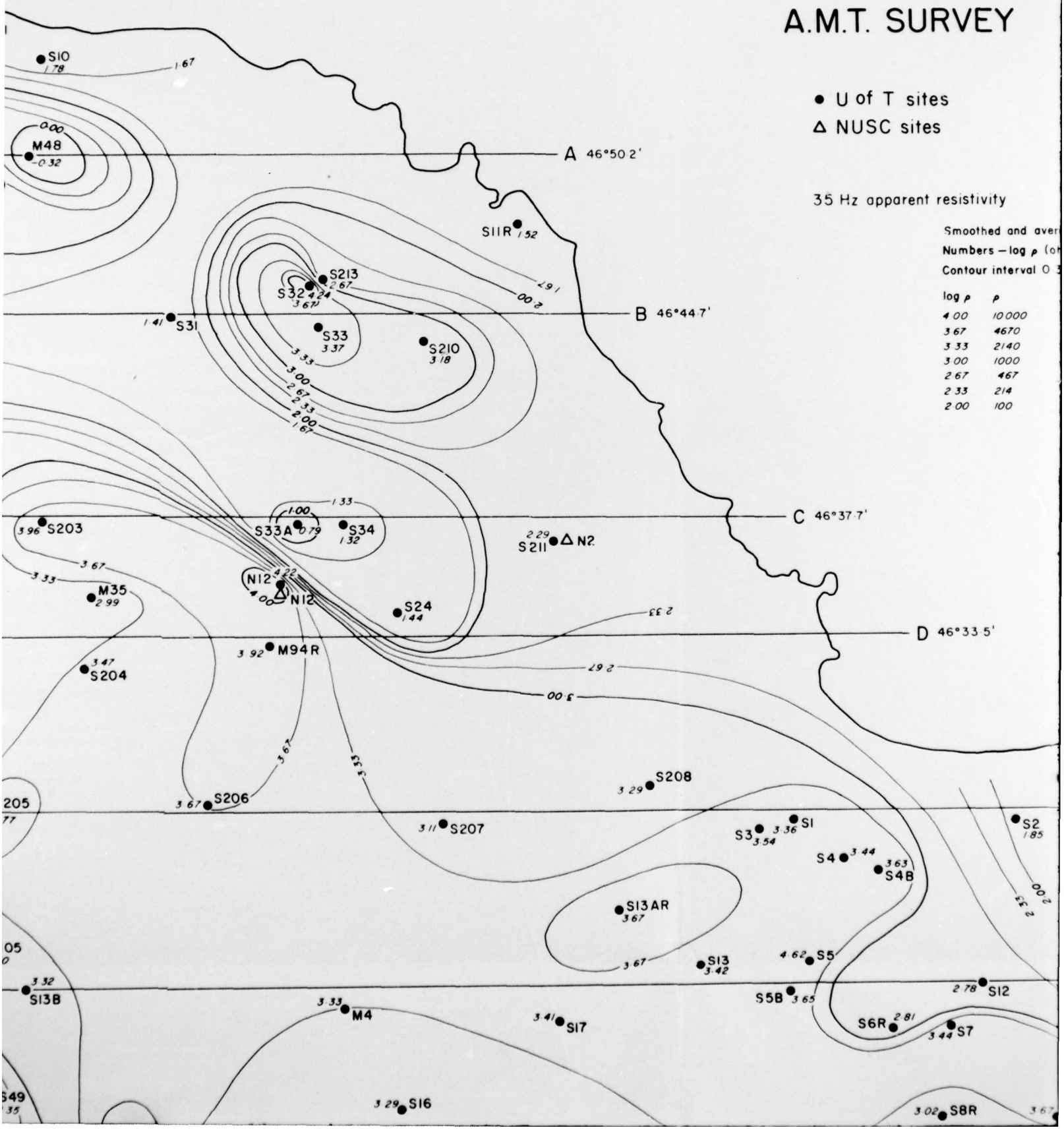

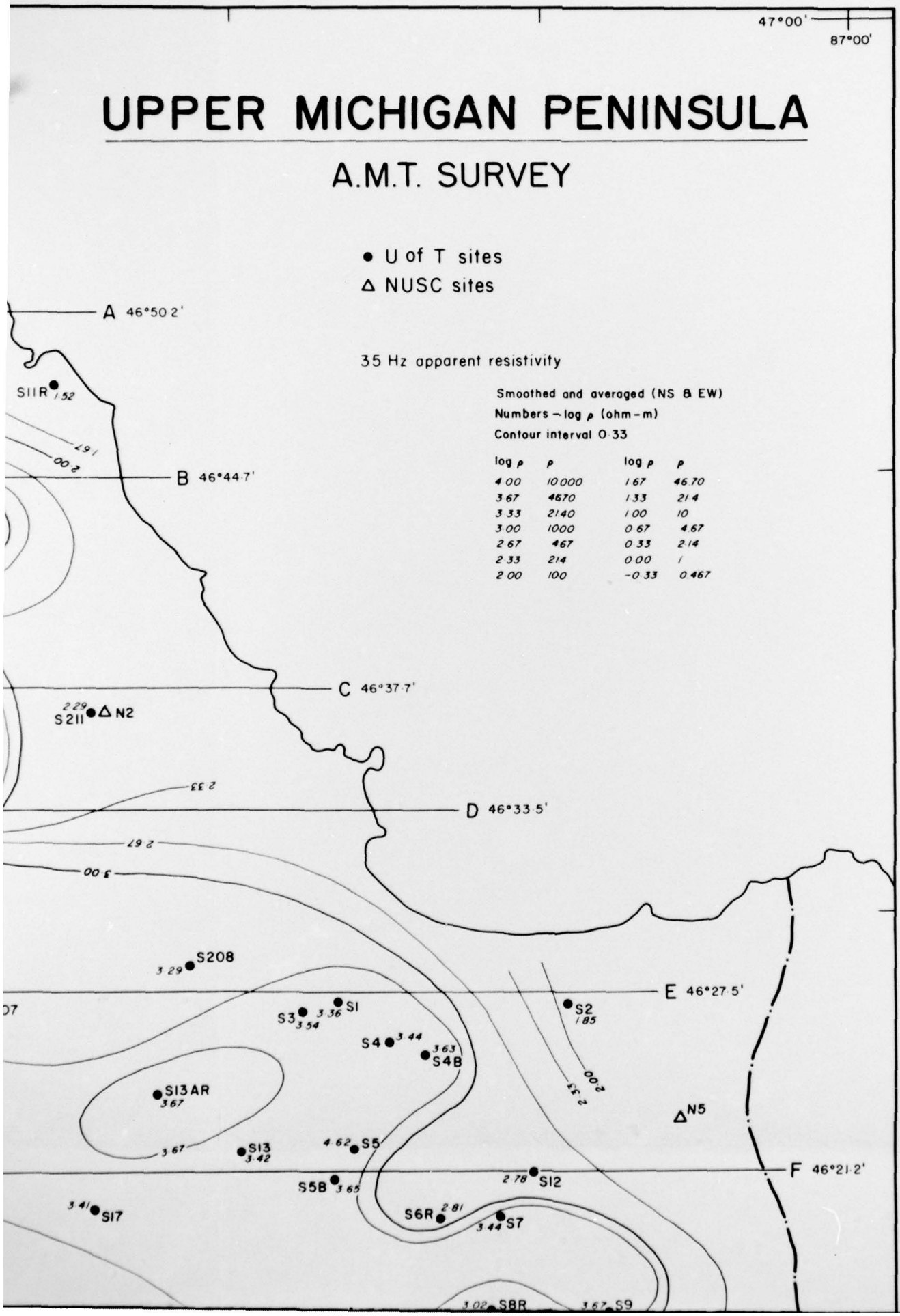
47°00'
87°00'
UPPER MICHIGAN PENINSULA
A.M.T. SURVEY
• U of T sites
△ NUSC sites
35 Hz apparent resistivity
Smoothed and averaged (NS & EW)
Numbers – log ρ (ohm-m)
Contour interval 0.33
log ρ ρ log ρ ρ
4.00 10000 1.67 46.70
3.67 4670 1.33 21.4
3.33 2140 1.00 10
3.00 1000 0.67 4.67
2.67 467 0.33 2.14
2.33 214 0.00 1
2.00 100 -0.33 0.467
A 46°50.2'
B 46°44.7'
C 46°37.7'
D 46°33.5'
E 46°27.5'
F 46°21.2'
S11R 1.52
S211 2.29
N2
S208 3.29
S3 3.54
3.36 S1
S4 3.44
3.63 S4B
S13AR 3.67
S13 3.42
4.62 S5
S5B 3.65
3.41 S17
S6R 2.81
3.44 S7
2.78 S12
S2 1.85
N5
3.02 S8R
3.67 S9
1.67
2.00
2.33
2.67
3.00

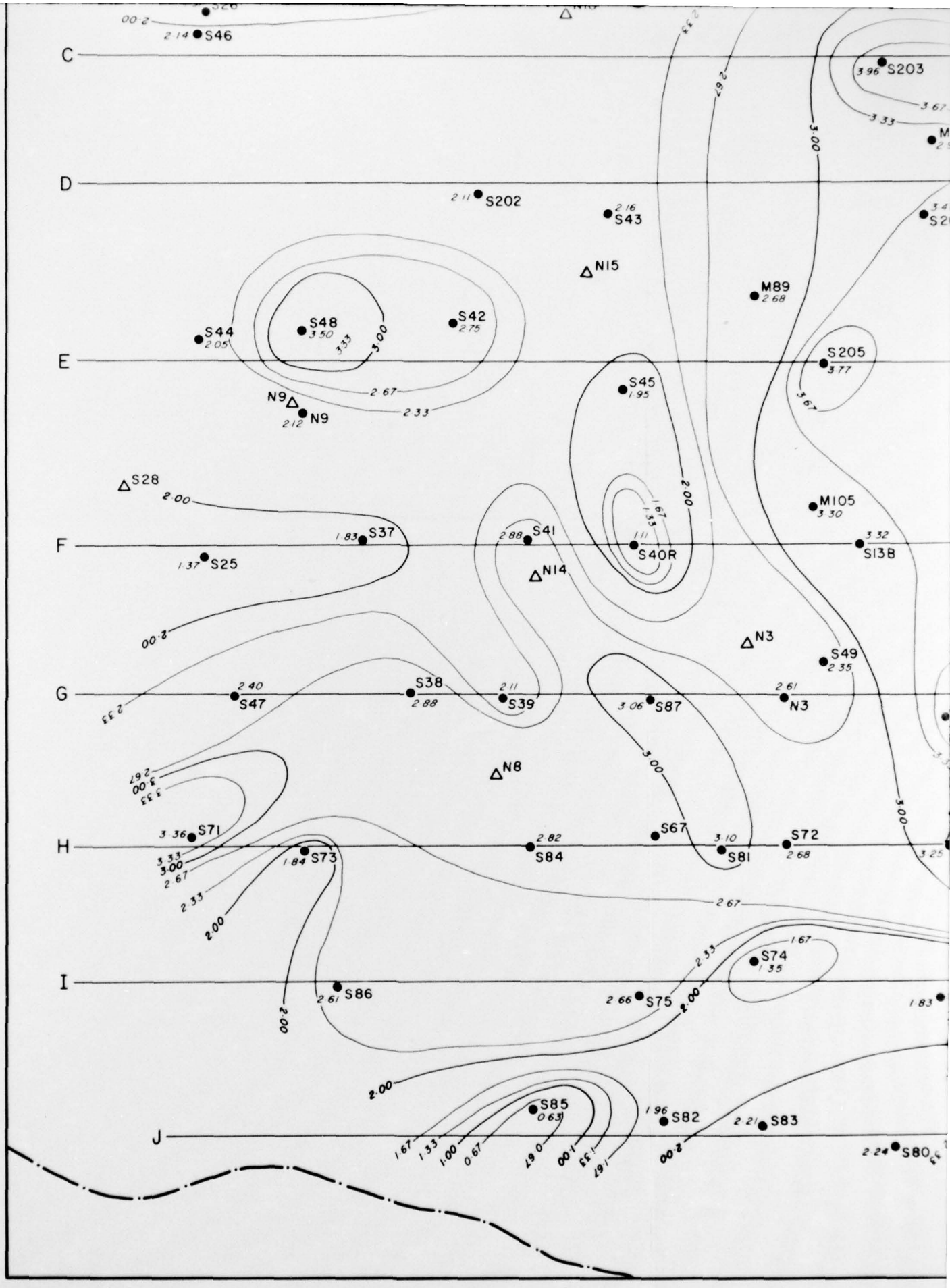
C
D
E
F
G
H
I
J
S46
S203
S202
S43
N15
M89
S44
S48
S42
S205
S45
N9
S28
S37
S25
S41
S40R
N14
M105
S138
N3
S49
S47
S38
S39
S87
N8
S71
S73
S84
S67
S81
S72
S74
S86
S75
S85
S82
S83
S80

4

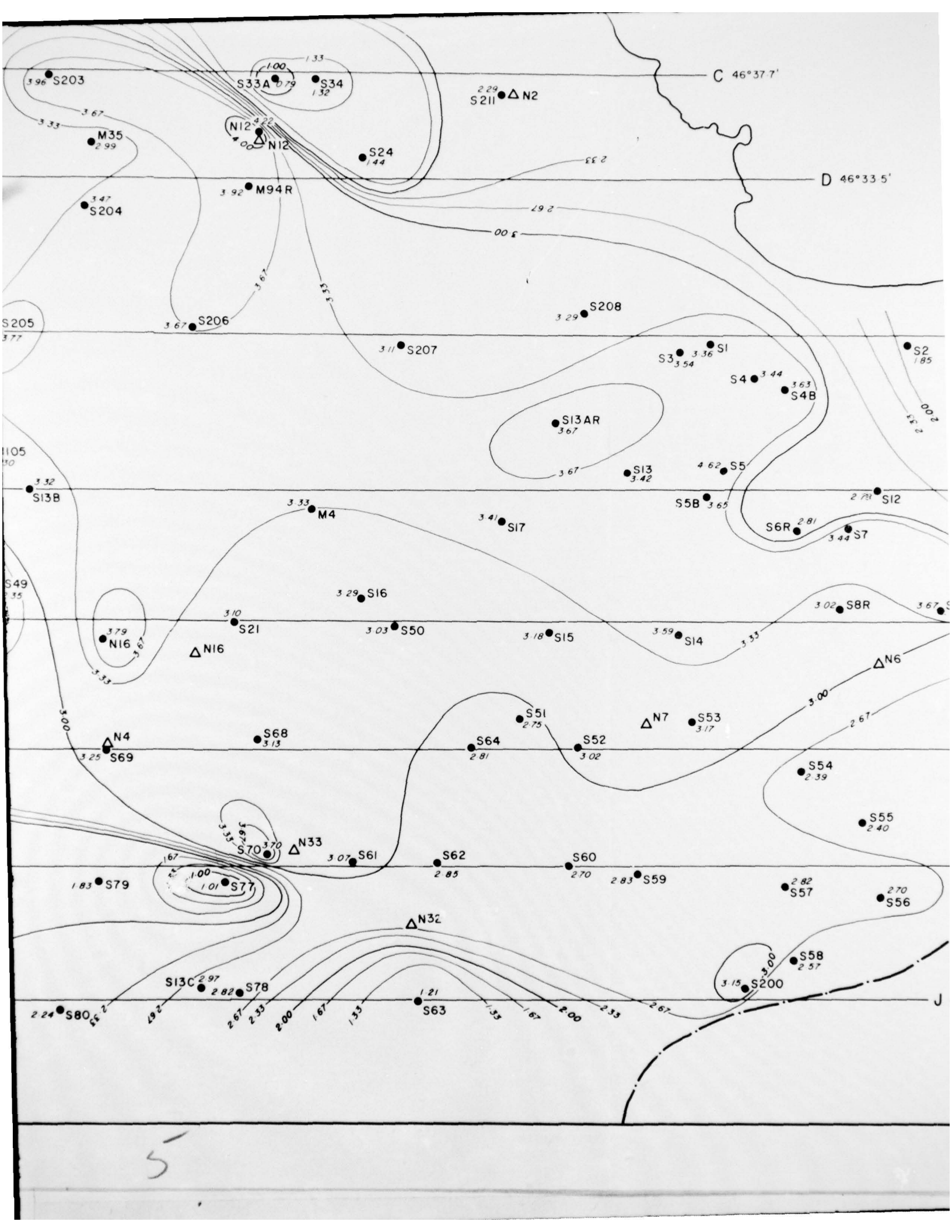
C 46°37.7'
D 46°33.5'
J
S203
S33A
S34
S211
N2
N12
M35
S24
M94R
S204
S206
S205
S208
S207
S1
S3
S2
S4
S4B
S13AR
S13
S5
S5B
S12
S13B
M4
S17
S6R
S7
S49
S16
S8R
S21
S50
S15
S14
N16
N6
S51
N7
S53
N4
S68
S64
S52
S69
S54
S55
S70
N33
S61
S62
S60
S79
S77
S59
S57
S56
N32
S58
S13C
S78
S200
S80
S63

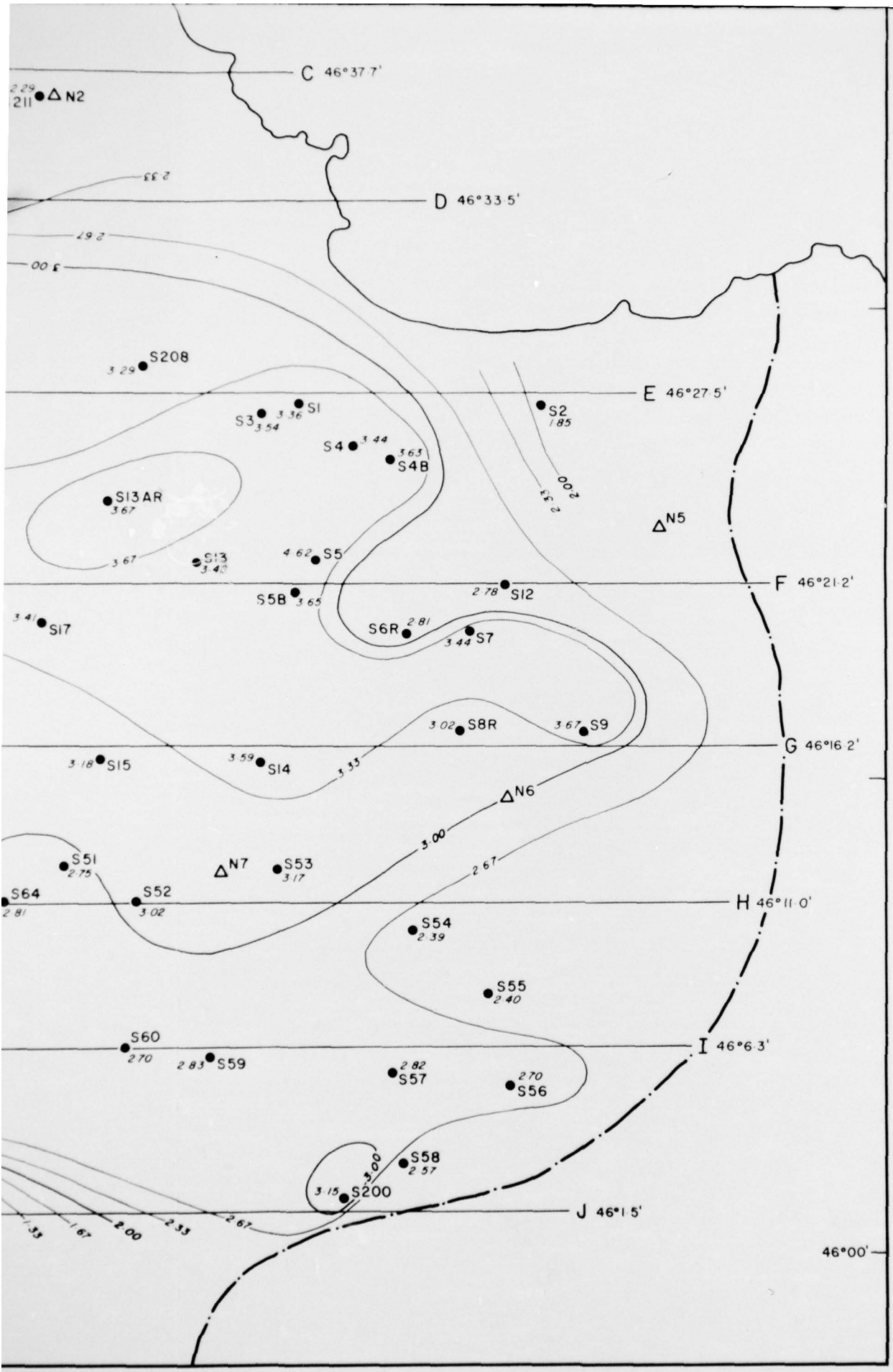
C 46°37.7'
D 46°33.5'
E 46°27.5'
F 46°21.2'
G 46°16.2'
H 46°11.0'
I 46°6.3'
J 46°1.5'
46°00'
N2
N5
N6
N7
S208
S1
S2
S3
S4
S4B
S13AR
S13
S5
S5B
S12
S17
S6R
S7
S8R
S9
S15
S14
S51
S53
S64
S52
S54
S55
S60
S59
S57
S56
S58
S200
2.29
2.11
3.29
3.36
3.54
3.44
3.63
1.85
3.67
3.40
4.62
3.65
2.78
3.41
2.81
3.44
3.02
3.67
3.18
3.59
3.33
2.75
3.17
2.81
3.02
2.39
2.40
2.70
2.83
2.82
2.70
2.57
3.15
3.00
2.67
2.33
2.00
1.67
1.33

6

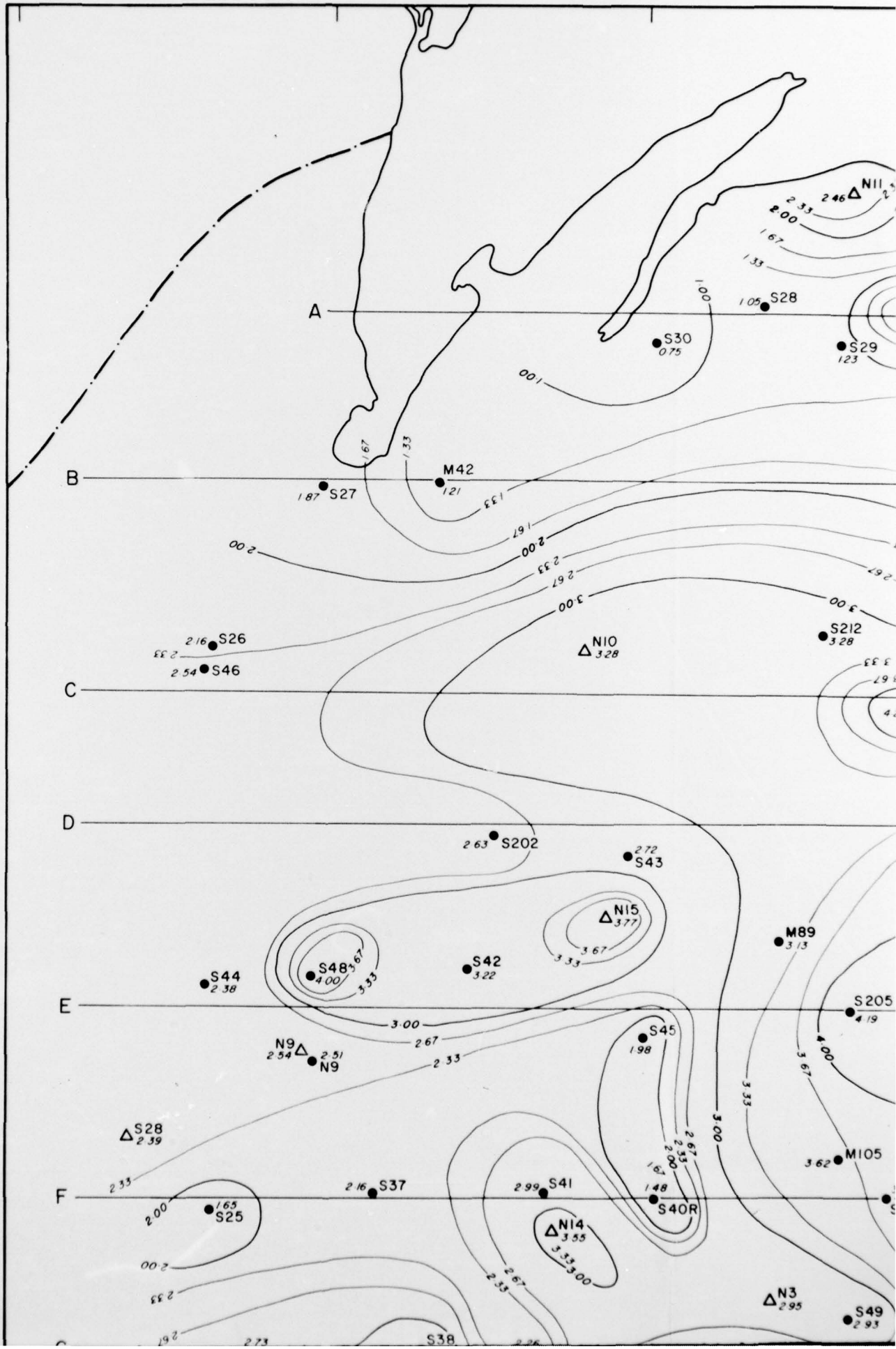
A
B
C
D
E
F
S28 1.05
S30 0.75
S29 1.23
M42 1.21
S27 1.87
S26 2.16
S46 2.54
N10 3.28
S212 3.28
S202 2.63
S43 2.72
N15 3.77
M89 3.13
S44 2.38
S48 4.00
S42 3.22
S205 4.19
N9 2.54
N9 2.51
S45 1.98
S28 2.39
M105 3.62
S37 2.16
S41 2.99
S40R 1.48
S25 1.65
N14 3.55
N3 2.95
S49 2.93
S38

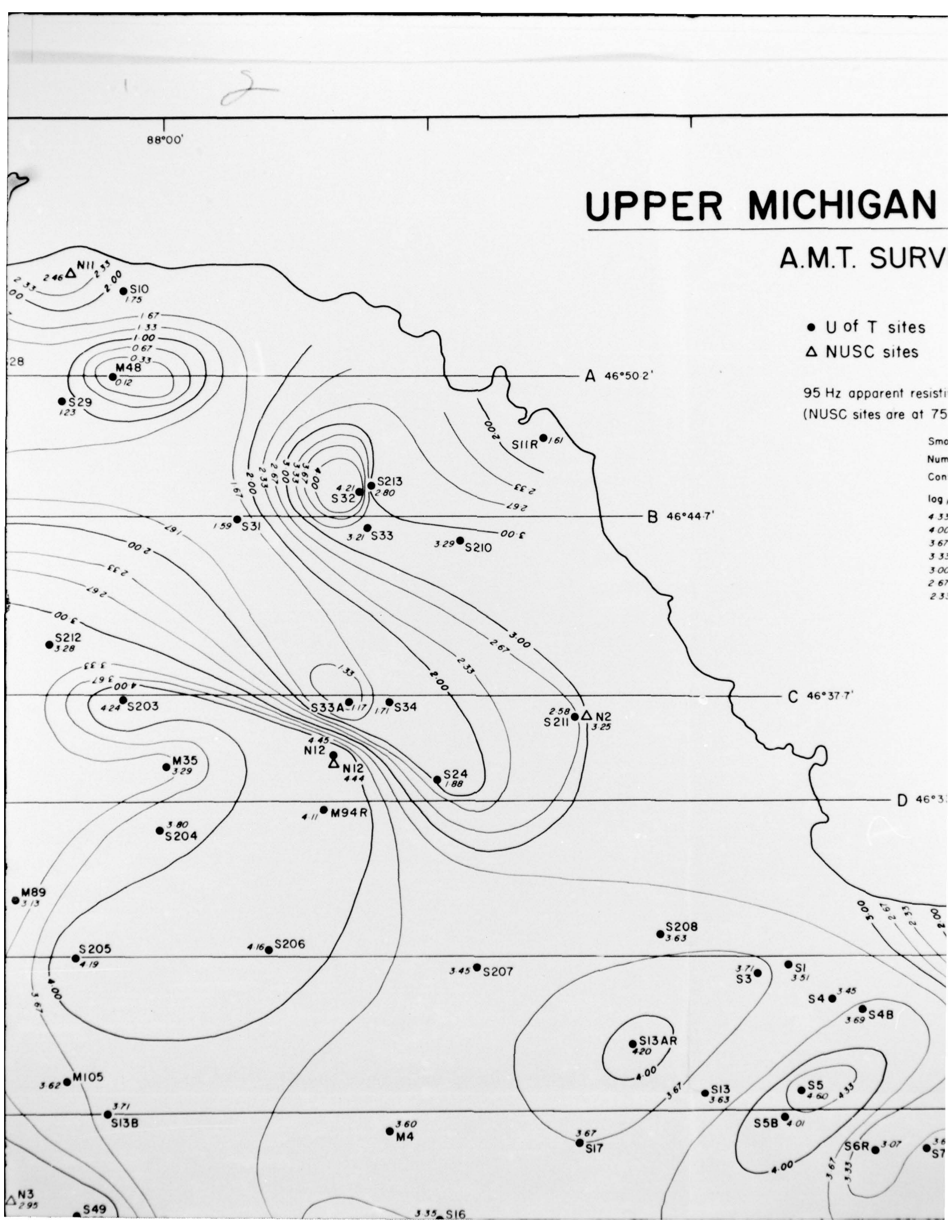
88°00'
UPPER MICHIGAN
A.M.T. SURV
• U of T sites
△ NUSC sites
95 Hz apparent resisti
(NUSC sites are at 75
A 46°50.2'
B 46°44.7'
C 46°37.7'
D 46°3
M48 0.12
S29 1.23
S10 1.75
N11 2.46
S11R 1.61
S213 4.21
S32 2.80
S31 1.59
S33 3.21
S210 3.29
S212 3.28
S203 4.24
S33A 1.17
S34 1.71
N2 3.25
S211 2.58
N12 4.45
N12 4.44
S24 1.88
M35 3.29
M94R 4.11
S204 3.80
M89 3.13
S205 4.19
S206 4.16
S208 3.63
S207 3.45
S3 3.71
S1 3.51
S4 3.45
S48 3.69
S13AR 4.20
M105 3.62
S13B 3.71
S13 3.63
S5 4.60
S5B 4.01
M4 3.60
S17 3.67
S6R 3.07
N3 2.95
S49
S16 3.35

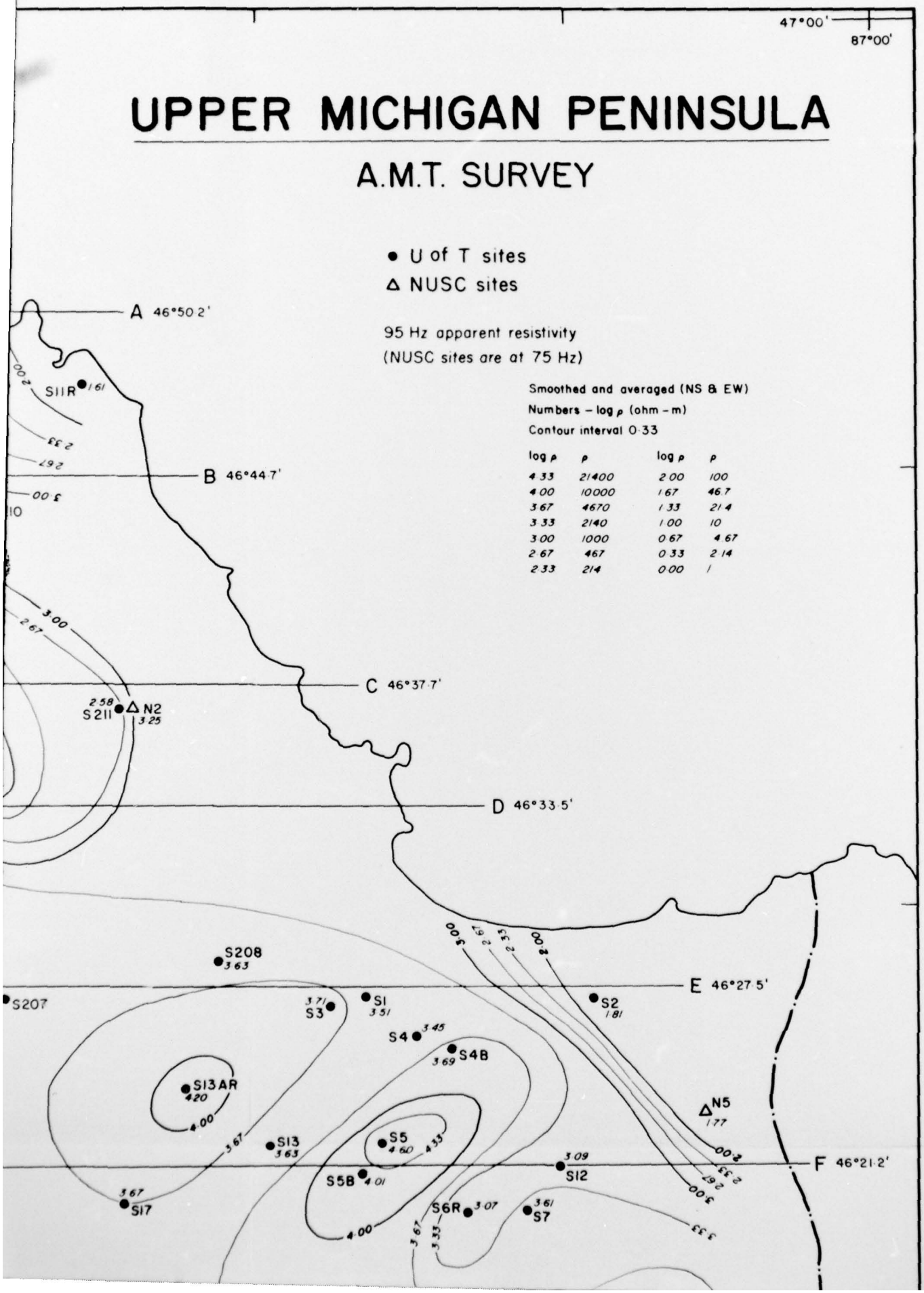
47°00'
87°00'
UPPER MICHIGAN PENINSULA
A.M.T. SURVEY
• U of T sites
Δ NUSC sites
95 Hz apparent resistivity
(NUSC sites are at 75 Hz)
Smoothed and averaged (NS & EW)
Numbers – log ρ (ohm – m)
Contour interval 0·33
log ρ ρ log ρ ρ
4·33 21400 2·00 100
4·00 10000 1·67 46·7
3·67 4670 1·33 21·4
3·33 2140 1·00 10
3·00 1000 0·67 4·67
2·67 467 0·33 2·14
2·33 214 0·00 1
A 46°50·2'
B 46°44·7'
C 46°37·7'
D 46°33·5'
E 46°27·5'
F 46°21·2'
S111R 1·61
S211 2·58
Δ N2 3·25
S208 3·63
S207
S3 3·71
S1 3·51
S2 1·81
S4 3·45
S4B 3·69
S13AR 4·20
S13 3·63
S5 4·60
S5B 4·01
S12 3·09
Δ N5 1·77
S17 3·67
S6R 3·07
S7 3·61
2·00
2·33
2·67
3·00
3·33
3·67
4·00

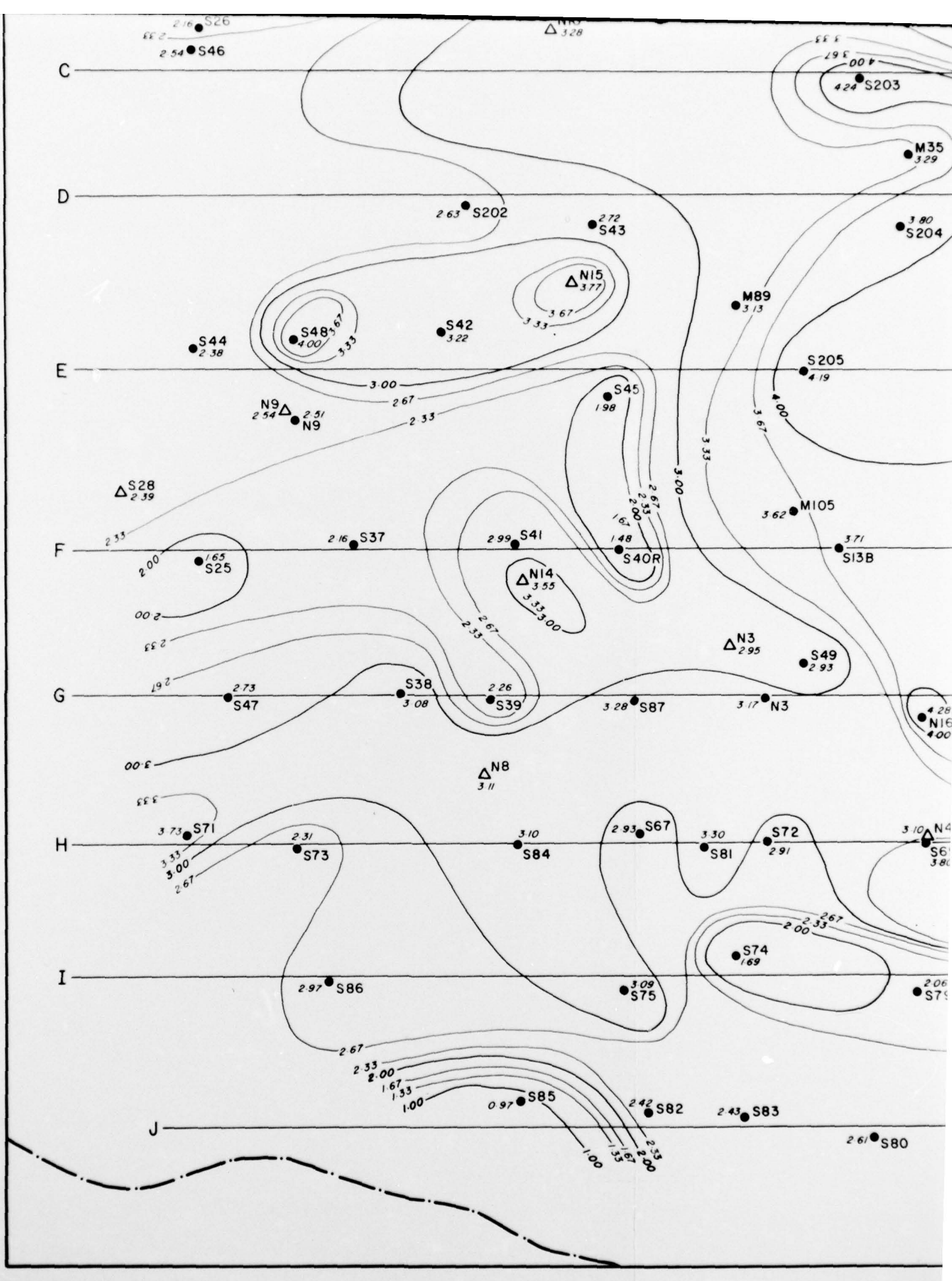
C
D
E
F
G
H
I
J
S26
S46
S203
M35
S202
S43
S204
N15
M89
S48
S42
S44
S205
S45
N9
S28
M105
S37
S41
S40R
S13B
S25
N14
N3
S49
S38
S47
S39
S87
N8
S71
S73
S84
S67
S81
S72
S74
S86
S75
S85
S82
S83
S80

4

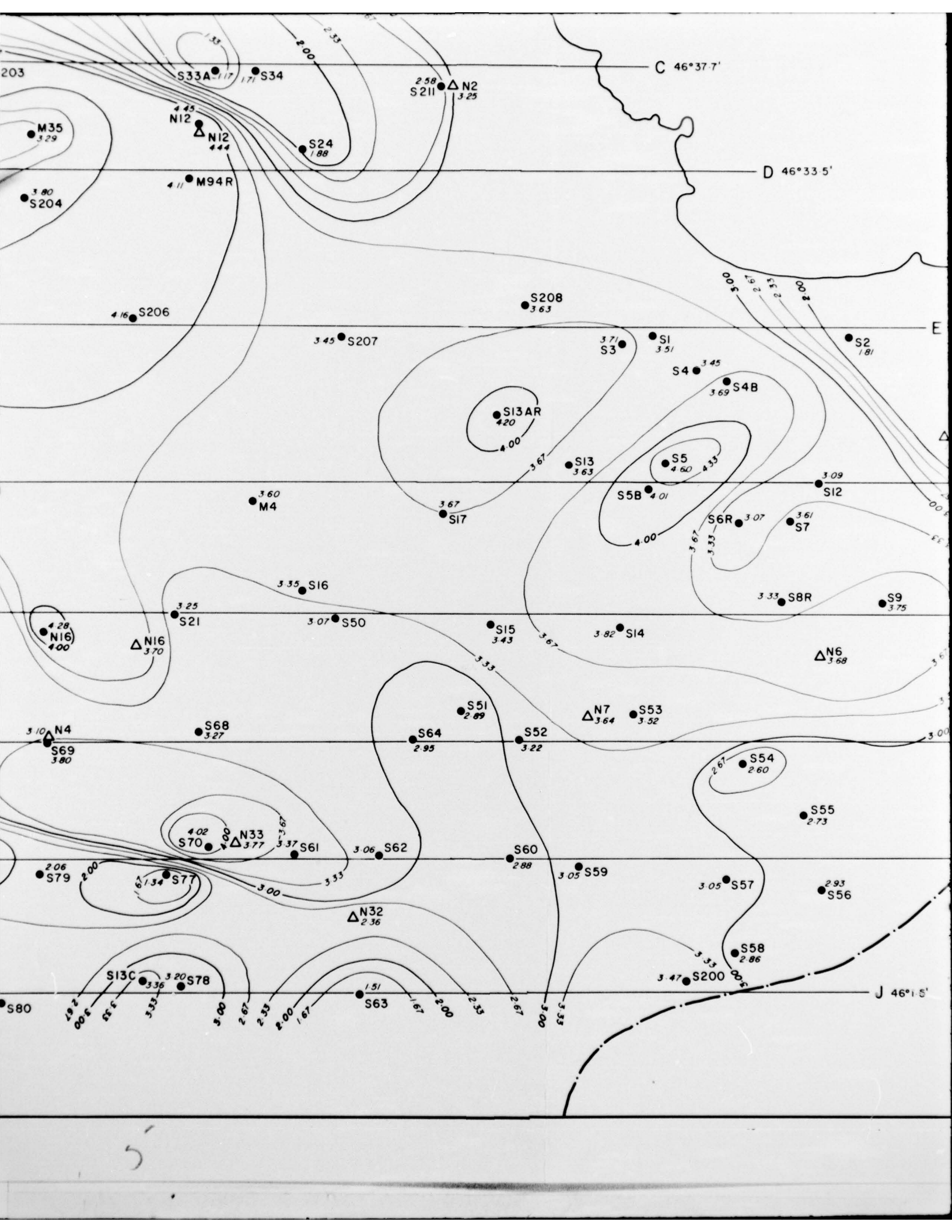
C 46°37.7'
D 46°33.5'
E
J 46°1.5'
S33A 1.17
S34 1.71
S211 2.58
N2 3.25
N12 4.45
N12 4.44
M35 3.29
S24 1.88
M94R 4.11
S204 3.80
S206 4.16
S208 3.63
S207 3.45
S3 3.71
S1 3.51
S2 1.81
S4 3.45
S4B 3.69
S13AR 4.20
S13 3.63
S5 4.60
S5B 4.01
S12 3.09
M4 3.60
S17 3.67
S6R 3.07
S7 3.61
S16 3.35
S21 3.25
S50 3.07
S8R 3.33
S9 3.75
N16 4.28
N16 3.70
S15 3.43
S14 3.82
N6 3.68
S51 2.89
N7 3.64
S53 3.52
N4 3.10
S68 3.27
S69 3.80
S64 2.95
S52 3.22
S54 2.60
S55 2.73
S70 4.02
N33 3.77
S61 3.37
S62 3.06
S60 2.88
S79 2.06
S77 1.34
S59 3.05
S57 3.05
S56 2.93
N32 2.36
S58 2.86
S200 3.47
S13C 3.36
S78 3.20
S80
S63 1.51
2.00
2.33
2.67
3.00
3.33
3.67
4.00

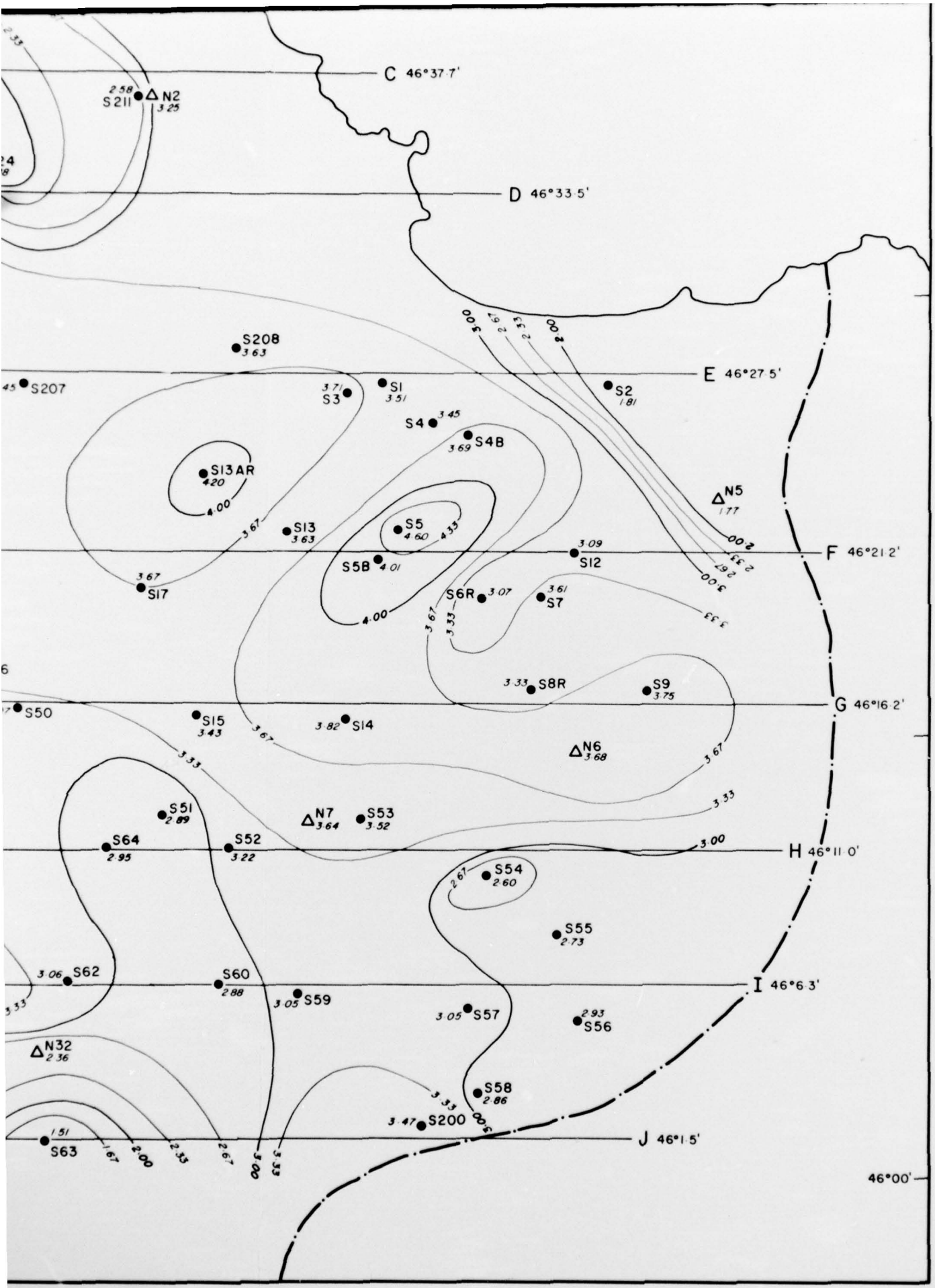
C 46°37.7'
D 46°33.5'
E 46°27.5'
F 46°21.2'
G 46°16.2'
H 46°11.0'
I 46°6.3'
J 46°1.5'
46°00'
S211 2.58
N2 3.25
S208 3.63
S207
S3 3.71
S1 3.51
S2 1.81
S4 3.45
S4B 3.69
S13AR 4.20
N5 1.77
S13 3.63
S5 4.60
S5B 4.01
S12 3.09
S17 3.67
S6R 3.07
S7 3.61
S8R 3.33
S9 3.75
S50
S15 3.43
S14 3.82
N6 3.68
S51 2.89
N7 3.64
S53 3.52
S64 2.95
S52 3.22
S54 2.60
S55 2.73
S62 3.06
S60 2.88
S59 3.05
S57 3.05
S56 2.93
N32 2.36
S58 2.86
S200 3.47
S63 1.51
2.00
2.33
2.67
3.00
3.33
3.67
4.00
4.33

6